DOE/SC-0148

Subsurface Biogeochemical Research

Subsurface Biogeochemical Research Annual Meeting

April 30-May 2, 2012

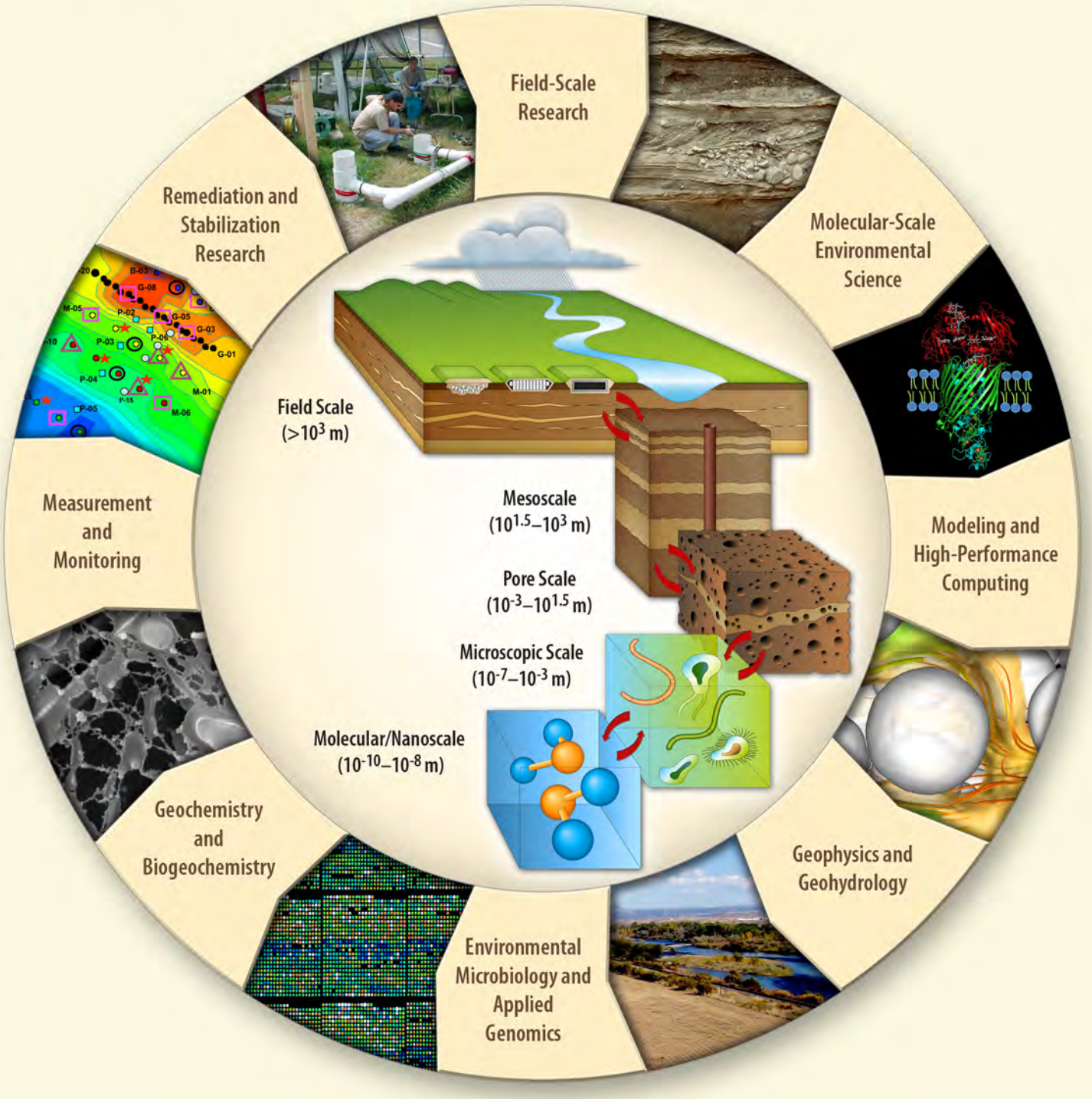

U.S. DEPARTMENT OF ENERGY | Office of Science

U.S. Department of Energy
Office of Science
[http://science.energy.gov/]
Office of Biological and Environmental Research
[http://science.energy.gov/ber/]
Subsurface Biogeochemical Research Program
[http://doesbr.org]

Program Managers

Paul Bayer: paul.bayer@science.doe.gov
David Lesmes: david.lesmes@science.doe.gov
Roland Hirsch: roland.hirsch@science.doe.gov
Arthur Katz: arthur.katz@science.doe.gov

An electronic version of this document is available at the SBR website:
http://doesbr.org/PImeetings/

DOE/SC-0148

U.S. DEPARTMENT OF ENERGY

Office of Science

U.S. Department of Energy Subsurface Biogeochemical Research Annual Meeting

Abstracts

Washington, D.C.

April 30-May 2, 2012

Prepared for the
U.S. Department of Energy
Office of Science
Office of Biological and Environmental Research
Germantown, MD 20874-1290
http://science.energy.gov/ber/

http://doesbr.org

Prepared by
Biological and Environmental Research Information System
Oak Ridge National Laboratory
Oak Ridge, TN 37830
Managed by UT-Battelle, LLC
For the U.S. Department of Energy
Under contract DE-AC05-00OR22725

Welcome

Subsurface Biogeochemical Research 2012 Annual Meeting

Welcome to the 2012 Subsurface Biogeochemical Research (SBR) Annual Meeting! There are four broad objectives for the meeting: (1) to provide opportunities to share research results and promote interactions among the SBR-funded scientists and other invited guests; (2) to evaluate informally the progress of each SBR-funded program or project; (3) to showcase the scientific expertise and research progress over the past year to senior managers within the DOE Office of Science, the technology offices within DOE, and other invited attendees from other federal agencies; and (4) to start a dialogue with the scientific community on future biogeochemical challenges for the BER and DOE mission areas.

Because of a significant reduction in the appropriated vs. proposed funding for fiscal year 2012 for the SBR program, and because outyear funding for the SBR program is expected to remain flat at the FY 2012 level, SBR program managers have significantly restructured all components of the SBR program. The scope of these changes will be presented. Future directions for the SBR program will be presented in the context of a new strategic plan for the Climate and Environmental Sciences Division (CESD) and a closer integration with CESD's Terrestrial Ecosystem Science (TES) program while maintaining close connections with BER's Genomic Science program. The plenary session on Monday morning will feature a CESD overview presentation by Dr. Gerald (Gary) Geernaert, the Director of CESD, and presentations by BER program managers on select BER programs.

In addition, the agenda includes an invited speakers session mid-Monday morning that is designed to feature speakers on topics that will set the stage for the afternoon breakout sessions. The speakers will include Philippe van Cappellen (University of Waterloo) on elemental biogeochemical cycles in subsurface environments, Evan DeLucia (University of Illinois) on the role of soil systems in sustainable feedstock production, and a split presentation from Bill Riley and Eoin Brodie (both from LBNL) on grand challenges for understanding carbon cycling in terrestrial ecosystems. Biological Systems Science Division (BSSD) Director Todd Anderson will provide an overview of BSSD science over lunch.

The concurrent breakout sessions planned for Monday afternoon are designed to enable the SBR-funded scientific community to explore research challenges for future investigation by SBR. Each session will have a different focus, and the discussions will be facilitated by lead SFA managers from LBNL, ORNL and PNNL. Research challenges identified in each breakout session will be captured by the facilitators, presented to all participants late Wednesday morning, and then further discussed among all meeting participants. We need your input to help guide our future planning efforts and look forward to hearing your suggestions.

On Tuesday, plenary sessions will continue in the morning and afternoon, and there will be a late morning and an evening poster session. Wednesday's plenary session will focus on selected highlights of research accomplishments from the IFRC sites and remaining scientific challenges at those sites.

We thank you in advance for your attendance, your presentations at this year's meeting, and your continued dedication and innovation to help advance the research to address BER and DOE mission areas. We are looking forward to meeting with you and not only discussing your research results, but also the opportunities for future challenges within the SBR program.

We also thank Patrick Horan of CESD, Jody Shumpert and Tracey Vieser of ORISE, and Marissa Mills and Sheryl Martin of ORNL for their important contributions to this meeting's technical and logistical aspects.

Finally, we congratulate Todd Anderson on his new position and thank him for his years of service in setting the strategic directions for the SBR program and for his attention to detail in managing the program.

Paul Bayer, Roland Hirsch, Arthur Katz, David Lesmes

April 30, 2012

Contents

Welcome iii

Contents v

Agenda vi

Hotel Map xii

Abstract List xiii

- University-Led Research 1
- Federal Agency-Led Research 71
- Integrated Field-Scale Subsurface Research Challenges (IFRC) 77
- Scientific Focus Areas (SFA) 103
- Early Career Awards 149
- Student Abstracts 151
- Facilities 161

Participants 163

Author Index 169

Institutional Index 175

Agenda

Correct as of April 19, 2012

Sunday, April 29

5:00–7:00 pm	Evening Registration

Monday, April 30

7:00–8:00 am	Registration	
8:00–9:20 am	Welcome and Introductory Comments	
	8:00–8:20 am	Gary Geernaert, Director, Climate and Environmental Sciences Division
	8:20–8:50 am	David Lesmes (DOE-CESD) *SBR Program Update*
	8:50–9:05 am	Dan Stover (DOE-CESD) *TES Program Update*
	9:05–9:20 am	Susan Gregurick (DOE-BSSD) *Systems Biology Knowledgebase Update*
9:20 am–12:00 pm	*New Frontiers for Subsurface Biogeochemical Research: Scientific Grand Challenges*	
	9:20–10:05 am	Philippe van Cappellen, University of Waterloo *Elemental Biogeochemical Cycles in Subsurface Environments*
	10:05–10:35 am	Break
	10:35–11:20 am	Evan DeLucia, University of Illinois *Scientific Grand Challenges for Understanding the Role of Soil Systems in Sustainable Feedstock Production*
	11:20–11:40 am	Bill Riley, Lawrence Berkeley National Laboratory *Challenges for Understanding and Modeling Carbon and Nutrient Cycling and Microbiological Processes in Terrestrial Ecosystems – Part I*
	11:40 am–12:00 pm	Eoin Brodie, Lawrence Berkeley National Laboratory *Challenges for Understanding and Modeling Carbon and Nutrient Cycling and Microbiological Processes in Terrestrial Ecosystems – Part II*
12:00–2:00 pm	**Lunch and Presentation** Speaker: Todd Anderson, Director, Biological Systems Science Division	
2:00–5:30 pm	Breakout Sessions *New Frontiers for Subsurface Biogeochemical Research*	

2:00–5:30 pm	***Breakout Session 1: Elemental Biogeochemical Cycles in Terrestrial Environments*** **Session Chairs:** Harry Beller (LBNL), Liyuan Liang (ORNL), and John Zachara (PNNL) **Panelists:** Derek Lovley (University of Massachusetts), Francois Morel (Princeton University), Tim Scheibe (PNNL), Jeremy Smith (University of Tennessee), Anne Summers (University of Georgia), and Philippe van Cappellen (University of Waterloo) **Objective:** The EMSP/NABIR/SBR programs have defined the state of fundamental science in contaminant biogeochemistry and metal/radionuclide fate and transport over the past 10 years. Seminal impacts to this scientific area have been made by many publications, the development of multidisciplinary approaches, and the performance of sophisticated field studies of unique character. While previous research has focused on the subsurface environment, elemental cycling facilitated by biosphere-metal interactions occurs more broadly in terrestrial environments including soil, groundwater, and freshwater sediments. Biosphere-metal interactions critically affect all ecosystems and respond in a dynamic manner to climatic and other environmental changes on all scales. Scientific understanding of these diverse, complex, and far-reaching processes, together with their rates, interactions, and impacts, is uneven. The intent of this session is to identify impactful scientific grand challenges (GCs) in elemental biogeochemical cycling (e.g., S, Fe/Mn, Si, trace elements, etc.) in terrestrial environments to guide future research. **Content:** A panel and audience discussion will identify fundamental scientific grand challenges (GC) in elemental biogeochemistry and multidisciplinary approaches to resolve them. Environments to be considered include soils, the vadose zone, groundwater, the groundwater-river mixing zone, and the hyphoreic zone. The focus will be on elemental cycling challenges that involve coupled microbiologic, hydrologic, and geochemical processes and that require a combination of molecular, mechanistic, and systems-scale approaches for comprehensive resolution and environmental prediction. The session will also consider responses of elemental biogeochemical cycling to climatic and other dynamic environmental changes. Discussions will identify two to three impactful grand challenges, example environments where they could be evaluated, balances between fine-scale and systems-scale research, and new modeling approaches that might be required.

2:00–5:30 pm	***Breakout Session 2: Toward an Integrated, Process-Level View of Biogeochemical Cycling and Carbon Flow within Terrestrial Systems*** **Session Chairs:** Baohua Gu (ORNL), Susan Hubbard (LBNL), and Alan Konopka (PNNL) **Panelists:** Jon Chorover (University of Arizona), Evan DeLucia (University of Illinois), Mary Firestone (UC Berkeley), TC Onstott (Princeton University), and Bill Riley (LBNL) **Objective:** Managed and natural terrestrial ecosystems are critically important for sustaining life. The interactions between the solid, aqueous, and biological components of ecosystem soils and underlying sediments regulate the geochemical fluxes of most life-critical elements, control the production of food and biofuel feedstock, and regulate greenhouse gases. Despite decades of research on carbon cycling in terrestrial ecosystems and the clear importance of these systems for bioenergy and climate change, a predictive understanding of the physical, chemical, and biological interactions that occur across scales and through various linked compartments of the system (atmosphere-plant-soil-vadose zone-groundwater-surface water) remains elusive. The lack of understanding hinders our ability to predict and optimize ecosystem behavior, both under current and future environmental conditions. BER has the potential to advance such a predictive understanding through the linkage of the SBR, Terrestrial Ecosystem Science (TES), Climate Science, and BSSD programs. Recognition of the hierarchical nature and complex interactions between system components, innovative multi-disciplinary approaches, sophisticated new instrumental platforms and "omics" technologies, and multi-scale mechanistic models developed through SBR research on contaminant biogeochemistry have great potential to advance a process-level understanding of biogeochemical cycles and carbon fluxes within terrestrial ecosystems. Such understanding is required for improved predictions and ultimately for sustainable management of natural and managed ecosystems. This breakout session will explore grand challenges that leverage SBR multi-process expertise to questions of how biogeochemical cycles coupled to hydrological fluxes impact carbon dynamics in multi-compartment terrestrial systems. **Content:** The breakout session will identify research grand challenges (GCs) related to developing a predictive understanding of the biogeochemical basis (broadly defined) of carbon cycling; carbon storage, transformation, and sequestration; and C exchange and redistribution in complex, multi-compartment terrestrial systems. The GCs will involve coupled processes; explicitly consider the range of space and time scales relevant to energy and environmental sustainability; have field relevance and linkage; be complementary to research directions in TES; and benefit from the research perspectives and approaches developed collectively by the SBR community including environmental "omics," molecular spectroscopy and analysis, multi-process modeling, and field characterization, monitoring, and experimentation. Deliberations will refine candidate GCs to a few examples and identify associated (i) science questions to guide scale-specific studies, (ii) molecular- to field-scale experimental and monitoring approaches that might be applied, (iii) ecosystem field site characteristics desirable for performing impactful science, and (iv) opportunities for the development of robust, process-level biogeochemical models of carbon cycling in multi-scale terrestrial systems. The session will conclude with an important discussion on how process-level models of biogeochemical cycles could contribute to improved management of ecosystem-level carbon fluxes and transformation rates.

2:00–5:30 pm	***Breakout Session 3: Subsurface Biogeochemical Processes Associated with Energy Production, Usage, and Storage*** **Session Chairs:** Scott Brooks (ORNL), Jim Fredrickson (PNNL), and Carl Steefel (LBNL) **Panelists:** Rick Colwell (Oregon State University), Li Li (Penn State University), George Redden (INL), Ken Williams (LBNL), and Mavrik Zavarin (LLNL) **Objective:** Many energy-related activities perturb the biogeochemistry of the subsurface or are themselves influenced by biogeochemical processes. A prime example is the design of geological nuclear waste repositories, where the impact of biogeochemical processes on far-field radionuclide transport will be substantial. Microbially-enhanced hydrocarbon recovery (MEHR) is another example in which perturbation of the subsurface microbiological and biogeochemical environment is used for energy extraction purposes. More knowledge is also needed of how greenhouse gas fluxes are modified by biogeochemical processes in the subsurface; the release of methane from methane hydrates due to global warming is now treated as a purely physical/hydrological process but is likely to be far more complex. Another example involves the leakage of geologically stored CO_2 into drinking water aquifers, where acidification may significantly alter the biogeochemical status and where toxic metals may be potentially mobilized. The objective of this breakout session is to address the question of how energy production, usage, and storage of byproducts can impact the biogeochemistry of the subsurface, as well as to consider how the ambient or perturbed biogeochemical environment can impact the energy production and storage schemes. **Content:** The breakout session will identify fundamental biogeochemical grand challenges associated with the production, usage, and storage of energy in the subsurface. While these topics have been addressed by applied DOE programs for improving process efficiencies, a firm scientific underpinning for understanding the full system behavior is lacking. An overall goal is to identify cross-cutting fundamental science issues or knowledge gaps associated with multi-scale, biogeochemical reactive transport whose resolution could advance safe extraction, isolation, or storage technologies. The breakout will consider the far-field impacts of biogeochemistry on the effective design of geological nuclear waste repositories, the effects of enhanced gas recovery and carbon sequestration on subsurface microbiologic communities and their biogeochemical function, and perturbations to the subsurface as a result of inadvertent hydrocarbon releases. The effect of biogeochemistry on carbon fluxes in the deep subsurface (as distinct from the soil environment) as related to climate change will also be addressed. A desired outcome is the identification of fundamental biogeochemical research topics applicable to multiple emerging DOE mission areas.
6:00–8:30 pm	Poster Session I

Tuesday, May 1		
8:00–10:00 am	Plenary Session I	
	8:00–8:20 am	Robin Gerlach, Montana State University *Mixing-, Reaction-, and Transport-Controlled Microbial Activity and Carbonate Mineral Precipitation in Porous Media*
	8:20–8:40 am	Gemma Reguera, Michigan State University *Extracellular Reduction of Uranium via* Geobacter *Conductive Pili as a Cellular Protective Mechanism*
	8:40–9:00 am	Derek Lovley, University of Massachusetts *New Biological Paradigms Emerging from Bioremediation Research*
	9:00–9:20 am	Eric Roden, University of Wisconsin *Microbial Oxidation of Insoluble Fe(II)-Bearing Minerals Relevant to the Hanford 300 Area and Other Subsurface Environments*
	9:20–9:40 am	David Richardson, University of East Anglia *Exploring the Biology of Microbe-to-Mineral Electron Transfer at Nanometer Resolution*
	9:40–10:00 am	Kevin Rosso, Pacific Northwest National Laboratory *Molecular Structure and Electron Transfer in Microbial Cytochromes*
10:00–10:30 am	Break	
10:30 am–12:30 pm	Poster Session II	
12:30–1:30 pm	Lunch	
1:30–5:30 pm	Plenary Session II	
	1:30–1:50 pm	Kim Hayes, University of Michigan *Impact of Iron Sulfide on the Oxidative Dissolution of Reduced Uranium*
	1:50–2:10 pm	Paul Tratnyek, Oregon Health and Science University *Technetium Reduction and Long-Term Sequestration by Iron/Iron-Sulfide Nanoparticles*
	2:10–2:30 pm	Yu Yang, Auburn University *Coupling Microscale Processes with Macroscale Migration for Actinides: From Dissolution and Reduction of Crystals to Column Transport*
	2:30–2:50 pm	Kathy Nagy, University of Illinois at Chicago *On the Stickiness of Mercury(II) to Soil Components and EFPC Soils*
	2:50–3:10 pm	Anne Summers, University of Georgia *Bacteria in the Global Mercury Cycle: From Y-12 to Clean Coal and Beyond*
	3:10–3:30 pm	Jeremy Smith, University of Tennessee S*imulations of Mercury: Inside and Outside the Bacterial Cell*
3:30–4:00 pm	Break	
4:00–5:30 pm	*New Insights for Subsurface Microbial Ecology*	
	4:00–4:30 pm	Chris Marx, Harvard University *Evolution and Modeling of Synthetic Microbial Communities*
	4:30–5:00 pm	Jill Banfield, University of California at Berkeley *Novel Organisms and Pathways Contribute to Coupled Carbon and Geochemical Cycling in Complex Subsurface Microbial Communities*
	5:00–5:30 pm	Tim Scheibe, Pacific Northwest National Laboratory *Complex Challenges in Science-Based Predictive Simulation: From Fundamental to Field Scales*
6:00–8:30 pm	Poster Session III	

Wednesday, May 2		
8:00–9:30 am	Plenary Session III *IFRC Presentations*	
	8:00–8:20 am	Baohua Gu, Oak Ridge National Laboratory *Oak Ridge-IFRC Science Talk*
	8:20–8:50 am	Scott Brooks, Oak Ridge National Laboratory *Accomplishments and Remaining Challenges*
	8:50–9:10 am	Xingyuan Chen, Pacific Northwest National Laboratory *Hanford-IFRC Science Talk*
	9:10–9:40 am	John Zachara, Pacific Northwest National Laboratory *Accomplishments and Remaining Challenges*
	9:40–10:00 am	Steve Yabusaki, Pacific Northwest National Laboratory *Old Rifle-IFRC Science Talk*
	10:00–10:30 am	Phil Long, Lawrence Berkeley National Laboratory *Accomplishments and Remaining Challenges*
10:30–11:00 am	Break	
11:00 am–12:30 pm	Plenary Discussion	
	11:00–11:20 am	Report Out: Breakout Session 1
	11:20–11:40 am	Report Out: Breakout Session 2
	11:40 am–12:00 pm	Report Out: Breakout Session 3
	12:00–12:30 pm	Discussion
12:30 pm	Final Announcements and Adjourn	

Hotel Map

Washington Marriott Wardman Park

2660 Woodley Road NW
Washington, District Of Columbia 20008 USA
Phone: 1-202-328-2000
Fax: 1-202-234-0015

LOBBY LEVEL

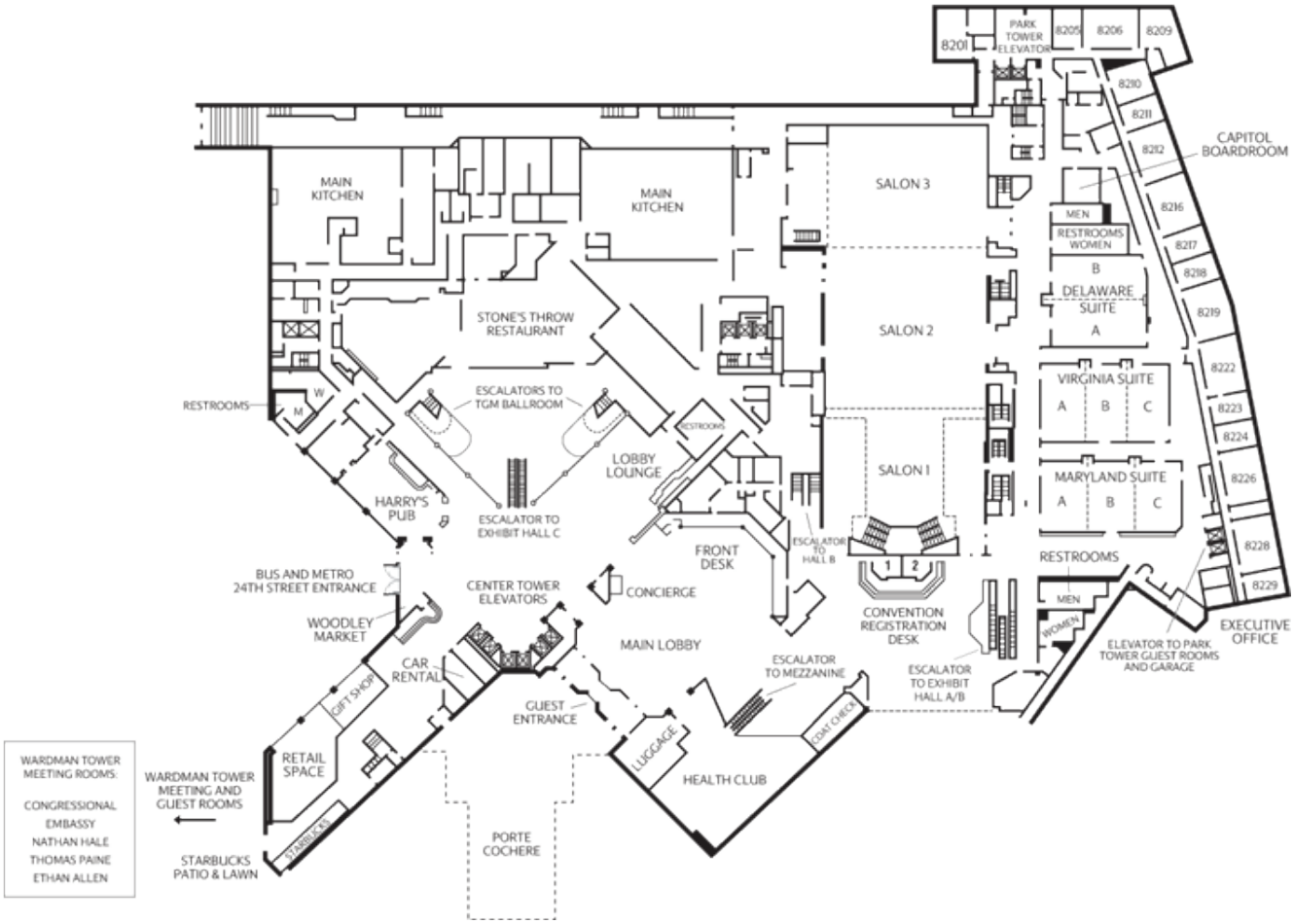

Abstract List

University-Led Research 1

Induced Polarization Signature of Biofilms in Porous Media: From Laboratory Experiments to Theoretical Developments and Validation 1

Estella A. Atekwana (PI), *Oklahoma State U.*; Andre Revil, *Colorado School of Mines*; Mariana Patrauchan, *Oklahoma State U.*

Integrated Microscopic and Metagenomic Analysis of Subsurface Microorganisms that Contribute to Carbon and Metal Cycling 2

Luis R. Comolli, Birgit Luef, Cindy J. Castelle, Sirine C. Fakra—*LBNL*; Kyle R. Frischkorn, Sean W.A. Mullin, Kelly C. Wrighton, *U. of California Berkeley*; Brian J. Anderson, Michael J. Wilkins, *PNNL*; Roseann Csencsits, Mary S. Lipton, *PNNL*; Steven W. Singer, Jillian F. Banfield (PI), *U. of California Berkeley*

Understanding the Subsurface Reactive Transport of Transuranic Contaminants at DOE Sites 3

M. Barnett (PI), *Auburn U.*; T. Albrecht-Schmitt, *U. of Notre Dame*; J. Saiers, *Yale U.*; D. Shuh, *LBNL*

Microscale Metabolic, Redox and Abiotic Reactions in Hanford 300 Area Subsurface Sediments 4

Haluk Beyenal (PI, beyenal@wsu.edu), *Washington State U.*; Jim Fredrickson, *PNNL*; Jeffrey S. McLean, *J. Craig Venter Institute*; Bin Cao, *Washington State U., PNNL*; Paul D. Majors, *PNNL*
Collaborators: Kenneth M. Kemner, Bhoopesh Mishra, Maxim I. Boyanov—*ANL*; Matthew J. Marshall, Liang Shi, David W. Kennedy, Roslyn N. Brown, Yijia Xiong, Margaret F. Romine, Mary S. Lipton, Nancy G. Isern—*PNNL*

Isotopic Characterization of Biogeochemical Pools of Mercury and Determination of Reaction Pathways for Mercury Methylation 5

J.D. Blum (PI), J. Demers—*U. of Michigan*; B. Gu (lead co-I), F. He, W. Zheng—*ORNL*

Reactivity of Iron-Bearing Phyllosilicates with Uranium and Chromium Through Redox Transition Zones 6

William D. Burgos (PI, wdb3@engr.psu.edu), *Penn State*; Hailiang Dong, (dongh@muohio.edu), *Miami U.*; Kenneth Kemner, *ANL*; Fubo Luan, *Penn State*; Michael Bishop, Paul Glasser—*Miami U.*

Inorganic Controls on Neptnium-237 Mobility in the Subsurface 7

Peter C. Burns (PI, pburns@nd.edu), Jessica M. Morrison, Enrica Balboni, Ernest M. Wylie—*U. of Notre Dame*

***In Situ* Generation of Iron-Chromium Precipitates for Long-Term Immobilization of Chromium at the Hanford Site** 8

E. Butler (PI, ecbutler@ou.edu), L. Chen, L. Krumholz, A. Madden—*U. of Oklahoma*; C. Hansel—*Harvard U.*

Field-Deployable Nanosensing Approach for Real-Time Detection of Free Mercury Speciation and Quantification in Surface Stream Waters and Groundwater Samples at the U.S. DOE Contaminated Sites 9

A.D. Campiglia (PI), F.E. Hernandez (co-PI), E.C. Heider, W. Chemnasiry, K. Trieu, C. Diaz, V. Diaz, A.F. Moore—*U. of Central Florida*; S.C. Brooks (co-PI)—*ORNL*

Dominant Mechanisms of Uranium-Phosphate Reactions in Subsurface Sediments 10

J.G. Catalano (PI), D.E. Giammar, F. Maillot, V. Mehta—*Washington U. St. Louis*; Z. Wang—*PNNL*

Isolation of Fe-Oxidizing Microorganisms from the Rifle IFRC Site: Toward Understanding Post-Biostimulation Permeability Reduction and Oxidative Processes 11

Clara Chan (PI), Kevin Cabaniss, Chaofeng Lin—*U. of Delaware*; Ken Williams, *LBNL*

Uranium and Strontium Fate in Waste-Weathered Sediments: Scaling of Molecular Processes to Predict Reactive Transport..... 12

Jon Chorover (PI/PD, chorover@cals.arizona.edu), *U. of Arizona*; Karl Mueller (co-PI), *PNNL*; Peggy O'Day (co-PI), *U. of California Merced*; Carl Steefel (co-PI), *LBNL*; Wooyong Um (co-PI), *PNNL*; John Zachara, *PNNL*; Nico Perdrial, *U. of Arizona*; Masa Kanematsu, *U. of California Merced*; Eric Poweleit, *Penn State*; Guohui Wang, *PNNL*

Sequestration of Uranium in Iron-Rich Sediments under Sequential Reduction-Oxidation Conditions 13

C.S. Criddle (PI), W.-M. Wu, X. Du, S. Fendorf—*Stanford U.*; J. Bargar—*SLAC*; T. Mehlhorn, K. Lowe, D.B. Watson—*ORNL*; B. Li, T. Zhang—*U. of Hong Kong*; J. Zhou—*U. of Oklahoma*

Subsurface Conditions Controlling Uranium Incorporation in Iron Oxides: A Redox Stable Sink.....14

M. Massey, M. Jones, G.E. Brown Jr., S. Fendorf (PI)—*Stanford U.*; J. Lezama, J. Bargar—*SSRL*; P. Nico, *LBNL*; Ravi Kukkadapu, *PNNL*

Microbial Community Trajectories in Response to Accelerated Remediation of Subsurface Metal Contaminants 15

Rebecca A. Daly, Katerina Estera —*U. of California Berkeley*; HsiaoChien Lim, *LBNL*; Ping Zhang, *U. of Oklahoma Norman*; Yongman Kim, *LBNL*; Zhili He, *U. of Oklahoma Norman*; Tetsu K. Tokunaga, Jiamin Wan—*LBNL*; Jizhong Zhou, *LBNL and U. of Oklahoma Norman*; Eoin L. Brodie, *LBNL*; Mary K. Firestone, *U. of California Berkeley and LBNL* (PI, mkfstone@berkeley.edu)

Combined Effects of Hydrology, Geochemistry, and Biology on the Remediation of U(VI) in Microfluidic Experimental Systems (Micro Models) 16

Kevin T. Finneran (PI), Timothy Strathmann (co-PI), Charles Werth (co-PI)—*Clemson U.*

Long-Term Colloid Mobilization and Colloid-Facilitated Transport of Radionuclides in a Semi-Arid Vadose Zone.....17

Markus Flury (PI), Jim Harsh—*Washington State U.*; Fred Zhang, Glendon Gee—*PNNL*; Peter Lichtner, *LANL*; Earl Mattson, *INL*

Ecophysiology and Extracellular Electron Transfer by the Metal-Reducing Bacterium *Geobacter daltonii* FRC32^T 18

Y. Gorby (PI), *U. of Southern California*; M. Fields, *Montana State U.*

A Universal Framework for Predicting Deposition and Transport Behavior of Microorganisms in Subsurface Environment.....19

YueYun Li, Xin Wang, JiaYi Shi, Sinan Muftu, KaiTak Wan, April Z. Gu (PI, april@coe.neu.edu)—*Northeastern U.*

Assessing the Role of Iron Sulfides in the Long-Term Sequestration of Uranium by Sulfate-Reducing Bacteria (SRB) 20

Kim F. Hayes (PI, ford@umich.edu), Sung Pil Hyun, Yuqiang Bi, Julian Carpenter—*U. of Michigan*; Bruce E. Rittmann (co-PI, rittmann@asu.edu), Raveender Vannela, Chen Zhou—*Arizona State U.*; James A. Davis (co-I, jadavis@lbl.gov), *LBNL*; John Bargar, *SSRL*; Ravi K. Kukkadapu, *PNNL*

Biotic Controls on Uranium Sequestration and Release by Framboidal Pyrite in Bioreduced Sediments 21

Michael F. Hochella Jr. (PI), *Virginia Tech*; Nikolla P. Qafoku, *PNNL*; Amy Pruden, Harish Veeramani, Maria V. Riquelme Breazeal, Gargi Singh—*Virginia Tech*; Brandy Gartman, *PNNL*
Collaborators: Ravi Kukkadapu, *EMSL-PNNL*; Philip E. Long, *LBNL*

Assessment of the Bioavailability and Methylation Potential of Mercury Sulfides with Sediment Slurry Experiments 22

T. Zhang, K.H. Kucharzyk, H. Hsu-Kim (PI), M.A. Deshusses (co-PI)—*Duke U.*

Effects of Pore-Scale Physics on Uranium Geochemistry in Hanford Sediments 23

Qinhong Hu (lead PI; maxhu@uta.edu), *U. of Texas*; Robert P. Ewing (co-PI; ewing@iastate.edu), *Iowa State U.*

Fate of Uranium During Transport Across the Groundwater–Surface Water Interface 24

P.R. Jaffe (PI), P. Koster van Groos—*Princeton U.*; D.I. Kaplan, D. Li—*SRNL*; A.D. Peacock, *Microbial Insights*; K. Scheckel, *EPA*; H.S. Chang, *U. of Georgia*

Impact of Biostimulation on Permeability and C-13 Stable Isotope Probing of Biostimulation Experiments to Identify Acetate Utilizers 25

P. Jaffe (PI), *Princeton U.*; H. Tan, L. Kerkhof, L. McGuinness, A. Peacock, *Microbial Insights*; K. Williams, P. Long—*LBNL*

Integrated Geophysical Measurements for Bioremediation Monitoring: Combining NMR, Magnetic Methods and SIP 26

K. Keating (PI), D. Ntarlagiannis, L. Slater—*Rutgers-Newark U.*; K. Williams—*LBNL*

Translation of Geophysical Log Responses to Estimate Subsurface Hydrogeologic Properties at the Hanford 300 Area 27

T.C. Kenna (PI), M.M. Herron—*Lamont-Doherty Earth Observatory*; A. Ward, *PNNL*

Development of Surface Complexation Models of Cr(VI) Adsorption on Soils, Sediments, and Model Mixtures of Kaolinite, Montmorillonite, γ-Alumina, Hydrous Manganese and Ferric Oxides, and Goethite 28

C.M. Koretsky (PI, Carla.koretsky@wmich.edu), T.J. Reich, A. MacLeod, A. Gilchrist, D. Wyman—*Western Michigan U.*

Chromate Reduction in Heterogeneous Porous Media 29

Li Wang, Li Li (PI)—*Penn State*

Monitoring Microbial Uranium Reduction at the Oxic-Anoxic Interface 30

R. Sanford, A. Basu, C. Lundstrom, T. Johnson—*U. of Illinois Urbana-Champaign*; J. Merryfield, G. Walshe—*U. of Tennessee*; K. Kemner, M. Boyanov—*ANL*; K. Pennell, *Tufts U.*; K. Ritalahti, F. Löffler (PI)—*U. of Tennessee and ORNL*

Multi-Scale Modeling Framework for Optimizing Uranium Bioremediation 31

Jiao Zhao, Kai Zhuang, Eugene Ma—*U. of Toronto*; Melissa Barlett, *U. of Massachusetts*; G. Tartakovsky, A. Tartakovsky, Yilin Fang—*PNNL*; Radhakrishnan Mahadevan, *U. of Toronto*; Timothy Scheibe, *PNNL*; Derek Lovley (PI, dlovley@microbio.umass.edu), *U. of Massachusetts*

Molecular Mechanisms Underlying the Metallic-Like Conductivity of *Geobacter* Pili 32

Madeline Vargas, *U. of Massachusetts and College of the Holy Cross*; Nikhil S. Malvankar, Pier-Luc Tremblay, Kelly Flanagan, Pranav Patel, Manju L. Sharma, Derek R. Lovley (PI; dlovley@microbio.umass.edu)—*U. of Massachusetts*

Influence of Protozoa on Anaerobic Groundwater Bioremediation 33

Ludovic Giloteaux, Dawn E. Holmes—*U. of Massachusetts*; Jeffrey D. Silberman, *U. of Arkansas*; Kenneth H. Williams, *LBNL*; Kelly C. Wrighton, *U. of California Berkeley*; Michael J. Wilkins, *PNNL*; Derek R. Lovley (PI; dlovley@microbio.umass.edu), *U. of Massachusetts*

Electrode-Based Approaches for Monitoring Microbial Activity and Carbon Cycling in Soils and Sediments 34

Kelly P. Nevin, Roberto Orellana—*U. of Massachusetts*; Kenneth H. Williams, *LBNL*; Derek R. Lovley (PI; dlovley@microbio.umass.edu), *U. of Massachusetts*

Catalytic DNA Biosensors for Radionuclides and Metal Ions 35

Yi Lu (PI), Yu Xiang, Hannah E. Ihms—*U. of Illinois Urbana-Champaign*

Development of U Isotope Fractionation as an Indicator of U(VI) Reduction in U Plumes 36

A.E. Shiel, P. Laubach, C.C. Lundstrom (PI), T.M. Johnson (co-PI), R.A. Sanford—*U. of Illinois Urbana-Champaign*; K.H. Williams, P.E. Long—*LBNL*

Linking As, Se, V, and Mn Behavior to Natural and Biostimulated Uranium Cycling 37

Brian J. Mailloux (PI), *Barnard College*; Alison Spodek Keimowitz, *Vassar College*; James F. Ranville, Valerie Stucker, Linda Figueroa—*Colorado School of Mines*; Kenneth H. Williams, *LBNL*

Colloids, Deposits, and Clogging in Groundwater Remediation 38

David C. Mays (PI), Eric J. Roth, Tim C. Lei—*U. of Colorado Denver*; Jonathan Ajo-Franklin, Benjamin Gilbert—*LBNL*

Radiochemically-Supported Microbial Communities: A Potential Mechanism for Biocolloid Production of Importance to Actinide Transport 39

D.P. Moser (PI), J.C. Fisher, J.C. Bruckner, C. Russell—*Desert Research Institute*; T.C. Onstott, *Princeton U.*; K. Czerwinski, *U. of Nevada Las Vegas*; B. Sherwood Lollar, *U. of Toronto*; M. Zavarin, M. Conrad—*LBNL*; L.M. Pratt, S. Young—*Indiana U.*

Electrical Responses of Grain Surfaces Measured by Spectral Induced Polarization and Atomic Force Microscopy 40

N. Hao, R. Chen, D. Dean, S. Moysey (PI)—*Clemson U.*; D. Ntarlagiannis, K. Keating—*Rutgers-Newark U.*

Role of Sulfhydryl Sites on Bacterial Cell Walls in the Biosorption, Mobility, and Bioavailability of Mercury 41

S.C.B. Myneni (PI), *Princeton U.*; J. Fein, *U. of Notre Dame*, B. Mishra, *ANL*

Mercury Release from Organic Matter (OM) and OM-Coated Mineral Surfaces 42

K.L. Nagy (PI), K. Kearney, K. Stallings—*U. of Illinois Chicago*; J.N. Ryan, B.A. Poulin—*U. of Colorado Boulder*, G.R. Aiken, *USGS*; A. Manceau, *CNRS and U. Joseph Fourier*

Molecular Mechanisms and Kinetics of Microbial Anaerobic Nitrate-Dependent U(IV) and Fe(II) Oxidation 43

Peggy A. O'Day (PI), Maria Pilar Asta, Samuel Traina—*U. of California Merced*; Peng Zhou, Carl Steefel, Harry R. Beller—*LBNL*

Effects of Pore Structure Change and Multiscale Heterogeneity on Contaminant Transport and Reaction Rate Upscaling 44

C.A. Peters (PI), M.A. Celia—*Princeton U.*; W.B. Lindquist, *SUNY Stony Brook*; K.W. Jones, *BNL*; W. Um, M. Rockhold—*PNNL*

Design and Application of Proteomics Workflows to Monitor and Predict *In Situ* Activity of Metal-Reducing Bacteria 45

K. Chourey, X. Liu, S. Nissen—*ORNL*; F.E. Löffler, *U. of Tennessee*; M. Shah, R.L. Hettich—*ORNL*; K. Ritalahti, T. Vishnivetskaya, A. Layton, G. Sayler, S.M. Pfiffner (PI)—*U. of Tennessee*

Development of a Self-Consistent Model of Plutonium Sorption: Quantification of Sorption Enthalpy and Ligand-Promoted Dissolution 46

B.A. Powell (PI), Y. Arai (co-PI), H. Emerson, S. Estes, S. Herr, A. Hixon, T. Miller, Y. Xie—*Clemson U.*; U. Becker (co-PI), R.C. Ewing (co-PI), S. Fernando, J. Zhang—*U. of Michigan*; D.I. Kaplan (co-PI), *SRNL*

Scale-Dependent Fracture-Matrix Interactions and Their Impact on Radionuclide Transport 47

Harihar Rajaram (PI, hari@colorado.edu), *U. of Colorado*; Russell Detwiler (PI, detwiler@uci.edu), *U. of California Irvine*

From Nanowires to Biofilms: An Exploration of Novel Mechanisms of Uranium Transformation Mediated by *Geobacter* Bacteria 48

Dena L. Cologgi, Sanela Lampa-Pastirk, Allison M. Speers—*Michigan State U.*; Shelly Kelly, *EXAFS Analysis*; Gemma Reguera (PI, reguera@msu.edu), *Michigan State U.*

Geoelectrical Surveys at the Oak Ridge Field Research Center 49

A. Revil (PI), *Colorado School of Mines*; S. Hubbard, *LBNL*; M. Karaoulis, M. Skold—*Colorado School of Mines*; N. Spycher, *LBNL*; D. Watson, *ORNL*; Y. Wu, *LBNL*

Microbial Communities Associated with Anaerobic Metabolism and U(VI) Reduction in ORFRC Area 2 Sediment Amended with Acetate or Ethanol 50

E. Roden (PI), B. Converse, T. Wu, E. Shelobolina—*U. of Wisconsin*; R. Findlay, *U. of Alabama*; Q. Jin, *U. of Oregon*

Processes Affecting Iodine-127,129 Speciation and Mobility in Two Contaminated DOE Plumes 51

Peter H. Santschi (PI, Santschi@tamug.edu), R. Brinkmeyer, K.A. Schwehr, S. Zhang, C. Xu, H-P. Li—*TAMUG*; D. Kaplan, K.A. Roberts—*SRNL*; C. Yeager, *LANL*

The Role of Natural Organic Matter in Immobilizing or Re-mobilizing Plutonium in the Far Field of the Savannah River Site, USA 52

Peter H. Santschi (PI, Santschi@tamug.edu), Kathleen A. Schwehr, Chen Xu—*TAMUG*; Patrick G. Hatcher, Nicole DiDonato—*Old Dominion U.*

Uranium Attenuation and Release Investigated at the Molecular and Column Scales: Responses to Geochemical Gradients in Geologic Media 53

K. Savage (PI), Wenyi Zhu—*Wofford College*; M.O. Barnett, *Auburn U.*

Hg(II) Uptake and Methylation in Iron-Reducing Bacteria 54

J.K. Schaefer (PI, jschaefe@princeton.edu), O. Baars, R. Anwar—*Princeton U.*; L. Liang, B. Gu—*ORNL*; F.M.M. Morel, *Princeton U.*

Electron Transfer and Atom Exchange between Aqueous Fe(II) and Structural Fe(III) in Clays: Role in U and Hg(II) Transformations 55

A. Neumann, M.M. Scherer (PI), M. Barger—*U. of Iowa*; C. Johnson, B. Beard, L. Wu—*U. of Wisconsin Madison*; K.M. Rosso, V. Alexandrov—*PNNL*; K. Kemner, M. Boyanov, E. O'Loughlin—*ANL*

Coupled Biological and Micro-XAS/XRF Analysis of *In Situ* Uranium Biogeochemical Processes 56

J.O. Sharp (PI), D. Drennan, S. Hollenback, D. Silverman—*Colorado School of Mines*; S.M. Webb, J.R. Bargar—*SSRL*

Molecular Mechanisms of the *mer* Operon and Hg(II)-Ligand Interactions: Combined Experimental and Computational Studies 57

J.C. Smith (PI), H. Guo—*U. of Tennessee*; A. Johs, L. Liang—*ORNL*; S. Miller, *U. of California San Francisco*; J.M. Parks, *ORNL*; D. Riccardi, *U. of Tennessee*; A.O. Summers, *U. of Georgia*; S.J. Tomanicek, *ORNL*; Q. Xu, *U. of Tennessee*

Field Investigations of Microbially Facilitated Calcite Precipitation for Immobilization of Strontium-90 and Other Trace Metals in the Subsurface 58

R.W. Smith (PI), *U. of Idaho*; Y. Fujita, *INL*; T.R. Ginn, *U. of California Davis*; S.S. Hubbard, B. Dafflon—*LBNL*; M. Delwiche, *INL*; T. Gebrehiwet, *U. of Idaho*; J.R. Henriksen, *INL*; J. Peterson, *LBNL*; J.L. Taylor, *U. of Idaho*

Uranium Biomineralization by Natural Microbial Phosphatase Activities in the Subsurface 59

Patricia A. Sobecky (PI, psobecky@ua.edu), *U. of Alabama*; Martial Taillefert (co-PI, martial.taillefert@eas.gatech.edu), *Georgia Institute of Tech.*; Robert J. Martinez, Melanie J. Beazley—*U. of Alabama*; Cindy Wu, *LBNL*; Terry C. Hazen, *U. of Tennessee*; Gary L. Andersen, *LBNL*; Karen Kinsella, David J. Schlyer, Joanna S. Fowler—*BNL*

The Molecular-Cellular-Field Continuum of Mercury Detoxification 60

A.O. Summers (PI), *U. of Georgia Atlanta*; S.M. Miller, *U. of California San Francisco*; C. Momany, *U. of Georgia Atlanta*; I. Artsimovitch, *Ohio State U.*; J. Blum, *U. of Michigan*; L. Liang, *ORNL*; J. Smith, *U. of Tennessee and ORNL*; T. Barkay, *Rutgers U.*; H. Guo, *U. of Tennessee*; B. Gu, *ORNL*; R.A. Scott, *U. of Georgia Atlanta*; J.D. Gross, R. Stroud—*U. of California San Francisco*

Identifying Mechanisms of Toxic Metal Stress with Global Proteomics 61

A.O. Summers (PI), S. LaVoie, L. Olliff, M.K. Johnson, R.A. Scott—*U. of Georgia Atlanta*; S.M. Miller, B. Polacco—*U. of California San Francisco*; M.S. Lipton, S.O. Purvine, E.M. Zink—*EMSL-PNNL*

Manganese Redox Mediation of UO_2 Stability and U Fate in the Subsurface: Molecular and Meter-Scale Dynamics 62

B.M. Tebo (PI, tebo@ebs.ogi.edu), S.-W. Lee—*OHSU*; Z. Wang, D.E. Giammar—*Washington U. St. Louis*; K.L. Plathe, R. Bernier-Latmani—*ÉPFL*; J.S. Lezama Pacheco, J.R. Bargar—*SLAC*; K.H. Williams, P.E. Long—*LBNL*

Firmicutes and Their Roles in Uranium Immobilization 63

F. Yang, J. Tiedje (PI, tiedjej@msu.edu), J. Zhou (jzhou@ou.edu), T.L. Marsh (marsht@msu.edu)—*Michigan State U. and U. of Oklahoma*

Differential Proteomics Analysis of GASP (Growth Advantage in Stationary-Phase) Phenotype of *Geobacter sulfurreducens* under "Famine" Conditions 64

Reema Bansal Agarwal (rzb12@psu.edu), Ruth A. Helmus, Susan Brantley, Ming Tien (PI)—*Penn State*

Technetium Reduction and Permanent Sequestration by Abiotic and Biotic Formation of Low-Solubility Sulfide Mineral Phases 65

P. Tratnyek (PI), B. Tebo, R. Anitori, D. Fan—*OHSU*; J. Szecsody, J. McKinley, D. Jansik—*PNNL*

Microbiological-Enhanced Mixing Across Scales During *In Situ* Bioreduction of Metals and Radionuclides at Department of Energy Sites 66

A.J. Valocchi (PI), C.J. Werth, W-T. Liu, R. Sanford—*U. of Illinois Urbana-Champaign;* K. Nakshatrala, *U. of Houston;* M. Oostrom, C. Zhang—*PNNL*

Development of New and Integrated Stable Isotope Tools for Understanding Nitrogen-Uranium Interactions in Subsurface Environments 67

Scott D. Wankel, Yuanzhi Tang, Colleen M. Hansel, David T. Johnston (PI)—*Harvard U.*

Viral Infection of Subsurface Microorganisms and Metal/Radionuclide Transport 68

Karrie A. Weber (PI), Don Pan, Zheng Huan Tan—*U. of Nebraska*; Kelly S. Bender, *S. Illinois U.*; Yusong Li, *U. of Nebraska*

Investigation on U(VI) Sorption / Desorption on Nanopores Goethite, and Structures of Ferrihydrite Nano-Mineral 69

Huifang Xu (PI/co-PI, hfxu@geology.wisc.edu), Eric E. Roden (PI/co-PI, eroden@geology.wisc.edu)—*U. of Wisconsin Madison*; Kenneth M. Kemner (PI/co-PI, Kemner@anl.gov), *ANL*; Hiromi Konishi, Hun-Bok Jung—*U. of Wisconsin Madison*

Emulsified Vegetable Oil Stimulates Sulfate-Reducing Communities for U(VI) Reduction at a Contaminated Aquifer Via Pyrosequencing of Dissimilatory Sulfite Reductase Genes 70

Ping Zhang, Yujia Qin, Joy D. Van Nostrand, Liyou Wu, Zhili He (PI/co-PI, zhili.he@ou.edu), Ye Deng—*U. of Oklahoma*; Terence L. Marsh (PI/co-PI, marsht@msu.edu), James M. Tiedje (PI/co-PI, tiedjej@msu.edu)—*Michigan State U.*; Jizhong Zhou (PI/co-PI, jzhou@ou.edu), *U. of Oklahoma*

Federal Agency-Led Research 71

Multiscale Assessment of Prediction Uncertainty in Coupled Reactive Transport Models 71

G. Curtis (PI), *USGS*; M. Ye, *Florida State U.*; P. Meyer, S. Yabusaki—*PNNL*; D. Rodriguez, *Colorado School of Mines*

Upscaling of U(VI) Desorption and Transport from Decimeter-Scale Heterogeneity to Plume-Scale Modeling 72

G. Curtis (PI), J.W. Lane Jr., M. Kohler—*USGS*; J. Davis, *LBNL*; D. Rodriguez, *Colorado School of Mines*; F.D. Day-Lewis, M. Hay, A.K. Gallagher, J.B. Ong—*USGS*

Geoelectrical Measurement of Multi-Scale Mass Transfer Parameters 73

Frederick D. Day-Lewis (PI), *USGS*; Kamini Singha, *Penn State*; Andrew Binley, *Lancaster U.*; Roy Haggerty, *Oregon State U.*; John W. Lane Jr., *USGS*; Jeremy Clifford, *Lancaster U.*; Ryan D. Swanson, *Penn State*; Timothy C. Johnson, *PNNL*; Kristina Keating, *Rutgers U.*

Advanced Simulation Capability for Environmental Management (ASCEM): Development and Demonstrations 74

Mark D. Freshley (PI), *PNNL*; J. David Moulton, *LANL*; Ian Gorton, *PNNL*; Susan S. Hubbard, *LBNL*; Vicky L. Freedman, *PNNL*; Gregory Flach, *SRNL*; Carl I. Steefel, Stefan A. Finsterle—*LBNL*; Paul Dixon, *LANL*; the ASCEM Team

Effects of Textural-Scale Heterogeneity on the Release of Uranium from Contaminated Sediments 75

Melanie A. Mayes (PI), Vijay A. Loganathan, Guoping Tang—*ORNL*; John M. Zachara, *PNNL*

Integrated Field-Scale Subsurface Research Challenges (IFRC) 77

Reducing the Hydrologic and Geochemical Uncertainty for Modeling Uranium Migration at the Hanford 300 Area by Assimilating Multi-Scale and Multi-Type Data 77

X. Chen (PI, Xingyuan.chen@pnnl.gov), G. Hammond, C. Murray, J. Zachara—*PNNL*

Impact of Soil Grain Size on Modeling Uranium Surface Complexation at the Hanford 300 Area IFRC Site 78

G. Hammond (PI, glenn.hammond@pnnl.gov), X. Chen, J. Zachara—*PNNL*

Investigating Field-Scale Properties and Processes that Influence Uranium Behavior at the Hanford 300 Area IFRC Using Advancements in Electrical Geophysical Imaging 79

T. Johnson (PI), W. Greenwood, M. Rockhold, E. Wallin, J. Zachara—*PNNL*; R. Versteeg, *Sky Research*; L. Slater, *Rutgers U.*

Geochemical Model, Model Uncertainty, and Pore-Scale Insights for Uranyl Reactive Transport in Hanford 300A Smear Zone Sediments 80

Chongxuan Liu (PI, Chongxuan.liu@pnnl.gov), John Zachara, Jianying Shang, Changyong Zhang, Zhi Shi, Paul Majors—*PNNL*; Deborah Stoliker, Douglas Kent—*USGS*; Xiaoying Zhang, Bill Hu—*Florida State U.*

The Effects of Columbia River Stage on Contaminant U Concentrations and Groundwater Compositions at the 300 Area IFRC 81

James P. McKinley (PI), Thomas C. Resch, Micah D. Miller, Rachael M. Lund, Vince R. Vermeul, Christopher J. Murray, John M. Zachara—*PNNL*

Reactive Transport Field Experiments at the Hanford IFRC 82

V.R. Vermeul, M.D. Freshley, B.G. Fritz, R.D. Mackley, J.P. McKinley, K.R. Parker, J.M. Zachara (PI)—*PNNL*

Multi-Scale Mass Transfer Processes Controlling Natural Attenuation and Engineered Remediation: An IFRC Focused on Hanford's 300 Area Uranium Plume 83

J.M. Zachara (PI), M.D. Freshley, B.N. Bjornstad—*PNNL*; J.N. Christensen, M.S. Conrad—*LBNL*; J.K. Fredrickson, *PNNL;* R. Haggerty, *Oregon State U.*; G. Hammond, T. Johnson—*PNNL*; D.B. Kent, *USGS*; A. Konopka, *PNNL*; P.C. Lichtner, *LANL*; C. Liu, J.P. McKinley, C. Murray, M.L. Rockhold—*PNNL*; Y. Rubin, *LBNL*; V.R. Vermeul, *PNNL*; R.J. Versteeg, *Sky Research*; C. Zheng, *PNNL*; K.M. Thompson, *DOE-RL*

Data Management Efforts for the Hanford 300 Area and Rifle IFRCs 84

R. Versteeg (PI), *Sky Research, Inc.*; *Hanford IFRC Team (PI: John Zachara)*
Rifle IFRC Team (PI: Philip Long)

Utilizing Azimuthal Seismic First-Arrival Tomography (ASFT), Time-Lapse Electrical-Resistivity Tomography (TLERT), and Other Geophysical Methods for the Detection and Characterization of Physical Controls on Hydrologic Transport 85

G.S. Baker (PI), M. Edmunds—*U. of Tennessee*; S. Hubbard, E. Gasperikova—*LBNL*; D. Watson, T. Mehlhorn, K. Lowe, S. Brooks—*ORNL*

Multiscale Investigations on the Rates and Mechanisms of Targeted Immobilization and Natural Attenuation of Radionuclides and Co-Contaminants in the Subsurface 86

Scott C. Brooks (PI), David B. Watson—*ORNL*; Greg S. Baker, *U. of Tennessee*; Maxim Boyanov, *ANL*; Craig C. Brandt, *ORNL*; Craig S. Criddle, *Stanford U.*; Baohua Gu, *ORNL*; Susan S. Hubbard, *LBNL*; Ken Kemner, *ANL*; Joel E. Kostka, *Florida State U.*; Jack C. Parker, *U. of Tennessee*; Chris W. Schadt, *ORNL*; Wei-Min Wu, *Stanford U.*; Trevor Zimmerman, Fan Zhang—*ORNL*; Joe Zhou, *U. of Oklahoma*

Nitrate Attenuation and the Impact of pH on the Predominant Denitrifying Microbial Groups in the OR-IFRC Subsurface 87

Joel E. Kostka (PI), *Georgia Institute of Tech.*; Stefan J. Green, *U. of Illinois Chicago*; Om Prakash, *Georgia Institute of Tech.*; Puja Jasrotia, *Florida State U.*; Lavanya Rishishwar, *Georgia Institute of Tech.*; Chris Schadt, David Watson, Scott Brooks—*ORNL*

Effect of Spatially and Temporally Variable Recharge on Subsurface Reactive Transport of Contaminants at Oak Ridge Integrated Field Research Site 88

Jitendra Kumar (PI), *ORNL*; Peter C. Lichtner, *LANL*; Richard T. Mills, *ORNL*

Geochemical pH Controls and Dynamics of Metals and Radionuclides in a Highly Contaminated, Acidic Aquifer 89

B. Gu (PI), T. Zimmerman, G. Tang, D. Watson—*ORNL*; W.-M. Wu, *Stanford U.*; K.M. Kemner, *ANL*; C. Schadt, *ORNL*; G.S. Baker, *U. of Tennessee Knoxville*; S. Hubbard, *LBNL*; Puja Jasrotia, J. Kostka—*Georgia Institute of Tech.*; S. Brooks, *ORNL*

New Isolates of *Geobacter*, *Desulforegula*, *Desulfovibrio*, and *Pelosinus* and Their Roles in a Low Diversity Consortia During Sustained *In Situ* Reduction of U(VI) 90

C.W. Schadt (PI), T.M. Gihring, S.L. Carroll, T.L. Mehlhorn, Z.K. Yang, M.K. Kerley, D.A. Elias, D.B. Watson, S.C. Brooks—*ORNL*; C.M. Doktycz—*Michigan State U.*; J.R. Merryfield—*U. of Tennessee*; J.E. Kostka, *Georgia Institute of Tech.*

Modeling Hydrobiogeochemical Dynamics in a Field Emulsified Vegetable Oil (EVO) Injection Test at the Oak Ridge IFRC 91

Guoping Tang (PI, tangg@ornl.gov), Scott C. Brooks, David B. Watson, Chris W. Schadt—*ORNL*; Jack C. Parker—*U. of Tennessee*; Wei-Min Wu, *Stanford U.*

Diffusion/Deposition/Remobilization of Uranium in Bioreduced Zones 92

D. Watson (PI), G. Tang, J. Earles, S. Brooks—*ORNL*

Impact of "Flow Tubes" within Structured Media on Groundwater Transport and Surface/Groundwater Interactions 93

D. Watson (PI), T. Mehlhorn, K. Lowe, C. Schadt, J. Howe, J. Earles, S. Brooks—*ORNL*; S. Hubbard, C. Ulrich, J. Peterson—*LBNL*; G. Baker, R. Storniolo—*U. of Tennessee*; D. Phillips, *Queens U.*; J. Kostka, *Georgia Institute of Tech.*

Application of GGKbase to Analyze "Omic" Data from Acetate-Stimulated Subsurface Microbial Communities 94

Brian C. Thomas, Kelly C. Wrighton, Ken-ichi Ueda, Andrea Singh, Jill Banfield (PI)—*U. of California Berkeley*

Sensitivity of Predictions of Uranium Plume Persistence at the Rifle IFRC Site to Reactive Transport Geochemical Parameters and Initial Conditions 95

James A. Davis (PI, jadavis@lbl.gov), *LBNL*; Janek Greskowiak, *U. of Oldenburg, Germany*; Michael B. Hay, *USGS*; Patricia M. Fox, Kenneth H. Williams, Philip E. Long—*LBNL*

Coupled Abiotic Fe, S, and U Redox Reactions in Rifle IFRC sediments 96

Patricia M. Fox (PI, pmfox@lbl.gov), James A. Davis—*LBNL*; Ravi Kukkadapu, *PNNL*; Sung Pil Hyun, *U. of Michigan*; David M. Singer, Hua Guo—*LBNL*; John R. Bargar, *SSRL*; Kim F. Hayes, *LBNL*

Manipulating Uranium Desorption and Redox Status in an Alluvial Aquifer: Overview of *In Situ* Electron Donor and Bicarbonate Amendment Experiments at the Rifle, Colorado IFRC 97

P. Long (PI), K. Williams—*LBNL*; J. Banfield, K. Wrighton, K. Handley—*U. of California Berkeley*; J. Bargar, *SSRL*; D. Lovley, *U. of Massachusetts*; M. Lipton, Mike Wilkins, S. Yabusaki, C. Murray—*PNNL*; R. Hettich, N. VerBerkmoes—*ORNL*; J. Davis, P. Fox, B. Luef, L. Comolli, S. Fakra—*LBNL*; P. Jaffe—*Princeton*; the Rifle IFRC Science Team

Floodplain-Scale Hydrological, Isotopic, Geochemical, and Geophysical States and Fluxes at DOE's Rifle Integrated Field Research Challenge Site 98

Kenneth H. Williams (khwilliams@lbl.gov), Mark Conrad—*LBNL*; Manish Gupta, Elena Berman—*Los Gatos Research, Inc.*; Jennifer Druhan, Craig Ulrich, Baptiste Dafflon, John Peterson, Susan Hubbard, Philip E. Long (PI)—*LBNL*

Geostatistical Modeling of Physical and Geochemical Properties for Reactive Transport Modeling, Rifle IFRC 99

C. Murray (PI, Chris.Murray@pnnl.gov), N. Qafoku, B. Gartman, Y. Bott, K. Draper, J. Greenwood, D. Newcomer, S. Yabusaki—*PNNL*

Molecular-Scale Characterization of Natural Organic Matter From A Uranium Contaminated Aquifer and its Utilization by Native Microbial Communities 100

Paula J. Mouser (PI), *Ohio State U.*; Michael J. Wilkins, *PNNL*; Kenneth H. Williams, *LBNL*; Donald Smith, Ljiljana Paša-Tolić—*EMSL and PNNL*; Philip E. Long, *LBNL*

Genome-Centered Analysis of Biogeochemical Cycling 101

K.C. Wrighton (PI), B.C. Thomas, I. Sharon, C.J. Castille—*U. of California Berkeley*; M.J. Wilkins, *PNNL*; N.C. VerBerkmoes, *ORNL*; C.S. Miller, *U. of California Berkeley*; R.L. Hettich, *ORNL*; M.S. Lipton, *PNNL*; K.H. Williams, P.E. Long—*LBNL*; J.F. Banfield, *U. of California Berkeley*

Integrating *In Silico* Modeling and Proteomics into Field-Scale Simulations of Uranium Biogeochemical Reactive Transport 102

Steve Yabusaki (PI), Yilin Fang, Mike Wilkins—*PNNL*; Radhakrishnan Mahadevan, *U. of Toronto*; Tim Scheibe, *PNNL*; Derek Lovley, *U. of Massachusetts*; Phil Long, *LBNL*; and the Rifle IFRC Science Team

Scientific Focus Areas (SFA) 103

Temporal Monitoring of Microbial Community Dynamics Under Iron- and Sulfate-Reducing Conditions via "Now-Generation" DNA Sequencing-Enabled Molecular Environmental Microbiology 103

D. Antonopoulos (PI, dion@anl.gov), M. Boyanov, J. Brulc, E. Johnston, M.J. Kwon—*ANL*; P. Long—*LBNL*; T. Marsh, *Michigan State U.*; M. McCormick, *Hamilton College*; F. Meyer, K. Skinner—*ANL*; K. Williams, *LBNL*, D. Sholto-Douglas, E. O'Loughlin, K. Kemner—*ANL*

Understanding Uranium Transformations in Reduced Sediments: An Integrated Bottom-Up and Top-Down X-Ray Spectroscopy Approach 104

M. Boyanov (PI, mboyanov@anl.gov), E. O'Loughlin, D. Latta, B. Mishra, K. Skinner—*ANL*; M. Scherer—*U. of Iowa*; W.-M. Wu, C. Criddle—*Stanford U.*; F. Yang, T. Marsh—*Michigan State U.*; R. Sanford—*U. of Illinois Urbana-Champaign*; F. Löffler—*U. of Tennessee and ORNL*; M. Mueller, T. Mehlhorn, K. Lowe, D. Watson, S. Brooks—*ORNL*; K. Kemner—*ANL*

The Argonne Subsurface Biogeochemical Research Program Scientific Focus Area.....105

K. Kemner (PI, kemner@anl.gov), E. O'Loughlin, M. Boyanov, D. Antonopoulos, D. Latta, T. Flynn—*ANL*; S. Brooks, *ORNL*; E. Carpenter, *Virginia Commonwealth U.*; C. Criddle, *Stanford U.*; J. Fredrickson, *PNNL*; F. Löffler, *U. of Tennessee*; T. Marsh, *Michigan State U.*; M. McCormick, *Hamilton College*; B. Mishra, *Illinois Institute of Tech.*; R. Sanford, *U. of Illinois Urbana-Champaign*; C. Segre, *Illinois Institute of Tech.*; M. Scherer, *U. of Iowa*; W. Wu, *Stanford U.*; J. Zachara, *PNNL*; C. Giometti, *ANL*

Ligand and Surface Effects on the Reduction of Hg^{II} by Fe^{II} 106

Bhoopesh Mishra (PI, bmishra3@iit.edu; bmishra@anl.gov), *Illinois Institute of Tech. and ANL*; Timothy Pasakarnis, *U. of Iowa*; Maxim I. Boyanov, Edward J. O'Loughlin—*ANL*; Michelle M. Scherer, *U. of Iowa*; Kenneth M. Kemner, *ANL*

Effects of Fe^{III} Oxide Mineralogy and Electron Donor on the Biogeochemical Dynamics of Fe, S, and C under Sulfate- and Iron-Reducing Conditions 107

E. O'Loughlin (PI), M.J. Kwon, D. Antonopoulos, M. Boyanov, J. Brulc, T. Flynn, E. Johnston, K. Skinner—*ANL*; P. Long, K. Williams—*LBNL*; M. McCormick, *Hamilton College*; K. Kemner, *ANL*

Experimental Studies and Modeling of Mineral Precipitation in Mixing Zones Controlled by Parallel Flow and Double Diffusion.....108

D. Fox, *INL*; T. Gebrehiwet, *U. of Idaho*; L. Guo, J.R. Henriksen, H. Huang, C. Lu, Y. Fujita—*INL*; A. Tartakovsky, *PNNL*; G. Redden (PI, George.redden@inl.gov), *INL*

Understanding and Controlling Precipitation Reaction Fronts in Subsurface Environments: The Idaho National Laboratory SBR Scientific Focus Area.....109

G. Redden (PI, George.redden@inl.gov), H. Huang, Y. Fujita, D. Fox, L. Guo, J.R. Henriksen, M. McIlwain—*INL*; T. Gebrehiwet, *U. of Idaho*, T. Johnson, *PNNL*; A. Revil, *Colorado School of Mines*; L. Slater, *Rutgers-Newark U.*; R. Smith, *U. of Idaho*, A. Tartakovsky, *PNNL*; C. Zhang, *Rutgers-Newark U.*

Mineral Precipitation Fronts in Porous Media: Modeling Using A Fully Coupled Fully-Implicit Simulator and Monitoring Using Spectral Induced Polarization (SIP) 110

Chi Zhang (chi.zhang@inl.gov), *Rutgers U. Newark and INL*; Luanjing Guo, George Redden (PI), Hai Huang, Don Fox, Yoshiko Fujita—*INL*; Lee Slater, *Rutgers U. Newark*; Timothy Johnson, *PNNL*

Use of Metagenomic and Meta-Transcriptomic Analysis to Interpret Biogeochemical Processes Mediated by Hanford 100H Aquifer Bacteria (Lab and Field Studies).....111

H.R. Beller (PI), R. Han, U. Karaoz, H.C. Lim, L. Yang, B. Faybishenko, E.L. Brodie—*LBNL*

Field-Scale Estimation and Simulation of Biogeochemical Heterogeneity 112

J. Chen (PI), *LBNL*; H. Wu, L. Li—*Penn State*; K.H. Williams, M.B. Kowalsky, Carl Steefel, S.S. Hubbard—*LBNL*

Highly Depleted Gypsum Veins at the Rifle Site Attributed to Multiple Episodes of Redox Cycling.....113

Mark E. Conrad (PI), Kenneth H. Williams, Jennifer L. Druhan, Wayne W. Lukens—*LBNL*

Integrating Geochemical, Reactive Transport, and Facies-Based Modeling Approaches to Assess U(VI) Contamination at the Savannah River F-Area.....114

S.A. Bea, N. Spycher, H. Wainwright, S. Mukhopadyay, S.S. Hubbard, Carl Steefel, J. Davis (PI)—*LBNL*

Isotopic Signature of Calcium and Sulfur Partitioning during Biostimulation: Experiments and Simulations.....115

Jennifer L. Druhan (PI), Carl I. Steefel, Kenneth H. Williams, Mark E. Conrad, Donald J. DePaolo—*LBNL*

LBNL Sustainable Systems Scientific Focus Area 116

S.S. Hubbard (PI), H. Beller, J. Davis, C. Steefel, K.H. Williams, J. Ajo-Franklin, E. Brodie, R. Chakraborty, J. Chen, J. Christensen, M. Conrad, D. DePaolo,W. Dong, B. Faybishenko, M. Kowalsky, B. Moses, P. Nico, D. Silin, N. Spycher, E. Sonnenthal, T. Tokunaga, J. Wan, L. Yang, Y. Wu—*LBNL*; M. Denham, *SRNL*, J. Hunt, *U. of California Berkeley*, J. Istok, *Oklahoma State U.*, Y. Fujita, *INL*, L. Li, *Penn State*

Reactive Facies: An Approach for Parameterizing Plume-Scale Reactive Transport Models Using Multi-Type Multi-Scale Datasets 117

H.M. Wainwright, D.S. Sassen, S.A. Bea, J. Chen, S.S. Hubbard (PI)—*LBNL*

Pore-Scale Modeling of Permeability Evolution due to Reactive Processes 118

S. Molins (PI), D.B. Silin—*LBNL*

Competing Evidence for Enzymatic Versus Abiotic Reduction of Cr(VI) in Hanford 100H Flow-Through Columns 119

Charuleka Varadharajan, Ruyang Han, Sergi Molins, Mark Conrad, John Christensen, Markus Bill, Carl Steefel, Joern Larsen, Li Yang, Eoin L. Brodie, Harry R. Beller, Peter S. Nico (PI)—*LBNL*

Reactive Transport Modeling of Hanford 100H Lab- and Field-Scale Experiments 120

E.L. Sonnenthal (PI), S. Molins, C. Wanner, C.I. Steefel, H.R. Beller—*LBNL*

Determining the Plume Source Discharge, Trailing Edge, and Natural Attenuation Timeframe: The F-Area Savannah River Site 121

T.K. Tokunaga (PI), J. Wan, W. Dong, J.N. Christensen, M.S. Conrad, M. Bill—*LBNL*; M. Denham, *SRNL*; S.S. Hubbard, *LBNL*

U(VI) Mobility in Acidic Waste Plumes: Laboratory Experiments and Surface Complexation Modeling using F-Area Savannah River Site Sediments 122

Wenming Dong, Jiamin Wan (PI), Tetsu K. Tokunaga, Hua Guo, Patricia M. Fox, James A. Davis—*LBNL*

Actinide NMR Research at Lawrence Livermore National Laboratory 123

H. Mason, S. Harley, P. Huang, S. Carroll (PI), R. Maxwell, M. Zavarin, A. Kersting—*LLNL*

Environmental Transport of Plutonium: Biogeochemical Processes at Femtomolar Concentrations and Nanometer Scales 124

A.B. Kersting (PI), M. Zavarin, J. Begg, P. Zhao, P. Huang, Z. Dai, R. Tinnacher, R. Kips, H. Mason, S.A. Carroll, R. Maxwell, R. Williams, S. Tumey—*LLNL*; B.A. Powell, J. Wong—*Clemson U.*

Influence of Natural Organic Matter on the Subsurface Fate and Transport of Plutonium 125

B.A. Powell (PI), N. Conroy, L. Simpkins, J. Wong, T. Zimmerman—*Clemson U.*; A.B. Kersting, M. Zavarin, J. Begg, P. Zhao, R. Tinnacher—*LLNL*

Adsorption and Desorption of Plutonium on Na-Montmorillonite over a Ten Order of Magnitude Range in Concentration 126

J.D. Begg, M. Zavarin (PI), S.J. Tumey, P. Zhao, A.B. Kersting—*LLNL*

Biogeochemical and Molecular Mechanisms Controlling Contaminant Transformation in the Environment 127

Laboratory Research Manager: Liyuan Liang (PI, liangl@ornl.gov), *ORNL*
Research Staff: C. Brandt, S. Brooks, S. Brown, D. Elias, B. Gu, F. He, A. Johs, C. Miller, M. Podar, J. Parks—*ORNL*
Current Collaborators: C. Gilmour, *Smithsonian Environmental Research Ctr.*; S. Miller, *U. of California San Francisco*; J.C. Smith, *U. of Tennessee Knoxville*; A. Summers, *U. of Georgia*; J. Wall, *U. of Missouri Columbia*

Biogeochemical Processes and Hg Cycling in Contaminated Sediments of East Fork Poplar Creek, Oak Ridge, TN (Hg SFA at ORNL) 128

Scott C. Brooks (PI, brookssc@ornl.gov), Carrie Miller, Craig Brandt, David Kocman, Ami Riscassi, Xiangping Yin, Yun Qian—*ORNL*; Rich Landis, Jim Dyer—*DuPont*

Spatial and Seasonal Relationships Between Surface Water Total and Methylmercury, Dissolve Organic Matter and Particulates in East Fork Poplar Creek, Oak Ridge, TN 129

Carrie Miller (millercl@ornl.gov), Scott C. Brooks (PI), David Kocman, Ami Riscassi, Xiangping Yin, Yun Qian—*ORNL*

Mercury Methylation: Microbial Communities Involved in Hg Transformations (ORNL Hg SFA, Microbial Genetics and Transformations) 130

James G. Moberly, Richard A. Hurt, Tatiana A. Vishnivetskaya, Steven D. Brown, Craig C. Brandt, Mircea Podar, Anthony V. Palumbo, Dwayne A. Elias (PI, eliasda@ornl.gov)—*ORNL*

Mercury Methylation: Genetics and Physiology of Methylmercury Production (ORNL Hg SFA, Microbial Genetics and Transformations) 131

Andrew M. Graham, *Smithsonian Environmental Research Center*; Romain Bridou, *U. of Missouri*; Richard A. Hurt, Steven D. Brown, Mircea Podar—*ORNL*; Steven D. Smith, *U. of Missouri*; Anthony V. Palumbo, *ORNL*; Judy D. Wall, *U. of Missouri*; Cynthia C. Gilmour, *Smithsonian Environmental Research Ctr.*; Dwayne A. Elias (PI, eliasda@ornl.gov), *ORNL*

Effects of Molecular Structure and Functional Groups of Organic Ligands on Photochemical Transformation of Mercury and Methylmercury 132

Feng He, Yun Qian, Wang Zheng—*ORNL*; Jason Demers, *U. of Michigan*; Balaji Rao, Xiangping Yin—*ORNL*; Joel Blum, *U. of Michigan*; Liyuan Liang, Baohua Gu (PI)—*ORNL*

Mercury Redox Cycling and Species Transformation Affected by Complex Interactions with Natural Organic and Thiolate Compounds 133

Baohua Gu (PI), Wang Zheng, Haiyan Hu, Feng He, Balaji Rao, Liyuan Liang—*ORNL*

Structural and Computational Analysis of MerR's Unique Allosteric Activation of *mer* Operon Transcription 134

A. Johs, S.J. Tomanicek, H.-B. Guo, L. Liang (PI)—*ORNL*; A.O. Summers, L. Olliff—*U. of Georgia*; M. Sharp, *ESS Sweden*; J.C. Smith, *U. of Tennessee Knoxville and ORNL*

ORNL SFA Task 4: Molecular-Scale Interactions and Transformations of Mercury in the Environment 135

A. Johs, J.M. Parks, H.-B. Guo, S.J. Tomanicek, L. Hong, L. Liang—*ORNL*; M. Sharp—*ESS Sweden*; M. Ohl, *FZ Jülich*; L. Shi, *PNNL*, R. Nauss, S.M. Miller—*U. of California San Francisco*; A.O. Summers, L. Olliff—*U. of Georgia Atlanta*; D. Riccardi, J.C. Smith (PI)—*U. of Tennessee Knoxville and ORNL*

Quantifying the Influences of Ecological Drift, Selection and Dispersal in Subsurface Microbial Communities 136

J.C. Stegen, X. Lin, J.K. Fredrickson, X. Chen, D.W. Kennedy, C.J. Murray, M.L. Rockhold, A.E. Konopka (PI, allan.konopka@pnnl.gov)—*PNNL*

Biogeochemical Investigations Across Oxidation-Reduction Boundaries at the Hanford Site SFA 137

J.P. McKinley (PI), C.T. Resch, M.D. Miller, R.M. Lund, X. Li, A.E. Konopka, C.J. Murray, J.M. Zachara—*PNNL*

Electron Transfer to the Microbe-Mineral Interface at Nanometer Resolution 138

D.J. Richardson (PI), *U. of East Anglia UK*

Relating Differences in Mineral Reaction Rates to Microenvironment Creation and Heterogeneous Pore-Scale Phase Distribution at the Hanford Site 139

K. Rosso (PI), A. Felmy, C. Pearce, J. Liu, O. Qafoku—*PNNL*; S. Heald, D. Latta, M. Boyanov, K. Kemner—*ANL*; E. Arenholz, *LBNL*; E. Buck, L. Shi, J. McKinley, D. Moore, T. Resch, T. Schaef, M. Bowden—*PNNL*

Isolation and Characterization of a Novel Fe(II)-Oxidizing *Alphaproteobacterium* from the Hanford 300 Area Subsurface 140

E. Roden (PI), E. Shelobolina, J. Benzine, E. Percak-Dennett, B. Converse—*U. of Wisconsin*; L. Shi, A. Plymale, S. Reed, J. Fredrickson—*PNNL*

Identification and Characterization of Microbial Proteins Important for Extracellular Electron Transfer Reactions 141

Liang Shi (PI), Juan Liu, Kevin M. Rosso—*PNNL*; Gaye White, *U. of East Anglia UK*; Zhi Shi, Alice C. Dohnalkova, Zheming Wang, David W. Kennedy—*PNNL*; Marcus Edwards, Julea N. Butt, Thomas Clarke—*U. of East Anglia UK*; Kathy Byrne-Bailey, John Coates—*U. of California Berkeley*; David J. Richardson, *U. of East Anglia UK*; John M. Zachara, James K. Fredrickson—*PNNL*

Role of Microenvironments and Transition Zones in Reactive Subsurface Biogeochemistry: The PNNL SFA 142

J.M. Zachara (PI), J.K. Fredrickson (PI)—*PNNL*, J. Davis, *LBNL*; A. Felmy, G. Hammond—*PNNL*; K. Kemner, *ANL*; A.E. Konopka, C. Liu, J. McKinley, C. Murray, C. Pearce—*PNNL*; D. Richardson, *U. of East Anglia UK*; E. Roden, *U. of Wisconsin*; K. Rosso, T. Scheibe, L. Shi, M. Wilkins—*PNNL*; B. Wood, *Oregon State U.*

SLAC SFA Project Overview: Biogeochemical Processes Governing the Speciation, Dynamics, and Stability of Uranium in Reduced Aquifers 143

J.R. Bargar (PI), *SLAC*; R. Bernier-Latmani, *ÉPFL*; G.E. Brown Jr., S.E. Fendorf—*Stanford U.*; D.E. Giammar, *Washington U. St. Louis*

SLAC SFA: Speciation of Uranium in Biologically Reduced Sediments During Iron and Sulfate Reduction in the Old Rifle Aquifer 144

J.R. Bargar (PI), J.S. Lezama Pacheco, N. Janot—*SLAC*; J.E. Stubbs, *U. of Chicago*; D.S. Alessi, E.I. Suvorova, G.M. Stylo, R. Bernier-Latmani—*ÉPFL*; K.H. Williams, P.E. Long, J.A. Davis, P.M. Fox—*LBNL*; Kim M. Handley, *U. of California Berkeley*; Jose M. Cerrato, Daniel E. Giammar—*Washington U. St. Louis*

SLAC SFA: U(IV) Biomineralization and Stability of Monomeric U(IV) Species 145

Rizlan Bernier-Latmani (PI), Daniel S. Alessi, Paul P. Shao, Malgorzata Stylo—*ÉPFL*; Juan S. Lezama-Pacheco, Noemie Janot, John R. Bargar (lead PI, bargar@slac.stanford.edu)—*SLAC*; Philip E. Long, Luis R. Comolli—*LBNL*

SLAC SFA: Biogeochemical Processes and Diffusive Transport Limitations Affecting the Stability of Biogenic U(IV) 146

Daniel E. Giammar (PI), Jose M. Cerrato, Mathew N. Ashner, Zimeng Wang, Vrajesh Mehta—*Washington U. St. Louis*; Juan S. Lezama-Pacheco, John R. Bargar (lead PI)—*SLAC*; Daniel S. Alessi, Rizlan Bernier-Latmani—*ÉPFL*

SLAC SFA: Structural Basis for Ferrihydrite Reactivity in Subsurface Environments 147

F.M. Michel (PI), J.S. Lezama-Pacheco, J.R. Bargar—*SLAC*; A.C. Cismasu, G.E. Brown Jr.—*Stanford U.*; K.H. Williams, P.E. Long—*LBNL*

Early Career Awards 149

Multi-System Analysis of Microbial Biofilms 149

M.J. Marshall (PI, matthew.marshall@pnnl.gov), S.M. Belchik, E.A. Hill, L.A. Kucek, A.C. Dohnalkova—*PNNL*
Collaborators: H. Beyenal, *Washington State U.*; B. Cao, *Nanyang Technological U.*

Nanoscale Mercury Sulfide-Organic Matter Interactions: Implications for Mercury Methylation Potential in Sediments 150
H. Hsu-Kim (PI), A. Morris, T. Zhang, K. Kucharzyk, Y. Liu, M.A. Deshusses—*Duke U.*

Student Abstracts 151

Hg Stable Isotope Measurements in Fish Tissue as Indicators of Hg Chemical Transformations in East Fork Poplar Creek, TN 151
G. Bartov,* T.M. Johnson (PI)—*U. of Illinois Urbana-Champaign*

Characterizing the Biological Mechanism of Uranium Reduction Using Novel Voltammetric Techniques 152
Keaton Belli,* *Georgia Institute of Tech.*; Philippe Van Cappellen, *U. of Waterloo Canada*; Thomas DiChristina, Martial Taillefert (PI)—*Georgia Institute of Tech.*

Studies on Abiotic Mechanisms and Kinetics of Chemogenic Uraninite Oxidation in the Presence of Mackinawite and its Implication in Uranium Remediation 153
Yuqiang Bi,* *U. of Michigan Ann Arbor*; Kim Hayes (PI)

Microbial Oxidation of Hg(0): Its Effect on Hg Stable Isotope Fractionation and Methylmercury Production 154
Matthew Colombo,* Nathan Yee, Juyoung Ha, John Reinfelder—*Rutgers U.*; Tom Johnson, *U. of Illinois Urbana-Champaign*; Tamar Barkay (PI), *Rutgers U.*

Quantifying the Enthalpy and Entropy of Europium-Hematite Surface Species Using Variable Temperature Batch Experiments and EXAFS 155
Shanna L. Estes,* Yuji Arai (co-PI)—*Clemson U.*; Rodney C. Ewing (co-PI), Jiaming Zhang—*U. of Michigan*; Tomohiro Shibata—*Illinois Institute of Tech., ANL*; Brian A. Powell (PI)—*Clemson U.*

Chromium Responses and Biofilm Formation in *Desulfovibrio vulgaris* RCH-1, a Sulfate-Reducing Bacterium Isolated from 100H Chromium-Contaminated Groundwater, are Temperature-Dependent 156
L.C. Franco,* *Montana State U.*; Y.A. Gorby, *U. of Southern California*; M.W. Fields (PI), *Montana State U.*

Effects of Temporal Error Correlation on Quantification of Predictive Uncertainty in Groundwater Reactive Transport Modeling 157
Dan Lu,* Ming Ye—*Florida State U.*; Gary P. Curtis (PI), *USGS*; Philip D. Meyer, Steve Yabusaki—*PNNL*

Formation and Stability of Uranium(VI) Phosphates under Groundwater Conditions 158
Vrajesh Mehta,* Dan Giammar (PI)—*Washington U. St. Louis*

Dynamics of Mercury Release in Flooded Soils from Oak Ridge, Tennessee 159
Brett A. Poulin,* *U. of Colorado Boulder and USGS*; George R. Aiken, *USGS*; Joseph N. Ryan, *U. of Colorado Boulder*; Kathryn L. Nagy (PI), *U. of Illinois Chicago*

Biostimulation at Rifle, CO: Impacts on Aqueous Arsenic Geochemistry 160
Valerie K. Stucker,* *Colorado School of Mines*; Kenneth H. Williams, *LBNL*; James F. Ranville, *Colorado School of Mines*; Brian Mailloux (PI), *Barnard College*

*Student Presenter

Facilities 161

EMSL: A DOE Scientific User Facility for Biogeochemical and Subsurface Science Research 161

Donald Baer (EMSL Chief Scientist), Nancy Hess (Science Lead for Geochemistry/Biogeochemistry and Subsurface Science)—*EMSL*

A Liquid Sample Interface for Rapid 14C Analysis by Accelerator Mass Spectrometry 162

T.P. Guilderson (PI), T. Ognibene, A. Thomas, P. Daley, G. Bench—*LLNL*

Induced Polarization Signature of Biofilms in Porous Media: From Laboratory Experiments to Theoretical Developments and Validation

Estella A. Atekwana (PI), *Oklahoma State U.*; Andre Revil, *Colorado School of Mines*; Mariana Patrauchan, *Oklahoma State U.*

Our newly funded grant is focused on characterizing the major components and processes within bacterial biofilms contributing to detectable biogeophysical signals, spectral induced polarization (SIP) signatures in particular. Although the SIP technique has emerged as the technique most sensitive to the presence of microbial cells and biofilms in porous media, mechanistic aspects of the relationships between biological interactions with geologic media and the ensuing SIP response remain poorly understood largely because of competing effects of a myriad of contributing factors. Thus it is often difficult to unambiguously distinguish the impact of multiple and often competing processes that occur during *in situ* biostimulation activities on the SIP signatures. Through geophysical laboratory column experiments, coupled with time-lapsed synchrotron based X-ray microtomography (CMT) and Scanning Confocal Laser Microscope (SCLM) analysis of biofilms we propose to: (i) evaluate the contribution of biofilm components to SIP signatures using field relevant organisms, (ii) determine the contribution of nanoparticulate biogenic minerals in biofilms to SIP signatures, (iii) determine if the SIP signatures can be used to quantify the rates of biofilm formation and biogenic mineral accumulation in subsurface media, (iv) develop a fundamental understanding of potential underlying polarization mechanisms at low frequencies (<40 kHz) resulting from the presence of microbial cells and biofilms, and (v) evaluate the use of reactive transport models to predict the geophysical response associated with the development of biofilms in field conditions.

Although we are still in the very early stages of our project, so far we have started by expanding the POLARIS model initially developed to model the induced polarization response of silicate materials to the modeling bacteria growth in porous media. Our model results suggest that the polarization of the electrical double layer coating the surface of bacteria increases the quadrature conductivity of the porous material. Thus the change in quadrature conductivity can be directly related to changes in the specific surface area of the bacteria and to the increase in cell density/population due to bacterial growth. We tested this new model using the experimental dataset of Davis et al. (2006) and found that the model is able to reproduce the magnitude of the polarization in the experimental dataset. We conclude that this new model allows us to quantitatively assess SIP signatures of bacterial growth in complex environments.

The next phase in our project is to evaluate the contribution of biofilm components to SIP signatures using field relevant organisms. We will begin by examining the effects of exopolymeric substances (EPS) and assess how the latter differs from the effect of high cell density.

Integrated Microscopic and Metagenomic Analysis of Subsurface Microorganisms that Contribute to Carbon and Metal Cycling

Luis R. Comolli, Birgit Luef, Cindy J. Castelle, Sirine C. Fakra—*LBNL*; Kyle R. Frischkorn, Sean W.A. Mullin, Kelly C. Wrighton, *U. of California Berkeley*; Brian J. Anderson, Michael J. Wilkins, *PNNL*; Roseann Csencsits, Mary S. Lipton, *PNNL*; Steven W. Singer, Jillian F. Banfield (PI), *U. of California Berkeley*

Our research is conducted at the Department of Energy's (DOE) Rifle Integrated Field Research Challenge (IFRC) site in Rifle, Colorado, USA. Microscopic analyses have advanced our understanding of well-studied bacteria that proliferate during initial subsurface acetate biostimulation and provided insight into the novel diversity that appears during secondary stimulation.

Geobacter species are important planktonic Fe-reducing bacteria (FeRB) abundant during primary stimulation (2010). We applied a new sample preparation method in which samples were cryo-plunged directly on site immediately after sampling (Comolli *et* al. 2011). Cells and cell-associated minerals were analyzed using 2D and 3D cryo-TEM, high resolution TEM (HRTEM), energy dispersive spectroscopy (EDS) and scanning transmission X-ray microscopy (STXM). Confocal laser scanning microscopy (CLSM) performed on cells labeled with *Geobacter*-specific fluorescence *in situ* hybridization (FISH) probes confirmed cell identities. This approach revealed that *Geobacter* accumulate remarkable aggregates of Fe-oxyhydroxide nanoparticles capable of providing sufficient electron acceptor to support planktonic growth and cell motility. To characterize relevant physiological states and expressed metabolic pathways more completely, correlated cryo-TEM and proteomic profiles associated with different growth stages and electron acceptors for *Geobacter* grown in laboratory experiments are under way. The development of antibody-based high-resolution image labeling is under way using *c*-type cytochromes detected in outer-membrane and extracellular protein fractions.

An experiment was designed partly to test the hypothesis that novel "Candidate Division" (CD) bacteria are active during secondary acetate biostimulation (2011). Clone library analysis of filtrate that passed through a 0.2 μm filter but is retained on 0.1 μm filter revealed that CDs OD1 and OP11 were dominant members of the community. Flash-frozen cryogenic groundwater samples (09/03/2011) were characterized via 2D and 3D cryo-TEM. We have identified and characterized highly unusual, ultra-small cells (200 - 250 nm in diameter), and are currently elucidating the 3D ultrastructure and associations. These data show median cell sizes below previously estimated lower size limits for life (NRC 1999). Evidence of unique spatial optimization strategies are evident in their 3D architecture, such as: a very compact packaged genome, distribution of ribosomes and polysomes, and cell wall-attached ribosomes. The cell wall has a novel architecture, with a remarkable and distinct surface layer, and several appendages. Higher resolution structure determination of the macromolecular components is under way. While uncultured, both OD1 and OP11 cells are inferred from Rifle community genomics data to have small genomes, lack a Gram-negative cell envelope, and encode pili, consistent with these observations (Wrighton et al., submitted). Work is ongoing to perfect fluorescence *in situ* hybridization probes that would correlate cell structure with identity. Metagenomic analysis suggests that both OD1 and OP11 are obligate fermentative bacteria, and likely play a carbon cycling role in the Rifle subsurface.

Understanding the Subsurface Reactive Transport of Transuranic Contaminants at DOE Sites

M. Barnett (PI), *Auburn U.*; T. Albrecht-Schmitt, *U. of Notre Dame*; J. Saiers, *Yale U.*; D. Shuh, *LBNL*

Our primary hypothesis is that Np and Pu can interact with surfaces in fundamentally different ways than other metals, metalloids, and oxyanions – namely by reductive surface precipitation from undersaturated solutions. We are testing our hypotheses by studying the sorption of Pu and Np and their analogues to representative heterogeneous subsurface materials from Savannah River Site (SRS).

The sorption of Np(V), the dominate oxidation state of Np in the environment, onto sand from the SRS does not occur under any environmentally relevant conditions. In contrast, Np(V) is sorbed onto clay substrate under slightly basic conditions. XPS and EDS spectroscopy were used to probe the specific minerals that the Np(V) is associated with, and invariably the Np(V) is found associated with Fe minerals. In addition, the transport of Np(V) has been shown to be mitigated by the precipitation of U(VI) minerals that act as carriers for Np(V).

Th(IV) [as an analogue for Pu(IV)] transport experiments are being conducted using columns packed with SRS geomedia. At low pH (pH=4) and high ionic strength (I=0.1 M) conditions, Th(IV) transport is strongly retarded by the soil. However, a decrease in ionic strength to I=0.001 M caused colloids to be released from the geomedia. In addition to colloids, high concentrations of Th(IV) were also detected in the effluent samples immediately after the change in solution chemistry. However, after measuring dissolved and total Th(IV) concentrations, it was determined that colloid-facilitated transport was not the predominant cause for peaks in Th(IV) concentration up to ten times that of the influent solution. Instead, a drop in pH caused by the change in solution chemistry was responsible for the peaks in Th(IV) concentration. Depending on the surface charge of the geomedia, fluctuations in ionic strength can cause pH fronts to occur, producing dramatic effects on the transport of strongly actinides that can cause effects more pronounced than conventional colloid-facilitated transport.

The Advanced Light Source-Molecular Environmental Sciences (ALS-MES) Beamline scanning transmission X-ray microscope (STXM) successfully imaged and conducted near-edge X-ray absorption fine structure (XAFS) spectroscopy studies on sets of particulates derived and prepared from several sources within the project. One of the most interesting results supported by the STXM experiments, in addition to laboratory studies, was that U interactions with the non-hydrophobic components of the humic acids studied were more important than anticipated. Additional STXM experiments on particulates obtained from column experiments provided information about elemental associations and the presence of C on the particles. Upcoming STXM experiments will continue these investigations and will initiate new experiments as beamtime permits. Hard X-ray XAFS studies were also conducted on representative U, Np, and Pu materials obtained from selected materials from the sorption experiments.

Microscale Metabolic, Redox and Abiotic Reactions in Hanford 300 Area Subsurface Sediments

Haluk Beyenal (PI, beyenal@wsu.edu), *Washington State U.*; Jim Fredrickson, *PNNL*; Jeffrey S. McLean, *J. Craig Venter Institute*; Bin Cao, *Washington State U., PNNL*; Paul D. Majors, *PNNL*
Collaborators: Kenneth M. Kemner, Bhoopesh Mishra, Maxim I. Boyanov—*ANL*; Matthew J. Marshall, Liang Shi, David W. Kennedy, Roslyn N. Brown, Yijia Xiong, Margaret F. Romine, Mary S. Lipton, Nancy G. Isern—*PNNL*

The U.S. Department of Energy Hanford 300 Area (300A) site experiences periodic hydrologic influences from the nearby Columbia River as a result of changing river stage, which causes changes in groundwater elevation, flow direction and water chemistry. An important question is the extent to which the mixing of Columbia River water and groundwater impacts the speciation and mobility of uranium (U). This year, we designed experiments to mimic interactions among U, oxic groundwater or Columbia River water, and 300A sediments in the subsurface environment of Hanford 300A. The results revealed that U was immobilized by 300A sediments predominantly through reduction (80-85%) when the column reactor was fed with oxic, organic-amended synthetic groundwater (OA-SGW). The reduced U in the 300A sediments fed with OA-SGW was relatively resistant to remobilization by oxic Columbia River water. Oxic Columbia River water resulted in U remobilization (~7%) through desorption, and most of the U that remained in the 300A sediments fed with OA-SGW (~93%) was in the form of uraninite nanoparticles. These results revealed that: 1) the reductive immobilization of U through OA-SGW stimulation of indigenous 300A sediment microorganisms may be viable in the relatively oxic Hanford 300A subsurface environments and 2) with the intrusion of Columbia River water, desorption may be the primary process resulting in U remobilization from OA-SGW-stimulated 300A sediments at the subsurface of the Hanford 300A site.

In continuation of our work related to understanding how heavy metals interact with subsurface biofilms at the microscale, noninvasive nuclear magnetic resonance imaging (MRI) and spectroscopy (MRS) approaches were used to monitor spatiotemporal responses of live *S. oneidensis* MR-1 biofilms to U(VI) and Cr(VI). MRI and spatial mapping of diffusion in the biofilms revealed that, although the overall biomass distribution was not significantly altered upon exposure to U(VI) or Cr(VI), microenvironments in the biofilm matrix changed as indicated by localized changes (~ 20 microns) of water diffusivity in the biofilms, suggesting potentially important contaminant-induced changes in structural or hydrodynamic properties of biofilm matrix upon exposure to the metals. We also quantitatively demonstrate that the responses of cellular metabolism in biofilms interacting with environmental contaminants are spatially stratified, implying the possibility that the strategies for detoxification or adaptation utilized by cells in biofilms may be altered in response to the local microenvironments. Lastly, we developed a 2-dimensional mathematical model to predict substrate utilization and metabolite production rates in *Shewanella oneidensis* MR-1 biofilms as well as U immobilization by considering reduction and adsorption processes in the cells and in the extracellular polymeric substances (EPS). The model included the production of EPS using the experimental data we generated last year. The EPS bound to the cell surface and distributed in the biofilm were considered as bound EPS (bEPS) and loosely-associated EPS (laEPS), respectively. COMSOL® Multiphysics finite element analysis software was used to solve the model numerically. We used a custom designed biofilm reactor placed inside a nuclear magnetic resonance (NMR) micro-imaging and spectroscopy system, and monitored substrate utilization and metabolite production rates to compare model with experimental data.

Isotopic Characterization of Biogeochemical Pools of Mercury and Determination of Reaction Pathways for Mercury Methylation

J.D. Blum (PI), J. Demers—*U. of Michigan*; B. Gu (lead co-I), F. He, W. Zheng—*ORNL*

The project objective is to use stable Hg isotope measurements to reveal locations of Hg methylation in the Poplar Creek (PC) watershed, TN and place new constraints on the processes that lead to methyl mercury (MeHg) production, transport and degradation. We seek to better understand the decoupling of inorganic Hg and MeHg concentrations in the East Fork PC (EFPC) ecosystem. We are using a two-pronged approach that involves 1) an ecosystem level study of natural samples, and 2) experimental studies of Hg isotope fractionation. Natural samples are being collected from wetland sediments, stream sediments and waters, stream bottom periphyton and, as a monitor of the MeHg in the ecosystem, young-of-year herbivore/ detritivore stoneroller minnows and omnivore/piscivores redbreast sunfish. During the first 6 months of this new project we: 1) completed a sampling campaign for water, sediment and periphyton from EFPC, Hinds Creek and adjacent wetlands, 2) obtained archived samples of fish tissues from the ORNL Ecol. Assess. Group, 3) obtained splits of samples of Clinch River, PC, and EFPC sediments from TN Dept. of Envir. and Conser., 4) completed Hg isotopic analyses of sediments, suspended particulates and periphyton, and 5) conducted preliminary experiments on Hg(0) oxidation by natural organic matter (NOM) to investigate Hg isotope fractionation.

Sediment samples from the Clinch River upstream of the confluence with PC (and from Hinds Creek) establish very low background Hg concentrations [Hg] of 11-23 ng/g. The background mass dependent isotopic composition displays a narrow range ($\delta^{202}Hg_{NIST-3133}$ = -1.43 to -1.46‰) and there is a deficit of the odd mass isotopes ($\Delta^{199}Hg$ = -0.24 to -0.29‰). Two samples from the Clinch River downstream of PC have elevated [Hg] of 242 and 763 ng/g, with Hg isotopic compositions ($\delta^{202}Hg$ = -0.26 and -0.31‰; $\Delta^{199}Hg$ = -0.07 and -0.08‰) that are highly contrasting from background values. Sediments from PC below EFPC have even more highly elevated [Hg] (2150 to 3870 ng/g) and isotopic compositions close to the downstream Clinch River samples ($\delta^{202}Hg$ = -0.13 to 0.07‰; $\Delta^{199}Hg$ = -0.02 to -0.13‰). Suspended sediment in EFPC collected near the Y-12 outflow pipe has $\delta^{202}Hg$ = -0.63‰ and $\Delta^{199}Hg$ = 0.03‰. Isotopic values of suspended sediment and periphyton change systematically with distance downstream reaching values of $\delta^{202}Hg$ = 0.07‰ and $\Delta^{199}Hg$ = -0.12‰ after 19 km. Patterns in Hg isotopic variation in stream sediments around the PC watershed can be summarized as follows. 1) Background sediment [Hg] is very low with a narrow range of Hg isotopic composition. 2) Sediments in EFPC near Oak Ridge have much higher [Hg] and have $\delta^{202}Hg$ and $\Delta^{199}Hg$ that are highly contrasting from background values. 3) $\delta^{202}Hg$ and $\Delta^{199}Hg$ in EFPC sediments vary with distance downstream likely due to fractionation associated with chemical transformations of Hg. 4) When PC mixes into the Clinch River the [Hg] and Hg isotopic compositions of sediments shifts dramatically; consistent with the addition of ~10% sediment from PC.

Preliminary experiments were conducted to investigate Hg isotope fractionation during dark and photochemical oxidation of Hg(0) by NOM. Results from dark oxidation of Hg(0) by reduced soil humic acid suggest that both mass dependent and mass independent isotope fractionation occur, and that the oxidation enriches heavy isotopes in the product Hg(II), which is opposite to the Hg(II) reduction processes. Results of photo-oxidation experiments indicate that the presence of NOM can substantially enhance the oxidation rate of Hg(0) particularly in EFPC water.

Reactivity of Iron-Bearing Phyllosilicates with Uranium and Chromium Through Redox Transition Zones

William D. Burgos (PI, wdb3@engr.psu.edu), *Penn State*; Hailiang Dong, (dongh@muohio.edu), *Miami U.*; Kenneth Kemner, *ANL*; Fubo Luan, *Penn State*; Michael Bishop, Paul Glasser—*Miami U.*

Operational extractions for the measurement of valence state-specific concentrations of Fe, U and Cr need to minimize secondary reactions that might occur in extract solutions. Because the reduction potentials for Fe and U species are similar, the thermodynamic favorability of one particular redox transformation (e.g., U(IV) O_2 oxidation by Fe(III)) may increase during the extraction phase but may not have been important under the geochemical conditions in which the sample was collected. In this scenario, the measured concentrations of U(IV/VI) and Fe(II/III) would not reflect the speciation in the sample but instead the speciation in the extract solution. To avoid these analytical problems when working iron(II/III)-bearing phyllosilicates, U(IV/VI), and Cr(III)/Cr(VI), we have developed a sequential extraction method as an alternative method for the conventional parallel extractions for (e.g., HF-H_2SO_4-phenanthroline for clay-Fe(II), and $NaHCO_3$ for U(VI)). We demonstrate that any extraction artifacts can be eliminated by using a sequential extraction procedure where U is first solubilized into H_3PO_4 and physically separated from the clay by centrifugation, and then the clay-Fe(II) is measured by HF-H_2SO_4-phenanthroline. A similar procedure is developed for Cr measurement. Using this this new procedure, we demonstrate excellent stoichiometric agreement.

Using the new procedure, we have performed Cr reduction experiments using clay-Fe(II). Nontronite (iron-rich smectite), smectite, chlorite, and Hanford site sediments were first bioreduced with *Geobacter sulfurreducens*. After pasteurization and removal of aqueous Fe^{2+}, clay-Fe(II) was used to reduce Cr(VI) at 10°, 20°, and 30°C to mimic natural conditions at DOE contaminant sites and to obtain activation energy of the reaction. The clay reactivity was strongly dependent on temperature. At 10°C, nontronite was most reactive and chlorite was not reactive at all, despite a large amount of Fe(II) in its structure. The reactivity of the Hanford site sediments was between these two end members. At the end of Cr(VI) reduction, there were various amounts of Fe(II) remaining in the clays. In order to estimate the capacity of clay-Fe(II), multiple spikes of Cr(VI) were added to the system. The rate of Cr(VI) reduction slowed with each spike. At the end of several spikes, there was still 20% structural Fe(II) in nontronite remaining that was considered not reactive. At 30°C, the rates of Cr(VI) reduction by clay-Fe(II) were several times higher than at 10°C. Nontronite was still most reactive and its structural Fe(II) was fully consumed upon two spikes of Cr(VI). At this temperature, even chlorite became reactive, but about 50% structural Fe(II) was still remaining after several spikes of Cr(VI).

Scanning and transmission electron microscope (SEM and TEM) observations revealed that reduced Cr was present in micro-structural associations with the clay minerals. Focused ion beam (FIB)-SEM and TEM observations and electron energy loss spectroscopy (EELS) revealed that reduced Cr was likely in the form of $Cr(OH)_3$. The association of reduced Cr with low-permeability clay minerals would minimize any chance of Cr reoxidation and remobilization. The clay minerals are currently undergoing redox cycling to assess any change of clay properties and their reactivity toward Cr under redox-fluctuating conditions.

Inorganic Controls on Neptnium-237 Mobility in the Subsurface

Peter C. Burns (PI, pburns@nd.edu), Jessica M. Morrison, Enrica Balboni, Ernest M. Wylie—*U. of Notre Dame*

Objective

Neptunium-237 has a long half-life (2.14 million years) and is highly soluble in near-surface groundwater in the pentavalent oxidation state. It is identified as a subsurface contaminant of concern by the DOE. As co-precipitation of Np into minerals may be important in determining the long-term behavior of this radionuclide in the subsurface, we aim to develop a detailed understanding of the factors, including structural constraints, that impact co-precipitation of Np(V) into minerals. To achieve this aim, we have the following working objectives:

1. To develop syntheses that show incorporation of Np(V) by rock-forming minerals, and
2. To investigate the structural mechanisms through which Np(V) is incorporated
3. To facilitate a comparative investigation of the inorganic factors valid to understanding the environmental fate of Np(V)

Results/Plans

The synthesis of a variety of mineral phases has allowed us to make preliminary contaminant uptake comparisons based on the steric constraints of the mineral structures. As of March 2012, fourteen mineral phases have been synthesized for this study. These include carbonates, sulfates, nitrates, phosphates, and a borate. Stage 1, the optimization of these mineral phases, is complete.

In the second stage, the mineral phases are synthesized in the presence of actinides—uranium and neptunium, separately. As of March 2012, eight mineral phases have been synthesized in the presence of uranium and neptunium for this study. These include carbonates, sulfates, and a borate.

Methods of synthesis, including a new method for the synthesis of calcite, and characterization of the phases by ICP-MS in solid and solutions modes will be presented and discussed. We will present hypothetical models for the incorporation of Np(V) into the crystalline structures of carbonates and sulfates along with a side-by-side comparison of the neptunium uptake potential for a variety of mineral phases.

In Situ Generation of Iron-Chromium Precipitates for Long-Term Immobilization of Chromium at the Hanford Site

E. Butler (PI, ecbutler@ou.edu), L. Chen, L. Krumholz, A. Madden—*U. of Oklahoma*; C. Hansel—*Harvard U.*

In situ Cr immobilization involves either microbial or abiotic reduction of Cr(VI), followed by precipitation of the much more insoluble Cr(III), typically in the form of a Fe(III)-Cr(III) (Fe-Cr) precipitate when Fe minerals are present. Numerous geochemical variables can impact the solubility of such Fe-Cr precipitates, including the rates of Cr(VI) reduction and Fe-Cr precipitation, particle size, and the Fe:Cr ratio. Poorly crystalline minerals, typically formed upon rapid precipitation, tend to be more soluble than highly crystalline minerals that are precipitated more slowly. Reoxidation of Cr(III) to Cr(VI) by manganese (Mn) oxides is well known, with the reaction taking place between dissolved Cr(III) and the solid Mn(III/IV) oxide surface. This means that many factors that influence the solubility of Fe-Cr precipitates also likely influence the rate of Cr(III) oxidation by Mn oxides.

The overall objective of this research is to determine the factors that most strongly influence the solubility of Fe-Cr precipitates formed in microbial and abiotic systems. Specific objectives are to: (1) measure the rates of Cr(VI) reduction by Fe(II) minerals and microorganisms (in separate microcosms) and measure the equilibrium solubility of the resulting Fe-Cr precipitates; (2) characterize the size, crystal structure, and composition of selected Fe-Cr precipitates that vary in solubility; and (3) measure oxidation rates of dissolved Cr(III) in equilibrium with Fe-Cr precipitates by birnessite. Abiotic systems will contain FeS or dithionite-reduced iron-rich nontronite. Microbial systems will contain one of three pure cultures of Cr(VI)-reducing bacteria isolated from the Hanford site, along with small quantities of hematite, Al-substituted goethite, or iron-rich nontronite as a source of Fe. Work to date includes preliminary experiments with pure cultures of Cr(VI) reducing bacteria and preparation/purification of Fe(III) oxides and clay minerals.

We hope that this research will lead to a more systematic understanding of how specific methods for *in situ* Cr immobilization in the presence of Fe (e.g., microbial reduction in the presence of Fe(III) oxides or abiotic reduction by Fe(II) minerals) affect the structure and solubility of the resulting Fe-Cr precipitate, and, in turn, how these properties affect the rate of reoxidation of Fe-Cr precipitates to Cr(VI) by birnessite. This knowledge will lead to a better understanding of how to generate Fe-Cr precipitates *in situ* that will be oxidized to Cr(VI) to the smallest extent over long time periods.

Field-Deployable Nanosensing Approach for Real-Time Detection of Free Mercury Speciation and Quantification in Surface Stream Waters and Groundwater Samples at the U.S. DOE Contaminated Sites

A.D. Campiglia (PI), F.E. Hernandez (co-PI), E.C. Heider, W. Chemnasiry, K. Trieu, C. Diaz, V. Diaz, A.F. Moore—*U. of Central Florida*; S.C. Brooks (co-PI)—*ORNL*

Our proposition targets a critical element of the Environmental Remediation Science Program (ERSP) research portfolio, which is the development of enabling scientific tools for characterizing the spatial and temporal evolution of complex subsurface systems. We are developing a field-portable, on-site sensing device for real-time speciation of elemental and inorganic mercury in surface stream waters, groundwater, and sediment samples. The sensing device relies on the combination of two well-known phenomena, i.e. the amalgamation of metallic mercury (Hg(0)) and gold (Au) and the Surface Plasmon Resonance (SPR) of gold nanorods (Au NR). When Au NR are exposed to the presence of Hg(0), its amalgamation to Au causes a reduction of the effective aspect ratio of NR and a blue shift of the maximum absorption wavelength of the longitudinal mode band. The linear correlation that exists between the aspect ratio of Au NR and the position of the maximum wavelength of the longitudinal mode of the SPR makes quantitative analysis possible. Efforts have been primarily directed towards the following: (a) Development of an immobilization procedure for Au NRs to produce Hg (0) detection substrates; (b) Analytical figures of merit for Hg (0) detection with various types of Au NRs when in solution and immobilized on the detection substrate under static conditions; (c) Interference studies with synthetic interference mixtures; (d) Evaluation a flow injection analysis (FIA) system for Au nanoparticles detection; and (e) Development of Hg (II) and Hg (I) reduction techniques and speciation strategy.

Scanning electron microscopy (SEM) and absorption spectroscopy confirm a well-dispersed deposition of NRs on the surface of the solid substrates. Calibration curves with NRs in aqueous solutions were built for six NRs samples with different maximum absorption wavelengths (610, 615, 630, 690, 730 and 740). The 630nm NRs exhibited the greatest slope and were the most sensitive to the concentration of Hg (0). Their limit of detection was approximately 10^{-20} M/NR. The immobilized NRs showed a limit of detection (10^{-19} M/NR) approximately one order of magnitude better than their counterparts suspended in liquid solutions. Exposure of Au NRs substrates to several inorganic ions showed no interference. A one-line and a two-line FIA system were implemented in our lab to monitor Au nanoparticles in water flows. On-going studies are focusing on the following: (a) extending FIA measurements to monitor Au NRs substrates exposed to ORNL contaminated water flows; (b) reducing mercury species via a cyclic voltammetry (CV) speciation procedure; and (c) combining CV with SPR-Au NRs spectroscopy for the detection of mercury species.

Dominant Mechanisms of Uranium-Phosphate Reactions in Subsurface Sediments

J.G. Catalano (PI), D.E. Giammar, F. Maillot, V. Mehta—*Washington U. St. Louis*; Z. Wang—*PNNL*

Widespread subsurface contamination at DOE sites has resulted from past mining, processing, and waste disposal processes. *In situ* remediation technologies can sequester uranium on site by transforming uranium to stable, low solubility species. While substantial recent research has investigated biogeochemical U(VI) reduction, this approach may have limited long-term sustainability because of the potential for reoxidation to occur. Phosphate addition is an alternative approach that can enhance the sequestration of uranium without requiring sustained reducing conditions. However, the geochemical factors that determine the dominant immobilization mechanisms are insufficiently understood to design efficient remediation strategies or accurately predict uranium transport in treated systems.

The overall objective of our project is to determine the dominant mechanisms of U(VI)-phosphate reactions in subsurface environments. Specific objectives are to: (1) resolve uncertainty regarding the specific U(VI) phosphate solids that form in homogeneous solutions; (2) determine the molecular mechanisms controlling U(VI) speciation in heterogeneous phosphate-bearing systems and the conditions where specific mechanisms dominate; (3) characterize how the interaction of competitive and cooperative reactions controls uranium speciation in sediments; (4) identify chemical divides that separate regimes where specific mechanisms dominate U(VI) speciation in subsurface sediments. In the first six months of this project our team has focused on meeting objectives 1 and 2.

For objective 1 we have investigated homogeneous precipitation of U(VI) phosphates to determine the conditions where specific phases forms. Studies to date have focused on systems lacking simple inorganic electrolyte cations in order to characterize the relative stability and occurrence of chernikovite [$H_3OUO_2PO_4 \cdot 3H_2O$] and uranyl orthophosphate [$(UO_2)_3(PO_4)_2 \cdot 4H_2O$]. Precipitation is initially rapid upon supersaturation and equilibrium is approached within 4 days. Chernikovite forms at all conditions studied; it may co-form with uranyl orthophosphate at pH 4 and high phosphate conditions. Solid characterization by XRD, SEM, EXAFS, and TRLFS is in progress. We plan to explore the effects of electrolyte cations (Na, Ca) and competition with calcium phosphate precipitation over the next six months.

For objective 2 we have investigated U(VI) and phosphate co-sorption on smectite to determine if substantial ternary complexation occurs and to characterize the transition between adsorption and precipitation. Wet chemistry studies show that phosphate has little effect on U(VI) adsorption at pH 4, 6, and 8 prior to the onset of U(VI) phosphate precipitation. Phosphate adsorption is low and these observations suggest that, unlike for iron oxide minerals, little U(VI)-phosphate ternary complexation occurs on smectite. The effect of phosphate on U(VI) adsorption mechanisms and U(VI) phosphate nucleation on smectite is currently being investigated by an integrated series of EXAFS and TRLFS measurements. Over the next six months we plan to determine the effects of Ca on U(VI) adsorption to smectite in the presence of phosphate and extend this work to goethite. Our efforts will then transition to characterizing U(VI)-phosphate reactions in sediments obtained from the Rifle and Hanford IFRCs.

Isolation of Fe-Oxidizing Microorganisms from the Rifle IFRC Site: Toward Understanding Post-Biostimulation Permeability Reduction and Oxidative Processes

Clara Chan (PI), Kevin Cabaniss, Chaofeng Lin—*U. of Delaware*; Ken Williams, *LBNL*

In order to optimize bioremediation of subsurface uranium contamination, we need to understand effects on aquifer permeability, as well as biogeochemical processes that occur after biostimulation ceases. At the Rifle IFRC, injection of organic carbon stimulates the production of reduced Fe and S chemical species and also results in significant permeability decreases especially within injection wells. After biostimulation ceases, reduced Fe and S species may be oxidized by microbes that produce Fe oxides, elemental S(0), and biomass that can clog pores. Additionally, Fe oxides may sorb uranium, thereby influencing its mobility. The overall goal of our exploratory project is to evaluate whether Fe and S oxidizers are indeed present, active, and contributing to post-biostimulation element cycling and pore-scale modification at the Rifle site.

Our first step involved demonstrating the presence of Fe- and S-oxidizing microorganisms (FeOM and SOM) in the Rifle aquifer. We use culturing methods because (1) we are still discovering the diversity of FeOM, so gene (e.g. 16S) similarity will not necessarily reveal FeOM presence and (2) because there are no well-characterized Fe oxidation genes to definitely show presence and activity. In order to sample active FeOM, we periodically monitored wells with a downhole video camera and sampled soon after the appearance of Fe floc. In December 2011, we sampled 3 wells: CU01, a background well; CD03, a well downgradient from injection wells, exposed to acetate in 2010 and 2011; and P101, a well that experienced acetate biostimulation in 2008 and 2009. We also sampled background sediment, which had not been exposed to acetate amendment. We enriched for aerobic Fe and S-oxidizers in gradient tubes, using a mineral medium and FeS or $FeCO_3$ substrate. Only the biostimulated wells CD03 and P101 showed S-oxidizers. All groundwater and sediment samples yielded FeOM growth, confirming the presence of FeOM in both amended and unamended areas of the Rifle aquifer.

Next, we are in the process of isolating model FeOM for biomineral characterization and microslide chamber growth experiments. Initial DGGE results indicate that cultures are highly enriched, possibly pure; purity will be checked by 16S rRNA sequencing and analysis. Transmission electron microscopy and selected area electron diffraction show that CD03 cultures contain curved rod cells and lepidocrocite. Uninoculated controls also formed lepidocrocite, suggesting that the observed mineralogy is a function of aqueous chemistry.

Our future work includes laser-scanning microscopy (LSM)-monitored microslide chamber experiments with isolates and enrichments; these will allow us to visualize pore-scale processes in real time and to test hypotheses relevant to permeability alteration. We will also perform field incubations of sediments in wells during and after planned biostimulation field experiments. Field and lab samples will be analyzed by LSM, SEM, TEM, and energy dispersive X-ray spectroscopy to identify newly formed material, and quantify biomass and porosity changes. Comparison of field and lab results will give insight on how to apply experimental results to the field. The project outcomes will help achieve the Rifle and SFA goals of relating pore-scale phenomena to intermediate- and field-scale processes. The results will contribute not only to improvement of biostimulation approaches, but also towards understanding of contaminant fate post-amendment.

Uranium and Strontium Fate in Waste-Weathered Sediments: Scaling of Molecular Processes to Predict Reactive Transport

Jon Chorover (PI/PD, chorover@cals.arizona.edu), *U. of Arizona*; Karl Mueller (co-PI), *PNNL*; Peggy O'Day (co-PI), *U. of California Merced*; Carl Steefel (co-PI), *LBNL*; Wooyong Um (co-PI), *PNNL*; John Zachara, *PNNL*; Nico Perdrial, *U. of Arizona*; Masa Kanematsu, *U. of California Merced*; Eric Poweleit, *Penn State*; Guohui Wang, *PNNL*

The need for better prediction of contaminant transport motivates multi-faceted lines of inquiry to build a strong bridge between molecular- and field-scale information. By focusing multiple lines and scales of observation on a common experimental design, our collaborative team seeks to reveal non-linear and emergent behavior in contaminated weathering systems. In prior work, we have successfully coupled weathering, adsorption and transport in geochemical models of sediments impacted by *hyperalkaline* waste streams. A goal of the current project is to expand our modeling capabilities to include *acidic* weathering reactions that, as described above, are expected to result in profoundly different products that will nonetheless undergo analogous silicate and non-silicate transformation, ripening and aging processes. We predict that these weathering reactions will vary with waste stimulant chemistry in ways that can be directly incorporated into the model structure.

Objectives of the project: (1) Determine process coupling between mineral transformation and uranium speciation change in acid waste-weathered Hanford sediments; (2) Establish linkages between molecular-scale contaminant speciation and meso-scale contaminant lability, release and reactive transport; (3) Make conjunctive use of molecular- to field-scale data to constrain the development of a reactive transport model that includes contaminant sorption-desorption and mineral transformation reactions.

Hypotheses: (1) Uranium speciation in legacy sediments from the U-8 and U-12 Crib sites can be reproduced in bench-scale weathering experiments conducted on unimpacted Hanford sediments from the same formations; (2) Reactive transport modeling of future U releases from the vadose zone of acid-waste weathered sediments can be constrained by combining molecular-scale information on contaminant bonding environment with grain-scale information on contaminant phase partitioning, and meso-scale kinetic data on contaminant release from the waste-weathered porous media; (3) Although field contamination and laboratory experiments differ in their diagenetic time scales (decades for field vs. months to years for lab), sediment dissolution, neophase nucleation, and crystal growth reactions that occur during the initial disequilibrium induced by waste-sediment interaction leave a strong imprint that persists with memory effects over subsequent longer-term equilibration time scales.

Research approach: We are developing an iterative measure-model approach that is applicable to elucidate mechanistic underpinnings of reactive contaminant transport in weathering geomedia.

Experimental design: Hypotheses are being tested by comparing the geochemical transformations and transport behaviors that occur in bench-scale studies of waste-sediment interaction with parallel solid-phase analyses of core sample extractions (scheduled for 2012-2013) from the acid uranium waste impacted U-8 and U-12 Cribs at Hanford. Crib waste aqueous simulants are being reacted with Hanford sediments in batch and column systems. Coupling of contaminant uptake to mineral weathering is being monitored using a suite of methods both during waste-sediment interaction, and after, when waste-weathered sediments are subjected to infusion with circumneutral background pore water solutions.

Results: We are currently in year 1 of the project, and have initiated a set of bench-scale batch weathering experiments where we are reacting Hanford Sediment with acidic, uranium bearing synthetic crib waste (SCW) solutions comprising a range in pH, uranium and phosphate concentrations. Parallel homogeneous nucleation experiments are being conducted to assess precipitation of reference uranium-bearing phases from supersaturated aqueous solution. Geochemical modeling is being conducted to assess aqueous speciation and the solubility envelopes of uranium-bearing solids as a function of system composition. These initial data streams guide follow-on experimental design and reactive transport modeling. These initial data streams guide follow-on experimental design and reactive transport modeling to understand the fate and transport of U in the Hanford subsurface.

Sequestration of Uranium in Iron-Rich Sediments under Sequential Reduction-Oxidation Conditions

C.S. Criddle (PI), W.-M. Wu, X. Du, S. Fendorf—*Stanford U.*; J. Bargar—*SLAC*; T. Mehlhorn, K. Lowe, D.B. Watson—*ORNL*; B. Li, T. Zhang—*U. of Hong Kong*; J. Zhou—*U. of Oklahoma*

Integrated field and laboratory studies indicate that iron species play a critical role in the sequestration of uranium at DOE sites with the relatively high iron content of sediments (up to 5-6% as w/w). In a long-term study conducted in Area 3 of the ORIFRC site, intermittent addition of ethanol stimulated sulfate and Fe(III) reduction with a concomitant decrease in soluble U to low levels. Re-oxidation with oxygen and nitrate led to a rebound in soluble U. Solid phase analyses revealed the formation of Fe(III)-U(IV) solids.

Well-defined solutions of dissolved Fe(II) reduced soluble U(VI) (50 mg/L) to U(IV) precipitates when pH was increased to values that were favorable for U(VI) reduction (pH>5.5 for these systems). When solutions containing U(IV) were then exposed to oxygen, U(IV) species were oxidized, as confirmed by XANES analysis, but almost all the oxidized U(IV) was bound to Fe(III) solids. Aqueous phase U(VI) levels were low (<0.01 mg/L) at pH > 5.5. This result establishes that U can be sequestrated in the presence of Fe(III) solids. A long-term (1210-day) microcosm experiment was performed to monitor the effects of dissolved oxygen (DO) on the sequestration of bioreduced U. Two bottles containing sediment from the bioreduced zone (1404 mgU/kg) were allowed to oxidize through long-term exposure to headspace air. As oxygen penetrated the sediment, aqueous uranium initially increased from <0.03 mg/L to a peak concentration of 0.1 mg/L at 400 days, but then decreased to <0.03 mg/L. Aqueous U concentrations remained at < 0.03 mg/L, at pH 7.0-7.2, despite the presence of 5-6 mg DO/L, 0.5 mM Ca and 2 mM HCO_3. This indicates that the uranium was strongly attached to the solid phase. To evaluate the impact of nitrate on U sequestration, nitrate (1.2 mM) was added to one of these bottles. A change in sediment color from black to brown indicated that the sediment was oxidized, but aqueous U concentrations did not increase. The U remained sequestered under the conditions of this incubation. Long-term field testing at ORIFRC Area 3 (over 1,000 days) has continued to examine the effects of exposure of bioreduced sediments to nitrate. Nitrate-contaminated groundwater was allowed to invade the bioreduced area via natural groundwater inflow. The geochemical response was variable depending on the proximity to the influx of contaminated groundwater from the highly contaminated source zone located up gradient. In general, the nitrate concentrations in the previously bioreduced area increased gradually from near zero to ~50-300 mM and then stabilized. The pH declined from post manipulation levels of 6.2-6.7 to below 5.0 as the site was recontaminated. Uranium concentrations rebounded in all monitoring wells but were well below upgradient contaminated groundwater levels for two years or more after active bioreduction stopped. In several monitoring wells uranium levels rebounded, declined, then a slowly rebounded as contaminated groundwater reentered the bioreduced zone. The results indicates significant sequestration of U when nitrate was a allowed to re-enter the bioreduced zone. The change in microbial communities in the subsurface was monitored in relation to the reduction and oxidation processes and functional microorganisms for iron and U reduction and oxidation were identified. The results suggest that reduction followed by re-oxidation could be an effective *in situ* U sequestration strategy for iron-rich sediments.

Subsurface Conditions Controlling Uranium Incorporation in Iron Oxides: A Redox Stable Sink

M. Massey, M. Jones, G.E. Brown Jr., S. Fendorf (PI)—*Stanford U.*; J. Lezama, J. Bargar—*SSRL*; P. Nico, *LBNL*; Ravi Kukkadapu, *PNNL*

Although large quantities of uranium can be potentially immobilized through microbially mediated U(VI) reduction, the potential for re-oxidative mobilization causes long-term stabilization to be technically challenging. Within natural environments, however, uranium often correlates with iron rather than existing as a discrete uranium oxide phase; uranium incorporation into iron oxides is a mechanism that can explain the co-occurrence of these two elements and may represent a natural attenuation pathway for uranium. Further, incorporated U(VI/V) within Fe (hydr)oxides appears stable with respect to oxidative dissolution, representing a potential means for long-term sequestration of uranium in the subsurface. Within this project we are examining the molecular mechanisms by which uranium is retrained by iron oxides, conditions optimal for retention, and the long-term stability of sequestered uranium.

Uranium incorporation into an iron (hydr)oxide lattice is dependent on Fe(II) propagated transformation of ferrihydrite. However, Fe(II) can also induce reduction of U(VI) to U(VI), with subsequent precipitation of UO_2, and thus represents a competing retention process for uranium. Deciphering (bio)geochemical factors influencing the predominance of each pathway is therefore critical to determine uranium fate within the subsurface. To elucidate the factors controlling uranium retention, we first conducted batch incubations where ferrihydrite slurries (100 mL of ~180 mg L^{-1}) were reacted with U(VI) and Fe(II) under varying water compositions (varying U(VI), Fe(II), and Ca concentrations, with total carbonate at 3.8 mM and pH buffered at 7.0). Using high-resolution synchrotron X-ray powder diffraction and extended X-ray absorption fine structure (EXAFS) spectroscopy, we identified the reaction products and thus the retention pathway. Incorporation of U into goethite is the dominant sequestration pathway at < 10 μM aqueous U concentration, with lesser amounts of UO_2 and U(VI) adsorption contributing to uranium retention. Similarly, low Fe(II) concentrations (<0.3 mM) promote incorporation over reductive precipitation of UO_2. Importantly, conditions conducive to the formation of uranyl-calcium-carbonato complexes were critical for incorporation, retarding reduction of U(IV). However, at high Fe(II) concentrations (3 mM), reduction was the dominant sequestration pathway independent of uranyl speciation or concentration. We further investigated the impact of mineralogical impurities common to the subsurface and found that although Al can inhibit ferrihydrite transformation, U(VI/V) incorporation occurred even at Al contents as high as 20% in Al-ferrihydrite. The combination of Ca-UO_2-CO_3 aqueous complexes and structural Al in ferrihydrite, however, resulted in limited incorporation or reduction. Our results demonstrate that U incorporation can be a major U sequestration pathway across a variety of aqueous phase and mineralogical conditions. However, multiple retention processes of uranium will occur in the subsurface and it is critical to appreciate the dominant pathway when considering the long-term fate of this hazardous element.

Microbial Community Trajectories in Response to Accelerated Remediation of Subsurface Metal Contaminants

Rebecca A. Daly, Katerina Estera —*U. of California Berkeley*; HsiaoChien Lim, *LBNL*; Ping Zhang, *U. of Oklahoma Norman*; Yongman Kim, *LBNL*; Zhili He, *U. of Oklahoma Norman*; Tetsu K. Tokunaga, Jiamin Wan—*LBNL*; Jizhong Zhou, *LBNL and U. of Oklahoma Norman*; Eoin L. Brodie, *LBNL*; Mary K. Firestone, *U. of California Berkeley and LBNL* (PI, mkfstone@berkeley.edu)

The objectives of our project are to: (1) Determine if the trajectories of microbial community structure, composition, and function following organic carbon (OC) amendment can be related to, and ultimately predicted through evaluation of key determinants. (2) Assess the relative importance of the characteristics of the indigenous microbial community, sediment, groundwater, and OC supply rate as major determinants of microbial community functional response and bioremediation capacity. We are using sediments from three DOE sites: Oak Ridge, TN; Rifle, CO; and Ringold formation, Hanford, WA; in a full-factorial reciprocal transplant experiment that includes sterile controls. Each sterilized sediment/inoculum combination receives OC supplied as sodium-acetate at two concentrations in synthetic groundwater that approximates the *in situ* conditions at each site. Sediments from the three sites were sieved, homogenized and a portion sterilized by gamma-irradiation. Sterilized sediments were inoculated with a small mass (2.0 g) of "live" sediment, thoroughly mixed and packed into flow-cells. The 2.0 g mass of inocula was selected following a gene-sampling-effort relationship experiment using PhyloChip and GeoChip arrays to determine the minimum mass required to provide inocula with reproducible phylogenetic content and functional capacity.

The 174 flow-cells constructed for this experiment are operating in an anaerobic chamber with synthetic anaerobic groundwater. All cells received groundwater without OC for approximately 6 weeks. The first destructive sampling of flow-cells (T0) occurred prior to OC addition to establish a baseline for the subsequent trajectory analysis. The remaining flow-cells are supplied with two OC supply rates: 0.1 and 1.0 mmol OC/kg/day. The OC supply rates were chosen based on prior experiments using Oak Ridge, TN sediment. Early results suggest inoculum and sediment-specific functional responses. Trajectory analysis will be performed as communities evolve over several months of biostimulation.

Remediation of subsurface metal contaminants at DOE sites involves microbial mechanisms of oxidation/reduction or complexation; which is controlled in large part by the ecology of the microbial community. Recognizing and quantifying the relationships between community structure, function, and key environmental factors may yield quantitative understanding that can inform future decisions on remediation strategies.

Combined Effects of Hydrology, Geochemistry, and Biology on the Remediation of U(VI) in Microfluidic Experimental Systems (Micro Models)

Kevin T. Finneran (PI), Timothy Strathmann (co-PI), Charles Werth (co-PI)—*Clemson U.*

The objective of this work has been to characterize the combined effects of hydrology, geochemistry, and biology on the bioremediation of U(VI). Our underlying hypothesis was *bioremediation of U(VI) in groundwater is controlled by transverse mixing with an electron donor along plume margins, and that* ***iron*** *bioavailability in these zones critically affects U(VI) reduction kinetics and U(IV) re-oxidation*. Our specific objectives are to a) quantify reaction kinetics mediated by biological versus geochemical reactions leading to U(VI) reduction and U(IV) re-oxidation, b) understand the influence of bioavailable iron on U(VI) reduction and U(IV) re-oxidation along the transverse mixing zones, c) determine how transverse mixing limitations and the presence of biomass in pores affects these reactions, and d) identify microbial populations that develop along transverse mixing zones and how the community development is influenced by the presence of iron and the concentration of electron donor.

The experimental tasks have utilized etched silicon microfluidic pore networks (micromodels) to simulate micro-scale hydraulic mixing zones within aquifer material. These micromodels have been used previously to understand the influence of transverse mixing (of electron donor and electron acceptor), biomass architecture, and biogeochemical reactions on contaminant fate and transport. We have used micromodels in the presence and absence of ferric iron, to assess the critical role that total iron plays in uranium bioremediation. Electron donors including acetate and lactate, U(VI), and Fe(III)-reducing cells have been introduced to the micromodels in a controlled manner to characterize the mechanisms and kinetics of both U(VI) reduction and U(IV) reoxidation, and to correlate this with biofilm structure along the transverse mixing zone(s). We have also used strictly abiotic experimental systems to determine the influence of abiotic reductants such as sulfides and hydroquinones on U(VI) reduction in the presence and absence of Fe(III).

Experiments with batch cultures (to support the micromodel development) were run with Geobacter metallireducens and uranyl adsorbed to the surfaces of either ferrihydrite or aluminum oxide. U(VI) was reduced by hydroquinones (as a model reductant) irrespective of whether the system contained aluminum or iron, suggesting that adsorbed U(VI) is available even when iron is not present. However, the buffer selection and concentration of bicarbonate was critical to reduction in the presence or absence of iron. Increasing bicarbonate decreases reduction of U(VI) in both iron and aluminum suspensions. In addition, aqueous uranyl is not reduced in bicarbonate buffer, where it is immediately reduced in HEPES buffer. This has implications for past experiments in which HEPES buffered suspensions were used to establish rates and mechanisms of adsorbed uranyl reduction, as HEPES seems to increase the capacity for reduction, while bicarbonate (which is the environmentally relevant buffer) decreases uranyl reduction in the presence of solids.

In addition, the abiotic precipitation of uranium (U(VI)) was evaluated in a microfluidic pore network (i.e. micromodel) to assess the efficacy of using a phosphate amendment to immobilize uranium in groundwater and mitigate the risk of this contaminant to potential down-gradient receptor sites. U(VI) was mixed transverse to the direction of flow with hydrogen phosphate (HPO_4^{2-}), in the presence or absence of calcium (Ca^{2+}) or sulfate (SO_4^{2-}), in order to identify precipitation rates, the morphology and types of minerals formed, and the effects of mineral precipitates on pore blockage. Each reactant was initially at 100 mM. Precipitation occurred over the time scale of hours to days, and rates varied with influent conditions. Relative to when only U(VI) and HPO_4^{2-} were present, precipitation rates were 2.3 times slower when SO_4^{2-} was present, and 1.4 times faster when Ca^{2+} was present; larger crystals formed in the presence of SO_4^{2-}. Raman backscattering spectroscopy and micro X-ray diffraction (μ-XRD) results both showed that the only mineral precipitated was chernikovite, also known as hydrogen uranyl phosphate; UO_2HPO_4.

Long-Term Colloid Mobilization and Colloid-Facilitated Transport of Radionuclides in a Semi-Arid Vadose Zone

Markus Flury (PI), Jim Harsh—*Washington State U.*; Fred Zhang, Glendon Gee—*PNNL*; Peter Lichtner, *LANL*; Earl Mattson, *INL*

We have continued our work on microscopic characterizations and quantifications of colloid detachment by moving air-water interfaces. Experimental and theoretical results show that the advancing air-water interface was significantly more effective in detaching colloids from a glass surface than the receding interface. For hydrophilic colloids, the advancing interface movement generally exerts a stronger detachment force than the receding, except when the hysteresis of the colloid-air-water contact angle is small and that of the solid-air-water contact angle is large. To generalize these results, we expanded our work from spherical colloids to colloids of different shapes (barrels, ellipsoids, disks). Direct measurements of capillary forces acting on natural sediment particles from Hanford showed that particle shape (and surface roughness) is an important factor controlling the magnitude of capillary forces. We experimentally distinguished between the maximum capillary force and the snap-off force when the air-water interface detaches from the particle.

We continued the monitoring of colloid transport in the field lysimeters at the Hanford 300N Lysimeter Site. The facility consists of six lysimeters, each 7.6 m deep. Fiberglass wicks were installed at 1, 2, 4, and 7 ft below surface to collect vadose zone water. We applied Eu-hydroxycarbonate colloids to the lysimeters. Small amounts of Eu colloids were detected in the deepest wick sampler (7-feet depth) only 2.5 months after application and cumulative precipitation of only 20 mm. Large water infiltration, mimicking Chinook snowmelt events in late winter/early spring, caused peaks of Eu in the wick outflow. A main peak of Eu outflow was detected in 4- and 7-feet depth in December 2011 and January 2012 (2.5 years after colloid application). Our results indicate rapid transport of Eu colloids under natural precipitation and artificial irrigation, i.e., the leading edge of the Eu colloids moved at a velocity of at least 3 cm/day within the first two months after application. The main peak of Eu colloids, however, moved at a rate consistent with long-term recharge estimates.

To elucidate the combined effects of water content and flow rate on colloid transport in unsaturated porous media, we conducted colloid transport experiments under different water contents and flow rates. To independently control flow rates and water contents, we used the geocentrifuge at the Idaho National Laboratory. This unique experimental setup allowed us to run a series of colloid transport experiments at different water contents (effective saturation of 1.0, 0.6, 0.32, 0.19) but identical pore water velocity (10.6 cm/min). In general, decreasing water content led to increased colloid retention inside the columns. A portion of the retained colloids could be released by changing the solution chemistry, indicating that colloids had been retained in the secondary energy minimum. A DLVO analysis supports this assumption. We attribute unrecovered colloids in the outflow to the presence of flow stagnation zones.

Ecophysiology and Extracellular Electron Transfer by the Metal-Reducing Bacterium *Geobacter daltonii* FRC32^T

Y. Gorby (PI), *U. of Southern California*; M. Fields, *Montana State U.*

Geobacter daltonii FRC32^T is an iron(III) and uranium(VI)-reducing bacterium isolated from uranium-contaminated subsurface sediments at the DOE ORFRC. Structural and functional gene analysis has confirmed that strain FRC32^T is abundant and active in those sediments. *G. daltonii* was cultivated in bioreactors using a chemically defined medium with acetate as the electron donor and fumarate as the electron acceptor. Under electron acceptor limited conditions, FRC32^T produced branched extracellular appendages that are morphologically similar to conductive nanowires those produced by *Geobacter sulfurreducens* strain PCA. *G. daltonii* also grew in chemostat cultures with oxygen as the sole terminal electron acceptor, but only when provided at growth-limiting concentrations. Amending the medium with amino acids to support the production of protein increased the production of extracellular filaments under electron acceptor limitation and increased the ability of this organism to reduce and transform solid phase iron oxide and dissolved forms of oxidized uranium.

This presentation provides an update on the molecular and electronic properties of extracellular filaments produced by *G. daltonii*. Novel cultivation methods will be described that can be used to more fully evaluate the enzymatic transformation of heavy metals and radionuclides across defined redox gradients. Information gained from this research will be used to better understand the biogeochemical processes that influence the fate and transport of uranium and other contaminants at the Oak Ridge Integrated Field Research Center. Understanding the components and mechanisms of charge transfer to extracellular electron acceptors by this and other environmentally-relevant organisms is an important step in realizing their full potential as tools for remediation of contaminated subsurface systems.

A Universal Framework for Predicting Deposition and Transport Behavior of Microorganisms in Subsurface Environment

YueYun Li, Xin Wang, JiaYi Shi, Sinan Muftu, KaiTak Wan, April Z. Gu (PI, april@coe.neu.edu)—*Northeastern U.*

Objectives: This project aims to explore and develop new AFM-enabled techniques for micro-/ nano-scale characterization and quantification of microbe cell surface properties and cell-surface interactions with the aim to correlate the conventional macroscopic deposition-transport measurement with the microscopic single cell characterization. Nano-scale cellular surface properties that govern the macro-scale cell-cell aggregation and cell-surface attachment tendencies for a number of IFRC-relevant microorganisms are obtained and, new theoretical and mathematical framework for microbe transport model in subsurface environments is proposed.

Material and Methods: In addition to comprehensive surface characterization of a number of DOE relevant microorganisms, the nature, magnitude and range of intersurface forces and surface potential at cell-cell and cell-substrate interfaces are quantified using Atomic Force Microscopy (AFM) combined with developed computation methods. Recognizing the complexity of factors dictating the cell-surface interactions and subsequent cell attachment behavior, an integrated and dimensionless parameter, Tabor value, μ, was proposed by us with the aim to parameterize the micro-scale cell-surface interactions in order to predict macro-scale cell deposition behavior. An improved theoretical model based on the DLVO theory but incorporating microorganism-specific features is constructed, aiming to generalize the transport behavior of a wide spectrum of microbes in water-saturated porous media. The microbial transport model will ultimately be extended to include other factors influencing microbe deposition to allow the prediction of cell deposition under different fluid condition, ionic strength and relevant sub-surface environments.

Results and Discussion: The sample microorganisms exhibit distinctive aggregation tendency and attachment efficiency via transport through porous media, indicating microbial bio-originated factors that influence the microbe movement. The attachment efficiency (α) ranges widely from 0.93 for strong microbe-substrate attachment to 0.06 for weak attachment, depending on the bacteria strain as well as the ionic strength of the aqueous environment. The electrolyte concentration is found to have significant influence on the cell stiffness and adhesion-detachment kinetics. No consistent correlation is found between α and any individual conventional micro-scale physicochemical properties such as electrophoretic mobility, hydrophobicity and extracellular polymeric substance. Mathematical calculation of interaction energy based on current DLVO formula failed to predict the deposition rates observed, indicating that the current DLVO model is not sufficient for predicting microbial deposition. AFM analysis allowed for quantification of the range and magnitude of the repulsive/attractive surface forces, including both short-ranges forces such as van der Waal and electrostatic and long-range forces such as those due to the presence of cellular surface substances (CSS) with varying thickness and density for each strain. A modified Tabor parameter based on classical colloidal and adhesion science is proposed, which collectively quantify the microscopic cell behavior and interfacial properties. Tabor values determined for the organism studied correlated well with the macroscopic attachment efficiencies measured by flow-through column experiments. This indicates that the rudimentary solid-mechanics model is promising to reliably predict the deposition-transport behavior by the Tabor parameter. For microorganism that have much larger *Ka* (reflect relative particle size to electrostatic layer thickness and density) value than colloids and with soft shell nature, the inevitable elastic deformation couples caused by the presence of both repulsive energy barrier and an attractive secondary minimum in the DLVO surface potential drastically alters the adhesion-detachment mechanism. We derive the theoretical description of distribution of 1st and 2nd minimum force associated to the detachment of a spherical / cylindrical shell of bacteria from an adhering substrate. An experimental verifiable grand theory of microbial deposition will ultimately be constructed to account for static-dynamic behavior of strains in porous media.

Assessing the Role of Iron Sulfides in the Long-Term Sequestration of Uranium by Sulfate-Reducing Bacteria (SRB)

Kim F. Hayes (PI, ford@umich.edu), Sung Pil Hyun, Yuqiang Bi, Julian Carpenter—*U. of Michigan*; Bruce E. Rittmann (co-PI, rittmann@asu.edu), Raveender Vannela, Chen Zhou—*Arizona State U.*; James A. Davis (co-I, jadavis@lbl.gov), *LBNL*; John Bargar, *SSRL*; Ravi K. Kukkadapu, *PNNL*

This UM/ASU research seeks to identify the potential for reduced iron sulfide minerals to inhibit the rate of oxidation of reduced U solid phases formed by sulfate reducing bacteria (SRB). Sulfate-reducing bacteria (SRB) utilize sulfate as a terminal electron acceptor and produce sulfide. When iron is also present, iron sulfide solids are produced. At DOE sites contaminated with U, aqueous phase U concentrations can be effectively lowered by reducing dissolved U(VI) species to insoluble U(IV) solids such as uraninite (UO_2(s)). SRB can accomplish this reduction step either directly by enzymatic electron transfer processes, or indirectly, through chemical reduction by the sulfides species produced. ***The working hypothesis of this study is that iron sulfides are preferentially oxidized over U(IV) solids when oxidants such as oxygen, denitrification products, or Fe(III) are introduced present.***

Batch studies were performed to continue the examination of the mechanism and kinetics of FeS protection against UO_2 oxidation under typical groundwater conditions. Experimental results show that mackinawite serves as an effective oxygen scavenger to inhibit the fast oxidation of chemogenic uraninite under simulated groundwater conditions. The kinetic profiles of dissolved uranium indicate that 5 g/L mackinawite inhibits UO_2 oxidative dissolution for about 60 hr under pH = 7, P_{O2} = 0.02 atm, and P_{CO2} = 0.05 atm. During the lag time, oxidation of structural Fe(II) and S(-II) of mackinawite control the DO levels, leading to the formation of iron hydroxides and elemental sulfur, respectively. After FeS is depleted, UO_2 oxidative dissolution occurs at a faster initial rate relative to the control experiments where mackinawite is absent. The kinetic data, along with XRD, Mössbauer, and XAS characterization of reaction products, suggest that the rapid uptake of U(VI) by FeS oxidation products during the initial stages of UO_2 oxidation is responsible for the accelerated rate of UO_2 oxidative dissolution compared to the control in absence of FeS. Ongoing research is testing groundwater conditions (including pH, pCO_2, pO_2) to understand the effects of these geochemical constraints in uranium reoxidation.

Sterile column experiments were performed to observe abiotic UO_2(s) oxidation by oxygen and denitrification products in natural sediments from Rifle CO. Both oxidation studies started with two RABS sediment columns supplemented with (1) chemogenic FeS (0.58g FeS(s)/kg) and UO_2(s) (0.5g UO_2(s)/kg) or (2) UO_2(s) alone (0.5g UO_2(s)/kg), sterilized with 5 Mrad gamma irradiation and by a 0.2 μm cartridge filter. For the oxygen columns, dissolved oxygen was passed through the columns, and for the denitrification products columns, nitrite, nitrous oxide, and dissolved oxygen were passed through sequentially. Effluent concentrations of uranium, sulfate, hydrogen sulfide, in combination with solid phase extractions on uranium, iron, and elemental sulfur show that under abiotic flow-through conditions: (a) iron sulfides protect uraninite from oxidation by dissolved oxygen and oxidizing minerals in RABS, (b) the terminal oxidation state for sulfide is elemental sulfur, (c) nitrite and nitrous oxide are not effective uranium or iron sulfide oxidants, and (d) oxidized RABS has a significant oxidizing capacity for uraninite. Upcoming experiments will further test the oxidizing potential of denitrification products, and will use sterilized bio-reduced sediment columns to better replicate natural systems undergoing oxidative U remobilization.

Biogenic iron sulfide minerals were produced by *Desulfovibrio vulgaris* supplied with various iron sources. Biogenic mackinawite production was demonstrated using either soluble iron or Fe (III) (hydr)oxide minerals in presence of *D. vulgaris*. The biogenic mackinawite derived from soluble Fe^{3+} was less crystallized than the mackinawite derived from soluble Fe^{2+}. By reducing Fe(III) (hydr)oxide solids and sulfate, *D. vulgaris* produced poorly crystalline mackinawite. XRD data further suggested that, in addition to mackinawite, residual Fe(III) (hydr)oxides, elemental sulfur, and vivianite [$Fe_3(PO_4)_2 \cdot 8(H_2O)$] were formed. Soluble iron, however, resulted in spectra containing only mackinawite patterns. The electron donor (lactate or pyruvate) did not have great impact on crystallization of mackinawite, except for soluble Fe^{3+}, where pyruvate led to more crystalline mackinawite. Residual Fe(III) (hydr)oxides and vivanite were present in the final solid products when pyruvate was the electron donor. These results illuminate the impact of the iron source coupled with the electron donor on the biogenic formation of iron sulfide solids that can be used to protect reduced uraninite from reoxidation in natural settings.

Biotic Controls on Uranium Sequestration and Release by Framboidal Pyrite in Bioreduced Sediments

Michael F. Hochella Jr. (PI), *Virginia Tech*; Nikolla P. Qafoku, *PNNL*; Amy Pruden, Harish Veeramani, Maria V. Riquelme Breazeal, Gargi Singh—*Virginia Tech*; Brandy Gartman, *PNNL*
Collaborators: Ravi Kukkadapu, *EMSL-PNNL*; Philip E. Long, *LBNL*

Uranium-containing framboidal pyrite, recently discovered in both IFRC/SFA sites at Rifle and Hanford, may play a significant role in controlling the fate and transport of subsurface contaminant U(VI). Biofilm-associated bacteria present on the framboidal pyrite surfaces could potentially influence the fate of uranium through enzymatic redox processes in the subsurface. Alternatively, framboidal pyrite-associated microbes could also play an indirect role in governing U(VI) bioreduction by catalyzing the initial formation of framboidal pyrite via iron-monosulfide precursors that can subsequently engage in non-enzymatic redox processes leading to U reduction and immobilization. Identifying framboidal pyrite-associated microbes and their distribution in biofilms may provide key insight into electron transfer processes driving U uptake and/or release.

An initial batch microcosm study was conducted to examine the relationship between biostimulants (lactate and acetate), pyrite (non-framboidal) amendment, and the microbial community dynamics using Rifle background sediment that was initially devoid of pyrite. A subsequent study will be conducted using synthetic-framboidal pyrite to amend the batch microcosms and compared with naturally bioreduced sediments to gain insight into the broader indigenous microbial community associated with framboidal pyrite. Several chemical synthesis methods involving aging of amorphous iron monosulfide are being employed to reproducibly generate substantial yields of pure framboidal pyrite for additional microcosm and parallel column studies. A key challenge in most synthesis methods involves scaling-up the production and ensuring phase purity. Flow-through column studies are being designed to evaluate uranium uptake and release by framboidal pyrite and compare uranium sorption and desorption behavior to the field site. Multivariate and statistical approaches applied to analyze microbial communities observed in the Rifle sediment and column studies will identify key groups of microbes associated with framboidal pyrite and help explain uranium removal under different test conditions. The biofilms formed on the surface of framboidal pyrite will also be visualized using fluorescence *in situ* hybridization (FISH) and confocal microscopy. Additionally, advanced microscopy and surface-sensitive spectroscopic techniques will be applied to probe molecular-scale redox interactions between framboidal pyrite and uranium. This exploratory research effort will help gain an understanding of interfacial biogeochemical processes impacting framboidal pyrite, the microbial population and activity, and U interactions in heterogeneous natural systems. This new insight in turn will aid in the development of molecular models to predict the rate and extent of U attenuation, as well as its long-term mobility, in bioreduced sediments. Further, the ability to stimulate these interactions may offer a new remediation strategy for DOE sites.

Assessment of the Bioavailability and Methylation Potential of Mercury Sulfides with Sediment Slurry Experiments

T. Zhang, K.H. Kucharzyk, H. Hsu-Kim (PI), M.A. Deshusses (co-PI)—*Duke U.*

In the natural aquatic environment, neurotoxic methylmercury (MeHg) mainly originates from anaerobic microbes that methylate inorganic forms of mercury in sediments. MeHg production rates can vary widely across aquatic ecosystems, sometimes by orders of magnitude. Accurate prediction of mercury methylation potential in the environment has remained elusive, partly because the mechanisms by which anaerobic microbes take up and methylate mercury are not well known. The overall goal of our research is to establish a quantitative relationship between the geochemical speciation of mercury in sediment pore water and the bioavailability of mercury to the methylating bacteria. In our previous work with pure cultures of sulfate reducing bacteria (SRB), we have demonstrated that the availability of mercury for methylation decreased during aging of mercury in sediments, a process in which mercury is expected to transform from dissolved Hg-sulfides to nanoparticulate and microparticulate forms of HgS.

To better capture the complexity of real sediment systems, we performed sediment slurry microcosm experiments to investigate the aging effect on the availability of Hg for methylation. For our slurries, we selected sediments and water at two locations in the San Francisco Bay-Delta estuary (California, U.S.A.) to represent sediments in freshwater and saline settings. The slurries were amended with one of the three forms of mercury: dissolved $Hg(NO_3)_2$ freshly mixed with Na_2S, HgS nanoparticles (<30 nm), and HgS microparticles (>1000 nm). In these HgS treatments, we compared the net MeHg production and other water quality parameters relative for Hg speciation. Our results showed that SRB were predominantly responsible for mercury methylation and their activity and subsequent MeHg production could be limited by the supply of sulfate and/or labile organic carbon. In the presence of abundant sulfate and carbon source, the bioavailability of Hg was the limiting factor for microbial methylation. The net MeHg production in the slurries amended with $Hg(NO_3)_2$+Na_2S was found to be the largest of the three types of Hg treatments, similar to our previous experiments with SRB in pure culture. Likewise, the methylation potential of nano-HgS was higher than that of micro-HgS. Nevertheless, the chemistry in natural sediments is more complex than that found in pure cultures of bacteria. Partitioning of Hg to bulk-scale mineral particles and colloids (especially FeS) may considerably influence the speciation of mercury and MeHg production. As a result, dissolved Hg in the bulk porewater (i.e., Hg remained in the supernatant after ultracentrifugation) in sediment pore water may not accurately represent the available fraction of Hg for methylation. Additional approaches targeting the Hg species that are likely taken up by the methylating bacteria (e.g., Hg-thiol complexes) are needed to assess the Hg availability in natural samples.

Effects of Pore-Scale Physics on Uranium Geochemistry in Hanford Sediments

Qinhong Hu (lead PI; maxhu@uta.edu), *U. of Texas*; Robert P. Ewing (co-PI; ewing@iastate.edu), *Iowa State U.*

The Hanford 300 Area sediments are mainly river cobble and gravel, with sands and fines (silt + clay) variably filling the voids in between. Fines comprise only 1.78% of the total sediment mass, but hold a disproportionately large fraction of the total U. However, the coarser sediments (e.g., >2 mm), with their larger mass fraction, may serve as a long-term U release pool despite their lower U concentration. We hypothesized that slow U release at the 300 Area is partly due to low connectivity of intra-granular pores. The objectives of this project are to evaluate the U distribution in 2-8 mm size sediments, to determine whether low pore connectivity affects U distribution and release from Hanford 300 Area sediments, and if so, to assess its implications for long-term release. Our approach integrates laboratory experiments (ICP-MS instrumentation to measure multiple elemental concentrations in liquid samples, laser ablation (LA)-ICP-MS for elemental mapping of 2-8 mm sized basaltic clasts) and pore-scale network modeling.

Over the last year we performed the following tasks with associated results:

1. Conducted complementary laboratory tests (stirred flow cell, saturated column, and batch reactor) to study U release behavior from each of five size fractions (<75 μm, 75-500 μm, 500-2000 μm, 2-8 mm, and a <2 mm composite). The stirred flow cell results indicate that 8.7% of the total U is in the 2-8 mm fraction, significantly reducing uncertainty in the U inventory. In addition, released U concentration shows a power-law relationship to elution volume (i.e., elution time) for all size fractions (published in *J. Environ. Radioact.*). Numerical simulations are being developed to recreate both stirred cell and saturated column experiments to better characterize U release rate constant distributions, and evaluate rate constant uncertainty for different size fractions.
2. Assessed concentration distributions of U and other elements in a 2-8 mm basaltic clast as a function of distance from the grain's surface. A second 2-8 mm basaltic clast was mapped and compared to the first mapped clast, examining fewer layers but to deeper depths. U concentration was power-law distributed with distance from the grain surface (published in *Environ. Sci. Technol.*).
3. Tested a pore-scale network model to examine pore connectivity issues in contaminant retention and release. The model supports our hypotheses about accessible porosity and anomalous patterns of contaminant release, and predicts U concentration distributions consistent with those observed in (2). A finite-difference model closely matches the network model results, indicating that we correctly captured how porosity and diffusion change with distance (published in *Water Resour. Res.*).
4. Carried out 3-D elemental mapping of a 2-8 mm basaltic clast, after vacuum saturation with a suite of nonsorbing and sorbing tracers, to better assess the edge-accessible porosity distribution; data processing and analysis are underway.
5. Performed unsaturated column transport experiments for 2-8 mm size fraction (at water saturations of 77% and 14%) and <2 mm size fraction (at 88% water saturation). Uranium release from 14% saturation is greater than that from 77% saturation under otherwise identical conditions, probably because at lower saturation, flow paths have more contact and interaction with the grains.

Fate of Uranium During Transport Across the Groundwater–Surface Water Interface

P.R. Jaffe (PI), P. Koster van Groos—*Princeton U.*; D.I. Kaplan, D. Li—*SRNL*; A.D. Peacock, *Microbial Insights*; K. Scheckel, *EPA*; H.S. Chang, *U. of Georgia*

Discharge of contaminated groundwater to surface waters is of concern at many DOE facilities. Essentially all surface or subsurface contaminants will move vertically through a vadose zone to an underlying aquifer and then laterally until it reaches some riparian zone or wetland. For example, at F-Area and TNX-Area on the Savannah River Site, contaminated groundwater, including uranium, is already discharging into natural wetlands. It is at this interface where contaminants come into contact with the biosphere. These wetlands exist in humid as well as arid regions. Furthermore, the numerous sharp biogeochemical transitions occurring in wetlands have profound effects on the ultimate fate of redox-sensitive trace metals and radionuclides, including uranium.

The goal of this research is to provide new insights on how plant-induced alterations to the sediment biogeochemical processes affect the key uranium reducing microorganisms, the uranium reduction, its spatial distribution, the speciation of the immobilized uranium, and its long-term stability. For this purpose we have formulated the following three **hypotheses**. (1) U(VI) discharged from ground- to surface-waters can be immobilized effectively as U(IV) in the sediments at the groundwater-surface water interface. The electron donor required to stimulate the microorganisms capable of reducing U(VI) is provided by wetland plants via their root exudates and root turnover. (2) Oxygen released into the sediments by plants reoxidizes Fe(II), forming iron oxy(hydroxi)des, which provide the bioavailable Fe(III) for long-term bacterial iron-reducing activity, which is key for a sustained biological uranium reduction. (3) Because wetland sediments are anaerobic and wetlands are usually nitrogen limiting, uranium immobilized as U(IV), which is readily oxidized in the presence of nitrates, will remain stable in the sediments for extended time periods.

To test these hypotheses we initiated a series of greenhouse **mesocosm studies** in which we will simulate the discharge of uranium contaminated groundwater into surface water through vegetated and non-vegetated sediments. These mesocosm studies, which will give information regarding macroscopic-scale processes and kinetics, will be augmented with laboratory batch studies to isolate the effect of specific variables. This characterization will be to determine the role the root-induced biogeochemical dynamics have on Fe speciation (to be determined via micro-XRD and Mössbauer analyses), microbiologic activities (^{13}C stable isotope pulse chase experiments coupled with ^{13}C phospholipid fatty acid analysis and pyrosequencing), and their role in controlling U speciation/oxidation states (via X-ray Absorption and X-ray fluorescence Spectroscopy) and U partitioning between the solid and aqueous phases. Spatial distribution of these characterizations and processes from the root surface to the bulk sediment will be quantified to gain detailed new insights into these biogeochemical processes and their overall impact onto the dynamics of uranium at the groundwater-surface water interface.

The project has just been initiated and we will show initial results of the microcosm operation, specifically the microbial community differences, including *Geobacter sp.* numbers as we move away from the root surface into the rhizosphere and into sediments where root growth has been excluded. Characterization of three U-contaminated wetland sediments from the SRS have shown that the U is only slightly more preferentially associated (1.5x) with the fine particle fraction (<2- µm or <0.5-µm), whereas Th(IV) was strongly concentrated (29x) in the finer particle size fraction. A sequential extraction of these sediments revealed that ~50% of the U in these heavily contaminated sediments was organically bound (sodium pyrophosphate extractable),7% was either associated with amorphous or crystalline Fe-oxides (extractable with ammonium oxalate or dithionite extractable), and another ~25% was exchangeable (acetic acid exchangeable). Uranium extractions were not similar to Th(IV) extractions, suggesting that some of the U may exist in the +6 oxidation state. Together these data indicates that: 1) the soil organic carbon is responsible for most of the sequestration of uranium in the wetland, and 2) a vast majority of the uranium in these wetland sediments may be in a labile state associated with organic matter, exchangeable fraction, and iron oxides in this dynamic chemical system.

Impact of Biostimulation on Permeability and C-13 Stable Isotope Probing of Biostimulation Experiments to Identify Acetate Utilizers

P. Jaffe (PI), *Princeton U.*; H. Tan, L. Kerkhof, L. McGuinness, A. Peacock, *Microbial Insights*; K. Williams, P. Long—*LBNL*

Here we are reporting results of two separate experiments. First we are conducting column experiments to study the link between biostimulation and changes in permeability. For this purpose seven columns were built that allow for dissolved species sampling and pressure change measurements along their vertical axis, and the experiment has been operating now for approximately one year. One column is equipped with electrodes to determine the induced polarization (IP) and link this to changes in permeability and to IP measurements that have been conducted at Rifle during previous biostimulation experiments. Results of this ongoing experiment show that there was a small and gradual (seemingly linear) increase in pressure over time during the first 200 days of biostimulation. Then, after about 220 days of biostimulation, we see a significant change in pressure along the longitudinal axis of the columns. This corresponds to approximately 50 days after sulfate is completely reduced. Effluent analyses show that by this time, methane is near solubility. A column that was sacrificed after ca. 90 days of biostimulation revealed that methanogen counts were the highest among microbial community members sampled. Although Rifle field experiments, focusing on dissolved groundwater samples have not reported significant presence of Archaea, these results, that focused on sediment analyses, seem to indicate that Archaea, in this case methanogens, might be a key organism competing for electron donors during biostimulation. In terms of permeability changes in response to biostimulation, we conclude that Under Rifle flow conditions, and with acetate as the electron donor, permeability changes are expected to be negligible, at least until separate-phase methane is building up.

A separate experiment was conducted to determine which microorganisms take up acetate during biostimulation and how the uptake of acetate by specific organisms, especially *Geobacter* species, changes over time, a 120-day column biostimulation experiment was performed. Eight columns were loaded with Rifle sediments and operated under continuous flow conditions using Rifle groundwater, amended with 3 mM C-12 acetate. At regular time intervals, C-12 acetate flow into a specific column was switched to C-13 acetate. That column was then operated under C-13 acetate amendment for 36 hours before it was sacrificed for detailed geochemical and microbiological analyses. Column operation started under iron reduction (based on the measured Fe(II) in the column effluent), while sulfate reduction (based on removal of sulfate between influent and outflow), was noted at about 25 days of operation. The microbial characterization consisted of phospholipid fatty acid analysis (PLFA) and stable isotope probing (SIP), while differentiating between the C-12 and C-13 incorporation into the biomass. Results showed that there was a differentiation between the community that was taking up acetate actively throughout the 120 days of operation and the overall microbial community. Of interest was that the fraction of *Geobacter* population remained fairly constant throughout the duration of the experiment, as well as its acetate uptake. Based on previous results conducted strictly during iron reduction, we estimate that of the acetate incorporated into the overall biomass, about 20% or less, was incorporated into *Geobacter* biomass. These results are key for the proper numerical simulations of biostimulation via acetate amendment and the biostimulation of *Geobacter*.

Integrated Geophysical Measurements for Bioremediation Monitoring: Combining NMR, Magnetic Methods and SIP

K. Keating (PI), D. Ntarlagiannis, L. Slater—*Rutgers-Newark U.*; K. Williams—*LBNL*

Our research aims to develop borehole measurement techniques to monitor subsurface processes, such as changes in pore geometry and iron/sulfur geochemistry, associated with remediation of heavy metals and radionuclides. Previous work has begun to identify methods that are capable of surveying the subsurface environment. One such method, spectral induced polarization (SIP), has been used to monitor the progress of subsurface contaminant remediation; however, its interpretation is of limited value in isolation. In our research we aim to combine measurements from multiple geophysical methods, i.e. nuclear magnetic resonance (NMR), and magnetic susceptibility (MS), with SIP, to allow us to reduce or overcome the limitations associated with using one measurement alone. The integration of measurements from multiple geophysical methods, each sensitive to mineral form and/or mineral-fluid interfaces, will provide better constraints on subsurface biogeochemical processes and evolution of pore geometries and significantly improve our understanding of processes impacting contaminant remediation.

In the first year of the research project, NMR and MS borehole logging measurements were collected at the Rifle Integrated Field Research Challenge (IFRC) site. The Rifle IFRC site is located at a former uranium ore-processing facility in Rifle, Colorado. Although removed from the site by 1996, leachate from spent mill tailings has resulted in residual uranium contamination of both groundwater and sediments within the local aquifer. Since 2002, research at the site has primarily focused on quantifying uranium mobility associated with stimulated biogeochemical processes. Ongoing studies at the site include an acetate amendment strategy, in which stimulation of native microbial populations by introduction of a carbon source serves to alter local redox conditions and immobilization of uranium in insoluble forms. NMR and MS logging measurements were taken before, during, and after acetate amendment. Changes in these signals were expected to correlate with changes in redox conditions and iron speciation. Experimental data were collected from two wells upstream of the acetate amendment, used as controls, and from three downstream wells.

The MS measurements revealed vertically stratified magnetic mineralization, likely the result of a detrital magnetic fraction within the bulk alluvium. Data were highly replicable over the monitoring interval, with little to no change observed in the MS measurements, suggesting negligible production of magnetic phases (e.g. magnetite, pyrrhotite) as a result of sulfidogenesis. NMR measurements had high levels of noise contamination requiring significant signal processing, and ongoing analysis suggests that any changes due to stimulated microbial activity may be difficult to differentiate from simultaneous changes in water content.

In the second year of the project we will collect laboratory SIP, NMR, and MS measurements on columns packed with sediments from the Rifle IFRC site as the columns are amended with acetate; changes in the geochemistry and pore geometry inferred from these measurements will be verified by standard, independent laboratory measurements. We will integrate the field and laboratory results to develop a strategy for the interpretation of coupled SIP, NMR and MS measurements during biostimulation.

Translation of Geophysical Log Responses to Estimate Subsurface Hydrogeologic Properties at the Hanford 300 Area

T.C. Kenna (PI), M.M. Herron—*Lamont-Doherty Earth Observatory*; A. Ward, *PNNL*

The geology and chemistry of the subsurface environment are fundamental factors controlling contaminant fate and transport, and thus play a critical role in remediation efforts at DOE sites. However, the subsurface is often heterogeneous and not well characterized. Petrophysical models that relate borehole neutron and gamma ray data to reservoir properties such as clay content, matrix density, porosity, and permeability are critical in the formation of meaningful reactive transport models.

The objectives of our research are to: 1) Analyze core and/or outcrop samples from representative facies for a variety of mineralogical, chemical and physical properties, 2) Predict the response of a variety of neutron and gamma logging tools based on these measurements, and 3) Develop algorithms to translate log responses into formation properties such as matrix density, lithology, porosity, and permeability, which are useful for input in flow and reactive transport models.

Our analysis of selected core samples from Hanford 300 Area boreholes reveals significant correlations between K, Th, and U concentrations and both matrix density and total clay, as determined by pycnometry and Dual Range Fourier Transform Infrared spectroscopy (DR-FTIR), respectively. Based on these relationships, we developed algorithms to predict total clay and matrix density from existing spectral gamma logs. The availability of laboratory bulk density data allows us to compute porosity estimates for some of our samples. The comparison of clay content and porosity reveals a relationship that is consistent with the relationship observed by Marion et al. (1992) and others, suggesting the existence of both clay-supported and framework (or grain) supported domains and the ability to estimate porosity from clay content. Further, the availability of total clay, matrix density, and porosity permit application of the k-Lambda model as a means to estimate permeability. We will present new data from wells distributed within 300 Area IFRC 399-3-31 (C6214), 399-2-30 (C6217), and 399-2-31 (C6218) and deeper wells from the surrounding Hanford_300 Area for which both geophysical logs and bulk density measurements are available - 399-1-23 (C5000), 399-3-19 (C5001), and 399-3-20 (C5002). Based on these new data, we will present refined algorithms for matrix density, clay content, porosity and permeability.

In addition, we have developed new environmental correction algorithms based on least-squares regression techniques that include uncertainty in the data, and propagation of errors with respect to the predicted correction factors. Goodness of fit evaluation of the new algorithms yields reduced chi-square that are lower than the Hanford algorithms and acceptable chi-square probabilities (>0.001). When these new algorithms are applied to existing log data along with an empirical detector based efficiency correction, a significant improvement in the accuracy and precision of the SGLS derived K, U, and Th concentrations are achieved as indicated by the reduction in uncertainties and good agreement between core and log data.

Development of Surface Complexation Models of Cr(VI) Adsorption on Soils, Sediments, and Model Mixtures of Kaolinite, Montmorillonite, γ-Alumina, Hydrous Manganese and Ferric Oxides, and Goethite

C.M. Koretsky (PI, Carla.koretsky@wmich.edu), T.J. Reich, A. MacLeod, A. Gilchrist, D. Wyman—*Western Michigan U.*

Cr(VI) is a toxic contaminant that has been introduced into aquifers and shallow sediments and soils via many anthropogenic activities. Cr(VI) contamination is a problem or potential problem in the shallow subsurface at several DOE sites, including Hanford, Idaho National Laboratory, Los Alamos National Laboratory and the Oak Ridge Reservation (DOE, 2008). To accurately quantify the fate and transport of Cr(VI) at DOE and other contaminated sites, robust geochemical models, capable of predicting changes in chromium speciation resulting from sorption, dissolution, precipitation and redox reactions, are required. The objectives of this study are to: (1) measure Cr(VI) adsorption kaolinite, montmorillonite, hydrous manganese oxide, γ-alumina as a function of ionic strength, pH, pCO_2 and sorbate/sorbent ratio, (2) develop surface complexation model descriptions of Cr(VI) sorption for these systems, (3) test component additivity predictions for Cr(VI) adsorption on mixtures of six well-characterized sorbents, (4) measure Cr(VI) adsorption on four bulk natural soils and sediments before and after four step-wise sequential extractions, and (5) develop methods for extending the component additivity approach to natural soils and sediments.

Significant adsorption of Cr(VI) occurs on γ-alumina (5 g/L solid; 10^{-4} or 10^{-5} M Cr) at low pH, with 50% of the Cr(VI) adsorbed between pH 6.5 and 8. Adsorption is suppressed with increasing ionic strength, especially at high pCO_2. Surface complexation models provide adequate fits to individual adsorption edges, but generally fail to reproduce the full range of observed ionic strength and sorbate/sorbent ratio dependence of sorption. Significantly less Cr(VI) occurs on hydrous manganese oxide, although 100% of 10^{-5} M Cr(VI) is sorbed on 20 g/L HMO at low pH. Increasing ionic strength (0.001 to 0.1 M $NaNO_3$) significantly decreases Cr(VI) sorption. Cr(VI) sorption is slow, failing to reach steady state after 2 weeks, and nearly irreversible with pH changes from 3 to 10 on untreated kaolinite. Pretreatment with 0.5 M HCl, 0.4 M hydroxylamine HCl or 30% H_2O_2 greatly increase the rate of adsorption, as well as the total quantity of sorbed Cr(VI). Cr(VI) is similarly irreversible on untreated montmorillonite, but is much more rapid than on kaolinite. Pretreatment with 30% H_2O_2 dramatically decreases the quantity of Cr(VI) sorbed on montmorillonite. These data suggest that Fe(II) in the lattice of these clay minerals is responsible for the irreversible sorption of Cr(VI), presumably by promoting reduction to Cr(III). Adsorption edges were measured on an organic-rich soil from Kleinstuck Marsh, MI, before and after stepwise removal of four target fractions (exchangeable, carbonate, reducible and oxidizable) for periods of 24 hrs to 2 weeks. For all sediments except those with the oxidizable portion removed, Cr(VI) sorption increases with time below pH 7, reaching a maximum of 100% sorbed at pH 3 and decreasing with increasing pH. Below pH 7, all Cr remaining in solution is Cr(VI), but above pH 7, dissolved Cr(III) increases with time, with the largest increases occurring at the highest pH, demonstrating reduction of Cr(VI) in contact with sediments. Cr(VI) sorption is greatly diminished after removal of the oxidizable fraction, suggested that the bulk of the Cr(VI) binds to organic matter or Fe(II)-bearing clays.

Chromate Reduction in Heterogeneous Porous Media

Li Wang, Li Li (PI)—*Penn State*

Chromate is a common groundwater contaminant at the U.S. Department of Energy (DOE) Hanford Site and poses a long-term threat to the water quality because of its high toxicity and aqueous solubility. Reduction of Cr(VI) to Cr(III), followed by the precipitation of Cr(III) hydroxide and / or mixed Fe/Cr (oxy) hydroxides, is one of the promising strategies to attenuate dissolved Cr(VI). Both aqueous and solid Fe(II) are abundant in Hanford sediments (biotite, clinochlore, magnetite, and ilmenite) and can serve as effective reductant for Cr(VI).

Under well-mixed laboratory conditions, the reduction of Chromate by aqueous Fe(II) often occur at a time scale of minutes. In natural systems, however, high Fe content sediments are typically unevenly distributed, with its majority in clay-rich low permeability zones. This can have a large impact on Fe(II) availability for the reduction of Cr(VI) and therefore the reduction rate of Cr(VI). The objective of this work is to investigate how and to what extent spatial distribution of Fe(II)-rich clay determine the rate of Cr(VI) reduction.

Column experiments with different mineral distribution patterns will be conducted, with quartz and illite representing the major solid components at the Hanford site. Illite will be pre-sorbed with Fe(II). Three columns will be set up, with one of the columns having Fe-saturated illite evenly distributed within the quartz matrix across the whole column (mixed column), while the other two having Fe-saturated illite distributed as one or three layers embedded within the sand matrix (1-layer column and 3-layer column). The total mass ratios of illite and quartz in the three columns will be kept constant. To investigate the effects of spatial distribution on the rate of Fe (II) desorption and Cr(VI) reduction under different geochemical conditions, flows at different pH conditions will be used. As the Fe(II) desorption and Cr(VI) reduction reactions are highly pH dependent and are sensitive to local geochemical conditions, a series of batch experiments is being conducted to determine 1) the suitable pH conditions for the Cr(VI) reduction in the column experiments, 2) the difference between Cr(VI) reduction rates with Fe(II) and with Fe(II)-sorbed illite. Understanding from batch reactor experiments will be used later to examine the difference between rates at the laboratory scale and the rates at the column scale. Reactive transport modeling will be used to quantify the rates under different conditions, to understand the role of heterogeneity, and to upscale laboratory rates to the field scale.

Monitoring Microbial Uranium Reduction at the Oxic-Anoxic Interface

R. Sanford, A. Basu, C. Lundstrom, T. Johnson—*U. of Illinois Urbana-Champaign*; J. Merryfield, G. Walshe—*U. of Tennessee*; K. Kemner, M. Boyanov—*ANL*; K. Pennell, *Tufts U.*; K. Ritalahti, F. Löffler (PI)—*U. of Tennessee and ORNL*

This collaborative, multi-investigator research project aims to develop innovative molecular and biogeochemical tools to enhance understanding of the microbiology controlling the redox state of metals and radionuclides in subsurface environments and near oxic-anoxic interfaces. Diverse groups of microorganisms affect the oxidation state of metals and, therefore, affect many biogeochemical processes including carbon turnover and the mobility of toxic radionuclides in subsurface environments. Relevant to uranium (U) transport are bacteria that can reduce the relatively water-soluble and mobile hexavalent U(VI) to the less-soluble U(IV) redox state.

We have applied physical, chemical and biological tools to analyze the fate of U under various geochemical conditions. Using EXAFS analysis we found that phosphate concentrations and the specific metal-reducing bacterial population can affect the form of reduced U(IV), indicating that a diversity of mononuclear U(IV) forms may be commonly formed during bioreduction. Using high precision mass spectrometry, we have also shown that significant U isotopic fractionation occurs during U(VI) reduction. During microbial reduction, the U(VI) remaining in solution becomes isotopically lighter; however, different U(VI)-reducing species resulted in different fractionation extents, and a new *Shewanella* isolate reduced U(VI) efficiently but without fractionation. These results indicate that different U reduction pathways/mechanisms operate that yield different products and can lead to varying amounts of isotopic fractionation. *c*-type cytochromes have been implicated in electron transfer to oxidized metal species, and using metaproteomic analysis we identified specific proteins expressed in cultures of *Anaeromyxobacter dehalogenans* strain 2CP-C, *Geobacter daltonii* strain FRC-32, and *Shewanella oneidensis* strain MR-1. Cytochromes expressed in response to the presence of specific electron acceptors provide information about the physiological state of the microbe, thus making predictions of metal-reducing activity possible.

To better investigate the spatial relationship associated with flow in a groundwater system we have completed the design of a rectangular Plexiglass flow-through column that will allow the simultaneous measurements of nucleic acid and protein biomarkers, U isotopes, and *in situ* EXAFS and XANES in a zone of controlled redox transition changes (i.e., the oxic-anoxic interface). The combined application of these tools will monitor the responses of metal-reducing bacteria and advance our understanding of the relevant microbiology and processes that determine the fate of electron donors (e.g., carbon) and electron acceptors (e.g., oxidized metals and radionuclides, oxygen) near oxic-anoxic transition zones.

Application of the new tools to DOE IFRC or relevant field sites will demonstrate their value to assess, monitor, and predict *in situ* reductive processes. The comprehensive understanding of the mechanisms and pathways affecting metal speciation, in particular U precipitation and mobilization, will contribute to the development of models that predict the long-term fate of metals in redox transition zones.

Multi-Scale Modeling Framework for Optimizing Uranium Bioremediation

Jiao Zhao, Kai Zhuang, Eugene Ma—*U. of Toronto*; Melissa Barlett, *U. of Massachusetts*; G. Tartakovsky, A. Tartakovsky, Yilin Fang—*PNNL*; Radhakrishnan Mahadevan, *U. of Toronto*; Timothy Scheibe, *PNNL*; Derek Lovley (PI, dlovley@microbio.umass.edu), *U. of Massachusetts*

Reductive immobilization of hexavalent uranium to uraninite by stimulation of indigenous bacteria has been extensively investigated as an efficient remediation strategy for subsurface U(VI) contamination. The challenge is how to achieve a sustainable, cost-effective and efficient U(VI) immobilization under specific and various sedimentary conditions. The overall objective of the project is to address this complex and systemic challenge by developing a multi-level computational framework capable of predicting uranium mobility for a long period of time under different conditions.

We have made progress in six parts that complement each other for achieving the project goal. These six parts cover every detailed aspect of the study of bioremediation process through computational modeling approaches, i.e. from very small test environment to field sites, from individual microorganism to microbial community, from regular biostimulation to optimal control of chemical amendments, and from single computer processor to grid engine. These six parts can be summarized as follows: 1) We have built a more complex mechanistic model that incorporates the latest research findings on both biotic and abiotic processes in subsurface sediments, providing insights into uranium immobilization that cannot be obtained by experiments alone. We have shown the value of model by validating its predictions under dramatically different environmental conditions; 2) We have performed a preliminary construction and analysis of the *Anaeromyxobacter dehalogenans* model at the genome scale and we are planning to incorporate this organism into our computational framework due to its diverse and wide-ranged metabolic capabilities relevant to the reduction of iron oxides, selenium, nitrate, chlorophenols and uranium for growth; 3) We have investigated the interaction of *Geobacter* and sulfate-reducing bacteria both in sediment incubations and with *in silico* metabolic modeling, revealing that Fe(III) availability, rather than competition with sulfate-reducing bacteria, is the key factor limiting the activity of *Geobacter* during *in situ* uranium bioremediation; 4) We have developed an optimization framework based on optimal control theory to maintain the uranium concentration below the environmental safety standard while minimizing the cost of the acetate and Fe(III) addition rates as well as the difference between the predicted and target uranium concentration; 5) We have succeeded in optimizing and parallelizing our preliminary 3D research codes containing different kinds of kinetic and equilibrium equations. We then adapted the model to be executed on Grid Infrastructure through OpenMP implementation, achieving good speedups that are close to the theoretical maximum speedups; and 6) We have incorporated a genome-scale metabolic model of *Geobacter sulfurreducens* into a pore-scale simulation of reactive transport and microbial growth to assess the manifestation of pore-scale variability (microenvironments) in terms of apparent Darcy-scale microbial reaction rates. We are trying to ultimately integrate all of these individual components to build a multilevel model framework for assisting the design of an effective and efficient bioremediation strategy.

Molecular Mechanisms Underlying the Metallic-Like Conductivity of *Geobacter* Pili

Madeline Vargas, *U. of Massachusetts and College of the Holy Cross*; Nikhil S. Malvankar, Pier-Luc Tremblay, Kelly Flanagan, Pranav Patel, Manju L. Sharma, Derek R. Lovley (PI; dlovley@microbio.umass.edu)—*U. of Massachusetts*

The discovery of long-range electron transport along the pili of *Geobacter sulfurreducens* via metallic-like conductivity is a paradigm shift in biological electron transfer and materials science with important implications in bioremediation and bioenergy. The metallic-like conductivity of the *Geobacter* pili differs significantly from previously described biological electron transport in which electrons hop or tunnel between discrete redox-active molecules, such as cytochromes. This finding also contradicts the long-standing belief that biological proteins act as insulators and can not be conductive. In the last year we have made significant progress in understanding the mechanisms for the metallic-like conductivity of *Geobacter* pili and the role of pili in extracellular electron transfer.

Additional evidence for metallic-like conductivity along pili was the finding that decreasing the pH of the pili preparations enhanced conductivity by as much as 100 fold. This response is characteristic of materials with metallic-like conductivity, but inconsistent with the alternative model of electron hopping/tunneling via cytochromes. In fact, the highest conductivity was observed at pH 2, a pH at which cytochromes are denatured.

Structural studies of *Geobacter sulfurreducens* pili using X-ray diffraction revealed overlapping pi orbitals. This is significant because pi orbital stacking is the basis for the metallic-like conductivity observed in synthetic conducting polymers, such as polyaniline. This finding led to the hypothesis that aromatic amino acids exposed on the outer surface of the pili play a key role in establishing the metallic-like conductivity of the pili.

In order to investigate this possibility, we genetically constructed mutant strains in which alanine was substituted for individual aromatic amino acids located at the carboxyl terminus of PilA, the structural pilin protein. Through these studies we identified an aromatic amino acid moiety that is required for the conductivity of pili sheared from the cells and for long-range electron transfer via pili attached to viable cells. The strain with this single amino acid substitution continued to produce pili that were functional in other aspects, such as promoting attachment to surfaces. These results are consistent with the hypothesis of metallic-like conductivity, but inconsistent with the alternative model of cytochromes mediating electron transport along pili.

Although *c*-type cytochromes can not account for conduction along pili, the cytochromes OmcS and OmcE are positioned outside the cell and are involved in electron transfer to Fe(III) oxide. Previous studies have demonstrated that OmcS is localized on the pili and is thought to facilitate electron transfer from pili to Fe(III) oxide. In order to localize OmcE, whole cells were treated with antibodies raised to OmcE, followed by secondary gold-labeled antibodies. Examination with transmission electron microscopy revealed that, unlike OmcS, OmcE is associated with the outer cell surface rather than the pili. These results suggest that a potential role of OmcE is to facilitate electron transfer to the pili. However, the ability to cells to adapt to deletion of the gene for OmcE indicates that there may be multiple proteins capable of this electron transfer step, a possibility that will be evaluated with adaptive evolution studies.

Influence of Protozoa on Anaerobic Groundwater Bioremediation

Ludovic Giloteaux, Dawn E. Holmes—*U. of Massachusetts*; Jeffrey D. Silberman, *U. of Arkansas*; Kenneth H. Williams, *LBNL*; Kelly C. Wrighton, *U. of California Berkeley*; Michael J. Wilkins, *PNNL*; Derek R. Lovley (PI; dlovley@microbio.umass.edu), *U. of Massachusetts*

The importance of bacteria in the anaerobic bioremediation of groundwater polluted with organic and/or metal contaminants is well recognized and in some instances so well understood that modeling of the *in situ* metabolic activity of the relevant subsurface microorganisms in response to changes in subsurface geochemistry is feasible. However, a potentially significant impact on bacterial growth and activity in the subsurface that has not been adequately addressed is protozoan predation of the microorganisms responsible for bioremediation. In order to evaluate the potential role of protozoa, anaerobic bioremediation studies were conducted at a uranium-contaminated aquifer located in Rifle, CO in which microbial reductive precipitation of uranium was stimulated with the addition of acetate to the groundwater. As observed in previous field experiments, acetate amendments initially promoted the growth of metal-reducing *Geobacter* species followed by the growth of sulfate-reducers. Analysis of 18S rRNA gene sequences revealed a broad diversity of sequences closely related to known bacteriovorous protozoa in the groundwater prior to the addition of acetate. In 2010, 41 different protozoan species were detected in the untreated groundwater and 37 species were detected in 2011. The bloom of *Geobacter* species associated with added acetate was accompanied by a specific enrichment of protozoa most closely related to the amoeboid flagellate, *Breviata anathema*, which accounted for over 80% of the recovered protozoan sequences. The abundance of *Geobacter* species declined following the rapid emergence of *B. ananthema*. The subsequent growth of sulfate reducers in the acetate-amended groundwater was accompanied by another specific enrichment of protozoa, but with sequences most similar to the diplomonad flagellate, *Hexamita inflata*, which accounted for over 80% of the protozoan sequences recovered during this phase of the bioremediation. These results suggest a prey-predator response during uranium bioremediation with specific protozoa responding to increased availability of preferred prey bacteria. Thus, quantifying the influence of protozoan predation on the growth, activity, and composition of the subsurface bacterial community is essential for predictive modeling of bioremediation strategies. It is expected that protozoa may play an important role in controlling the activity of microorganisms in a diversity of anaerobic soils and sediments.

Electrode-Based Approaches for Monitoring Microbial Activity and Carbon Cycling in Soils and Sediments

Kelly P. Nevin, Roberto Orellana—*U. of Massachusetts*; Kenneth H. Williams, *LBNL*; Derek R. Lovley (PI; dlovley@microbio.umass.edu), *U. of Massachusetts*

There is a compelling need for strategies to simply and inexpensively monitor the activity of microorganisms in soils and sediments. This is true not only for the microbial monitoring that is required during subsurface bioremediation, but also for assessing changes in microbial activity due to environmental perturbations, such as climate change. Current methods typically involve invasive sampling of the environment, which can alter microbial activities, and require the addition of tracers or indicators, adding complexity and expense. Furthermore, these traditional methods are not amenable to real-time monitoring of *in situ* activity.

Our previous studies at the Integrated Field Research Challenge (IFRC) site in Rifle, CO demonstrated that microbially generated current was a good predictor of the amount of acetate reaching downgradient monitoring wells when acetate was added to the subsurface to promote uranium reduction. This monitoring system worked well even though the graphite anodes deployed in monitoring wells were connected to cathodes located 5 m away at the surface. Low levels of current were detected with anodes deployed in monitoring wells in control zones not amended with acetate, presumably due to microorganisms producing current from acetate, and possibly other electron donors, steadily produced over time from the natural degradation of complex organic matter in the subsurface.

Therefore, we hypothesized that it might be possible to monitor microbial activity in a diversity of anaerobic soils and sediments in real time based on the amount of current generated from anodes deployed in the environments of interest. Our primary goal for this project is to monitor microbial activity in unamended sites at Rifle to evaluate the relationship between indigenous rates of anaerobic microbial activity and the degree of uranium removal via the natural attenuation of microbial U(VI) reduction. Field experiments will be validated by laboratory studies using Rifle-derived microflora and natural organic matter concentrated from a variety of locations across the Rifle floodplain. However, as an initial proof-of-concept we evaluated current production versus rates of methane production in freshwater methanogenic sediments, because monitoring methane production in these sediments provided a simple independent means of estimating rates of carbon turnover under different conditions.

There was a strong correlation between rates of methane production in sediments and rates of current produced by electrodes emplaced in the sediments. Although the sediments were methanogenic, microorganisms in the family *Geobacteraceae* accounted for 69% of the 16S rRNA gene sequences recovered from the anode surface. It is likely that the *Geobacteraceae* living on the electrode surface were utilizing acetate, and possibly other intermediates of anaerobic metabolism in the methanogenic sediments with electron transfer to the electrode. Thus, these results suggest that current production is likely to respond to changes in rates of carbon turnover in the same manner as natural terminal electron accepting processes. Therefore, it is expected that electrodes can provide an inexpensive noninvasive method for monitoring microbial activity and carbon cycling not only in groundwater, but also in a diversity of soils and sediments.

Catalytic DNA Biosensors for Radionuclides and Metal Ions

Yi Lu (PI), Yu Xiang, Hannah E. Ihms—*U. of Illinois Urbana-Champaign*

We are developing novel field-portable catalytic DNA biosensors to detect and quantify bioavailable radionuclides such as uranium, technetium, strontium, and plutonium as well as metal contaminants such as mercury and chromium. The sensors will be highly sensitive and selective, not only for different metal ions, but also for different oxidation states of the same metal ion (such as U(IV) vs. U(VI), or Cr(III) vs. Cr(VI)). To achieve the goals, we are using the combinatorial biological technique called *in vitro* selection to obtain catalytic DNAs that are highly specific for a given radionuclide or metal ion. We also use state-of-the-art biochemical and biophysical techniques to elucidate the structural elements responsible for high selectivity. These DNA have been transformed into fluorescent or colorimetric sensors by labeling the DNA with fluorophores or gold nanoparticles through catalytic beacon and nanoparticle assembly technologies developed in the PI's group, with detection limit down to 11 ppt and over millions-of-fold selectivity of uranyl over other radionuclides and metal ions. These sensors have been developed into commercially available sensor products that allow detection and quantification of radionuclides and metal ions in less than 2 min.

In the past year, we have made significant progresses in two areas. In the first area of developing novel catalytic DNA sensors for radionuclides and metal ions, we have demonstrated that functional DNA-linked gold nanoparticles can detect and quantify mercury ion in aqueous solution, with high sensitivity and selectivity. This system has been converted into a dipstick test using lateral-flow devices, making it even more practical for on-site and real-time detection. Furthermore, to lower the cost of quantitative detection, we have taken advantage of the wide availability and low cost of the pocket-sized personal glucose meter and demonstrated a method to use such meters to quantify radionuclides such as uranium with 9.1 nM detection limit. The method is based on the target-induced release of invertase from a functional-DNA–invertase conjugate. The released invertase converts sucrose into glucose, which is detectable using the meter. The approach should be easily applicable to the detection of many other radionuclides and metal ions. In the second area of fundamental understanding of metal ion selectivity in order to design more selective sensors, we have studied metal-ion-dependent folding of a uranyl-specific DNAzyme and obtained insight into the selectivity and function from fluorescence resonance energy transfer studies. In addition, we have also discovered the importance of peripheral sequences in determining the metal selectivity of an in vitro-selected Co^{2+}-selective DNAzyme.

Detecting and quantifying radionuclides and metal contaminants onsite and in real-time in a simple and cost-effective way will impact many other areas of research under the SBR program. For example, it will enhance geochemistry/biogeochemistry research by lowering the costs of characterization and by providing more accurate information of the radionuclides and metal contaminants at the DOE sites. This information will strengthen the correlations between results obtained from microbial ecology and community dynamic analyses and DOE site properties, improve the understanding of the mechanisms of biotransformation, and provide deeper insight into biomolecular science and engineering. Practical applications of these sensors will not only help assess the effectiveness of science-based solutions for remediation performed by researchers and engineers, but will also contribute to the long-term monitoring of DOE contaminated sites by DOE staff members, state and local regulation agents, and concerned citizens around the sites.

Development of U Isotope Fractionation as an Indicator of U(VI) Reduction in U Plumes

A.E. Shiel, P. Laubach, C.C. Lundstrom (PI), T.M. Johnson (co-PI), R.A. Sanford—*U. of Illinois Urbana-Champaign*; K.H. Williams, P.E. Long—*LBNL*

We are evaluating U isotope ratios ($\delta^{238}U$) as a tool for monitoring U(VI) reduction in the controlled field setting at the Rifle, CO IFRC site. The increased understanding of the biogeochemical behavior of U can guide remedial strategies and long-term stewardship activities at DOE sites. Several key questions are under investigation: (1) Are there confounding processes that complicate efforts to use $^{238}U/^{235}U$ as an indicator of U(VI) reduction (e.g., adsorption, mixing of distinct U from different flow paths)? (2) Is the U isotopic fractionation factor ($\varepsilon = (\alpha 1) \times 10^3$; $\alpha = {}^{238}U/^{235}U_{product}/^{238}U/^{235}U_{reactant}$) for U(VI) reduction constant? (3) Does the fractionation factor for U(VI) reduction differ between natural and stimulated conditions? (4) How do effective (field experiments) and intrinsic (laboratory experiments) fractionation factors compare? (5) Can reoxidation be detected using $^{238}U/^{235}U$? (6) Can biotic and abiotic reduction be distinguished by $^{238}U/^{235}U$?

$\delta^{238}U$ was measured in groundwater samples from the 2010–11 experiment to evaluate the degree of isotopic fractionation due to (1) bicarbonate induced U(VI) desorption and (2) acetate amended U(VI) reduction (occurring with or without bicarbonate amendment). Samples from a well impacted only by bicarbonate amendment reveal no significant U isotopic fractionation resulting from adsorption/desorption of U(VI) from aquifer solids. Samples from a well impacted by only acetate amendment show a similar shift in $\delta^{238}U$ to that observed for the 2007 biostimulation experiment [1] ($\Delta^{238}U$ =1.35‰ and 1.05‰, respectively), where ^{238}U is preferentially removed as reduced U(IV). In addition, the 2010–11 results give us, for the first time, $\delta^{238}U$ measurements during rebound of U(VI) concentrations after acetate amendment is terminated. In a well impacted only by acetate amendment, groundwater U(VI) concentration and $\delta^{238}U$ return to preinjection values within 128 days. Lack of an increase of $\delta^{238}U$ above preinjection values implies the primary source of U is advection of U(VI) rather than reoxidation of U(IV). This is particularly important, as the long-term success of this remediation technique depends on the stability of sequestered U(IV). Notably, the recovery of U(VI) concentration and $\delta^{238}U$ is much slower for a well impacted by both bicarbonate and acetate amendments; by 201 days after acetate injection stopped, U(VI) concentrations returned to preinjection values, yet $\delta^{238}U$ remained significantly lower (0.43‰) than initial conditions, possibly reflecting resorption of upgradient U.

Rifle floodplain samples exhibit limited but significant variation in U concentration and $\delta^{238}U$. The three surface waters collected north of the site are characterized by a mean U concentration and $\delta^{238}U$ of 36.9 ppb and 0.12‰, respectively. Similarly, the background well LR01 (not impacted by mill operations) is characterized by a U concentration and $\delta^{238}U$ of 44.5 ppb and 0.19‰, respectively. The remaining site floodplain samples exhibited significantly higher U concentrations ranging from 111 to 327 ppb and $\delta^{238}U$ from 0.05 to 0.24‰. The total variation, 0.43‰, is greater than the long-term uncertainty, 0.09‰ (2× root mean square difference between measurements of 16 full sample duplicates). Among floodplain samples, as the U concentration increases, a corresponding increase is observed in the $\delta^{238}U$ value. This relationship may be due to mixing between background U coming into the site with contaminant U remaining from historical U mill operations.

[1] Bopp, C.J. et al. (2010) Environ. Sci. Technol. 44, 5927–5933.

Linking As, Se, V, and Mn Behavior to Natural and Biostimulated Uranium Cycling

Brian J. Mailloux (PI), *Barnard College*; Alison Spodek Keimowitz, *Vassar College*; James F. Ranville, Valerie Stucker, Linda Figueroa—*Colorado School of Mines*; Kenneth H. Williams, *LBNL*

Biogeochemical redox cycles in groundwater systems frequently mobilize metals and metalloids that directly impact human health. These same biogeochemical cycles can also alter uranium speciation and mobility thus directly impacting groundwater quality at DOE legacy sites. Interestingly, the reducing conditions that immobilize uranium may be optimal for mobilizing metals such as As, Mn, Se, and V. These processes are occurring at the Department of Energy's Field Research Challenge (IFRC) site near Rifle, Colorado and offer a unique opportunity to study biogeochemical redox cycles. At well U01 near the Colorado river, natural redox fluctuations occur with changing river stages. When the river stage is high the aquifer appears oxidized. When the river stage is low the aquifer becomes reducing and Mn, As, and sometimes Fe becomes mobilized. Interestingly, little change in U concentrations are observed. During biostimulation at the IFRC As concentrations dramatically increase in the groundwater. During Fe(III) reduction, As levels increase to concentrations similar to levels observed in well U01 (~1.0 μM). However under sulfate reducing conditions As concentrations can be over ten times higher. Initial speciation work by IC-ICP-MS from samples collected during the "Super 8" experiment in 2011 indicated that arsenite was the dominant species during Fe(III) reduction but thioarsenates, in particular trithioarsenate, become dominant during sulfate reduction. No thioarsenites were observed. Speciation results were in close agreement with geochemical modeling. Future work will focus on understanding the sorption properties of thioarsenates along with the observed speciation during natural redox fluctuations. The goal is to better constrain the mobility of thioarsenate species and the species present and extent of As transport under natural and stimulated redox conditions.

Colloids, Deposits, and Clogging in Groundwater Remediation

David C. Mays (PI), Eric J. Roth, Tim C. Lei—*U. of Colorado Denver*; Jonathan Ajo-Franklin, Benjamin Gilbert—*LBNL*

This poster describes ongoing research (DE-SC0006962) aimed at linking colloidal phenomena and clogging in groundwater remediation. Colloids—particles between 1 nm and 10 μm—include bacteria, precipitates, and clay minerals that are ubiquitous in natural porous media. Soil science and filtration engineering indicate that colloidal phenomena (*i.e.*, colloid deposit morphology) can cause clogging that is detrimental for groundwater remediation. Can we avoid or manage clogging in groundwater remediation though better understanding of deposit morphology? To address this question, the current research comprises three components:

First, a series of laboratory experiments is being performed to simultaneously measure colloid accumulation, clogging, and deposit morphology. Here we report the first ever measurements of deposit morphology in flow cells, using a novel application of static light scattering in refractive index matched porous media (*i.e.*, Nafion) that quantifies deposit morphology as a fractal dimension. Details are given in the companion poster by Roth, Mont-Eton, and Mays. Ongoing experiments will measure how colloid accumulation, clogging, and deposit morphology vary over a range of physical (*i.e.*, fluid velocity) and chemical (*i.e.*, ionic strength) conditions.

Second, we have developed the first iteration of a clogging model that quantitatively accounts for the effect of deposit morphology. This clogging model is adapted from the literature on water treatment, in which a basic process is removal of colloid aggregates by settling, which provides a link between permeability and aggregate fractal dimension: Settling velocity depends on aggregate permeability, which in turn depends on fractal dimension. This new clogging model provides a framework for interpretation of the laboratory work above.

Third, we have planned a suite of measurements that will link the laboratory and modeling efforts with other research sponsored by the Department of Energy. Specifically, we plan to measure the fractal dimension of colloid suspensions taken from (1) laboratory experiments and (2) the Old Rifle field site. Task (1) links this work to ongoing research on chemical precipitation, x-ray computed microtomography, and nanogeochemistry. Task (2) links this work to conditions at the Old Rifle Integrated Field Research Challenge (IFRC) in Colorado.

Radiochemically-Supported Microbial Communities: A Potential Mechanism for Biocolloid Production of Importance to Actinide Transport

D.P. Moser (PI), J.C. Fisher, J.C. Bruckner, C. Russell—*Desert Research Institute*; T.C. Onstott, *Princeton U.*; K. Czerwinski, *U. of Nevada Las Vegas*; B. Sherwood Lollar, *U. of Toronto*; M. Zavarin, M. Conrad—*LBNL*; L.M. Pratt, S. Young—*Indiana U.*

This work focuses on the hypothesis that radiogenic substrates such as H_2 at DOE sites may support the growth of microorganisms, and thus indirectly influence the mobility of redox-sensitive radionuclides. Consistent with this hypothesis are early project results indicating the presence of H_2 and SSU rRNA genes, closely related (up to 99% sequence identity) to candidatus *Desulforudis audaxviator*, in fluids from underground nuclear test cavities (U12N.10 tunnel and ER-EC-11) at the Nevada National Security Site (NNSS). In deep South African mines, *D. audaxviator* is believed to utilize H_2 and SO_4^{2-} from radiochemical reactions; and until recently, this region was thought to define the geographic limit of the genus. Thus, the detection of *D. audaxviator* in radioactive subsurface water at the NNSS supports a radiochemical lifestyle for *D. audaxviator*. The current project builds upon these observations with the sampling of new sites, detailed microbial community and chemistry assessments, and radiochemical modeling.

In 2011, groundwater was obtained from six new wells from the NNSS and Nevada Test and Training Range: ER-20-5 #1 and #3 (4/26/11), ER-20-8 (6/27/11), ER-20-4 (9/21/11), U12N vent hole #2 (10/5/2011), and ER-EC-12 (11/28/11). These samples are currently being analyzed for dissolved ions, gases, and radiologic components. All samples contained sulfate (3 mg/L to ~140 mg/L) but only the U12N sample contained measurable H_2S (~6 μM). Four of six sulfate samples have been analyzed for sulfur isotopes, with $\delta^{34}S$ values ranging from +4.43‰ to +17.44‰. H_2S fractionation values are pending. Corresponding DNA extracts are currently undergoing molecular community assessments including T-RFLP, SSU rRNA gene libraries and 454 pyrotag analysis. Various physiotypes were also cultivated using defined media based on NNSS groundwater. Aerobic heterotrophs were present at all sites analyzed, with densities ranging from 10^4-10^6 cells mL^{-1}. Sulfate-reducing bacteria were also present (~10^3-10^4 cells mL^{-1}) at sites ER-EC-11 and U12N. Enrichments from U12N grew equally well in the presence or absence of ^{239}Pu, suggesting a community adapted to a high radiation environment.

To better constrain the abundance of *D. audaxviator* in the U12N.10 tunnel and ER-EC-11 samples, DNA extracts were subjected to pyrotag analysis (~20,000 reads, M. Sogin Lab, MBL). Sequences from the Actinobacteria, Deinococcus-Thermus, Firmicutes, and Proteobacteria phyla were detected in both ER-EC-11 and U12N.10; the U12N.10 tunnel sample also contained Bacteroidetes, Chlorobi, and Nitrospirae. Over 40 genera of *Clostridia* were present, with *Symbiobacterium* and *Dethiobacter* dominating the ER-EC-11 and U12N.10 libraries, respectively. *Clostridia* comprised 25% of the U12N.10 library, and this sample also produced many sequences affiliated with *D. audaxviator* (93-99% similar). Flow cytometric cell sorting was performed (six 384 well plates, Bigelow Lab. R. Stepanauskas) on a cellular retentate washed free of radioactivity from U12N, with subsequent multiple displacement amplification (MDA) yielding ~60 useable sequences. Full genome sequencing will follow if a single amplified genome (SAG) from a North American *D. audaxviator* is obtained.

Electrical Responses of Grain Surfaces Measured by Spectral Induced Polarization and Atomic Force Microscopy

N. Hao, R. Chen, D. Dean, S. Moysey (PI)—*Clemson U.*; D. Ntarlagiannis, K. Keating—*Rutgers-Newark U.*

Quantitatively describing the spectral induced polarization (SIP) response (a.k.a complex conductivity) of the subsurface is a problem that spans nanometer to meter length scales. We are combining surface-sensitive, micron-scale polarization and atomic force microscope (AFM) techniques with column scale SIP observations to bridge these scales. Recently we have been evaluating whether complex conductivity measurements of grain surfaces can be obtained using AFM. Initial AFM calibration measurements were performed on glass slides with different geometries to confirm that complex surface conductivity values could be achieved. After accounting for geometry, we found consistent patterns in the real conductivity change with frequency for different slide geometries and a very strong capacitive response; the order of the magnitude for the low frequency real conductivity was 10^{-11} S/m which is comparable with the theoretical values for glass (10^{-11} to 10^{-15}S/m). We then performed SIP experiments and AFM measurements using glass beads under four different experimental conditions: (1) unaltered, (2) etched with hydrofluoric acid, (3) calcite coated, and (4) iron oxide coated. The calcite coated beads showed a decrease in real conductivity of 10% compared to the plain beads for the SIP measurements and a decrease of approximately two orders of magnitude for the AFM measurements. This observation is consistent with the fact that surface charge maps obtained with the AFM also showed a decrease in surface charge density for the calcite coated beads. In contrast, both the etched and iron coated beads showed an increase in real conductivity relative to the plain beads, though the magnitude of increase was inconsistent between the SIP and AFM measurements. The iron oxide coated and etched beads increased in real conductivity by 34% and 12%, respectively, for the SIP measurements. For the AFM measurements the real conductivity of the iron coated beads doubled, whereas it increased by approximately an order of magnitude for the etched beads. The difference between the SIP and AFM response could be an indication that even though the etching created a larger impact on individual grain surfaces, the iron oxides bridge grains to create a continuous conductive surface pathway through the porous medium. The SIP measurements showed that the peak response of the imaginary conductivity shifted from approximately 0.03Hz for the plain beads to approximately 0.1Hz for the etched beads and 0.5Hz for calcite coated beads without a significant change in magnitude between any of these samples. In contrast, the imaginary conductivity of the iron oxide coated beads exhibited a shift in peak response to 0.05Hz, but doubled in magnitude relative to the other treated beads. Consistent phase measurements for the beads have not yet been obtained using the AFM.

Role of Sulfhydryl Sites on Bacterial Cell Walls in the Biosorption, Mobility, and Bioavailability of Mercury

S.C.B. Myneni (PI), *Princeton U.*; J. Fein, *U. of Notre Dame*, B. Mishra, *ANL*

Bacteria are ubiquitous in a wide-range of low temperature aqueous systems, and can strongly affect the distribution and transport of metals and radionuclides in the environment. However, the role of metal adsorption onto bacteria, via the reactive cell wall functional groups, has been largely overlooked. Previous macroscale metal sorption, and XAS studies have shown that carboxyl and phosphoryl functional groups to be the important metal binding groups on bacterial cell walls. However, our preliminary XAS studies indicated that Hg^{2+} binds to sulfhydryl groups in preference to the more abundant carboxyl and phosphoryl groups on cell walls when Hg concentration is submicromolar. The stoichiometry of these Hg-cysteine bacterial cell wall complexes also change as a function of aqueous Hg concentration, and the structures of such complexes can have a significant impact on the solubility and bioavailability of Hg. The overall goal of our study is to provide a quantitative and mechanistic understanding of the impact of bacterial sulfhydryl groups on the uptake, speciation, transport and bioavailability of Hg in the environment.

We examined the sorption and structure of Hg complexes on the cell membranes of *Bacillus subtilis*, *Shewanella oneidensis*, and *Geobacter sulfurreducens* as a function of pH, and Hg and Cl^- concentration. The concentration of reactive thiols on cell membranes are also characterized using a newly developed fluorophore technique. Mercury adsorbs strongly, and exhibits similar sorption trends for all bacterial species; however, our XAS and fluorescence spectroscopy studies indicate that Hg speciation is significantly different on methylating and non-methylating organisms. In the case of *S. oneidensis*, Hg forms HgS_3 (S= organic thiol) complex at nanomolar Hg concentration, and HgS_2 and HgS (S = cysteine) with increasing Hg concentrations in the sub-micromolar range. Mercury binds to carboxyls with further increases in Hg concentration, and this transition occurred in the range of 20-25 mM of Hg per gram of cells. Our fluorescence spectroscopy studies indicate that the concentration of reactive thiols is also in the same range on cell membranes of *S. oneidensis,* indicating saturation of all available thiol sites by Hg before binding to carboxylates. Whereas *G. sulfurreducens* exhibit HgS_2 and HgS complexes although it has more reactive thiols on its cell envelope when compared to *S. oneidensis*. *G. sulfurreducens* may exhibit HgS_3 complexes at much lower Hg concentration range, which is difficult to access using XAS. The presence of Cl^- reduced Hg adsorption on cells significantly because of the formation of Hg-chloro aqueous complexes. The XAS studies indicate that the structure of the Hg surface complex on the cell membranes is not affected by the presence of Cl^-.

Our current studies are in progress- i) to evaluate the site density of thiols on cell envelope, and how they vary between different organisms under different environmental conditions, and ii) the role of DOM on Hg interactions with different bacteria under different pH and NOM concentrations. Mercury is a common contaminant at several DOE sites, and our study provides important clues on the understanding of the ultimate fate and biological toxicity of Hg at these sites.

Mercury Release from Organic Matter (OM) and OM-Coated Mineral Surfaces

K.L. Nagy (PI), K. Kearney, K. Stallings—*U. of Illinois Chicago*; J.N. Ryan, B.A. Poulin—*U. of Colorado Boulder*, G.R. Aiken, *USGS*; A. Manceau, *CNRS and U. Joseph Fourier*

Mercury released to the environment at the U.S. Department of Energy's Oak Ridge Y-12 Site during the Cold War is now distributed downstream in the floodplain of East Fork Poplar Creek as Hg(II) bound to natural organic matter, mercury sulfide minerals, and methyl-mercury. Strong binding to reduced sulfur in soil or dissolved natural organic matter, organic matter coatings on mineral surfaces, or sulfide minerals may immobilize mercury(II) and/or inhibit methylation reactions. This project is focused on identifying and quantifying binding and release mechanisms of Hg to organic matter, clay minerals, and soils characteristic of the floodplain. We hypothesize that (1) Hg(II) release from reduced sulfur sites requires biogeochemical redox-active agents, whereas release from oxygen sites does not; (2) Mercury bonded to organic matter on clay mineral surfaces is immobilized to a greater extent than Hg(II) adsorbed to uncoated clays; and, (3) Release rates are proportional to the quantity and type of binding site, each of which has a different molecular configuration and therefore different binding strength.

We are investigating adsorption and release of Hg(II) in controlled laboratory experiments using single minerals and natural organic matter. Synopses of sub-projects and results in progress are as follows. (1) Mercury(II) uptake on vermiculite, which comprises 12 to 16% of all minerals in the floodplain soil (N 35°57.959; W 84°21.570), shows an adsorption edge between approximately pH 7.5 and 9.5 in experiments using ~11 mg of solid in 30 mL of an initial 100 ppb Hg(II) solution. Downward shifts of pH by around one pH unit across the edge do not result in mercury(II) release. Work is underway to measure Hg(II) uptake in the presence and absence of well-characterized dissolved organic matter similar to that leached during simulated flooding and drying experiments from floodplain soils (see below). (2) Mercury(II) release from cinnabar under reducing conditions is somewhat higher in the presence of simple quinones, is not pH-dependent over the range of 4.0 to 7.0, and decreases with increasing mass. (3) Using Hg-L_3 edge EXAFS spectroscopy we have characterized the kinetics of mercury(II) binding to dissolved organic matter. (4) To characterize Hg binding to the EFPC soils, we have reassessed how to quantify sulfur speciation in natural organic matter using S-K edge XANES spectra. We refined the Gaussian curve fitting method commonly applied and also used a new linear combination fitting approach to determine sulfur speciation.

We are characterizing mercury release from soil cores collected from the top few tens of cm at a stream bank and floodplain site along the East Fork Poplar Creek downstream from Oak Ridge in simulated flooding and drying experiments (Poulin et al., this volume). Mercury concentration, mercury physiochemical speciation via selective sequential extraction, organic matter content, elemental composition, cation exchange capacity, and soil mineralogy were determined in undisturbed, intact soil cores. Pore fluids during flooding periods were analyzed for total dissolved mercury, elemental indicators of redox state, dissolved sulfate and sulfide, dissolved organic carbon, and colloids. Distinct differences in mercury release kinetics and release mechanisms were observed between O and A horizons. Work is in progress on identifying Hg binding using S-K edge XANES and Hg-L_3 edge EXAFS spectroscopy.

Molecular Mechanisms and Kinetics of Microbial Anaerobic Nitrate-Dependent U(IV) and Fe(II) Oxidation

Peggy A. O'Day (PI), Maria Pilar Asta, Samuel Traina—*U. of California Merced*; Peng Zhou, Carl Steefel, Harry R. Beller—*LBNL*

In this project, we are combining molecular genetic, spectroscopic, and microscopic techniques with kinetic and reactive transport studies to describe and quantify biotic and abiotic mechanisms underlying anaerobic, nitrate-dependent U(IV) and Fe(II) oxidation, which influences the long-term efficacy of *in situ* reductive immobilization of uranium at DOE sites. In these studies, *Thiobacillus denitrificans*, an autotrophic bacterium that catalyzes anaerobic U(IV) and Fe(II) oxidation, is used to examine coupled oxidation-reduction processes under either biotic (enzymatic) or abiotic conditions in batch and column experiments with biogenically produced $U^{IV}O_2(s)$. Research is focused on identifying the primary redox proteins that catalyze metal oxidation, environmental factors that influence protein expression, and molecular-scale geochemical factors that control the rates of biotic and abiotic oxidation.

Biogenic $UO_2(s)$ was synthesized under anaerobic conditions (using *S. oneidensis* strain MR-1) following previously published methods. Mixtures of biogenic $UO_2(s)$ and quartz were packed into 1 mL or 5 mL polypropylene columns. For experiments in the presence of *T. denitrificans,* cells were harvested anaerobically, washed and resuspended, mixed with quartz and biogenic $UO_2(s)$, and packed into the columns. Oxidation experiments were carried out in the dark at 25±2°C in an anaerobic glove box (10%H_2, 90%N_2) in buffered solution (MOPS, pH ~ 7.2). In abiotic experiments, $UO_2(s)$ oxidation by nitrate (up to 20 mM) was relatively slow; higher dissolved U concentrations were observed in abiotic experiments with nitrite (up 20 mM). Reactive transport modeling (using Crunchflow) of abiotic column experiments, which included sorption of U(VI) in the column, simulated steady-state U release. In the presence of *T. dentrificans* and 10 mM nitrate, higher rates of dissolved U release were observed compared with abiotic controls, suggesting that *T. dentrificans* catalyzed the oxidative dissolution of $UO_2(s)$. Characterization by synchrotron XAS showed higher fractions of U(VI) compared to U(IV) in post-experiment solids reacted with higher dissolved nitrite concentrations. Structural analysis of biogenic $UO_2(s)$ by EXAFS suggested variable particle size and/or a variable degree of local structure disorder. Spatially resolved characterization of samples reacted with nitrite and Fe(II) solutions by SXTM showed association of U with C and Fe around edges of $UO_2(s)$ particles. Experiments examining Fe(II) and Fe(III) in coupled redox reactions are in progress.

Current work with *T. denitrificans* focuses on determining the enzymes responsible for anaerobic, nitrate-dependent Fe(II) oxidation. We previously reported that two *c*-type cytochromes, Tbd_0187 and Tbd_0146, were involved in anaerobic nitrate-dependent U(IV) oxidation in *T. denitrificans*. However, we have found that these same mutants were *not* defective in nitrate-dependent Fe(II) oxidation. Here we report on efforts to identify genes involved in anaerobic Fe(II) oxidation in *T. denitrificans* based on screening of its Tn*5* transposon mutant library; over 10,000 mutants have been screened to date, with defects in Fe(II) oxidation as great as 40%. One mutant that is 27% defective in Fe(II) oxidation relative to the wild-type has the Tn*5* transposon inserted in a putative *c*-type cytochrome. The insertion is downstream of the CXXCH heme-binding motif. A deletion knockout mutant for the disrupted gene is under construction, and more mutants from the library are being screened.

Effects of Pore Structure Change and Multiscale Heterogeneity on Contaminant Transport and Reaction Rate Upscaling

C.A. Peters (PI), M.A. Celia—*Princeton U.*; W.B. Lindquist, *SUNY Stony Brook*; K.W. Jones, *BNL*; W. Um, M. Rockhold—*PNNL*

Mineral dissolution and precipitation in porous media alters pore network structure and subsequent flow velocities, creating complex interactions between reaction and transport. This project investigates mineral reactions and alterations in flow permeability in a multi-scale, multi-dimensional study that combines experimentation, modeling and imaging. Primarily, we are targeting the reaction of highly caustic, radioactive waste solutions with subsurface Hanford sediments, and the immobilization of radionuclides.

(1) Reactive flow experiments. We are conducting experiments using reactive flow-through columns of several sizes. The most recent experiments performed at PNNL used 7.6-cm-long x 1.9-cm-diameter columns. Separate columns were packed with quartz sand and with Hanford sand to evaluate the influence of mineralogy on transport and reaction rates and changes in pore-structure resulting from contact with a synthetic tank waste liquid (STWL). Another column was flown through using STWL without Al, in which only dissolution is occurring, which results in porosity increases. Experiments have shown porosity changes ranging from 0.04 to 0.11, resulting in calculated permeability reductions on the order of 2 to 3 times. Also observed were changes in pore structure that would affect the unsaturated hydraulic properties of the sediments (moisture retention characteristics and relative permeability).

(2) Multiscale Imaging and Analysis. To examine the reaction-induced alterations of pore structure, we are using 3D X-ray computed microtomography, and 2D backscattered electron and energy-dispersive X-ray imagery. In our early work, columns reacted at PNNL were imaged using X-ray computed microtomography at BNL, but recently we are using an XMT system at EMSL (PNNL). The 3D images are analyzed in novel ways to quantify pore structure, mineral distribution, structural changes and fluid-air and fluid-grain interfaces. This informs pore network models for calculating expected changes in permeability and reactive surface area. At Princeton, using the method we have developed for sectioning the columns and using SEM and EDX for 2D imaging, sub-pore scale structural alterations have been observed. For example, secondary cancrinite precipitates were observed in reacted columns as a relatively uniform coating on all grain surfaces. 2D imaging also revealed that Hanford sediments have a large amount of intragranular porosity and that secondary precipitates were observed in intragranular space.

(3) Multiscale Modeling and Up-Scaling. This project involves modeling at several spatial scales. The column experiments are being modeled using the STOMP simulator to evaluate ways of representing effective reaction rates and feedback between changes in pore structure and the permeability relations needed for the continuum-scale. The column experiments have also been modeled using a custom reactive transport model to investigate the capacity for intragranular pore space in Hanford sediments to sequester and release radionuclides. Long-term leaching of Cs from intragranular pores is predicted to prolong the period of secondary contamination at the site. Finally, a specific application of our pore-network reactive transport modeling was aimed at understanding how CO_2-rich brines alter rocks containing fast-reacting minerals such as calcite and dolomite. These simulations of porosity and permeability evolution reveal the importance of considering different flow regimes (advection-controlled vs diffusion-controlled) and inlet fluid mixing scenarios. We have shown that there is not a unique continuum-scale permeability relationship that describes all reactive flow scenarios for even the same porous medium and that the spatial and temporal evolution of the network dictates the unique relationship between porosity and permeability.

Design and Application of Proteomics Workflows to Monitor and Predict *In Situ* Activity of Metal-Reducing Bacteria

K. Chourey, X. Liu, S. Nissen—*ORNL*; F.E. Löffler, *U. of Tennessee*; M. Shah, R.L. Hettich—*ORNL*; K. Ritalahti, T. Vishnivetskaya, A. Layton, G. Sayler, S.M. Pfiffner (PI)—*U. of Tennessee*

The expression of *c*-type cytochromes has been correlated with bacterial metal and U(VI) reduction activity. With recent advances in environmental proteomics, *c*-type cytochrome expression may serve as an indicator for microbial activity contributing to metal and U(VI) reduction. Cytochrome expression was studied in *Anaeromyxobacter dehalogenans* strain 2CP-C, *Geobacter daltonii* strain FRC-32, and *Shewanella oneidensis* strain MR-1, which represent bacterial clades commonly detected in U-contaminated soils and sediments. Based on the presence of characteristic heme-binding motifs, 68, 42 and 72 putative c-type cytochromes have been predicted for *A. dehalogenans*, *S. oneidensis* and *G. daltonii*, respectively. Biomass of each strain was collected from media amended with different electron acceptors, and global proteome measurements recovered protein datasets that were queried against predicted proteome databases via SEQUEST. Variable levels of *c*-type cytochrome expression were observed for each bacterial species grown with different electron acceptors. In *A. dehalogenan*s, 53 out of 68 predicted *c*-type cytochromes were detected across nine growth conditions tested. In *S. oneidensis*, 23 *c*-type cytochromes out of annotated 42 were identified. In *G. daltonii*, the expression of 29 out of 73 *c*-type cytochromes was noted; however, only three growth conditions have been tested so far. Extending this work to field samples, groundwater filters from the emulsified vegetable oil (EVO) demonstration (4 days post amendment) were selected for proteomic analysis. The peptide profiles were searched with two databases: (i) an artificial database of ~ 12 sequenced soil microbes and (ii) the database of three model species. Initial results confirmed that proteins, including *c*-type cytochromes, can be identified and that EVO injection resulted in metaproteome differences. Current efforts aim at the integration of quantitative DNA and RNA measurements with the proteomics datasets to obtain a refined picture of abundance and activity of bacteria relevant for metal and radionuclide reduction. Knowledge gained from these studies will help to better predict the fate of subsurface radionuclides, thus enabling science-based decision making for long-term site management.

Development of a Self-Consistent Model of Plutonium Sorption: Quantification of Sorption Enthalpy and Ligand-Promoted Dissolution

B.A. Powell (PI), Y. Arai (co-PI), H. Emerson, S. Estes, S. Herr, A. Hixon, T. Miller, Y. Xie—*Clemson U.*; U. Becker (co-PI), R.C. Ewing (co-PI), S. Fernando, J. Zhang—*U. of Michigan*; D.I. Kaplan (co-PI), *SRNL*

This project is focused on developing a fundamental understanding of the environmental behavior of plutonium through the development of a mechanistic model of plutonium speciation in subsurface environments. The speciation model will be a thermodynamic surface complexation model of plutonium sorption to mineral surfaces that is self-consistent with macroscopic batch sorption data, X-ray absorption spectroscopy (XAS) measurements, electron microscopy analyses, and quantum-mechanical calculations. The overarching hypothesis of the project that the strong interactions of actinides with mineral surfaces result from the formation of inner sphere complexes with a limited number of high-energy surface sites, and that displacement of solvating water molecules from the actinide and mineral surface during sorption is energetically favorable and results from a large increase in entropy.

In order to test the above hypothesis without involving the complex redox chemistry of plutonium, Eu(III) and Np(V) were selected as strongly and weakly hydrated, respectively, species. Sorption of Eu(III) to hematite increased strongly with temperature while Np(V) exhibited little change. This is consistent with our hypothesis showing that sorption of Eu(III) is entropically driven as hydrating waters are removed from the mineral surface and the Eu(III) ion upon sorption. A series of unique, high energy k-shell Eu EXAFS measurements were performed and confirmed at the coordination number of Eu(III) decreases upon sorption (consistent with the removal of hydrating waters) and that a bidentate, mononuclear surface species forms. Sorption enthalpy and entropy values were calculated using a surface complexation model and the van't Hoff equation. Consistent with the overarching hypothesis of this work, sorption of Eu(III) was entropically driven. This observation of the dominant entropy term is consistent with the experimental hypothesis that the energetic favorability of actinide surface complex formation is strongly influenced by positive sorption entropies, which are mechanistically driven by displacement of solvating water molecules from the actinide and mineral surface during sorption. These results are currently being compared with quantum mechanical models of Eu(III) sorption as both inner and outer sphere complexes.

Sorption of Pu(IV) and Pu(V) to goethite has exhibited a similar increase with increasing temperature. These experiments as well as many others in the literature, have observed surface mediated reduction of Pu(V) to Pu(IV) although the specific mechanism, including the reductant, is still unclear. Experiments are being performed to examine possible mechanisms. Experiments with multiple Pu isotopes (^{238}Pu and ^{242}Pu) have shown that alpha particle generated radiolysis does not appear to significantly influence the reduction rate. Attempts to remove trace Fe(II) during hematite nanoparticle synthesis by aeration did not influence the observed reduction rates. Furthermore, the reduction rate on the Pu(V) nanoparticles was significantly influenced by light, indicating that semiconducting properties of the mineral can influence the electron transfer reaction. It is possible that goethite may indirectly participate in Pu(V) reduction by acting as a catalyst or electron shuttling device to transfer charges between coadsorbates, as suggested by recent quantum mechanical modeling of uranyl reduction on goethite in the presence of hydrogen disulfide.

These Pu sorption studies will be used to develop thermochemically based surface complexation models as discussed above for the Eu(III)-hematite system. The surface complexation constants will be used to predict sorption of Pu to sediments from the Savannah River Site and the Hanford Site. Experiments quantifying sorption of Th(IV), Pu(IV), Pu(V), and Np(V) have been completed. Based on differences between systems with initially Np(V) and Pu(V), both sediments appear to facilitate surface mediated reduction of Pu(V) to Pu(IV).

Scale-Dependent Fracture-Matrix Interactions and Their Impact on Radionuclide Transport

Harihar Rajaram (PI, hari@colorado.edu), *U. of Colorado*; Russell Detwiler (PI, detwiler@uci.edu), *U. of California Irvine*

Matrix Diffusion and Adsorption within a rock matrix are important mechanisms for retarding transport of radionuclides in fractured rock. Due to computational limitations and difficulties in characterizing complex subsurface systems, diffusive exchange between a fracture network and surrounding rock matrix is often modeled using simplified conceptual representations. There is significant uncertainty in "effective" parameters used in these models, such as the "effective matrix diffusivity". Often, these parameters are estimated by fitting sparse breakthrough data, and estimated values fall outside meaningful ranges (e.g. effective matrix diffusivity much greater than free molecular diffusivity), because simplified interpretive models do not consider complex three-dimensional flow. There is also evidence for an apparent scale-dependence in effective matrix diffusivity, also a consequence of using over-simplified interpretive models. These observations raise questions on whether fracture-matrix interaction parameters estimated from small-scale tracer tests can be used for predicting radionuclide fate and transport at the scale of DOE field sites.

High-resolution three-dimensional Discrete-Fracture-Network-Matrix (DFNM) models based on well-defined local scale transport equations can help to address some of these questions. Due to tremendous advances in computational technology over the last 10 years, DFNM modeling in relatively large domains is now feasible. The overarching objective of our research is to use DFNM modeling to improve fundamental understanding of how effective parameters in conceptual models are related to fracture network structure and matrix properties. An advanced three-dimensional DFNM model is being developed, which combines upscaled particle-tracking algorithms for fracture-matrix interaction and a parallel fracture-network flow simulator. The particle-tracking algorithms allow complexity in flow fields at different scales, and track transport across fracture-matrix interfaces based on rigorous local approximations to the transport equations. This modeling approach can incorporate aperture variability, multi-scale preferential flow and matrix heterogeneity. The code can handle computational domains with about 1 Billion nodes for flow and 1 Billion particles for transport. The overarching goal is to obtain insights on (i) the relationship between effective fracture-matrix interaction parameters, network structure and matrix properties and (ii) their scale dependence in different types of fractured rock environments.

We will demonstrate results obtained using "high-resolution" particle tracking algorithms at the single fracture scale and at fracture intersections; and "upscaled" particle-tracking algorithms, which allow use of much larger time steps. The upscaled algorithms have been verified using the "very-high-resolution" simulation results as a benchmark, and hold significant promise as an efficient tool for field-scale simulation. A generalized approach for particle tracking in interfaces has been developed, which captures the complexities of Stokes flow through variable-aperture intersections with excellent accuracy. Flow simulations in fracture networks illustrate the important role of head variations along an intersection in driving flow through slow advective loops in dead-end fractures. Such loops have been postulated as potential mechanisms for producing long-tailed behavior even in the absence of true matrix diffusion, and often confused for matrix diffusion. Ongoing efforts are focused on extending the network flow and transport simulations to very large scales, and including the influence of adsorption.

The final stage of our research will specifically target applications at the Oak Ridge Field Research Center, former nuclear test sites in Nevada (e.g. the Shoal and Bullion tests), and other field sites (e.g. Mirror Lake) where tracer tests were conducted to obtain fracture-matrix interaction parameters for site-scale transport models. We will explain the differences in behavior observed at these sites using our network model and subsequently simulate radionuclide transport at the site scale and 100+ year time scales.

From Nanowires to Biofilms: An Exploration of Novel Mechanisms of Uranium Transformation Mediated by *Geobacter* Bacteria

Dena L. Cologgi, Sanela Lampa-Pastirk, Allison M. Speers—*Michigan State U.*; Shelly Kelly, *EXAFS Analysis*; Gemma Reguera (PI, reguera@msu.edu), *Michigan State U.*

An insufficient knowledge of the biological mechanisms of contaminant transformation often limits the performance of *in situ* subsurface bioremediation and long-term stewardship strategies. The *in situ* stimulation of Fe(III) oxide reduction by *Geobacter* bacteria, for example, leads to the concomitant precipitation of U(VI) from groundwater. However, the biological mechanism behind this reaction has remained elusive for almost two decades. Because Fe(III) oxide reduction requires the expression of conductive pili in *Geobacter*, we evaluated their contribution to uranium reduction in piliated an non-piliated strains of *Geobacter sulfurreducens*. We observed a direct correlation between the levels of piliation and the extent of U removal and reduction. Furthermore, pili expression also prevented the permeation of U in the cell envelope and its periplasmic mineralization. As a result, pili expression preserved the vital respiratory activities of the cell envelope and the cell's viability. Uranium preferentially precipitated along the pili as a mononuclear U(IV) complexed by carbon containing ligands and, to a lesser extent, on outer membrane redox-active foci. These results demonstrate a previously unrecognized role for *Geobacter* pili in the extracellular reduction of uranium and highlight its essential function as a catalytic and protective cellular mechanism that is of interest for the bioremediation of uranium-contaminated groundwater.

The expression of pili by *Geobacter* also promotes cell aggregation and biofilm formation. Thus, we investigated the contribution of biofilms of *G. sulfurreducens* to U transformations. Multilayered biofilms reduced substantially more U than planktonic cells and for prolongued periods of time. They also tolerated higher concentrations of U, making them an attractive option for the development of permeable biobarriers for U bioremediation. While U was immobilized by both monolayered and multilayered biofilms, only pili-expressing multilayered biofilms reduced the U. Similarly, a pili-deficient mutant, which is interrupted at the monolayer stage, immobilized but did not reduce U. Thus, the pili are also the primary U reductase in the biofilms. To gain more insights into how biofilms transform U, we screened a library of 4,000 transposon-insertion mutants and identified mutants with biofilm defects. After identifying the interrupted genes and their functions, we built a genetic model for biofilm formation that links biofilm development to the mechanisms of U transformations. This study confirmed the role of *Geobacter* pili in the biofilm formation and U reduction and identified molecular markers involved in biofilm electron transport and metabolism that can be used to predict and monitor the physiological state of *Geobacter* bacteria during the *in situ* bioremediation of U.

Geoelectrical Surveys at the Oak Ridge Field Research Center

Oak Ridge ORFRC (Principal Investigator: André Revil)

A. Revil (PI), *Colorado School of Mines*; S. Hubbard, *LBNL*; M. Karaoulis, M. Skold—*Colorado School of Mines*; N. Spycher, *LBNL*; D. Watson, *ORNL*; Y. Wu, *LBNL*

We performed a 3D resistivity survey and self-potential mapping at the Oak Ridge Field Research Center (ORFRC) to locate contaminant migration from the former waste disposal S3 ponds. The S3 area historically received liquid waste containing uranium and nitric acid, which has leached into the underlying groundwater. The pH of the contaminated groundwater is less than 4 and the electrical conductivity is very high, exceeding 5 S/m at several locations in the plume. The groundwater composition made it possible to detect zones of contaminant migration using electrical resistivity. A total of 17 resistivity profiles were collected along three sides and downgradient of the former S3 ponds. All but two profiles used an electrode spacing of 2 m with a total profile length of 126 m while the electrode spacing of the two 235 m long profiles was 5 m. The electrical conductivity of water samples collected from monitoring wells and inverted electrical conductivity at the same locations are correlated. The correlation provides evidence that ERT can be used to detect plumes with high total dissolved solids emanating from the former ponds. ERT measurements were also inverted to create a 3D resistivity model. Zones of low resistivity correspond to zones where contamination is observed. Time-lapse electrical resistivity measurements collected along one profile downgradient of the S3 ponds were inverted using a new time-lapse algorithm with an active time constrain approach to investigate the effect of infiltration on plume dilution and attenuation. Decreasing electrical resistivity was observed immediately after heavy rainfall and the greatest electrical resistivity was observed between May and September, which is the driest period during the year. Self-potential profiles were corrected for the presence of anthropogenic noise and provide further evidence for the location of the plumes.

In addition to the field measurements, we also investigated the petrophysical properties of saprolite core samples in the laboratory including complex conductivity and streaming potential coupling coefficients at different salinities and pH. Contaminated saprolite was neutralized in a separate column experiment. The results showed that complex conductivity was related to the pH and highlighted the large acidity accumulated in the sediments. The formation factor of saprolite samples measured in the laboratory was less than the formation factor estimated from field measurements. The difference is likely related to disturbance of the samples during sampling and repacking into columns. The electrical surface conductivity determined in the laboratory, on the other hand, corresponds to what was observed in the field and was related to the relative clay content of the samples. The background sample collected from the greatest depth (26 feet) contained more illite, smectite and chlorite than samples collected from 9 and 16 feet and also exhibited greater surface conductivity.

Microbial Communities Associated with Anaerobic Metabolism and U(VI) Reduction in ORFRC Area 2 Sediment Amended with Acetate or Ethanol

E. Roden (PI), B. Converse, T. Wu, E. Shelobolina—*U. of Wisconsin*; R. Findlay, *U. of Alabama*; Q. Jin, *U. of Oregon*

This project examined bulk terminal electron accepting processes (TEAPs) and U(VI) reduction in ORFRC Area 2 sediments undergoing biostimulation through ethanol or acetate amendment. The central hypothesis is that patterns of U(VI) reduction will be linked to shifts in the predominant TEAP and to changes in abundance and activity of different types of respiratory microorganisms. Bulk TEAPs, U(VI) reduction, and microbial community composition were monitored in semicontinuous culture reactors (SCRs) (10 day residence time) amended with different amounts acetate or ethanol (either 0, 0.1 or 0.2 mM d^{-1}, in duplicate, for a total of 10 reactors) over a ca. 8-month period. Overall TEAP patterns were similar in the acetate and ethanol-amended reactors. Complete consumption of incoming nitrate was observed in all amended reactors. Complete reduction of Fe(III) phases (oxides and clays) took place in sediments receiving the higher levels of electron donor addition, in which sulfate reduction became active after 2-3 months. Roll tube enumerations confirmed major stimulation of Fe(III)- and sulfate-reducing populations. Patterns of U(VI) reduction indicated that the extent of reduction was similar in acetate vs. ethanol-fed reactors, and proportional to the amount of electron donor added. A major increase in the accumulation of residual HNO3-extractable U (presumably uraninite) took place during the transition between Fe(III) and sulfate reduction, indicating significant contribution of sulfate reducing bacteria to U(VI) reduction. The microbial community response to electron donor amendment in the SCRs was assessed via quantitative PCR (q-PCR) analysis of taxa-specific 16S rRNA genes and selected functional genes, 16S rRNA gene pyrosequencing, and ^{13}C stable isotope probing (SIP) of bacterial PLFAs. The q-PCR analyses revealed a ca. 10-fold increase in total 16S rRNA gene copies in the amended reactors. *Betaproteobacterial* 16S rRNA gene and *nosZ* functional genes were most abundant, increasing ca. 5-fold in the amended reactors and indicating a predominance of nitrate-reducing biomass in the reactors. Densities of *Deltaproteobacterial* 16S rRNA genes were lower, but increased more dramatically (ca. 100-fold) in response to electron donor addition. Although a full analysis of the 16S rRNA gene pyrosequencing results (7 time points for each of the 10 reactors) is not yet available, data from ca. 4 months into the experiment revealed communities dominated by known *Betaproteobacterial* nitrate-reducing taxa (e.g. *Dechloromonas*, *Herbaspirillum*, *Azoarcus*). Metal- and sulfate-reducing taxa (e.g. *Anaeromyxobacter*, *Desulfotomaculum*) were present in the libraries, but their relative abundance was generally much lower than putative nitrate-reducers. Bacterial PLFAs showed dramatic shifts with ethanol or acetate amendment. Profiles from unamended sediments were dominated by the fatty acids 16:0 and cy17:0, while amended sediments showed increased importance 16:1w7 and 18:1w7 and a reduction in cy17:0. Short-term (3-day) SIP (^{13}C-labled ethanol or acetate) assays conducted periodically during the experiment showed incorporation of ^{13}C values into some but not all PLFAs. The most heavily labeled fatty acids in assays conducted at day 150 were associated with metal/sulfate-reducing bacteria and other anaerobic taxa (br17:1a, 10Me16:0, i15:0). The collective geochemical and microbial community analysis results provide the basis for application of a population-based biogeochemical reaction model to the SCR experiments.

Processes Affecting Iodine-127,129 Speciation and Mobility in Two Contaminated DOE Plumes

Peter H. Santschi (PI, Santschi@tamug.edu), R. Brinkmeyer, K.A. Schwehr, S. Zhang, C. Xu, H-P. Li—*TAMUG*; D. Kaplan, K.A. Roberts—*SRNL*; C. Yeager, *LANL*

Background: ^{129}I is among the key risk drivers at all DOE nuclear disposal facilities. In our on-going SBR project we developed several highly sensitive iodine speciation techniques and one of our key findings was that sediment bacteria are capable of influencing the chemical behavior of iodide, the most common form of iodine found in groundwater, via accumulation and oxidation to iodate. In turn, sediment bacteria, as well as reduced metals in the aquifer, are capable of reducing iodate to organo-iodine via iodide. Based on this conclusion and others, we proposed the following **hypotheses** and objectives. **H1:** Despite its thermodynamic stability, iodide is readily transformed to organic iodine and iodate, a transformation that is facilitated by biotic (e.g., non-specific oxidative enzymes) and abiotic (e.g., redox reactions by Mn(IV,II), Fe(III,II), or hydroquinone/quinone moieties in humic acids) factors. **H2:** Microbial mediated oxidation of iodine species irreversibly transfers I into natural organic matter, of which aromatically bound iodine is the most stable. **H3:** I mobility is dependent on physico-chemical speciation, which decreases from iodide to iodate to organic iodine, and from low molecular weight to high molecular weight to particulate organic I species. Our **approach** will determine how microbial activity, concentrations and chemical speciation (iodide, iodate, and organo-I) of ^{129}I and ^{127}I, as well as redox reactive metals and organic carbon, affect I mobility and isotopic fractionation in groundwater samples from contaminated SRS and Hanford site locations.

Highlights: A sensitive and rapid method was developed which enabled us to determine isotopic ratios (^{129}I/^{127}I) of speciated I via GC-MS [*1*]. The fact that I occurs in multiple oxidation states leads to complex biogeochemical cycling of I. We demonstrated that the mobility of I species greatly depends on the I concentration used [*2*], mostly due to covalent binding of I to a limited number of aromatic C moieties of the particle surface and in solution [*3-5*]. Bacterial accumulation of I^- followed by iodination of cellular organic molecules was demonstrated, but likely plays a minor role in the formation of organic I in the subsurface [*6*]. First-order calculations indicate that the modest increase of 0.7 pH units detected in the study site groundwater over the last 17 years since closure of the basins may be sufficient to produce the observed increased groundwater ^{129}I concentrations [up to 1 nCi/L; [*7*]. Removal of I from the groundwater through the formation of high molecular weight organo-I complexes is modified by the release of more mobile organo-I species [*8,9*]. Extracellular, enzymatic oxidation of I^- and organic acid production by bacteria significantly contribute to organo-I formation [10,11].

References: [*1*] Zhang, S. et al., 2010. *ES&T,* 44, 9042-9048. [*2*] Schwehr, K.A. et al. 2009. *ES&T,* 43, 7258–7264. [*3*] Zhang S. et al. 2011. *ES&T,* 45, 5543-5549. [*4*] Xu, C. et al. 2011. *ES&T,* 45, 9975–9983. [*5*] Xu, C. et al. 2012. GCA, in revision. [*6*] Li, H.-P. et al. 2011. *Appl. Env. Microbiol.* 77, 2153–2160. [*7*] Kaplan, D.I. et al. 2011. *ES&T,* 45, 489-495. [*8*] Otosaka, S. et al. 2011. *Sci. Tot. Env.* 409, 3857–3865. [*9*] Xu, C. et al. 2011. GCA, 75, 5716–5735. [*10*] Li, H.-P. et al. 2012, in press. [*11*] Li, H.-P. et al. 2012. *ES&T,* submitted.

The Role of Natural Organic Matter in Immobilizing or Re-mobilizing Plutonium in the Far Field of the Savannah River Site, USA

Peter H. Santschi (PI, Santschi@tamug.edu), Kathleen A. Schwehr, Chen Xu—*TAMUG*; Patrick G. Hatcher, Nicole DiDonato—*Old Dominion U.*

Plutonium (Pu) contamination of soils or groundwater can be a serious problem at DOE sites. Pu is an element with a complex chemistry, exhibiting a number of oxidation states in aquatic environments, predominantly Pu(IV) and Pu(V). In surface and subsurface waters, the prevailing Pu oxidation state depends on the abundance of natural organic matter (NOM) and selected minerals. NOM reducing moieties can significantly modify the mobility of Pu in the environment by producing colloidal organic carriers that strongly bind Pu, mostly as Pu(IV).

Objectives: *Objective 1:* Build on our successful characterization of the chemical composition of organo-Pu species in water leachates from the remediated RFETS site by using a similar approach on other soils or aquifer sediments from different Pu-contaminated DOE sites. These Pu-associated ambient colloidal organic leachates will then be compared to those that have formed over time when a Pu tracer was added to the same soils, and will be used for transport studies. *Objective 2:* Determine the biogeochemical factors that give mobility and/or immobility to the colloidal organic carrier molecule. This requires a full molecular level characterization of the chemical composition of strongly Pu-binding biopolymers in NOM extracted from laboratory incubation, leaching and column studies with these soils. *Objective 3:* Determine thermodynamic stability constants of Pu to the well-characterized Pu-carrying NOM compounds isolated from Pu contaminated soils.

Hypotheses: *H1:* Mobile organic Pu species from Pu contaminated soils contain biomarker compounds that can be used to predict the future spread of Pu contamination as well as Pu bioavailability. *H2:* Amphipilic EPS molecules of moderate molecular weight (e.g., 5-50 kDa) containing reducing moieties (e.g., hydroquinones, ferredoxins, or flavodoxins) with clustered ligand groups for Fe(III)-binding are most effective in immobilizing organo-Pu species that sorb to sediment particles, while colloids of ≤105 kDa molecular mass are potentially mobile in groundwater. *H3:* Binding constants of Pu to well characterized Pu-carrying NOM compounds isolated from Pu contaminated soils depend on applied Pu concentrations due to the well-known surface site heterogeneity effect.

Experimental Design: The objectives of this proposal will be accomplished through collaborative research at TAMUG and ODU, as well as researchers from national laboratories. **The potential benefits** of the project to DOE are a better understanding of the role and mobility of different organic bio- and geopolymeric Pu vectors that will greatly advance science in general, and in particular, biogeochemistry of Pu at low, environmental levels.

Preliminary Results: In the present study, SRS sediment cores collected from a reservoir lake, which was used as part of a cooling water loop for two production reactors during the period 1961 to 1964, is analyzed for elemental composition and plutonium content. A significant positive correlation is shown between NOM content and Pu concentration. Humic acid obtained from these sediments extracted following the IHSS standard method is prepared in different ways, and Kds of Pu to the humic acid fraction are calculated and compared. Pu bound NOM is further separated and purified using isoelectric focusing method [Xu et al., 2008. ES&T 42, 8211-8217]. Composition of the Pu enriched organic fraction is determined by elemental analysis, FT-IR, NMR, and FT-ICR-MS.

Uranium Attenuation and Release Investigated at the Molecular and Column Scales: Responses to Geochemical Gradients in Geologic Media

K. Savage (PI), Wenyi Zhu—*Wofford College*; M.O. Barnett, *Auburn U.*

Understanding relationships between physical and chemical processes at different scales is critical to effective prediction of contaminant mobility. This study addresses the molecular-scale response of dissolved uranium to advective chemical gradients, simulating ground water encountering soil and sediment matrices that are representative of subsurface environments at the Oak Ridge Integrated Field Research Challenge (ORIFRC) site.

Column experiments were devised to investigate the role of changing fluid composition on mobility of uranium through a sequence of geologic media. Synthetic ground waters were pumped upwards at 0.05 mL/minute for 21 days through layers of quartz sand alternating with layers of uncontaminated soil, quartz sand mixed with illite, quartz sand coated with iron oxides, and a second soil layer. Increases in pH or concentration of phosphate, bicarbonate, or acetate were imposed on the influent solutions after each 7 pore volumes while uranium (as uranyl) remained constant at 0.1mM. A control column maintained the original synthetic groundwater composition with 0.1mM U. Pore water solutions were extracted to assess U retention and release in relation to the advective ligand or pH gradients. Following the column experiments, subsamples from each layer were characterized using microbeam X-ray absorption spectroscopy (XANES) in conjunction with X-ray fluorescence mapping.

U retention of 55 – 67 mg occurred in phosphate >pH >control >acetate >carbonate columns. The mass of U retained in the first-encountered quartz layer in all columns was highest and increased throughout the experiment. The rate of increase in acetate- and bicarbonate-bearing columns declined after ligand concentrations were raised. U also accumulated in the first soil layer; the pH-varied column retained most, followed by the increasing-bicarbonate column. The mass of U retained in the upper layers was far lower.

A preliminary transport model that incorporates surface complexation, using the code PHREEQC (7, USGS, V.2.18), captures the major features observed in the carbonate and pH gradient experiments but is less successful for the phosphate column. The acetate column was not modeled. In the carbonate column, the model indicates that uranium complexes adsorbed to quartz can account for the observed U uptake and subsequent release. The pH-varied simulation showed increasing pH to lead to U retention, as observed.

Speciation of U, interpreted from microbeam XANES spectra and XRF maps of sediments collected from the columns, varied within and among the materials. Evidence of minor reduction to U(IV) was observed in the first-encountered quartz layer in the phosphate, bicarbonate, and pH columns while only U(VI) was observed in the control and acetate columns. Spectral evidence suggests poorly ordered precipitates in this layer of the phosphate, acetate, and pH columns. In the soil layer, the acetate and bicarbonate columns both indicate minor reduction to U(IV), but U(VI) predominated in all columns. Evidence of precipitates in the soil layer is restricted to the control column. These results will be used to inform and refine the transport models.

Hg(II) Uptake and Methylation in Iron-Reducing Bacteria

J.K. Schaefer (PI, jschaefe@princeton.edu), O. Baars, R. Anwar—*Princeton U.*; L. Liang, B. Gu—*ORNL*; F.M.M. Morel, *Princeton U.*

Mercury uptake and methylation by microorganisms is a key first step in the accumulation of methylmercury in aquatic ecosystems such as the East Fork Poplar Creek (EFPC) in the US DOE Oak Ridge Reservation. Our current model for this process in *Geobacter sulfurreducens* is that Hg(II) enters cells by active transport where it is methylated and rapidly exported as methylmercury. To determine the likely role of a divalent metal transporter in the uptake of Hg(II), we have tested mercury methylation in the presence of a variety of essential heavy metals to act as possible competitive substrates for Hg(II) uptake. Experiments are currently on-going. Further, we have performed knock-outs of a number of putative heavy metal transporters and are now testing these mutants for the ability to take up and methylate Hg(II). Although transport appears to be a critical first step in the methylation of Hg(II), it remains unclear whether methylation occurs in the cytosol or periplasm of these organisms. To clarify this, methylmercury production was monitored in lysed spheroplasts isolated from *G. sulfurreducens*, indicating a cytosolic location for Hg methylation. Thus, mercury must cross both the outer and inner membranes prior to its methylation, and we are actively trying to identify such transporters. In addition, we have observed differences in the type of cellular exudates released during growth of methylating and non-methylating iron-reducing bacteria which have significant impacts on Hg availability. For instance, *G. sulfurreducens* produces cysteine during growth which enhances Hg(II) uptake and methylation; while *Shewanella oneidensis*, a non-methylating species, excretes an unknown compound only during anaerobic growth which renders Hg(II) unavailable to both the parent strain and to *G. sulfurreducens*. Identification of the possible compound(s) by solid-phase extraction and electrospray mass spectrometry is on-going. These results will provide a greater understanding of the biological factors governing methylmercury production in known methylating strains which is critical for controlling its accumulation in the environment.

Electron Transfer and Atom Exchange between Aqueous Fe(II) and Structural Fe(III) in Clays: Role in U and Hg(II) Transformations

A. Neumann, M.M. Scherer (PI), M. Barger—*U. of Iowa*; C. Johnson, B. Beard, L. Wu—*U. of Wisconsin Madison*; K.M. Rosso, V. Alexandrov—*PNNL*; K. Kemner, M. Boyanov, E. O'Loughlin—*ANL*

Recent advances in spectroscopic and microscopic techniques, stable Fe isotope measurements, and theoretical calculations of mineral electronic structures have lead to a new conceptual framework for the reaction of aqueous Fe(II) with Fe oxides. Fundamental processes in the reaction of aqueous Fe(II) at the Fe(III) oxide-water interface include electron transfer between aqueous Fe(II) and structural Fe(III), bulk electron conduction, and Fe(II)-Fe(III) atom exchange.

In contrast, reactions of aqueous Fe(II) with clay minerals have received much less attention and descriptions of these reactions have been limited to surface or interlayer reactions such as ion exchange, surface complexation, and/or surface precipitation. Recently, however, we showed that interfacial electron transfer between aqueous Fe(II) and structural Fe(III) occurs in a clay mineral. Whether this observation can be generalized to all iron-bearing clay minerals and whether similar Fe atom exchange processes occur in clays as observed for the heterogeneous redox reaction in Fe(III) oxides is unclear.

Studies on chemical reduction of structural Fe in smectites have showed that the type of reductant as well as smectite structural properties determine the extent of Fe reduction, as well as the speciation of the resulting structural Fe(II). Here, we investigated the reaction of well-characterized smectites differing in structural Fe content, location of structural Fe (octahedral vs. tetrahedral), and location of excess layer charge (octahedral vs. tetrahedral) with aqueous Fe(II), a reductant abundant in natural anaerobic environments.

More specifically, we used stable isotope specific Mössbauer spectroscopy to determine the extent of reduction of structural Fe in smectites after exposure to aqueous ^{56}Fe(II), which is transparent in Mössbauer spectra. Experiments with aqueous Fe(II) enriched in ^{57}Fe were also carried out to determine the exchange of stable Fe isotopes between aqueous Fe(II) and structural Fe(III) in smectites. Different pools of Fe(II) and Fe(III) were investigated by sequential extraction procedures and solid reaction products were characterized with X-ray diffraction and electron-based microscopic methods.

Coupled Biological and Micro-XAS/XRF Analysis of *In Situ* Uranium Biogeochemical Processes

J.O. Sharp (PI), D. Drennan, S. Hollenback, D. Silverman—*Colorado School of Mines*; S.M. Webb, J.R. Bargar—*SSRL*

Biogeochemical processes play a critical role in reductive uranium immobilization in groundwater found at former uranium mining and processing locations throughout the United States and other parts of the world. While microbiological and molecular studies have brought insights regarding enzymes and candidate microbes involved in bioimmobilization in contaminated aquifers, we have not yet correlated the identity and distribution of organisms associated with metal redox transformations, functionality of extracellular proteins in these systems, and complex mineral-microbe processes influencing uranium immobilization at the micrometer scale. The objective of our newly funded exploratory two-year project is to merge existing toolsets to query microbial location and distribution in conjunction with geochemical alterations in sediments. Our work is currently exploring methodologies for labeling subsurface microorganisms in the presence of sediments using fluorescent dyes and nanomaterials coupled to visualization using microprobe x-ray absorption and fluorescence spectroscopy (micro-XAS/XRF) analysis. We are also bridging efforts with other currently funded DOE projects and the Rifle IFRC (PI's Mailloux, Ranville, and Williams) with the goal of extending our research scope to include arsenic biogeochemistry. This merged approach will enable the co-visualization of microbe-metal processes in sediments and provide a mechanism to increase our understanding of heterogeneities, redox state, mineral form, and targeted biostimulation. The work has implications both for fundamental field-scale biogeochemical science as well as engineering applications and monitoring tools targeting low-cost, minimally invasive remediation of contaminated aquifers.

Molecular Mechanisms of the *mer* Operon and Hg(II)-Ligand Interactions: Combined Experimental and Computational Studies

J.C. Smith (PI), H. Guo—*U. of Tennessee*; A. Johs, L. Liang—*ORNL*; S. Miller, *U. of California San Francisco*; J.M. Parks, *ORNL*; D. Riccardi, *U. of Tennessee*; A.O. Summers, *U. of Georgia*; S.J. Tomanicek, *ORNL*; Q. Xu, *U. of Tennessee*

Mercury resistant bacteria exert a strong influence on lowering toxic methylmercury levels at contaminated sites, with the proteins and enzymes of the *mer* operon functioning as an efficient detoxification system. The *mer* operon confers resistance to mercury by encoding specific genes that facilitate uptake of mercuric species, Hg-C cleavage of organomercurials, and reduction of Hg(II) to Hg(0). Combined experimental and computational approaches are used to investigate molecular mechanisms of the *mer* operon, including intramolecular transfer and reduction of Hg(II) by the mercuric reductase MerA, the roles of specific amino acids in the conformational transitions in MerR triggered by Hg(II) binding, and the energetics of Hg(II)-ligand binding interactions.

MerR responds specifically to nanomolar levels of Hg(II) by activating the transcription of *mer* genes. Binding of Hg(II) to MerR was found previously to induce a significant reorientation of the two DNA-binding domains relative to each other, which leads to underwinding of operator DNA followed by transcription. Four MerR mutants, Y27F, Y46F, K99T, and M106I, have been expressed and purified, and SAXS experiments are being performed to characterize the effects of these point mutations on the conformation of MerR. The results will reveal the roles of these key amino acids in propagating allosteric changes at the Hg(II) binding site to the DNA binding domains. MerA converts Hg(II) to less toxic Hg(0), and a pair of cysteines, C464 and C465, is involved in delivering Hg(II) to another pair of cysteines, C42 and C47, at the active site prior to reduction. The mechanisms of intramolecular Hg(II) transfer in MerA are not fully understood, as they are likely to be coupled to specific protonation/deprotonation events. A multi-step quantum mechanical/molecular mechanical (QM/MM) approach is applied to explore and compare the energetics of several possible Hg(II) transfer pathways. Multiple protonation states are considered, and the roles of various active site residues and solvent molecules are hypothesized. Solvation is expected to contribute significantly to the interaction energies involving Hg(II) and affect the relative stabilities of different states during the allosteric transition in MerR and the intramolecular Hg(II) transfer in MerA. However, such information has been lacking. To further determine the effects of solvation on the interactions involving Hg(II), density functional theory and polarizable continuum models are used to compute aqueous binding free energies for a number of complexes containing Hg(II). Excellent agreement with relative experimental data is achieved for both hydration and ligand binding free energies. The standard deviation of the average error (STDEV) in the binding free energies is around 1 kcal mol^{-1} using Solvent Model D (SMD) with two explicit water molecules for hydration of anions and Hg(II)-ligand complexes. The binding free energies are analyzed in terms of local and long-range contributions. It is demonstrated that solvation provides a key driving force for effectively enhancing the interactions between Hg(II) and functional groups in low-dielectric media.

Field Investigations of Microbially Facilitated Calcite Precipitation for Immobilization of Strontium-90 and Other Trace Metals in the Subsurface

R.W. Smith (PI), *U. of Idaho*; Y. Fujita, *INL*; T.R. Ginn, *U. of California Davis*; S.S. Hubbard, B. Dafflon—*LBNL*; M. Delwiche, *INL*; T. Gebrehiwet, *U. of Idaho*; J.R. Henriksen, *INL*; J. Peterson, *LBNL*; J.L. Taylor, *U. of Idaho*

Subsurface radionuclide and metal contaminants throughout the U.S. Department of Energy (DOE) complex pose one of DOE's greatest challenges for long-term stewardship. One promising stabilization mechanism for divalent ions, such as the short-lived radionuclide ^{90}Sr, is co-precipitation in calcite. We have previously found that that nutrient addition can stimulate microbial ureolytic activity, that this activity accelerates calcite precipitation and co-precipitation of Sr, and that higher calcite precipitation rates can result in increased Sr partitioning. We are conducting integrated field, laboratory, and computational research to evaluate the relationships between ureolysis and calcite precipitation rates and trace metal partitioning under environmentally relevant conditions, and investigating the coupling between flow/flux manipulations and precipitate distribution and metal uptake.

Our September 2010 experimental campaign at the Integrated Field Research Challenge (IFRC) site located at Rifle, CO was based on a continuous recirculation design; water extracted from well M-07 was amended with urea and molasses and re-injected into up-gradient well M-02. The recirculation experiment was followed by 14 months of geophysical and groundwater monitoring. Cross borehole electrical conductivity tomography indicated a very conductive, high porosity layer overlying a low conductivity unit within the recirculation cell. An increase in electrical conductivity, primarily in the top layer, was observed 40 days after the start of urea recirculation and was likely the result of urea hydrolysis occurring predominantly in the upper portion of the recirculation cell. This interpretation is supported by analysis of sediments from a core (BS-11-2) collected between the injection and extraction well 10 months following urea injection which showed high *ureC* gene copy numbers as well as much higher laboratory measured ^{14}C urea hydrolysis rates in the upper portion of the recirculation cell compared to the deeper portion of the cell.

Long term groundwater sampling of the injection and extraction wells showed an initial increase in urea concentration associated with injection activities followed by decreasing urea concentration and associated increases in ammonium and dissolved inorganic carbon (DIC) following the termination of injection. Preliminary estimates of urea loss yielded a first order rate constant for urea hydrolysis of 0.2 day^{-1}. This value is approximately 7 times higher than estimated for previous field experiments conducted in eastern Idaho. Additionally, DIC carbon isotope ratios were measured for the groundwater. Injected urea had a $\delta^{13}C$ of -40.62±0.36 ‰ compared to background groundwater DIC $\delta^{13}C$ of -16.62±0.27‰. Observed decreases in groundwater DIC $\delta^{13}C$ of up to -19.75‰ suggested that up to 41% of the post injection DIC resulted from urea hydrolysis. Aquifer solids incubated within the treatment zone retained high ureolytic activity 10 months after the cessation of active urea amendment. Sediments from background cores BS-01 collected in 2010, sediments recovered following 10 months incubation in experimental wells B-01, M-02, and M-04, and core BS-11-2 are being processed for trace metal speciation in different operationally defined sediment fractions as well as determination of the $\delta^{13}C$ for carbonate minerals.

Uranium Biomineralization by Natural Microbial Phosphatase Activities in the Subsurface

Patricia A. Sobecky (PI, psobecky@ua.edu), *U. of Alabama*; Martial Taillefert (co-PI, martial.taillefert@eas.gatech.edu), *Georgia Institute of Tech.*; Robert J. Martinez, Melanie J. Beazley—*U. of Alabama*; Cindy Wu, *LBNL*; Terry C. Hazen, *U. of Tennessee*; Gary L. Andersen, *LBNL*; Karen Kinsella, David J. Schlyer, Joanna S. Fowler—*BNL*

The project goal is to examine the role of phosphohydrolases in naturally occurring subsurface bacteria for the purpose of promoting the immobilization of uranium through the formation of insoluble uranium phosphate minerals. Our prior work focused on pure culture and soil column studies that utilized contaminated soils from the DOE Oak Ridge Field Research Center (ORFRC), demonstrating that microbial phosphatase activity liberated sufficient concentrations of inorganic phosphate (PO_4^{3-}) to promote uranium-phosphate mineral formation under oxic and anoxic conditions at different pH values (pH 5.5 and 7). Current objectives are to: (1) examine the diversity of the microbial communities present in Area 2 soil slurry incubations and examine treatments [glycerol-2-phosphate (G2P) or glycerol-3-phosphate (G3P) amendments at pH 5.5 or pH 6.8] conditions that promote intracellular polyphosphate formation, (2) examine the biochemistry of multiple acid phosphatases identified in the completed genomes of the ORFRC *Rahnella* strain Y9602 and reference strain *Rahnella aquatilis* ATCC 33071, and (3) examine the application of positron emission tomography (PET) to track subsurface bacteria in soil column studies. In collaboration with DOE LBNL investigators, we have examined microbial community dynamics of ORFRC Area 2 subsurface microbial populations responding to G2P and G3P amendments with the PhyloChip microarray. Within 36 days, treatments with G3P and G2P yielded 9.1 mM and 4.7 mM PO_4^{3-}, respectively. Treatments at pH 6.8 enriched members of the phyla *Crenarchaeota*, *Euryarchaeota*, *Bacteroidetes*, *Flavobacteria*, *Sphingobacteria*,and *Proteobacteria* while treatments at pH 5.5 enriched in the phyla *Crenarchaeota*, *Euryarchaeota*, and *Proteobacteria*. Electron microscopy of soil slurry treatments indicates that G2P (pH 5.5) enhanced intracellular polyphosphate formation. Our two *Rahnella* genome sequencing projects (*Rahnella* sp. Y9602 and *Rahnella aquatilis* ATCC 33071) led by JGI have been completed. Comparative genomic studies between the two strains are underway to examine possible influences the contaminated ORFRC had on the Y9602 strain. Five candidate low-molecular weight acid phosphatases have been cloned and biochemical analysis of substrate range(s) are underway and will be used examine alternative phosphate substrates as well as allow for real-time gene expression analysis of cultured and mixed community phosphate-solubilizing studies.

Our current collaboration with DOE BNL researchers has examined the use PET imaging as a method to visualize subsurface microbial processes. Our recently published studies demonstrated that the phosphate solublizing *Rahnella* sp. Y9602 labeled with 2-deoxy-2-(^{18}F)fluoro-D-glucose could be visualized in real-time after being introduced to soil columns. These initial studies demonstrate metabolically active subsurface microorganisms could be visualized under varying soil column conditions relevant to the ORFRC. The combined multiphasic approach of pure culture and soil slurry studies coupled to genome-enabled studies will provide a greater understanding of microbial community dynamics involved in phosphate-mediated U(VI) sequestration and biomineralization.

The Molecular-Cellular-Field Continuum of Mercury Detoxification

A.O. Summers (PI), *U. of Georgia Atlanta*; S.M. Miller, *U. of California San Francisco*; C. Momany, *U. of Georgia Atlanta*; I. Artsimovitch, *Ohio State U.*; J. Blum, *U. of Michigan*; L. Liang, *ORNL*; J. Smith, *U. of Tennessee and ORNL*; T. Barkay, *Rutgers U.*; H. Guo, *U. of Tennessee*; B. Gu, *ORNL*; R.A. Scott, *U. of Georgia Atlanta*; J.D. Gross, R. Stroud—*U. of California San Francisco*

Stewardship requires controlling bioavailability $MeHg^+$ and Hg^{2+}, the substrate for methylation. Effective Hg detoxifying proteins have evolved in many bacteria and archaea. Enhancing removal or sequestration of Hg^{2+}/$MeHg^+$ by naturally Hg resistant (HgR) bacteria means knowing how these proteins work. We study HgR genes of γ-proteobacteria and actinobacteria abundant in high Hg areas of the ORR and report here on the mechanisms of the *mer* reductase and demethylase and regulatory proteins that optimize their expression to rapidly and completely convert Hg^{2+} or RHg^+ to volatile, poorly biomagnified Hg^0.

ACTINOBACTERIAL MerA/MerB: Relatives of *Streptomyces lividans* are found in high Hg regions of the East Fork Poplar Creek of the ORR. We study their co-evolved MerA/MerB proteins. *S. lividans* MerA (SLMerA) lacks the tethered NmerA domain found in γ-proteobacterial MerA, and its MerB (SLMerB) lacks a cysteine of proteobacterial MerB essential for Hg^{2+} transfer to NmerA, but has a distinct C-terminal cysteine pair. To examine the role of this cysteine pair in RHg^+ binding and Hg^{2+} release, we generated an active site mutant with only the C-terminal cysteine pair (SSCCSLMerB) and a mutant with only the active site cysteines (CCAASLMerB). Results with wild type SLMerB and the mutants will be presented.

Hg ISOTOPE FRACTIONATION BY PURIFIED MerA: Distinct signatures in Hg isotope fractionation for different chemical processes are important for distinguishing biotic and abiotic contributions to natural Hg cycling. Kritee et al (2007) measured Hg isotope fractionation by intact cells expressing *mer* genes and proposed that MerA is largely responsible for the observed effects. To test this in vitro, we're measuring Hg isotope fractionation with a purified γ-proteobacterial MerA. Experimental design and progress will be presented.

PROTEOBACTERIAL REGULATION OF *mer* EXPRESSION: In γ-proteobacteria, repressor-activator MerR holds RNA polymerase (RNAP) at the *mer* operator-promoter (MerOP) until Hg^{2+} provokes it to let RNAP transcribe. MerR binds MerOP and Hg^{2+} tightly, so anti-activator, MerD, must stop expression when all Hg^{2+} is reduced. We've made MerD monoclonal antibodies for in vitro interaction studies with MerR, MerOP and RNAP. In vivo RT-qPCR shows *mer* mRNA declines once Hg^{2+} is reduced if *merD* is wildtype and are currently testing *merD* mutants. We also find Hg^{2+} binds a 38 bp MerOP DNA in the absence of thiols (as in acute Hg^{2+} exposure) at 3 distinct, high affinity sites (K_{form} ~10^{20} M^{-1}). EXAFS shows expected nitrogen ligandsbut TA:AT slippage, the believed basis of Hg^{2+} binding in artificial systems, cannot occur in MerOP. Free bases don't bind Hg^{2+}, so DNA's high affinity must involve base-pairing or -stacking, an idea we are testing. We also find *E.coli* cells bind >3-fold more Hg^{2+} via N or O ligands than their available thiols. So, cellular DNA may be a large sink of Hg^{2+} with unknown turnover rate.

ACTINOBACTERIAL REGULATION OF *mer* EXPRESSION: Actinobacteria control the *mer* operon with a simple ArsR-type repressor. *S. lividans* MerR (SLMerR) is a distinct clade of the ArsR family. Homology models based on ArsR regulators with 3D structures show a candidate Hg^{2+} binding site in SLMerR's DNA binding helix, a radical departure from metal sites in other ArsR regulators. SLMerR over-expression proved toxic in *E.coli* which lacks the tRNA profile to translate actinobacterial mRNA, resulting in ribosome malfunction. With help from the UT-ORNL group we synthesized an *S.lividans merR* gene optimized for expression in *E.coli* and anticipate good production of this unusual ArsR-type regulator.

Identifying Mechanisms of Toxic Metal Stress with Global Proteomics

A.O. Summers (PI), S. LaVoie, L. Olliff, M.K. Johnson, R.A. Scott—*U. of Georgia Atlanta*; S.M. Miller, B. Polacco—*U. of California San Francisco*; M.S. Lipton, S.O. Purvine, E.M. Zink—*EMSL-PNNL*

$MeHg^+$ and Hg^{2+} directly inactivate proteins by binding to their cysteine or selenocysteine residues. As previously reported (Polacco, et al. MCP, 2011), we have devised a high-throughput global proteomics method using the 7 stable isotopes of Hg to identify proteins of *E.coli* most vulnerable to forming stable adducts of phenylmercury ($PhHg^+$; a proxy for methylmercury). Analysis of the dataset of ~1.62 million total observed MS2 spectra continues and here we report establishment of a MySQL database for these data, an overview of the biological findings, independent confirmation of the stability of Hg-peptide adducts under the LC-MS/MS conditions used, and initial work extending this method to the Hg^{2+}-methylating bacterium, *Desulfovibrio* ND132.

Hg EXPOSOME DATABASE: Unlike transcriptomic's MIAME standards, there is no agreed protocol for storage, sharing, and reporting of basic proteomics data, much less those with adducts. So, using the relational database freeware, MySQL, we built our own repository and analytical tools. Housed on a dedicated server at the University of Georgia, the database records every experimental aspect from cell culture thru spectra collection to identification and quality scoring with three widely used algorithms. It is available to all members of our collaboration by password.

OVERVIEW OF BIOLOGICAL FINDINGS: From three complete biological replicates (developed via five full scale pilot experiments) we identified by two or more peptides 1301 of *E.coli* MG1655's 4249 encoded proteins (WISC_ASAP); an additional 261 proteins were identified by multiple observations of a single high quality peptide for a total of 1562 rigorously identified proteins (37% of total). There are 3654 cysteine-containing proteins encoded by MG1655 (86% of total); they vary widely in abundance and conditions for expression. We observed 303 cysteine-containing proteins modified by Hg (19.4% of identified proteins) and 85% of these have at least one cysteine that is highly modified (Def: >50% of observations have Hg-modification). These Hg-vulnerable proteins represent all metabolic functional groups, and especially energy generation, translation and amino acid biosynthesis (Zink et al, in preparation). Bulk cell properties altered by PhHg or Hg exposure include thiol homeostasis, electrolyte balance, and free iron (LaVoie et al, in preparation).

STABILITY OF Hg-PEPTIDES TO PROTEOMICS: The 4-fold lower recovery of cysteine containing proteins than expected has several possible physiological causes, including their differential occurrence under the aerobic growth conditions used and natural differential abundance. These can be resolved via ontological analysis underway; although absolute abundance is unknown for many proteins, it can be inferred from their functional class. Possible technical factors include differential stability to pre-column procedures, column conditions, and MS conditions. We're using our database to examine cysteine peptide/protein yield variation related to pre-MS variables. Experiments with pure Hg-adduct peptides show they are stable to the MS conditions.

Hg EXPOSOME OF A METHYLATING BACTERIUM: To identify proteins involved in Hg^{2+} uptake and methylation we've first grown *Desulfovibrio* ND132 facultatively without Hg^{2+} to test the efficacy of our modified proteomics method on it. The results (~1350 identified proteins of 3455 encoded) were slightly less than work on pyruvate or fumarate grown *Desulfovibrio* G20 (1900 identified proteins of 3258 encoded). Optimization of growth conditions for maximum methylation is underway and, since this project requires exposure to bivalent Hg^{2+}, we are adapting our Hg-proteomics method to identify the distinct peptides of pairs of Hg-crosslinked peptides. This work will also uncover cysteine peptides vulnerable to being missed because they are crosslinked.

Manganese Redox Mediation of UO_2 Stability and U Fate in the Subsurface: Molecular and Meter-Scale Dynamics

B.M. Tebo (PI, tebo@ebs.ogi.edu), S.-W. Lee—*OHSU*; Z. Wang, D.E. Giammar—*Washington U. St. Louis*; K.L. Plathe, R. Bernier-Latmani—*ÉPFL*; J.S. Lezama Pacheco, J.R. Bargar—*SLAC*; K.H. Williams, P.E. Long—*LBNL*

Successful bioremediation of U in the subsurface depends on the long-term stability of U(IV). As a strategy to immobilize U, injection of electron donors to the subsurface to stimulate U(VI) reduction is being tested. During the process, Mn and Fe oxides sequentially undergo reductive dissolution. Once the injection of electron donor is ceased, however, zones where U(IV) precipitated may return to oxidizing conditions and the stability of U(IV) affected by the formation of strong oxidants such as MnO_2. The focus of our project is 1) to determine how certain groundwater constituents affect the coupled Mn(II)/U(IV) oxidation process, 2) to examine the fate of U once it is oxidized by MnO_2 in both lab and field settings, and 3) to quantify the effects of physical and chemical parameters on MnO_2/UO_2 interaction.

The oxidation of U(IV) by Mn(II)-oxidizing bacteria and Mn oxides has been shown in laboratory experiments to occur very rapidly. To assess the effect of groundwater constituents typical of the Rifle field site and the form of U(IV) on coupled Mn(II)/U(IV) oxidation, we investigated the effect of O_2 and common groundwater chemical species (Ca^{2+}, Mg^{2+}, and HCO_3^-) on Mn(II) and U(IV) oxidation by a model Mn(II)-oxidizing organism, *Bacillus* sp. SG-1 spores. Increasing O_2 resulted in increased levels of U(IV) oxidation which were attributable to both direct oxidation of U(IV) by O_2 and to the formation of biogenic MnO_2 which subsequently oxidized U(IV). Interestingly, Ca^{2+}, Mg^{2+}, and HCO_3^- showed varying effects on coupled Mn(II)/U(IV) oxidation by exerting its impact on either Mn(II) or U(IV) oxidation.

To understand the reaction between U(IV) and MnO_2, biogenic UO_2 or monomeric U(IV) were embedded in agarose gels with SG-1 spores. 65% and 74% of the total U was oxidized in gels containing UO_2 and monomeric U(IV) respectively. Additionally, more loss of U was observed from gels incubated with O_2 in the absence of Mn(II), suggesting that the impact of Mn oxidation is U(IV) immobilization. Bulk XAS results showed that the majority of U after Mn(II) oxidation was in the U(VI) form. MicroXAS analyses showed, two main particle types associated with U(VI), single particles or aggregates of U(IV) and Mn oxide particles.

In order to gain a field-relevant understanding of U(IV) oxidation by Mn oxides, several columns were deployed in the Rifle field site, under Mn-oxidizing conditions. These columns contained sediment from the Rifle site that had been pre-loaded (*in situ*) with U(IV). Total digestion of the sediments carried out prior to deployment and after 2 months showed a large decrease (from 40-65%) in the amount of U present in sediments that received higher levels of Mn(II), indicating that Mn(II) oxidation may play a role in the oxidation of U(IV) species.

Finally, laboratory experiments have been performed to understand the physical and chemical factors controlling the interaction of MnO_2-UO_2. Experiments with a multi-chamber reactor with a permeable membrane that prevented direct contact between MnO_2-UO_2 indicated that physical contact or close proximity is required for effective oxidation of UO_2 by MnO_2. When contact was allowed, an increase in the MnO_2:UO_2 ratio significantly increased the UO_2 dissolution rate. The product of MnO_2-UO_2 interaction, U(VI), was substantially adsorbed to MnO_2 and the release of Mn was less than expected based on the stoichiometry of the reaction.

Firmicutes and Their Roles in Uranium Immobilization

F. Yang, J. Tiedje (PI, tiedjej@msu.edu), J. Zhou (jzhou@ou.edu), T.L. Marsh (marsht@msu.edu)—
Michigan State U. and U. of Oklahoma

Bioremediation of uranium in subsurface is a great challenge. To evaluate the natural occurring uranium-removing bacterial populations, we have anaerobically enriched uranium contaminated soil sediments (FW107, FW102-2, and FW102-3) collected from ORNL iFRC site (S3 area). Electron acceptors, NO^{3-}, Fe^{3+}, and U^{6+}, were supplemented in the enrichments as selection factors. We previously reported the shifts of bacterial community profiles in enrichments. After two serial transferring and enriching, bacterial 16S rRNA gene survey revealed that Fe^{3+} and U^{6+} supplemented enrichments shared similar community structures. Genus *Pelosinus* was found dominant in Fe^{3+} and U^{6+} enriched FW107 microcosms. This group of bacteria was also present in FW102-2 and FW102-3 enrichments but substantially less abundant. Unclassified *Clostridiales* and *Geobacter* groups were most abundant in Fe^{3+} and U^{6+} supplemented FW102-2 microcosms, respectively. Genus *Geobacter* was dominating the FW102-3 community after it was enriched with Fe^{3+} and U^{6+}. Hence, we suspect that Firmicutes might play a significant role in subsurface uranium removal.

With our goal of identifying unknown uranium immobilizers in mind, we have isolated 54 bacterial isolates from Fe^{3+} and U^{6+} supplemented enrichments. The growth rates of these isolates at 25°C vary from 6 hours to 22 hours per generation. All isolates belong to phylum Firmicutes and can be categorized into four groups, *Clostridium* XI, *Clostridium* XIVa, *Clostridium sensu stricto*, and *Pelosinus*, based on their 16S rRNA gene sequences. Majority of the sequences in *Clostridium* XIVa group were identical to the 16S rRNA gene sequence of *Desulfotomaculum guttoideum*, which is a rarely studied sulfate-reducing bacterium. At 95% to 97% similarity, sequences in *Clostridium sensu stricto* group were closely related to *Clostridium acetobutylicum*, C*lostridium butyricum,* and *Clostridium puniceum*. While *Clostridium acetobutylicum* was recently reported as a uranium reducing bacterium, the other two were mostly studied for their chemical producing ability, such as butanol and 1,3-propandiol. The *Pelosinus* isolates we have identified were closely related to *Pelosinus sp.* strain UFO1, which was recently reported for its ability in multi-mode uranium immobilization. Out of 54 isolates, only one was identified as *Clostridium venationis* in group *Clostridium* XI. However, no studies have been reported on this species. In light of these taxonomy information and literature reports, we are in the process of evaluating the uranium immobilization rate by these isolates. Preliminary studies have shown that these isolates are resistant to 250μM of U^{6+}. We also performed rep-PCR to select the representative isolates to determine their U^{6+} removal rates. Currently, we are studying the U^{6+} immobilization by these representatives as well as the co-cultures of these isolates to evaluate the importance of mixed Firmicute populations in U^{6+} bioremediation.

Differential Proteomics Analysis of GASP (Growth Advantage in Stationary-Phase) Phenotype of *Geobacter sulfurreducens* under "Famine" Conditions

Reema Bansal Agarwal (rzb12@psu.edu), Ruth A. Helmus, Susan Brantley, Ming Tien (PI)—*Penn State*

Geobacter sulfurreducens is used for bioremediation at heavy metal and readioactive waste contaminated sites. The organism typically encounter limited access to electron donors and/or electron acceptors in such environments. Therefore, gaining an understanding of how *Geobacter sulfurreducen* involved in bioremediation survive under such conditions is relevant for planning efficient bioremediation strategies. Previously we have demonstrated that *Geobacter sulfurreducens* displays five typical stages of growth: lag, log, stationary, death, and survival phases. The orgainsm acquire a growth advantage adaptation that begin to emerge during the stationary phase; this adaptation is termed "growth advantage in stationary phase," or GASP. The GASP strains can out-compete mid-log phase population when co-cultured under similar conditions. This work aims to study differential protein expression between different growth phases of *Geobacter sulfurreducens* grown under electron acceptor (fumarate) limiting conditions. We employed LC/MS- based iTRAQ methods to obtain information about relative changes in protein expression between mid-log, stationary and survival phases.

There were 80 proteins that were significantly up-regulated in survival phase organisms as compared to mid-log. Most of the up-regulated proteins (29%) were found to be involved in energy metabolism function. These included components of the ATP synthase and NADH dehydrogenase enzymes, as well as cytochrome c family proteins and all three components of the heterotrimeric fumarate reductase FrdCAB. In addition, several outer membrane proteins and putative lipoproteins involved in transport and binding were also up-regulated. About 40% of the total up-regulated proteins were found to be hypothetical or with unknown function.

We identified 66 proteins that were significantly down-regulated in survival phase organisms. Around 40% were ribosomal, transcription and translation proteins involved in protein synthesis. In addition 10 proteins (~15%) associated with energy metabolism, 5 (~8%) involved in nucleotide biosynthesis and 11 (~17%) hypothetical or unknown function proteins were also down-regulated. Two proteins that play a role in heme biosynthesis, the gene products of GSU3285 and GSU3453, were down-regulated. However, preliminary results did not indicate that total heme levels were lower in survival phase cultures compared with mid-log phase cultures. Of all the 146 proteins differentially expressed between mid-log and survival phases, the predicted cellular localization of 117 could be determined. A majority of the up-regulated proteins were predicted to localize in the membrane and periplasmic space, and most of the down-regulated proteins were predicted to be localized in the cytoplasm.

These results indicate that the composition of the inner and outer membranes of *G. sulfurreducens* changes drastically from mid-log to survival phase and may have important implications for organism's survival under famine conditions. Fewer changes in protein expression between mid-log and stationary phases as compared to mid-log and survival phases, indicate that the significant changes in survival expression cannot be detected at early stationary phase. Thus, study of long-term cultures is necessary to truly appreciate the nature of *G. sulfurreducens* dwelling in famine environments. The genetic basis of the GASP phenomenon and survival capacity will be further investigated by genomic sequencing. We will also determine the energy charge and reducing equivalents involved to gain insight into the energy metabolism of the organism.

Technetium Reduction and Permanent Sequestration by Abiotic and Biotic Formation of Low-Solubility Sulfide Mineral Phases

P. Tratnyek (PI), B. Tebo, R. Anitori, D. Fan—*OHSU*; J. Szecsody, J. McKinley, D. Jansik—*PNNL*

One way to minimize the mobility of the Tc^{VII} oxyanion pertechnetate (TcO_4^-) is to effect reduction under sulfidogenic conditions (generated abiotically by Fe^0 or biotically) to form TcS_x, which is significantly slower to oxidize than $Tc^{IV}O_2$. In sediment systems, TcS_x and other precipitates may oxidize more slowly due to oxygen diffusion limitations to these low permeability precipitate zones. In addition, the TcO_4^- reduction rate may be more rapid in the presence of sediment because of additional reductive surface phases. This project aims to provide a fundamental understanding of the feasibility of immobilization of TcO_4^- as TcS_x in the vadose zone or groundwater by application nano zero-valent iron (nZVI), and sulfide or sulfate.

Biotic batch experiments have used the sulfate-reducing bacterium (SRB) *Desulfotomaculum reducens*. The iron sulfide mineral mackinawite was generated under these conditions, while vivianite was formed in nZVI only controls. The sulfide/bacteria-containing system consistently reduced aqueous pertechnetate rapidly (> 95% in the first hour), a rate similar to that for the sulfide-free, nZVI only system. Reduced Tc (aged for 3 months) generated in both SRB/nZVI systems was highly resistant to reoxidation. In reduced samples, Tc was found associated with solid phases containing Fe and S (*D. reducens*/nZVI) or Fe (nZVI only). Experiments using *D. reducens* without nZVI provided some additional insights. Firstly, stationary phase cultures were able to slowly reduce pertechnetate. Secondly, addition of pertechnetate at the beginning of cell growth (lag phase) resulted in a faster rate of Tc reduction, possibly indicating a direct (e.g. enzymatic) role for *D. reducens* in Tc reduction.

Abiotic batch experiments were conducted with Na_2S as the sulfide source. Pertechnetate reduction was rapid in the presence of sulfide and nZVI, although the rate was suppressed at the higher S/Fe ratios tested. This suppression appeared to be due to the formation of Tc-containing colloids. As with the biotic experiments, pertechnetate reduced under sulfidic conditions was highly resistant to reoxidation. The microscopic morphology of abiotically-transformed nZVI particles varied significantly with those in the biotic experiment, although mackinawite was formed in both systems (as indicated by μXRD and Mössbauer spectroscopy). Preliminary XAS analysis pointed to a mixture of Tc-O and Tc-S binding in the abiotic sulfide/nZVI system, while the major reduced solids under non-sulfidic conditions were $TcO_2 \bullet nH_2O$. Further investigation of these phases in abiotic and biotic samples are currently in progress using XAS.

The presence of sediment and advective flow to the TcO_4^-/nZVI/sulfide system results in additional processes occurring. Although the natural Hanford sediment used has sufficient available ferrous iron to slowly reduce TcO_4^-, under anaerobic conditions, that rate is orders of magnitude slower than reduction by nZVI/sulfide. Batch and 1-D column experiments showed that the TcO_4^- reduction rate increased with the sediment surface area (with the same nZVI mass). As in batch systems, column studies showed that the presence of sulfide with TcO_4^- at low (2-5 mM) concentrations increased the TcO_4^- reduction rate and high (10-30 mM) sulfide decreased the rate. This change is attributed to the formation of sulfide precipitates on the nZVI and sediment surfaces. Injection of low and high sulfide (i.e. pretreatment) prior to TcO_4^-/sulfide injection also greatly decreased the TcO_4^- reduction rate, likely decreasing the generation of ferrous iron from the nZVI. Although the high sulfide systems have slower Tc reduction rates, 190 times more Tc mass precipitated than in the low sulfide systems and the highest fraction of Tc mass remained immobilized.

Microbiological-Enhanced Mixing Across Scales During *In Situ* Bioreduction of Metals and Radionuclides at Department of Energy Sites

A.J. Valocchi (PI), C.J. Werth, W-T. Liu, R. Sanford—*U. of Illinois Urbana-Champaign;* K. Nakshatrala, *U. of Houston;* M. Oostrom, C. Zhang—*PNNL*

Bioreduction is being actively investigated as an effective strategy for subsurface remediation and long-term management of DOE sites contaminated by metals and radionuclides (i.e. U(VI)). These strategies require manipulation of the subsurface, usually through injection of chemicals (e.g., electron donor) which mix at varying scales with the contaminant to stimulate metal reducing bacteria. There is evidence from DOE field experiments suggesting that mixing limitations of substrates at all scales may affect biological growth and activity for U(VI) reduction.

Although current conceptual models hold that biomass growth and reduction activity is limited by physical mixing processes, a growing body of literature suggests that reaction could be enhanced by cell-to-cell interaction occurring over length scales extending tens to thousands of microns. Our project is investigating two potential mechanisms of enhanced electron transfer. The first is the formation of single- or multiple-species biofilms that transport electrons via direct electrical connection such as nanowires through biofilms to where the electron acceptor is available. The second is through diffusion of electron carriers from syntrophic bacteria to dissimilatory metal reducing bacteria (DMRB). The specific objectives of this work are i) to quantify the extent and rate that electrons are transported between microorganisms in physical mixing zones between an electron donor and electron acceptor (e.g. U(IV)), ii) to quantify the extent that biomass growth and reaction are enhanced by interspecies electron transport, and iii) to integrate mixing across scales (e.g., microscopic scale of electron transfer and macroscopic scale of diffusion) in an integrated numerical model to quantify these mechanisms on overall U(VI) reduction rates.

We are testing these hypotheses with five tasks that integrate microbiological experiments, unique micro-fluidics experiments, intermediate-scale flow cell experiments, and multi-scale numerical models. Continuous fed-batch reactors will be used to derive kinetic parameters for DMRB, and syntrophic/DMRB systems. They will also be used to develop an enrichment culture for elucidation of syntrophic relationships in a complex microbial community. Pore and continuum scale experiments using microfluidic and bench top flow cells will be used to evaluate the impact of cell-to-cell and microbial interactions on reaction enhancement in mixing-limited bioactive zones, and the mechanisms of this interaction. The microfluidic experiments will be used to develop and test a pore scale model that considers direct cell-to-cell interactions during U(VI) reduction. The pore scale model will be incorporated into a multi-scale hybrid model that combines pore scale modeling at the reaction interface with continuum scale modeling. We will validate the multi-scale model by comparison with continuum scale bench top flow cell experimental results, and then explore opportunities to extend this model to larger systems and eventually to field sites.

Work to date for this new project has investigated developing an appropriate system of syntrophs and metal reducers for use in follow-up experiments. Preliminary results indicate that *Anaeromyxobacter dehalogenans* has the capability to grow syntrophically with *Syntrophobacter fumaroxidans* using propionate as an electron donor and ferric citrate or ferrihydrite as an electron acceptor. Similarly, *Geobacter lovleyi* has grown with *S. fumaroxidans* using propionate and ferrihydrite only. In contrast, *G. sulfurreducens* has not been capable of syntrophic growth. Preparatory work needed for design and fabrication of microfluidic flow cells has been completed. Finally, we are starting to formulate the mathematical model for diffusion and reaction with a biofilm consisting of both syntrophs and metal reducers.

Development of New and Integrated Stable Isotope Tools for Understanding Nitrogen-Uranium Interactions in Subsurface Environments

Scott D. Wankel, Yuanzhi Tang, Colleen M. Hansel, David T. Johnston (PI)—*Harvard U.*

As the most ubiquitous contaminant anion in sediments and groundwater at US DOE sites, high levels of nitrate (NO_3^-) also co-occur with one or more priority contaminant metals or radionuclides. This project seeks to improve the understanding of the multifaceted interactions between the nitrogen cycle and cycling of the widespread radionuclide uranium (U) in order to better predict its fate and transport in complex subsurface environments. For example, while bioremediation efforts have primarily focused on immobilizing uranium through stimulation of microbial reduction of U(VI) to U(IV), this process is inhibited by the presence of NO_3^-. Furthermore, the potential for introduction of nitrate-contaminated groundwater poses a direct and serious threat to the longevity and stability of uranium immobilization in subsurface sediments directly through the oxidation of U(IV) by NO_3^- and/or the reductive intermediate NO_2^-, or indirectly by coupling of N and Fe cycling. As such, the interpretation of the results of field–scale bioremediation studies are often complicated by the fact that several competing processes may occur simultaneously.

Through the use of new and integrated stable isotopic tools, which represent naturally occurring spatial and temporal integrators of cycling processes, this project aims to improve the detection and monitoring of biogeochemical changes in subsurface environments, particularly those involving the coupling of nitrogen cycling to uranium oxidation and mobilization. Specifically, the use of coupled isotope systems (e.g. $^{15}N/^{14}N$ and $^{18}O/^{16}O$ and the ratio of their respective fractionation or $^{18}\varepsilon:^{15}\varepsilon$) provides an even more powerful integrator for constraining the relative roles of simultaneously occurring cycling processes in the context of U(IV) oxidation.

Initial batch experiments were designed to characterize the kinetic isotope effects of abiotic NO_3^- reduction by Fe(II) as a starting point for understanding the potential for linkages among subsurface N, Fe and U cycling. Results have shown substantial reduction of NO_3^- by Fe(II) in the presence of iron oxyhydroxides mineral phases (goethite) and/or catalytic amounts of Cu(II). Kinetic isotope effects for NO_3^- reduction during these reactions have varied widely across experimental conditions ($^{15}\varepsilon_{NO3}$ = 6.8 to 32.7‰, $^{18}\varepsilon_{NO3}$ = 3.4 to 19.7‰). However, in all cases, abiotic NO_3^- reduction exhibited larger nitrogen isotope effects than oxygen isotope effects ($^{18}\varepsilon:^{15}\varepsilon$ = 0.36 to 0.83), which could suggest the involvement of abiotic Fe (II) based reduction of NO_3^- when observed in the environment. During the next phase of characterization, a full experimental series of 17 flow-through sediment columns, inoculated with subsurface sediment from a local study site, was run for approximately 60 days under anaerobic, reducing conditions. In a subset of columns, iron reduction was allowed to occur for the initial 30 days (allowing a buildup of Fe(II) sorbed onto mineral surfaces), followed by the addition of NO_3^-. Rapid NO_3^- and Fe(III) reduction was observed in all treatments. Results of NO_3^- stable isotope measurements from these flow-through experiments will be discussed in the context of potential linkages among subsurface N, Fe and U cycling. Based on these results, we posit that tracking changes in NO_3^- and NO_2^- concentration and $\delta^{15}N$ and $\delta^{18}O$ along with aqueous and solid phase U and Fe chemistry in future experiments will allow partitioning of the specific N reducing processes directly and indirectly related to U(IV) reoxidation and mobilization under advective flow.

Viral Infection of Subsurface Microorganisms and Metal/Radionuclide Transport

Karrie A. Weber (PI), Don Pan, Zheng Huan Tan—*U. of Nebraska*; Kelly S. Bender, *S. Illinois U.*; Yusong Li, *U. of Nebraska*

Microbially mediated metabolisms have been identified as a significant factor either directly or indirectly impacting the fate and transport of heavy metal/radionuclide contaminants. To date the role that viruses play influencing microbial mortality and the resulting community structure under varying redox conditions in subsurface sedimentary environments remains poorly understood. The objective of this project is to investigate viral infection of subsurface bacteria and the formation of contaminant-bearing viral particles. This objective will be approached by examining the following working hypotheses: (*i*) subsurface microorganisms are susceptible to viral infections by the indigenous subsurface viral community, and (*ii*) viral surfaces will adsorb heavy metals and radionuclides. In an effort to initially assess the significance of viral infection in subsurface microbial communities, the production of viral like particles in response to biostimulation of the microbial community was investigated by inoculating low nutrient culture medium containing acetate and nitrate with uranium and nitrate containing shallow subsurface sediment (25% mass/vol). No significant production of viral like particles was observed when acetate or nitrate was omitted from culture medium. Acetate was oxidized coupled to the reduction of nitrate to nitrite resulting in the increase in bacterial abundance and an initial increase in Viral Like Particles (VLP's) (Virus to Bacteria ration ca. 480 to 2,400 over the course of the study). During nitrate reduction to nitrite, VLP abundance increased from 1.1×10^5 to 4.6×10^7 VLP mL^{-1} (ca. increase of 430x). The production of 9mM nitrite resulted in a lag in nitrite reduction and a subsequent decrease in bacterial abundance. This also corresponded to a decrease in VLP abundance (4.9×10^6 VLP mL^{-1}). Interestingly when nitrite reduction resumed, VLP abundance again increased to 2.6×10^7 VLP mL^{-1} while bacterial abundance continued to decrease. In an effort to identify the viruses infecting indigenous bacteria, bacterial isolates were obtained. One nitrate reducing isolate, Alda10, was selected for further study. Analysis of the 16S rRNA gene sequence revealed the closest related organism in pure culture was *Pseudomonas fredricksbergensis* with 99%similarity. Mitomycin C induction of Alda10 resulted in the production of VLP's (1.9×10^6 VLPmL^{-1}). Transmission electron microscopy of the VLPs revealed particles similar to filamentous phage. Together these results suggest a lysogenic infection of *Pseudomonas* sp. Alda10. The production of VLP's in groundwater has implications for metal and radionuclide transport. Initial experiments indicate that metals will adsorb to the surface of *Escherichia coli* phage T4. It is therefore necessary to establish the potential relationship(s) between viruses, subsurface microbial communities, and contaminant metals/radionuclides to provide sufficient scientific understanding such that DOE sites would be able to incorporate coupled physical, chemical and biological processes into decision making for environmental remediation and long-term stewardship by establishing viral-microbial relationships and the subsequent fate and transport of heavy metals and radionuclides.

Investigation on U(VI) Sorption / Desorption on Nanopores Goethite, and Structures of Ferrihydrite Nano-Mineral

Huifang Xu (PI/co-PI, hfxu@geology.wisc.edu), Eric E. Roden (PI/co-PI, eroden@geology.wisc.edu)—*U. of Wisconsin Madison*; Kenneth M. Kemner (PI/co-PI, Kemner@anl.gov), *ANL*; Hiromi Konishi, Hun-Bok Jung—*U. of Wisconsin Madison*

Most reactive surfaces in clay-dominated sediments are present within nanopores (pores of nm dimension). The behavior of geological fluids and minerals in nanopores is significantly different from those in normal non-nanoporous environments. The effect of nanopore surfaces on U(VI) sorption/desorption and reduction is likely to be significant in clay-rich subsurface environments. Our research objective is to test the hypothesis that U(VI) sorption on nanopore surfaces can be greatly enhanced by nanopore confinement environments.

We investigated sorption and desorption of uranium on both natural nanoporous and non-porous goethite. U(VI) Desorption experiments of nanoporous goethite and non-porous goethite model systems show that all the sorbed U(VI) on non-porous goethite can be easily desorbed with low bicarbonate concentration. However, the most sorbed U(VI) on nanoporous goethite can not be desorbed even with high bicarbonate concentration. 50 mM bicarbonate solutions can only desorb ~ 10% of the sorbed uranium. The results also support that sorbed U(VI) in natural FRC sediments are bonded to both nanopore surfaces (strong sorption) and non-nanopore surfaces (weak sorption). Majority of sorbed U(VI) are associated with goethite nano-crystals. If we use Dithinote-Citrate-Bicarbonate (DCB) to remove goethite nano-crystals, it also removes more than 80% of U(VI). The amounts of labile Fe by BCD method is approximately 300 umol/kg.

Ferrihydrite nano-minerals are precursors for nanoporous goethite. Mechanism for highly reactive surfaces of ferrihydrite is not well explained, because ferrihydrite structure is still not well understood. We have determined structure and defects in a natural ferrihydrite using Z-contrast imaging. With spherical aberration-corrected scanning transmission electron microscopy (STEM), we can obtain locations of Fe atoms and vacancies in ferrihydrite directly from Z-contrast images with better than 0.1 nm spatial resolution. Two polymorphs are confirmed: ferrihydrite-4H (~ 2/3) and ferrihydrite-2H (~1/3). Intergrowth of the two polymorphs can also occur with (001) as interface. The 2H polymorph has ABAB packing for oxygen atoms, and the 4H polymorph has ABAC packing with doubled unite cell parameters along *a*- and *b*-directions with respect to the 2H polymorph. All Fe atoms occupy octahedral sites. Unit cell doubling along the *a*-, *b*-, and *c*-directions in ferrihydrite-4H is resulted from the ordering between Fe and vacancy in octahedral sites. Due to structural disordering between Fe and vacancies, ferrihydrite can be considered as 2-D crystals with two strong *(hk0)* diffraction peaks. The calculated XRD pattern based on the new structural models fits observed and reported XRD patterns well. Stoichiometry of 6-line ferrihydrite is close to $Fe(III)_{0.75}(O, OH)_2$ based on occupancy fitting, i.e., between $Fe(OH)_3$ and FeOOH, instead of between FeOOH and Fe_2O_3. Z-contrast images of ferrihydrite sorbed with U(VI) show that some of the adsorbed U atoms are right on Fe-sites. It is proposed that structural disordering could be a reason for very reactive surfaces of ferrihydrite.

Emulsified Vegetable Oil Stimulates Sulfate-Reducing Communities for U(VI) Reduction at a Contaminated Aquifer Via Pyrosequencing of Dissimilatory Sulfite Reductase Genes

Ping Zhang, Yujia Qin, Joy D. Van Nostrand, Liyou Wu, Zhili He (PI/co-PI, zhili.he@ou.edu), Ye Deng—*U. of Oklahoma*; Terence L. Marsh (PI/co-PI, marsht@msu.edu), James M. Tiedje (PI/co-PI, tiedjej@msu.edu)—*Michigan State U.*; Jizhong Zhou (PI/co-PI, jzhou@ou.edu), *U. of Oklahoma*

Sulfate reducing bacteria (SRB) are predominant and play an important role in accelerated, sustained reduction of U(VI) during bioremediation at contaminated sites, but the SRB community diversity, composition and structure are poorly understood. In this study, 454 pyrosequencing of dissimilatory sulfite reductase genes (*dsrA*) was used to analyze 44 groundwater samples collected from a U(VI)-contaminated aquifer (Oak Ridge, TN) undergoing bioremediation with an amendment of emulsified vegetable oil (EVO). Acetate was detected as a representative of the intermediates (e.g. H_2, CO_2, glycerol, propionate, butyrate) from EVO biodegradation, which stimulated the reduction of significant electron acceptors (sulfate, nitrate, Fe, Mn) and U(VI) in the seven downgradient wells during the entire experimental period of 269 days. A total of 82,537 sequences were obtained, and a total of 15,084 OTUs were defined at a 90% similarity level among all 44 samples. While a majority of the sequences (84%) were founde to be *Deltaproteobacteria*, 0.4% were related to *Desulfotomaculum* in *Firmicutes,* and a considerable portion (21% at the genus level) was novel *dsrA* sequences. Significantly different SRB communities (P<0.01) were observed after EVO amendment. While novel *dsrA* sequences were predominant (98%) in the samples before EVO addition, *Desulfovibrio* and to lesser degrees, *Desulfobacterium* and *Desulfococcus* species overwhelmingly dominated the SRB communities after EVO injection. A temporal dynamics of these organisms relative to EVO amendment was observed, which was coordinated with the succession of microbial communities as well as EVO biodegradation and U(VI) reduction. When both species relative abundance and relative frequency of occurrence were taken into account, *Desulfovibrio* (60-80% of the SRB community) and *Desulfococcus* (20%) were indicator species from 4 to 31 days, and *Desulfobacterium* (50%) characterized the community at 80 days when extensive EVO degradation and U(VI) reduction occurred. *Desulfovibrio* species remained important indicators by 269 days when acetate production and U(VI) reduction were still detected, suggesting a long-term modification of the community. The indicators of the non-EVO samples were aligned with cultured *Desulfotomaculum* strains and the *Firmicutes*-like sequences recovered in this study, suggesting that *dsrA* genes of non-EVO U(VI)-contaminated environments may be phylogenetically distant from those enriched by EVO amendment. A regression analysis showed a significant influence of *Desulfovibrio* dominance over the U(VI) concentration in groundwater (P<0.001). *Desulfovibrio* species could play an important role in the accelerated and sustained U(VI) reduction at this site. Further analysis of *in situ* activity of *Desulfovibrio* and their relationship with U (VI)-reduction should provide more information for bioremediation of this contaminated DOE site.

Multiscale Assessment of Prediction Uncertainty in Coupled Reactive Transport Models

G. Curtis (PI), *USGS*; M. Ye, *Florida State U.*; P. Meyer, S. Yabusaki—*PNNL*; D. Rodriguez, *Colorado School of Mines*

Reactive transport simulations provide a systematic framework for integrating hydrologic and biogeochemical conceptual process models into a quantitative description of subsurface behaviors, which can then be used to project future concentrations. Assessing the uncertainty associated with these projections is difficult, because subsurface environments are open and complex, and subject to multiple interpretations and conceptualizations. This challenge is addressed using the method of multimodel analysis, in which model predictions are based on a weighted average of predictions of multiple plausible models, each of which is associated with a model averaging weight. For the multimodel analysis, several theoretical issues on quantification of model and parametric uncertainty are resolved in this study. First, we developed a statistical method to evaluate effects of the correlation of temporal residuals on model averaging weights for both synthetic and column experimental data. Disregarding the temporal correlation of the residuals may result in unrealistic weights for individual models that cannot be realistically justified. This problem is resolved by estimating the residual correlation using time series theories; the method is general and can be applied to other reactive transport models. For quantification of parametric uncertainty, we found that parametric uncertainty quantified using simpler regression methods is similar to that based on computationally expensive Bayesian methods. Finally, a Bayesian method of data-worth analysis was developed for selecting the potential dataset that can maximize the reduction of predictive uncertainty. This method is unique in that it reduces both parametric and model uncertainty whereas conventional methods of are limited to considering parametric uncertainty.

Parametric and conceptual model uncertainty for the stimulated bioreduction of U(VI) by microbial processes at the Rifle IFRC site was evaluated using a 1-D reactive transport model abstracted from a realistic 3-D model of one of the field experiments. The sensitivities of key biogeochemical concentrations vary in space and time and model nonlinearities have a significant impact on calculated sensitivities. However, sensitivities computed at the optimal parameter estimates provided similar information to a global sensitivity screening method. Observed data constrained parameter values much more tightly than indicated by likely parameter ranges used in the global sensitivity analysis. This suggests that model nonlinearities may not invalidate estimates of uncertainty based on linear methods. Synthetic observations obtained with the 3-D model were that were evaluated using 1-D modeling framework showed systematic errors in the 1-D model parameter estimates. Without considering the impact of non-uniform flux, the predictive uncertainty of the 1-D model was significantly underestimated.

Parameter and model uncertainty were also evaluated for a tracer tests that had increased or decreased alkalinity that were conducted at the Naturita, CO, UMTRA site. Significant uncertainty results from imperfect knowledge of the adsorption reactions that immobilize uranium at the mineral surfaces. A calibration study of ion exchange reactions and alternative adsorption reactions to observations at four wells demonstrated that the most probable adsorption models all contained dicarbonato surface complexes. Cross validation studies using the most probable models showed that the model parameters were robust and gave good predictions of the experiments excluded in the cross validation study. In addition, predictions using the most probable calibrated models bracketed the observations at a fifth well that was not included in the calibration study.

Upscaling of U(VI) Desorption and Transport from Decimeter-Scale Heterogeneity to Plume-Scale Modeling

G. Curtis (PI), J.W. Lane Jr., M. Kohler—*USGS*; J. Davis, *LBNL*; D. Rodriguez, *Colorado School of Mines*; F.D. Day-Lewis, M. Hay, A.K. Gallagher, J.B. Ong—*USGS*

Applications of reactive transport modeling of contaminants in groundwater can often be limited by because experimental data are available at the centimeter scale but field-scale transport occurs on the kilometer scale. The focus of this project is to test approaches for defensibly incorporating small-scale information into field-scale simulations. The project is using extensive previously collected datasets at bench-, decimeter-, and tracer-test scales to support field-scale simulations of uranium transport in the shallow alluvial aquifer at the Naturita, Colorado UMTRA site. The decimeter scale experiments were conducted in 2 dimension tanks that provide a unique opportunity to impose chemical gradients in experiments with known heterogeneity. U(VI) adsorption was simulated using both one-site and two-site models which were calibrated to batch desorption data for three size fractions. These surface complexation models were then incorporated into multicontinuum mass-transfer models which were successfully calibrated to column, decimeter-scale and tracer test experimental results. High-resolution simulations of two new 2D tank experiments that have incorporated the bench-scale models have been conducted. Two 2D tank experiments will be conducted simultaneously based on the results of the high-resolutions simulations. The size of the tanks will be 2.4 m x 1.2 m x 7.6 cm and 2.4 m x 0.6 m x 7.6 cm.

Two tracer tests were conducted in the summer and fall of 2011 to observe *in situ* desorption processes over longer time scales compared with previous experiments. Whereas both tests were monitored by conventional groundwater sampling, the fall 2011 test was also monitored using time-lapse electrical resistivity tomography between two rows of down-hole electrodes augmented by several surface electrode arrays. Preliminary analysis of the combined time-lapse resistivity and geochemical sampling data provide insights into the spatial-temporal evolution of the tracer across the site. Work is ongoing to compare the geophysical and geochemical results to evaluate mass transfer and identify preferential flowpaths.

A combined analysis of data from these laboratory experiments and field tracer tests will be used to evaluate upscaling approaches at two distances from the injection gallery. Knowledge of the spatial distribution of sedimentary facies defined by previous geophysics studies, coupled with new sediment acquisition and characterization, will provide a better understanding of heterogeneity at the plume scale. Ultimately, plume-scale predictions of U(VI) transport for 13 years (1999-2012) will be compared with measured values in the aquifer, with upscaling of reactive transport parameters in accordance with the meter-scale studies.

Geoelectrical Measurement of Multi-Scale Mass Transfer Parameters

Frederick D. Day-Lewis (PI), *USGS*; Kamini Singha, *Penn State*; Andrew Binley, *Lancaster U.*; Roy Haggerty, *Oregon State U.*; John W. Lane Jr., *USGS*; Jeremy Clifford, *Lancaster U.*; Ryan D. Swanson, *Penn State*; Timothy C. Johnson, *PNNL*; Kristina Keating, *Rutgers U.*

Evidence of mass transfer at contaminated sites includes long "tailing" behavior and concentration rebound during remediation of groundwater. The lack of experimental methods to verify and measure mass transfer *in situ* or independently of tracer breakthrough results in significant uncertainties in estimates of controlling parameters. Our objectives are to develop geophysical strategies to measure mass-transfer parameters over a range of spatial scales, and to demonstrate these strategies to produce estimates of mass-transfer parameters for Hanford 300 Area materials. Here, we assess the utility of time-lapse electrical resistivity (ER) and complex resistivity (CR) to improve the basic and site-specific understanding of mass transfer.

During the second year of funding, we focused on (1) ER and CR laboratory experiments; (2) comparison of ER and CR results to nuclear magnetic resonance (NMR) measurements of mobile and immobile porosity; and (3) pore-network modeling of the electrical signature of mass transfer. Column ER/tracer-test experiments were performed using samples of the porous zeolite clinoptilolite, which has well defined mass-transfer properties. Parametric sweeps identified best-fit transport parameters. The estimated mobile and immobile porosities are consistent with measurements using NMR. Analysis of CR spectra measured on sieved fractions of the same zeolite, using a Debye decomposition approach, reveals different relaxation-time distributions. Time-lapse measurements of CR in columns under tracer loading show a time-/frequency-dependent response to reactive transport. These results also show a disconnection between real and imaginary components of the CR spectra relating to surface chemistry of the immobile and mobile domain. This method is currently being applied to a sieved-fraction composite sample from the Hanford 300 Area. Initial analysis of relaxation-time distributions indicate correlation with transport parameters and NMR relaxation-time results. Hanford materials have been obtained and are under study. We also are capitalizing on CR analyses performed for the IFRC on Hanford cores by collaborators at Rutgers U. Pore-network models qualitatively reproduce the hysteresis observed in time-lapse ER but indicate that the bicontinuum Archie model used previously systematically over-predicts the contribution of immobile porosity to bulk conductivity. A multiphase Archie model, which allows for different internal connectivity (i.e., formation factor) for mobile and immobile domains, provides a superior fit to the simulated bulk-fluid conductivity relation.

Fieldwork to install ER/temperature/sampling probes took place in March 2012 in preparation for summer field experiments. Infiltration and tracer experiments will assess the mass-transfer properties of the vadose zone and 'smear zone.' Additional ER and CR work on Hanford materials is ongoing, and publications on results from zeolites and pore network modeling are in preparation. To date, two papers acknowledging this project have been published. In the final year of our grant, we will focus on integrating insights from our pore-, laboratory-, and field-scale investigations.

Advanced Simulation Capability for Environmental Management (ASCEM): Development and Demonstrations

Mark D. Freshley (PI), *PNNL*; J. David Moulton, *LANL*; Ian Gorton, *PNNL*; Susan S. Hubbard, *LBNL*; Vicky L. Freedman, *PNNL*; Gregory Flach, *SRNL*; Carl I. Steefel, Stefan A. Finsterle—*LBNL*; Paul Dixon, *LANL*; the ASCEM Team

The U.S. Department of Energy Office of Environmental Management, Technology Innovation and Development is supporting development of the Advanced Simulation Capability for Environmental Management (ASCEM). ASCEM is a state-of-the-art scientific tool and approach for understanding and predicting contaminant fate and transport in natural and engineered systems. The modular and open source high performance computing tool facilitates integrated approaches to modeling and site characterization that enable robust and standardized assessments of performance and risk for EM cleanup and closure activities. The modularity of ASCEM enables new scientific understanding to be incorporated as it is developed. The open-source nature is envisioned to be critical for adoption of ASCEM by the scientific community for use in quantifying and understanding flow and transport associated with a variety of critical energy and environmental subsurface systems.

During the second full year of the project, ASCEM has continued to make significant progress in the development of Platform and Integrated Toolsets and a High Performance Computing (HPC) Multi-Process Simulator. The Platform, called Akuna, includes toolsets that support data management, parameter estimation, uncertainty quantification, and visualization of model input and output. The HPC capabilities target process model representations, toolsets for interaction with Platform, and verification and model confidence testing. The HPC simulator, called Amanzi, includes transient flow using both structured and unstructured grids implemented on a parallel computer using up to 1000 processors. Additional capabilities are now being added, including: transport and geochemical processes and interfaces with Platform capabilities. A build system is being developed to permit compiling on different desktop and supercomputers.

The ASCEM Project is working to complete a second demonstration focused on three working groups. The working groups include 1) Attenuation-Based Remedies for the Subsurface, focused at the Savannah River Site F Area, 2) the Hanford Site Deep Vadose Zone, and 3) a representative Waste Tank Performance Assessment. Progress on ASCEM development and demonstrations will be highlighted in this poster.

Effects of Textural-Scale Heterogeneity on the Release of Uranium from Contaminated Sediments

Melanie A. Mayes (PI), Vijay A. Loganathan, Guoping Tang—*ORNL*; John M. Zachara, *PNNL*

The vadose zone at the Hanford, Washington, 300-Area is contaminated with uranium (U) from historical disposal in settling ponds, and persistent contamination of the groundwater is observed. Release of U from the partially-saturated contaminated sediments will be a function of (1) the degree of connection between major flowpaths and fine-grained pockets of sorbed U, and (2) differential rates of desorption which are a function of the mineralogy active at a particular moisture content. The goal of this study is to perform column leaching experiments at variable moisture regimes with two textural scales, i.e. fine-texture (<2 mm) and field-texture (<31.5 mm). The objectives of this study are (1) to determine the dependence of mass transfer and to provide parameters to describe flow and transport as a function of water content and (2) to discover and quantify the factors controlling the exchange of U between different pore classes.

Contaminated vadose zone sediment was obtained from the "smear zone," located between the vadose zone and groundwater. The sediment was fractionated into different particle sizes that ranged from <0.053 – 12.5 mm. Chemical extractions, viz. dithionate-citrate-bicarbonate and formate, were performed to quantify total U and dominant reactive mineral fractions. Moreover, the labile form of U, i.e. expected total available U for desorption, was quantified using bicarbonate and synthetic groundwater extractions in batch systems. About 41% of the total U in the finer fractions existed as labile U. The boundary conditions and hydraulic parameters for unsaturated flow experiments were obtained using Hanford analog sediment that was composited to the mean smear zone particle size distribution. The saturated hydraulic conductivity in the field-textured column was about an order of magnitude higher when compared to the fine-textured column. A saturated column leaching experiment was performed using fine-textured contaminated sediment wherein bromide and pentafluorobenzoic acid were used as non-reactive tracers. Both the tracers confirmed the absence of physical nonequilibrium during stop-flow scenarios. Ongoing experiments include a saturated column experiment wherein the sediments are packed to field-textured particle size distribution. We expect that the field-textured column will exhibit physical nonequilibrium limiting the rate of release of U from the reactive fine-grained materials, and that the degree of rate-limited mass transfer will change as a function of moisture content. Currently, efforts are underway to evaluate the existing smear zone model to describe our batch and column results. This research will enable improved field-scale predictions of groundwater U mobility by capturing the coupled hydraulic and geochemical controls in the smear zone.

Integrated Field-Scale Subsurface Research Challenges (IFRC)

Reducing the Hydrologic and Geochemical Uncertainty for Modeling Uranium Migration at the Hanford 300 Area by Assimilating Multi-Scale and Multi-Type Data

Hanford IFRC (Principal Investigator: John Zachara)

X. Chen (PI, Xingyuan.chen@pnnl.gov), G. Hammond, C. Murray, J. Zachara—*PNNL*

In modeling the uranium migration within the Integrated Field Research Challenge (IFRC) site at the Hanford 300 Area, uncertainties arise from both hydrologic and geochemical sources. The hydrologic uncertainty includes the transient flow boundary conditions induced by dynamic variations in Columbia River stage and the underlying heterogeneous hydraulic conductivity field, while the geochemical uncertainty is a result of limited knowledge of the geochemical reaction processes and parameters at the field scale, as well as heterogeneity in uranium source terms. In this work, multiple types of data are sequentially assimilated across scales to reduce the hydrologic uncertainty, including the results from constant-injection tests, borehole flowmeter profiling, and conservative tracer tests. The hydrologic data assimilation is followed by geochemical data assimilation, which is conditioned on point measurements of sorbed uranium in the water table smear zone and uranium breakthrough curves from a desorption test that took place at high spring water table. Ensemble-based data assimilation techniques are used in our study, and their computational demand is managed by using the multi-realization capability within the parallel PFLOTRAN simulator.

Impact of Soil Grain Size on Modeling Uranium Surface Complexation at the Hanford 300 Area IFRC Site

Hanford IFRC (Principal Investigator: John Zachara)

G. Hammond (PI, glenn.hammond@pnnl.gov), X. Chen, J. Zachara—*PNNL*

Recent laboratory experiments based on Hanford 300 Area sediment have demonstrated a dependence of uranium [U(VI)] sorption properties on soil grain size. In that work, an additive approach was employed to develop a composite adsorption/desorption conceptual model for U(VI) based on unique surface complex selectivity coefficients and kinetic multirate parameters (i.e. mean and standard deviation of rate constants) assigned to each soil grain size fraction. This presentation demonstrates the impact of this enhanced geochemical conceptual model on field scale models of U(VI) migration within the Hanford 300 Area IFRC site. At the field scale, uncertainty in soil grain size distribution must be considered, and this geochemical uncertainty further complicates predictive modeling of U(VI) persistence at the IFRC site.

Investigating Field-Scale Properties and Processes that Influence Uranium Behavior at the Hanford 300 Area IFRC Using Advancements in Electrical Geophysical Imaging

T. Johnson (PI), W. Greenwood, M. Rockhold, E. Wallin, J. Zachara—*PNNL*; R. Versteeg, *Sky Research*; L. Slater, *Rutgers U.*

Accurate modeling and prediction of system-scale uranium behavior in the Hanford 300 Area requires information concerning the distribution of sediment textural properties and how those properties govern physical and geochemical interactions between groundwater and Columbia River water. Electrical geophysical imaging methods have demonstrated utility for providing such information at relatively high resolution over large areas. Improvements in Electrical Resistivity Tomography (ERT) made possible through high performance computing and inversion code advancements were used at the Hanford 300 IFRC to better understand field scale properties and processes controlling uranium transport. Efforts initiated or completed in 2012 include 1) a high-resolution, 3D, geostatistically-constrained ERT characterization of the IFRC well field, 2) time-lapse imaging of river water intrusion into the 300 Area during spring high stage, and 3) time-lapse imaging of surface recharge and infiltration through the contaminated vadose zone.

The IFRC well field was implemented with a dense array of 840 electrodes, enabling high-resolution ERT imaging. Using parallel processing and custom imaging constraints that enable the integration of prior information on known electrical conductivity boundaries and subsurface structural features, a geostatistically accurate image of bulk electrical conductivity was generated and validated with core scale measurements. The results of this constrained inversion displayed a significant improvement over the standard inversion methodology, and revealed subsurface structure that likely plays a significant role in uranium transport. Most notable of these is a thin, spatially continuous, low permeability region dividing the saturated zone that may inhibit vertical contaminant migration. This same region contributed to vertical well-bore flows previously discovered by IFRC researchers.

Exploiting the electrical conductivity contrast between 300 Area groundwater and Columbia River water, SBR project DE-FG02-08ER64561 led by Rutgers University demonstrated the capability to image near-shore groundwater river-water interaction with ERT. In the spring and summer months of 2011 (March to September), 2D ERT arrays were deployed further inland to monitor river water intrusion toward the IFRC well field during high river stage using time-lapse ERT imaging. Results revealed a prominent preferred flow pathway into the 300 Area that is generally consistent with a depression in the lower aquifer boundary unit assumed to be a paleochannel, thus discovering a significant control on groundwater river-water interaction in the 300 Area.

Surface recharge could play a significant role in transporting residual uranium from the vadose zone to the water table, contributing to the persistence of the uranium plume in the 300 Area. Efforts are currently underway to monitor precipitation-induced moisture migration within the vadose using time-lapse surface ERT, cross-hole ground penetrating radar, and neutron moisture logging. Initial results show moisture moving downward relatively rapidly after moderate precipitation events, and stopping at the boundary between backfill and native 300 Area materials. This may indicate backfill materials act as a partial capillary barrier to vertical flow, at least within the IFRC well field region. This effort is ongoing.

Improvements in electrical geophysical characterization and monitoring capabilities enabled by the IFRC are providing information concerning subsurface structure and processes that govern uranium transport in the 300 Area. Ultimately, this information must be used to inform 300 Area flow and transport models. We see significant scientific opportunities in this regard through coupled hydrogeological/geophysical modeling, enabling the use of time-lapse geophysical data for model calibration.

Geochemical Model, Model Uncertainty, and Pore-Scale Insights for Uranyl Reactive Transport in Hanford 300A Smear Zone Sediments

Chongxuan Liu (PI, Chongxuan.liu@pnnl.gov), John Zachara, Jianying Shang, Changyong Zhang, Zhi Shi, Paul Majors—*PNNL*; Deborah Stoliker, Douglas Kent—*USGS*; Xiaoying Zhang, Bill Hu—*Florida State U.*

This is a collaborative research to develop a consistent uranium geochemical model for Hanford 300A smear zone sediments, to assess model uncertainty for short- and long-term prediction of uranyl release from the sediments, and to provide pore-scale insights into the reactive transport in heterogeneous porous media. Experiments of batch, stirred flow-cell, and columns of variable sizes were performed to systematically investigate uranyl release from and reactive transport in different grain size fractions and their composites in a sediment composited from 300A smear zone sediments. A consistent geochemical model that integrates uranyl surface complexation reactions, aerobic denitrification, cation exchange, and calcite dissolution was developed to interpret the experimental results. A Bayesian-based Monte Carlo Markov Chain approach was developed to rigorously analyze the assumption and uncertainty of the rate parameters and their statistical distribution in the geochemical model and to assess the effect of the parameter uncertainty on the prediction of uranyl release from the sediment. X-ray computerized tomography (XCT), nuclear magnetic resonance relaxation (NMRR), and vacuum-drained pore water chemical analysis were used to provide insights into the pore-scale uranium distribution and release rates. Pore-scale micromodel and reactive transport simulations were used to investigate the coupling of advection and diffusion with surface reactions and to provide insights into the scale-dependent manifestation of the pore-scale geochemical reactions in both intragranular and inter-granular domains. The results showed that all grain size fractions ranging from clay/silt to gravel contributed to uranyl surface complexation reactions in the sediment. The desorption rates were similar in grains with <2mm sizes, but slower in the gravel fraction (2-8mm). The rate and extent of uranyl release was strongly affected by fluid chemical composition, which was collectively influenced by denitrification, calcite dissolution, and cation exchange. Uranyl release and reactive transport in the grain size composites (< 2mm and <8mm) were predictable from the linear addition of size-specific geochemical models, but were better simulated using a geochemical model for the composite. The results implied the importance of understanding microbial processes in the sediment that apparently led to the denitrification, which affected pH, calcite solubility, dissolved carbonate and calcium concentrations, which in turns affected uranyl surface complexation reactions. Besides the chemical composition effect, model simulations of the experimental results also indicated that uranyl release from individual grain size fractions and their composites was affected by diffusive mass transfer in intragranular and inter-granular domains, which was further confirmed by XCT and NMR tomographic analysis of sediment columns. Micromodel experiments and simulations revealed the importance of pore-scale coupling of geochemical reactions in controlling reaction rates at the Darcy scale. The coupling has a larger effect on faster reactions as they retarded the diffusion faster, which in turns affected more on surface reactions in interior diffusion domains. The developed uranium geochemical model contained uncertainty in its rate constants with slower rate constants having larger uncertainties. The uncertainty resulted from the assumption of the statistical distribution for the diffusive mass transfer rate constants in the model and from the time-scale limitation of laboratory experiments.

The Effects of Columbia River Stage on Contaminant U Concentrations and Groundwater Compositions at the 300 Area IFRC

Hanford IFRC (Principal Investigator: John Zachara)

James P. McKinley (PI), Thomas C. Resch, Micah D. Miller, Rachael M. Lund, Vince R. Vermeul, Christopher J. Murray, John M. Zachara—*PNNL*

Seasonal variations in contaminant uranium concentrations have long been observed at the Hanford site's 300 Area. A significant pool of uranium persists in the vadose zone; of particular interest is the uranium within the smear zone, the area traversed by the water table. The springtime snowmelt and the resultant long and short-term rise and fall in river stage drives a coupled undulation in the elevation of the water table along the river shoreline to a distance from the river of more than 250 m. Our objective was to determine whether groundwater captured uranium from the smear zone during water table rises, and whether the groundwater composition was affected by infiltration of river water during high-stage events. Because the timing and magnitude of river stage variations is dependent upon the accumulation of snow in the Columbia River catchment and the rapidity with which it is melted during the spring thaw, understanding the potential for U contributions to the local aquifer from the vadose zone required a multi-year sampling effort. To date, our efforts included sampling during the spring thaw for the years 2009-2011. Groundwater was sampled by pumping from the center of the well screen and by bailing from the top of the aquifer (sampling in 2011 was by pumping only) across the IFRC, and analyzed for major dissolved components and uranium.

Uranium concentrations prior to the seasonal groundwater rise were 30 -50 μg U L^{-1} across the site each year. In each year, the water table rose abruptly, but the date and magnitude varied significantly. In 2010, the advent of spring was relatively late, and the maximum elevation occurred in late June; in 2011, the maximum was three weeks earlier. The magnitude of the rise varied also, with maximum elevations of approximately 106.3, 106.8, and 107.9 m in 2009, 2010, and 2011, respectively. In each year, the uranium concentration increased differentially across the site, with the largest contributions occurring proximal to the south-most cluster of nested wells. For example, in 2010, the uranium concentration increased from 50 μg L^{-1} to 330 μg L^{-1} over the course of 4 days at the south end of the site. Uranium concentrations decreased as the water table crested. The uranium concentration across the site – the 'background' concentration – increased broadly to 60 – 70 μg L^{-1} over the course of the tests. Anion concentrations were used to assess the impact of river water infiltration. In 2009, no river water intrusion was detected; in 2010 river water comprised a maximum of approximately 80% of the groundwater at the eastern IFRC boundary, and was >90% in 2011. The groundwater impact was less toward the west, with the river water invading across the site to the northwest, and comprising less than 25% of the total at the western site boundary. The results demonstrated that the smear zone represented a significant source of uranium to groundwater, and that river water imposed significant compositional variation to the aquifer over the course of the test.

Reactive Transport Field Experiments at the Hanford IFRC

Hanford IFRC (Principal Investigator: John Zachara)

V.R. Vermeul, M.D. Freshley, B.G. Fritz, R.D. Mackley, J.P. McKinley, K.R. Parker, J.M. Zachara (PI)—*PNNL*

The Integrated Field-Scale Subsurface Research Challenge (IFRC) at the Hanford 300 Area addresses multi-scale mass transfer processes controlling U plume dynamics in a complex hydrogeologic setting. The site has 35 instrumented wells, which have been remediated to eliminate the effects of wellbore flow and focus testing on the uppermost portion of the aquifer, and an extensive monitoring system. During CY 2011, several significant, culminating experiments were performed on the revised well field, involving reactive transport. In the spring, an experimental campaign investigated U desorption and reactive transport processes in this uppermost aquifer zone. The experiment involved injecting groundwater containing low U concentrations and a conservative tracer over a two week period. The experimental objective was to create an extended zone of low U concentration groundwater within the IFRC well field that induced desorption of adsorbed U from the aquifer sediments. In the fall, a series of uranium adsorption and desorption experiments were conducted with the objective of providing information about uranium mass transfer processes and kinetics for high concentration U pulses released from the lower vadose zone. The experimental design for the first two injection experiments consisted of two operationally similar injections of groundwater containing elevated uranium concentrations mixed with make-up water of different chemical composition (one groundwater, the other filtered river water with a lower bicarbonate concentration). During each of the injections, the high U test solution (~ 600 μg/L, baseline concentrations within the wellfield were on the order of 100 to 150 μg/L) was spiked with a unique conservative tracer and injected into the uppermost, high permeability portion of the aquifer. These two injection tests were nearly identical except for the makeup water composition and anionic tracer species used. This test configuration made it possible to interrogate the effect of injection solution chemical composition on uranium mass transfer processes. The third experiment, which utilized an injection solution containing elevated uranium concentrations (750 μg/L), filtered river water as the make-up water, and a third unique ionic tracer, targeted a lower permeability intermediate depth interval of the aquifer. These injection experiments have collectively revealed that U retardation is very low in the extremely high permeability aquifer materials comprising the uppermost portion of the aquifer. Although U retardation is relatively small in the high permeability upper zone, a comparison of U transport response for the different solution chemical compositions demonstrated increased mass transfer for the lower bicarbonate concentration river water case. In addition, U adsorption/desorption processes were greatly increased in the lower permeability intermediate zone. The increasingly comprehensive field experimental results, along with the field and laboratory characterization, are leading to a new conceptual model of U flow and transport in the IFRC footprint and the 300 Area in general.

Multi-Scale Mass Transfer Processes Controlling Natural Attenuation and Engineered Remediation: An IFRC Focused on Hanford's 300 Area Uranium Plume

Hanford IFRC (Principal Investigator: John Zachara)

J.M. Zachara (PI), M.D. Freshley, B.N. Bjornstad—*PNNL*; J.N. Christensen, M.S. Conrad—*LBNL*; J.K. Fredrickson, *PNNL;* R. Haggerty, *Oregon State U.*; G. Hammond, T. Johnson—*PNNL*; D.B. Kent, *USGS*; A. Konopka, *PNNL*; P.C. Lichtner, *LANL*; C. Liu, J.P. McKinley, C. Murray, M.L. Rockhold—*PNNL*; Y. Rubin, *LBNL*; V.R. Vermeul, *PNNL;* R.J. Versteeg, *Sky Research*; C. Zheng, *PNNL*; K.M. Thompson, *DOE-RL*

The Integrated Field Research Challenge (IFRC) at the Hanford Site 300 Area uranium (U) plume addresses multi-scale mass transfer processes in a complex and dynamic subsurface biogeochemical setting where groundwater and river-water interact. The site has 35 instrumented wells that are screened in the upper layer of the unconfined, near-river aquifer. It has a deep borehole for microbiologic and biogeochemical research that is screened in the lower, semi-confined region of the aquifer.

Significant, impactful progress has been made in CY 2011 and early CY 2012 including: i.) geophysical monitoring of winter precipitation infiltration through the U-contaminated vadose zone and spring river water intrusion 150 m inland to the IFRC site, ii.) injection experimentation to probe the lower vadose zone and to evaluate the transport behavior of high U concentrations released from the smear zone in the spring, iii.) extended passive monitoring before, during, and after the period of water table rise and fall, and iv.) collaborative down-hole experimentation with the PNNL SFA on the biogeochemistry of the Hanford-Ringold contact and the underlying redox transition zone. Collaborative microbiologic studies with the PNNL SFA have established a census of microorganism types present with the IFRC, with research now evolving to investigations of *in situ* function and activity. Beyond these experimental efforts, geostatistical models of hydrologic and geochemical properties and adsorbed U distribution, and new hydrologic characterization measurements of the upper aquifer have been integrated into our site-wide reactive transport models (PFLOTRAN and eSTOMP). These increasingly robust models are being used to simulate past and recent U desorption-adsorption experiments performed under different hydrologic conditions, and to perform heuristic modeling to understand the complex functioning of the smear zone under dynamic hydroloigic conditions. Ongoing efforts to assimilate geophysical logging and 3D ERT characterization data into our site wide hydrophysical model have been successful, yielding a recently submitted manuscript.

Our increasingly comprehensive field experimental results and robust reactive transport simulators, along with multi-scale field and laboratory characterization, are leading to a new conceptual model of U(VI) flow and transport in the IFRC footprint and the 300 Area in general Important insights have resulted on the microbiological community and associated biogeochemical processes influencing N, S, C, Mn, and Fe under the highly varied redox conditions present at the site. Collectively, these findings and higher scale models are providing a unique and unparalleled system-scale understanding of the biogeochemical function of the groundwater-river interaction zone.

Data Management Efforts for the Hanford 300 Area and Rifle IFRCs

Hanford/Rifle IFRC—Versteeg

R. Versteeg (PI), *Sky Research, Inc.; Hanford IFRC Team (PI: John Zachara)*
Rifle IFRC Team (PI: Philip Long)

Both the scope of the IFRCs (in terms of duration, number of participants, and diversity of disciplines involved in each IFRC) as well as the amount of data collected is substantially larger than previous geoscience research projects sponsored by DOE. This required an organized effort for data management and curation. Over the past several years, an approach for data management.

was developed and implemented for the Hanford 300 Area(www.300areaifrc.org) and Rifle IFRC(www.ifrcrifle.org) . As the two IFRCs share a common approach, software components and (where appropriate) data models this has allowed for synergistic development and resource utilization. The approach has two main elements: (1) implementing data management as a web application (resolving issues of distributed applications and data inconsistencies) and (2) using the maximum amount of existing software components (both commercial and open source). This extends both to the standard components of a web application (such as the database and the server), and to the software components for mapping, display, and data presentation. To this end, the web application has been implemented in Zend Framework, an open source, object-oriented web application framework implemented in PHP 5 with a MySQL database. The web application makes use of several Google components (Google Maps and Calendars), as well as several open-source packages for wiki (phpBB), graphing (jpGraph,Visit), and data analysis (R).

The data management effort for the IFRCs has several objectives. The first is to capture all data collected as part of the IFRC in such a way that this data is easily available and accessible, both for the core IFRC group and for future researchers. The second is to provide tools for basic data exploration and visualization. The approach to data collection included (1) iterative development of a comprehensive data inventory; (2) implementation of a structure allowing individual scientists to upload their data in a relatively unstructured format in so-called data packages (a loose free form assembly of data with some basic amount of documentation—typically identical to the scientist specific organization); given that the IFRC project PIs (John Zachara and Phil Long) strongly encourage data package assembly and submittal, compliance with this effort is high; and (3) full integration of selected parts of the data contained in the data package into the database.

As data management is an ongoing effort which occurred over the life of the IFRC, both in the continued integration of novel data, as well as in the expansion of features in the web interface and in the refactoring of the database and underlying implementation datamanagement capabilities have been evolving over the life of the IFRC. Current capabilities provide for sample tracking and management, on-demand graphing and contouring of different datasets, generation of time series animations of field and modeling data, cross analysis of different datasets, and download of user selectable subsets of the data. In addition, by aggregating components such as Google calendar, weather, twitter feeds, and webcams, the website provides a central point of access for field activities. At the SBR meeting, an overview and live demonstration of the system will be given.

Utilizing Azimuthal Seismic First-Arrival Tomography (ASFT), Time-Lapse Electrical-Resistivity Tomography (TLERT), and Other Geophysical Methods for the Detection and Characterization of Physical Controls on Hydrologic Transport

ORNL IFRC (Principal Investigator: Scott Brooks)

G.S. Baker (PI), M. Edmunds—*U. of Tennessee*; S. Hubbard, E. Gasperikova—*LBNL*; D. Watson, T. Mehlhorn, K. Lowe, S. Brooks—*ORNL*

The Oak Ridge Integrated Field Research Challenge (ORIFRC) project was established to study the various biogeochemical processes involved in the remediation as well as natural attenuation of a large contaminant plume that is extant in the vicinity of the S-3 Pond area. The site in general consists of three hydrostratigraphic units: (1) a clayey saprolite, (2) a transition zone, and (3) more competent Nolichucky Shale bedrock. The saprolite is clayey, low permeability, typically between 3 and 10 m thick, and has some remnant fracturing. The transition zone includes an irregular region with higher permeability and contaminant transport than either the saprolite or bedrock, due to a combination of high fracture density and lower clay content. The primary fracture sets yield a strong degree of horizontal hydrologic anisotropy. The transition zone can have a hydraulic conductivity as high as 1×10^{-3} to 1×10^{-2} cm/s, where the saprolite and bedrock zones typically have hydraulic conductivities between 1×10^{-4} and 10^{-7} cm/s. Ground water flow is oriented predominantly along geological strike (i.e., bedding planes). The underlying Nolichucky Shale bedrock is highly fractured, with a large degree of horizontal hydrologic anisotropy, but yields much lower conductivities than the transition zone. We have utilized three main techniques for characterizing groundwater movement and physical controls on transport associated with these three hydrostratigraphic units.

First, we demonstrate azimuthal seismic first-arrival tomography (ASFT) as a novel technique for identifying and quantifying the horizontal anisotropy of the three layers present at the ORIFRC. The methodology involves acquisition of seismic first-arrival tomography profiles at 10° intervals rotated around a central point. The resultant tomograms are converted from XZ plane cross-sections to XY plane polar plots. Initial azimuthal velocity maps show an increase in seismic anisotropy with depth, correlating well with the three principle hydrostratigraphic units. Seismic data have been collected at a second site, and in conjunction with pump test and tracer data, we establish a correlation between observed seismic anisotropy and observed hydrologic anisotropy to establish an intermediary relationship between the two types of datasets.

Second, time-lapse surface and crosshole electrical resistivity tomography (TLERT) data, collected over a course of a year in conjunction with aqueous geochemical and rainfall data, are used to examine the impact of recharge on subsurface contamination near the S-3 ponds in response to vertical anisotropy in unsaturated flow. The data suggest that subsurface hydrogeological zonation plays a critical role in plume transient behavior.

Finally, we utilize a combination of traditional seismic first-arrival tomography, deep borehole core analysis, and additional shallow boreholes to identify a spatially confined along-strike fast-flow path, that exceeds fast-flow rates elsewhere in the transition zone. This flow path—initially identified as a low-seismic-velocity zone with continuity down hydrologic gradient and along strike of the S-3 ponds—has been correlated with regions of deepened weathering in the Nolichucky Shale associated with increased limestone composition, resulting in a thicker and more hydraulically conductive zone within the transition zone layer.

Multiscale Investigations on the Rates and Mechanisms of Targeted Immobilization and Natural Attenuation of Radionuclides and Co-Contaminants in the Subsurface

Oak Ridge IFRC (Principal Investigator: Scott Brooks)

Scott C. Brooks (PI), David B. Watson—*ORNL*; Greg S. Baker, *U. of Tennessee*; Maxim Boyanov, *ANL*; Craig C. Brandt, *ORNL*; Craig S. Criddle, *Stanford U.*; Baohua Gu, *ORNL*; Susan S. Hubbard, *LBNL*; Ken Kemner, *ANL*; Joel E. Kostka, *Florida State U.*; Jack C. Parker, *U. of Tennessee*; Chris W. Schadt, *ORNL*; Wei-Min Wu, *Stanford U.*; Trevor Zimmerman, Fan Zhang—*ORNL*; Joe Zhou, *U. of Oklahoma*

The Oak Ridge Integrated Field Research Challenge (ORIFRC) project comprises an integrated multi-disciplinary, multi-institutional research program whose goal is to provide an improved scientific understanding and predictive capability of subsurface contaminant fate and transport through experiments and observations at scales ranging from the molecular to the watershed. The influence of coupled processes on U, Tc, and co-contaminant NO_3^- fate and transport are being quantified along numerous contaminant pathways using subsurface manipulations and the assessment of natural attenuation processes throughout the watershed. These investigations are being integrated with multi-scale numerical simulations to address several coupled processes and assess their impact on contaminant transport. The research is identifying and quantifying key reactions, previously not addressed, that control contaminant fate and transport. The research approach is designed to enable the understanding gained and models developed to be broadly applicable to individual DOE sites.

The overall goal of the project is to advance the understanding and predictive capability of coupled hydrological, geochemical, and microbiological processes that control the *in situ* transport, remediation and natural attenuation of metals, radionuclides, and co-contaminants at multiple scales ranging from the molecular to the watershed. The specific objectives of this research are to: (i) quantify recharge pathways and other hydraulic drivers for groundwater flow and dilution of contaminants along flow pathways and determine how they change temporally and spatially during episodic events, seasonally, and long term; (ii) determine the rates and mechanisms of coupled hydrological, geochemical, and microbiological processes that control the natural attenuation of contaminants in highly diverse subsurface environments; (iii) explore novel strategies for enhancing the subsurface stability of immobilized metals and radionuclides; (iv) understand the long-term impacts of geochemical and hydrologic heterogeneity on the remobilization of immobilized radionuclides; and (v) improve our ability to predict the long-term effectiveness of remedial activities and natural attenuation processes that control subsurface contaminant behavior.

Significant progress towards our original project objectives has been achieved in the past five years and recent results are highlighted in the associated ORIFRC posters. Concurrently, new observations have raised new questions regarding the hydrogeological constraints on biogeochemical contaminant and nutrient transformations in coupled groundwater-surface water systems. These observations present new research challenges for the future that are summarized in operating hypotheses addressing (i) the structure of the subsurface flow network including shallow lateral storm flow and deeper flow paths, (ii) material property controls on the biogeochemical reaction path(s) followed along a flow path, (iii) controls on the concentration, speciation and reactions across the groundwater-surface water interface, (iv) dynamic mixing of distinct water sources and process kinetics, (v) disequilibrium and system response caused by external forcings that alter flow networks.

Nitrate Attenuation and the Impact of pH on the Predominant Denitrifying Microbial Groups in the OR-IFRC Subsurface

Joel E. Kostka (PI), *Georgia Institute of Tech.*; Stefan J. Green, *U. of Illinois Chicago*; Om Prakash, *Georgia Institute of Tech.*; Puja Jasrotia, *Florida State U.*; Lavanya Rishishwar, *Georgia Institute of Tech.*; Chris Schadt, David Watson, Scott Brooks—*ORNL*

The goal of this research is to understand the fundamental mechanisms controlling the fate and transformation of uranium, nitrate, and technetium under natural attenuation conditions. The fate and transport of uranium and nitrate are intimately linked through a variety of biogeochemical reactions. We hypothesize that microbial denitrification is the only biogeochemical mechanism for permanently decreasing nitrate flux, where the denitrification rate is governed by pH and electron donor concentrations. Specific objectives are to: 1) quantify the relative roles of dilution, assimilatory uptake, and denitrification as mechanisms of nitrate natural attenuation along the Bear Creek watershed flow paths, 2) identify and quantify the denitrifying bacterial populations that catalyze nitrate removal in groundwaters on a watershed scale in the uranium-contaminated subsurface, and 3) directly link denitrification activity to the abundance and phylogenetic structure of nitrate-respiring organisms through a tight coupling between geochemical and microbiological approaches.

The site-wide distribution of overall bacteria as well as the dominant denitrifying bacteria in subsurface groundwaters of the main OR-IFRC contaminant plume has been conclusively tracked, and the results are published. Two site-relevant denitrifying bacterial isolates have been described as a novel species, *Rhodanobacter denitrificans*, the description is now published in IJSEM, and the strains have been deposited into public culture collections. We continue to inform our field efforts using genome-based approaches with site-relevant isolates. A genome sequencing project was initiated to further elucidate the *in situ* function of the *Rhodanobacter* group, which has been found to dominate the bacterial communities in the highly uranium-contaminated OR-IFRC subsurface. The genomes have been sequenced for 5 *Rhodanobacter* strains isolated from different regions of the OR-IFRC site, including the described species.

The metabolic potential of the aerobic and denitrifying microbial community response was assessed in the OR-IFRC site subsurface in groundwater and sediment slurry experiments. These experiments demonstrate slow, but active denitrification even at acidic pH (<4), with higher rates and more complete denitrification (to N_2) at elevated pH. Low rates of aerobic respiration were also observed in the highly contaminated acidic, source zone. Background or pristine subsurface sediments showed higher rates of O_2 consumption but denitrification rates were below detection. In a pH threshold experiment, the maximum rate of denitrification in source zone subsurface sediments was observed at pH 5-6, matching the pH adaptation of *R. denitrificans.*

To address their potential role in contaminant transformation, we expanded our site-wide microbial community characterization to include the fungal community composition across the site. Fungal diversity was less dramatically impacted by pH in comparison to bacteria, but some low pH samples had very low diversity. Other factors, such as sampling time, and depth also contribute to the observed fungal community dynamics. Fungal communities were often dominated by fungi from the order Coniochaetales. Site-relevant fungal isolates were obtained in parallel with molecular characterization of subsurface fungal communities. In particular, members of the Coniochaetales, which are abundant in sequence libraries were isolated and shown to mediate denitrification.

Effect of Spatially and Temporally Variable Recharge on Subsurface Reactive Transport of Contaminants at Oak Ridge Integrated Field Research Site

ORNL IFRC (Principal Investigator: Scott Brooks)

Jitendra Kumar (PI), *ORNL*; Peter C. Lichtner, *LANL*; Richard T. Mills, *ORNL*

Recharge is one of the most fundamental components of groundwater systems which drives both flow and transport in the subsurface and plays an important role in the migration of contaminants. Spatial and temporal variation in the recharge in heterogeneous aquifers leads to corresponding variations in the velocity fields, which has a strong bearing on dispersive mixing and transport processes. The impact of temporal variations in recharge are significantly important at the Oak Ridge Integrated Field Research Challenge (ORIFRC) site, which receives an average of 137 cm of precipitation annually. Prediction of contaminant plumes from former waste disposal ponds at the site is desired for the design and deployment of bio-remediation and contaminant containment strategies. Long term monitoring of the contaminants at the site has been carried out using a series of monitoring wells providing point measurements for an array of chemical species of interest. Due to the complex geology of the region, however, a number of preferential flow pathways are present at the site resulting in highly fluctuating point measurements. In addition, temporally variable recharge may induce dynamics in flow leading to significant fluctuations in the ground water levels as well as concentrations of chemical species. To investigate these issues numerical simulations at the site were carried out using the massively parallel flow and reactive transport model PFLOTRAN to estimate the impact of spatially and temporally variable recharge on the migration of contaminant plumes at the site. A series of the details from the actual site (e.g., the gravel filled ditch around the S-3 ponds that receives high storm flow runoffs from the surface asphalt cover, gravel filled S-3 ponds after capping, among others) were incorporated in the model to realistically capture the dynamics of surface and subsurface hydrology at the site. The results were compared and validated against observation data from field monitoring wells.

Geochemical pH Controls and Dynamics of Metals and Radionuclides in a Highly Contaminated, Acidic Aquifer

B. Gu (PI), T. Zimmerman, G. Tang, D. Watson—*ORNL*; W.-M. Wu, *Stanford U.*; K.M. Kemner, *ANL*; C. Schadt, *ORNL*; G.S. Baker, *U. of Tennessee Knoxville*; S. Hubbard, *LBNL*; Puja Jasrotia, J. Kostka—*Georgia Institute of Tech.*; S. Brooks, *ORNL*

As part of the Oak Ridge Integrated Field Research Challenge (IFRC), the objective of this research is to determine geochemical dynamics and to evaluate feasibility of a controlled base addition for immobilizing uranium (as uranyl, UO_2^{2+}) and other contaminant metal ions such as aluminum (Al), nickel (Ni), cobalt (Co), and technetium (Tc) *in situ* through neutralization. The research is motivated by the fact that few effective remedial options are available to remove or immobilize uranium *in situ* in such a highly contaminated acidic aquifer, but pH adjustment can lead to sorption, precipitation/co-precipitation or immobilization of these contaminant metal ions. A field plot (~2×3 m) was established following laboratory studies, which showed that the addition of base can provide an effective means of sequestering U(VI) and other toxic metals in the soil and groundwater. Greater than 94% of soluble U(VI) and greater than 83% of Tc(VII) can be immobilized at pH about 4.5 by the co-precipitation and/or adsorption with Al-oxyhydroxides. *In situ* controlled base addition bega in late November 2010 and lasted 12 months, during which regular geochemical, microbiological, and geophysical analyses, and two bromide tracer tests were performed in order to assess the biogeochemical dynamics and potential groundwater flow path changes accompanying the pH increase. The pH of recirculated groundwater was slowly increased from an ambient value of approximately 3.5 to about 5.5 in the injection well, and the anticipated corresponding decrease in U and Al (> 90% reduction) was observed. Downgradient wells and the extraction well have shown similar behavior with approximately 80% decrease in U and Al, although the extraction well did not exhibit a discernible change in pH. Our results indicate that the field plot is being neutralized and acting as a barrier (or a sorbent) for Al, U and other toxic metals, thus validating our original hypothesis that the master variable for U, and possibly Tc, attenuation is pH. Al hydrolysis and the presence of carbonates are the dominant pH buffering reaction impeding U precipitation, adsorption, and transport at Oak Ridge IFRC.

New Isolates of *Geobacter*, *Desulforegula*, *Desulfovibrio*, and *Pelosinus* and Their Roles in a Low Diversity Consortia During Sustained *In Situ* Reduction of U(VI)

ORNL IFRC (Principal Investigator: Scott Brooks)

C.W. Schadt (PI), T.M. Gihring, S.L. Carroll, T.L. Mehlhorn, Z.K. Yang, M.K. Kerley, D.A. Elias, D.B. Watson, S.C. Brooks—*ORNL*; C.M. Doktycz—*Michigan State U.*; J.R. Merryfield—*U. of Tennessee*; J.E. Kostka, *Georgia Institute of Tech.*

Subsurface amendments of slow-release substrates (*e.g.*, emulsified vegetable oil; EVO) are potentially a pragmatic alternative to using short-lived, labile substrates for sustained bioimmobilization within contaminated groundwater systems. We previously tracked the dynamic changes in geochemistry and microbial communities for 270 days following a one-time EVO injection that resulted in decreased groundwater U concentrations that remained below initial levels for approximately 4 months. Pyrosequencing and quantitative PCR of 16S rRNA from monitoring well samples revealed a rapid decline in groundwater bacterial community richness and evenness after EVO injection, concurrent with increased 16S rRNA copy levels, indicating the selection of a very narrow group consisting of 10-15 dominant OTUs. Members of the Firmicutes family *Veillonellaceae* dominated after injection and most likely catalyzed the initial oil decomposition and utilized the glycerol associated with the oils and possibly energy sources associated with the small amounts of yeast extract in the EVO product. Sulfate-reducing bacteria from the genus *Desulforegula*, known for LCFA oxidation to acetate, also increased greatly shortly after EVO amendment and are thought to catalyze this process. Acetate and H_2 production during LCFA degradation appeared to also stimulate NO_3^-, Fe(III), U(VI), and SO_4^{2-} reduction by members of the *Comamonadaceae*, *Geobacteriaceae*, and *Desulfobacterales*. Methanogenic archaea flourished late in the experiment and at points constituted over 25% of the total microbial community.

Subsequent to the experiment we were able to isolate several of these organisms into pure culture including representatives of phylogenetically distinct isolates and/or species of *Geobacter* and *Desulforegula*, *Pelosinus* and *Desulfovibrio*. Physiological investigations into the substrate utilization patterns and end products in pure cultures of these isolates have largely verified the hypothesized model for the functioning of these limited communities that had been developed during the community investigations. *Pelosinus* IFRC1214 has the ability to ferment glycerol from triglycerides and produce acetate, while *Desulforegula* IFRC300 has the ability to use LCFAs producing acetate or acetate + propionate depending on the carbon chain length of the LCFA's while reducing sulfate. The endproducts above (largely acetate) have in turn been shown to support growth by *Geobacter* IFRC128 and *Desulfovibrio* IFRC170 isolates in laboratory studies of the isolates. Currently, in collaboration with the JGI, representative strains of the above isolates are undergoing full genome sequencing and future studies are planned to reconstitute the community and verify its function in synthetic consortia derived from the pure cultures above.

Modeling Hydrobiogeochemical Dynamics in a Field Emulsified Vegetable Oil (EVO) Injection Test at the Oak Ridge IFRC

ORNL IFRC (Principal Investigator: Scott Brooks)

Guoping Tang (PI, tangg@ornl.gov), Scott C. Brooks, David B. Watson, Chris W. Schadt—*ORNL*; Jack C. Parker—*U. of Tennessee*; Wei-Min Wu, *Stanford U.*

A pilot test was conducted involving a one-time 2-hour injection of emulsified vegetable oil (EVO) into an aquifer to reduce long-term U discharge to a stream. The objective of this work was to develop a coupled hydrological, geochemical and microbiological model to better describe and understand the complex processes in the field, and identify knowledge and data gaps for field scale bioremediation predictive simulation.

First, we developed a comprehensive biogeochemical model to couple hydrolysis of EVO, production and oxidation of long-chain fatty acids (LCFA), glycerol, acetate, and hydrogen, reduction of nitrate, Fe(III), U(VI) and sulfate, and methanogenesis with growth and decay of multiple functional microbial groups. By estimating a consistent set of EVO, LCFA and glycerol degradation rate constants, and using growth rate parameter values from the literature, the model matched observed sulfate, U(VI), and acetate concentrations and described microbial population dynamics in various microcosms amended with ethanol, oleate, and EVO and different levels of sulfate.

Using a kinetic Langmuir isotherm to approximate EVO sorption, we then applied the biogeochemical model to simulate observed acetate, nitrate, Fe, U, and sulfate concentrations, and the activities of multiple microbial functional groups during and after EVO injection. While lab-determined parameters were generally applicable in the field-scale simulation, the rate coefficient for EVO hydrolysis was estimated to be an order of magnitude greater in the field than in microcosms. Assuming *Pelosinus* was grew via glycerol fermentation, the model predicted later and less biomass production for these fermentative microorganisms than observed, indicating potential alternative pathways for *Pelosinus* growth. A lag time of about 50 days or alternative inhibitory mechanisms for acetoclastic methanogenesis was necessary to simulate the observed sustained acetate concentration.

The model predicted substantial accumulation of denitrifiers and sulfate reducers, and U(IV) near injection wells and along the side boundaries of the treatment zone where produced electron donors (e.g., acetate) met electron acceptors in the groundwater. While EVO retention and hydrolysis characteristics were expected to control treatment longevity, modeling results indicated that electron acceptors such as sulfate may not only compete for electrons but also play a role in degrading complex substrates and enhancing U(VI) reduction and immobilization.

Diffusion/Deposition/Remobilization of Uranium in Bioreduced Zones

ORNL IFRC (Principal Investigator: Scott Brooks)

D. Watson (PI), G. Tang, J. Earles, S. Brooks—*ORNL*

It is common practice to inject substrates and other reactants to reduce the mobility and/or toxicity of subsurface contaminants through bioreduction and other remediation techniques. These injections result in manipulated zones that are in a state of chemical disequilibrium. For example, bioreduction can significantly reduce the concentration of contaminants (like U) and other inorganics in groundwater but increase the concentration on the solid phase. Due to preferential transport through subsurface heterogeneities, there will be abrupt aqueous concentration gradients between well connected high permeability zones that receive a high concentration of treatment media (low U zone) and adjacent lower permeability zones that do not receive treatment media (high U zone). The objective of this study is to assess the diffusion of U into bioreduced zones from adjacent unreduced zones, deposition of the U in the bioreduced zone and remobilization of U after the bioreduction has stopped.

Laboratory bottle tests, field observations at the U.S. DOE Oak Ridge Integrated Field Research Challenge site during U bioreduction experiments and numerical modelling were employed to meet these objectives. U contaminated soils encapsulated in polyacrylamide hydrogels (Spalding et. al., 2010) were used in the lab and the field to determine U release and diffusion rates. A two site kinetic model was used to predict release and diffusion of U from unreduced zones to adjacent reduced zones.

The results of our study suggest that U will migrate from unreduced zones into reduced zones when bioreduction is active resulting in "extra" U being deposited in high permeability transport pathways. However, if bioreduction conditions are not maintained, an unintended consequence may be an increase in the U flux (relative to pre-bioreduced conditions) as the "extra" U is released as a result of oxygenated groundwater entering the previously reduced zone.

Spalding, B. P., S.C. Brooks and D. B. Watson. Hydrogel-Encapsulated Soil: A Tool to Measure Contaminant Attenuation *In Situ*. 2010. *Environ. Sci. Technol.* 44(8):3047-3051.

Impact of "Flow Tubes" within Structured Media on Groundwater Transport and Surface/Groundwater Interactions

ORNL IFRC (Principal Investigator: Scott Brooks)

D. Watson (PI), T. Mehlhorn, K. Lowe, C. Schadt, J. Howe, J. Earles, S. Brooks—*ORNL*; S. Hubbard, C. Ulrich, J. Peterson—*LBNL*; G. Baker, R. Storniolo—*U. of Tennessee*; D. Phillips, *Queens U.*; J. Kostka, *Georgia Institute of Tech*.

Recent studies at the ORIFRC site indicate that groundwater transport in structured media may behave as a system of parallel flow tubes. ORIFRC studies suggest that several dominant types of groundwater flow paths exist with the primary driver being the solid phase encountered (e.g., clays, carbonates, clastics) as contaminants migrate along the pathway. We have begun conducting preliminary geophysical, spectrographic, geochemical and microbiological studies to help determine if processes (solid phase reactions, recharge, diffusion, microbial interactions) that occur along the groundwater flow tubes have a significant impact on the reactions that occur when groundwater discharges and interacts with surface water. Groundwater geochemistry and contaminant concentrations reaching the Bear Creek tributaries can vary depending on the "tube" groundwater flows through and the solid phase encountered. For example, if a tube is rich in carbonate, the pH of the groundwater will increase and the U concentration will decrease but high nitrate concentrations are maintained. Low pH and high U conditions are likely to be more persistent in pathways with lower carbonate present in the solid phase.

As expected, preliminary studies show that surface/ground water interactions are dynamic; changing rapidly in time and space due to precipitation events. Under some flow conditions we have observed extreme contaminant stratification with depth in some deeper pools (2-3 feet deep). For example on 11/3/11 at NT1+250 the Specific Electrical Conductivity (SEC) at the creek bottom was 11,320 μS/cm and the pH was 4.4. Close to the surface SEC and pH were 732 μS/cm and 6.9, respectively. This suggests contaminated groundwater is entering at the bottom of these pools and remains temporarily trapped at the bottom due to density effects. As highly contaminated low pH and DO water at the bottom of the pool migrates upwards and interacts with surficial waters containing high pH and DO, mixing and contaminant transformation will occur. In this zone of mixing, kinetically controlled reactions are likely to occur that produce U, Al, Mn, Fe and other precipitates. Microbial sampling and DNA analysis of sediment and surface water samples collected from Bear Creek and tributaries are underway to help elucidate changes in microbial processes under different flow conditions.

Preliminary data shows that how and where surface water samples are collected can significantly impact the results, interpretation and estimation of surface water fluxes. The amount of mixing and reaction kinetics after discharge depends on the proportion of surface water and groundwater that enters the creek along the mixing zone. These processes are presently poorly understood and warrant further in-depth study to better understand and predict long-term contaminant fate, transport and discharge through the surface water exit pathway.

Application of GGKbase to Analyze "Omic" Data from Acetate-Stimulated Subsurface Microbial Communities

Brian C. Thomas, Kelly C. Wrighton, Ken-ichi Ueda, Andrea Singh, Jill Banfield (PI)—*U. of California Berkeley*

http://geomicrobiology.berkeley.edu/rifle/acd_ggkbase.html

Rifle IFRC project goal: To simultaneously analyze genomes reconstructed from community metagenomic data to provide functional insight.

Cultivation-independent approaches provide access to the wide diversity of microorganisms in natural environments. Sequence data (metagenomic information) is foundational to most studies of natural microbial communities. In addition to providing insight into metabolic potential, these data enable functional analysis through proteomics (proteogenomics) and provide context for transcriptomic and metabolomics information.

Given the vast sizes of metagenomic datasets, extraction of biological and biogeochemical insight is challenging. Here, we present GGKbase as a means for data management and analysis, demonstrating its utility through application to microbial community datasets collected during the early, mid, and late phase of iron-reduction (secondary stimulation) at DOE's Rifle IFRC site. The Kbase is designed for analysis of well-assembled datasets, where much of the data have been assigned to near-complete genome bins. Although relatively uncommon at this time, such datasets will be the norm in the near future, as sequencing and bioinformatics methods improve.

GGkbase is a multi-user, list-based, social/sharing approach for analysis of the metabolism of individual organisms and comparative metabolic analysis at the community level. For an individual organism, is possible to browse the gene content of genome fragments, to investigate the functional predictions, and to modify them. The linked pages also document sequence similarity to other organisms, and provide access to proteomic information. Individual genes or groups of genes belonging to a pathway can be assigned to one of more lists, as determined by the investigator, and these lists can be shared with other users (new users can be invited to participate in curating a list). Because the lists are driven by a keyword search (or EC number, GO term etc.), genes can be identified and classified simultaneously across the entire dataset. This establishes metabolic profiles using tens, hundreds, and potentially thousands of genes at a time. It is also possible to summarize the gene and pathway capacities across the dataset using "genome summary" visualization. This allows recognition of characteristics shared by multiple organisms, thus is useful for investigating the molecular underpinnings of ecosystem metabolic processes. Application to the Rifle metagenomic dataset comprising enabled efficient analysis of 87 genomic datasets. Genome summaries provide a means to rapidly communicate information about genome completeness (based on marker gene content) and metabolic strategies, e.g., obligate fermentation.

Development of GGKbase is supported by DOE's Knowledgebase Program, Susan Gregurick, Program Manager. Rifle IFRC research is supported by U.S. Department of Energy under Contract No. DE-AC02-05CH11231

Sensitivity of Predictions of Uranium Plume Persistence at the Rifle IFRC Site to Reactive Transport Geochemical Parameters and Initial Conditions

James A. Davis (PI, jadavis@lbl.gov), *LBNL*; Janek Greskowiak, *U. of Oldenburg, Germany*; Michael B. Hay, *USGS*; Patricia M. Fox, Kenneth H. Williams, Philip E. Long—*LBNL*

Surface complexation of U(VI) on mineral surfaces generally controls its transport in groundwater under oxic conditions. The degree of surface complexation is affected by several aqueous chemical variables, including pH and Ca, U(VI), and HCO_3^- concentrations. Sorption of U(VI) on Rifle sediments as a function of these variables has been studied in batch experiments and used to develop a surface complexation model (SCM) for the Rifle site (*1*). Hyun et al. also tested the ability of the SCM to predict field-measured U(VI) sorption on Rifle sediments collected by coring and found the model performed successfully. In a further test of the model, Fox et al. (*2*) observed in a field experiment that an abrupt increase in HCO_3^- concentration in Rifle groundwater required a kinetic sorption model to describe U(VI) desorption and transport, because groundwater velocity is fast relative to the time to reach sorptive equilibrium. A multi-rate, mass transfer model was applied to describe these data, using the SCM to describe equilibrium U(VI) conditions.

We have conducted 1-D reactive transport predictions for a likely groundwater flow path along a transect of the Old Rifle site. The model domain is 225m long, with input of relatively uncontaminated groundwater; the outlet is at the Colorado River near DOE well 310. Initial chemical conditions in the model were based on data collected in 1998 at DOE monitoring wells and the equilibrium SCM. Based on the flow velocity of (*3*), one pore volume passes through the domain in 2.2 yr. For a base case, the following assumptions were made: a) porosity = 25%, b) 35% of subsurface sediment mass is <2 mm with a surface area of 3.5 m^2/g (sediments >2 mm are inert), and c) slight calcite oversaturation was allowed, based on field observations. Using the equilibrium SCM, it is predicted that it would take approximately 15 yr (i.e., until 2013) for U(VI) concentrations to decrease to near the upgradient value of 0.2 μmol/L at the model outlet.

The simulations are sensitive to several parameters or assumptions of the base case. For example, assuming calcite equilibrium with groundwater increases the time to reach 0.2 μmol/L U(VI) at the river by 60% to 24 yr. The reason for this effect is that U(VI) sorption is very sensitive to the Ca^{2+} concentration because the major aqueous U(VI) species is $Ca_2UO_2(CO_3)_3^\circ$. Assuming a porosity of 35% or that 61% of the sediment mass is <2 mm has a similar impact, because of the increase in surface area in the aquifer. Assuming a porosity of 15% (or 27% sediment <2 mm) decreases the natural attenuation time by 30% to 10.5 yr (until 2009). If one applies the multi-rate kinetic rate model (*2*), U(VI) concentrations fall faster at first at the end of the domain but are then followed by a much longer tail, increasing the cleanout time by 40% to 21 yr.

Current (2011) field observations of U(VI) concentration near the river outlet for this flowpath are 0.84 μmol/L, which has decreased from a peak value of 1.5 μmol/L in 2004. The base case predicted the 2011 value would be achieved by 2007, but predicted a higher peak value (5 μmol/L) in 2000 that was not observed. The higher values of U(VI) observed at present in comparison to the base case could be due to oxidation of U(IV) in the sediments, which has been found in the Rifle aquifer. Several simulations illustrate the potential impact of oxidation of U(IV) on the natural attenuation times for the aquifer and the sensitivity to various model parameter values.

1. Hyun, S.P., Fox, P.M., et al., 2009, Surface complexation modeling of U(VI) adsorption by aquifer sediments from a former mill tailings site at Rifle, Colorado, Environ. Sci. Tech., 43, 9368-9373.
2. Fox, P.M., Davis, J.A., et al., 2012, Rate-Limited U(VI) desorption during a small-scale tracer test in a heterogeneous uranium contaminated aquifer, Water Resources Res., in press.
3. Yabusaki, S. B., Fang, Y. et al., 2007, Uranium removal from groundwater via *in situ* biostimulation: Field-scale modeling of transport and biological processes, J. Contam. Hydrol., 93, 216-235.

Coupled Abiotic Fe, S, and U Redox Reactions in Rifle IFRC sediments

Patricia M. Fox (PI, pmfox@lbl.gov), James A. Davis—*LBNL*; Ravi Kukkadapu, *PNNL*; Sung Pil Hyun, *U. of Michigan*; David M. Singer, Hua Guo—*LBNL*; John R. Bargar, *SSRL*; Kim F. Hayes, *LBNL*

Uranium (U) is a priority contaminant at DOE UMTRA sites, and the mobility of U is governed by a complex array of biogeochemical processes. Our work is a summary of several related laboratory studies of abiotic reactions and processes affecting U, in particular processes that are coupled with Fe and S abiotic redox reactions. In addition, a tracer test was conducted at the Rifle IFRC site in which Fe(II) was injected into the alluvial aquifer without an added electron donor.

When ^{57}Fe(II) is added to Rifle sediments in a batch reactor in an artificial groundwater solution, a large fraction (60–100%) is quickly oxidized to ^{57}Fe(III) on sediment surfaces. Mossbauer results indicate that the oxidation is coupled to transformation of a ferrihydrite-like mineral to a nanoparticulate, Fe(II)/^{57}Fe(III)-like mineral phase. The fraction oxidized decreases as Fe(II) loading increases, indicating a finite limit for oxidation per unit sediment. Increasing pH from 7.2 to 8.3 or including HCO_3^- had no effect on percent oxidation or mineral transformation.

The effect of Fe(II) addition on U reactions with sterilized Rifle sediment was studied in pH 7.2 and 8.3 solutions equilibrated with 400 ppm CO_2. XANES results indicate U(VI) reduction to U(IV) at both pH values, with the extent of U reduction increasing with increasing Fe(II) concentration. Greater levels of U reduction were observed at pH 8.3 compared to pH 7.2, and this effect may be due to the greater uptake of Fe(II) onto sediments at higher pH. For example, 18% of solid phase U was U(IV) at both pH 7.2 and 8.3 for similar Fe(II) loadings. Greater U reduction was observed in the absence of CO_2 compared to 400 ppm CO_2. At pH 8.3, 54% of U was reduced in the absence of CO_2 while 36% was reduced under 400 ppm CO_2 at an Fe(II) loading of 55 μmol/g.

Aqueous Fe(II) concentrations reach 50-100 μM in biostimulation experiments at the IFRC site. A field experiment was performed in which pulses of groundwater with added Fe(II) were injected into multi-level sampling wells. Groundwater had low dissolved O_2(g) (0.6-2.5μM), pH (7.1-7.4), aqueous U(VI) (0.18 μM), and low Fe(II) (0-4 μM). Aqueous Fe(II) in the injection wells increased with each pulse of added Fe(II), reaching injection concentrations (45 μM) after the 6th injection. In shallower ports (18, 21 ft bgs) the Fe(II) concentrations remained elevated during the 3 week experiment, while Fe(II) concentrations decreased more quickly in deeper ports (24 ft bgs). Despite the appearance of a conservative tracer (Br) in wells 0.8-1.4 m downgradient of the injections, no Fe(II) was detected in downgradient wells. A single pulse of high pH (pH 8.4) groundwater was injected following the Fe(II) injections in one of the wells. Little change in U(VI) concentration was observed in any of the wells at ambient pH, suggesting negligible or no U reduction occurred. Complex changes with time were observed following the high pH injection, which may have been caused by both U(VI) desorption and a small amount of U reduction.

Kinetics of abiotic U(VI) reduction by aqueous sulfide were also studied using a batch reactor. The effects of pH, dissolved carbonate, Ca(II), U(VI), and S(-II) concentration were evaluated in separate experiments. The U reduction rate increased with increasing S(-II) concentration, while it was slowed by increased dissolved carbonate or Ca concentration. The U reduction product was identified as nanoscale uraninite. Thermodynamic modeling showed that the concentrations of non-carbonato U(VI) species, which changed as a function of the experimental variables, correlated with observed changes in U reduction rate. At Rifle groundwater conditions, the U reduction was slow but measurable. Reactive transport modeling is needed to evaluate whether this reaction is of significance under sulfate-reducing conditions in Rifle biostimulation experiments.

Manipulating Uranium Desorption and Redox Status in an Alluvial Aquifer: Overview of *In Situ* Electron Donor and Bicarbonate Amendment Experiments at the Rifle, Colorado IFRC

Rifle IFRC (Principal Investigator: Philip Long)

P. Long (PI), K. Williams—*LBNL*; J. Banfield, K. Wrighton, K. Handley—*U. of California Berkeley*; J. Bargar, *SSRL*; D. Lovley, *U. of Massachusetts*; M. Lipton, Mike Wilkins, S. Yabusaki, C. Murray—*PNNL*; R. Hettich, N. VerBerkmoes—*ORNL*; J. Davis, P. Fox, B. Luef, L. Comolli, S. Fakra—*LBNL*; P. Jaffe—*Princeton*; the Rifle IFRC Science Team

Starting in 2002, field-scale biostimulation and desorption tracer experiments have been conducted in a uranium-contaminated, shallow alluvial aquifer. These experiment that have provided insight into the coupling of microbiology, biogeochemistry, and hydrogeology in the subsurface controlling mobility of U. Research at the Integrated Field Research Challenge site (IFRC) at Rifle, Colorado, USA, initially focused on testing the concept that Fe-reducing bacterial such as *Geobacter sp.* could enzymatically reduce soluble U(VI) to insoluble U(IV) during electron donor amendment (acetate) and that this could be used as a bioremediation strategy. Initial experiments correlated an increase in *Geobacter sp.* with decrease in U(VI) concentration, but also resulted in dominance of sulfate reduction 20 to 30 days after starting electron donor amendment (Anderson et al. 2003 AEM 69:5884-5891). Subsequent experiments directly linked gene expression in *Geobacter sp.* to U(VI) concentration. More recently it has been possible to sample and analyze proteomes, metagenomes, and single cells (cryo-TEM/STXM) during biostimulation, leading to an understanding of both the metabolic capability of the biostimulated microbial community and its active metabolic processes.

In parallel, desorption tracer tests involving both bicarbonate amendment and abiotic Fe-reducing conditions induced by amendment with ferrous sulfate have demonstrated both equilibrium and rate-limited U desorption and the absence of significant U reduction under abiotic Fe-reducing conditions at pH values typical of the Rifle aquifer (7.3±0.2). Results indicate the importance of enzymatic U reduction and suggest the ability to combine desorption and U reduction. Experiments conducted in 2010 ("Super 8") and in 2011 ("Best Western") combined bicarbonate promoted uranium desorption and acetate amendment. The rate of enzymatic U reduction was not decreased by the increased abundance of Ca-uranyl-carbonate aqueous complexes in the bicarbonate part of the experiment. Bicarbonate increases during acetate-only field experiments due to microbial activity promote U desorption during biostimulation and U adsorption following acetate amendment; both biotic and abiotic bicarbonate must be accounted for in order to estimate field-scale reduction rates for U. Future research at the Rifle IFRC will be focused on natural organic carbon and metal cycling (e.g. Fe, V, and U) in the context of the metabolic potential of the entire subsurface microbial community. Initial results from metagenomic sequencing show that assembly of nearly complete genomes for microbes present at the 0.5% level is possible (http://genegrabber.berkeley.edu/rifle_acd/). Coupled with proteomics, transcriptomics, and selected physiological studies, prediction of microbially-mediated C, Fe, U, and V cycling should be possible for typically oligotrophic conditions in the aquifer.

Floodplain-Scale Hydrological, Isotopic, Geochemical, and Geophysical States and Fluxes at DOE's Rifle Integrated Field Research Challenge Site

Rifle IFRC (Principal Investigator: Philip Long)

Kenneth H. Williams (khwilliams@lbl.gov), Mark Conrad—*LBNL*; Manish Gupta, Elena Berman—*Los Gatos Research, Inc.*; Jennifer Druhan, Craig Ulrich, Baptiste Dafflon, John Peterson, Susan Hubbard, Philip E. Long (PI)—*LBNL*

The objective of this research was compilation of a comprehensive inventory of geochemical and geophysical data providing insight into transport processes at DOE's Rifle Integrated Field Research Challenge (IFRC) site and its relation to surface water-groundwater interactions, aquifer heterogeneity, and uranium (U) plume dynamics. Over the past year and a half, we have assembled a spatially and temporally dense geochemical dataset (δD, $\delta^{18}O$, $\delta^{87}Sr$, $\delta^{34}S$-SO_4^{2-}, $^{234}U/^{238}U$, anions, cations, and inorganic/organic carbon) through bi-weekly to monthly sampling of Rifle groundwater and surface water bounding the site (e.g. springs, seeps, and Colorado River). We have interpreted this data within the context of floodplain scale surface and borehole geophysical measurements, including electromagnetic induction and magnetics data. Through data synthesis, we have developed a refined floodplain model that accounts for influx of U-bearing groundwater from off-site (i.e., non-tailings impacted) and the role that magnetic minerals may play in impeding natural flushing of U from the aquifer.

Analysis of groundwater and surface water samples from Dec-2010 to Mar-2012 for δD, $\delta^{18}O$, $\delta^{34}S$-SO_4^{2-}, U, and anion composition has been largely completed. Preliminary results suggest that recharge of the Rifle IFRC aquifer occurs primarily through influx of regional groundwater from the north, as evidenced by δD, $\delta^{18}O$, and $\delta^{34}S$ values shared between select surface water locations and Rifle groundwater. The isotopic composition of Colorado River water is distinct from most groundwater at the site, although seeps to the northeast of the site reflect infiltration from the City of Rifle's discharge lagoons, which receive treated drinking water sourced from the Colorado River. Geochemical data support a sharp water divide between this source term and regional groundwater infiltrating the majority of the Rifle site, with the latter containing naturally elevated levels of U (30-110ppb). Acquisition and processing of surface electromagnetic (EM) induction and magnetic data has been completed, with EM data suggestive of infiltration of spring/seep water from the north. Magnetic anomalies mapped using a surface gradiometer are corroborated by borehole magnetic susceptibility (MS) data, which reveal an elevated magnetic mineral volume fraction within the capillary fringe. Characterization of alluvial magnetite grains recovered during drilling operations reveals a close association of magnetite and U, with enrichment of up to 150mg/kg of magnetite.

Future research directions include (a) analysis of groundwater and surface water samples that continue to be collected, (b) identification of samples of interest for more-detailed analysis (e.g. $\delta^{87}Sr$, $^{234}U/^{238}U$), (c) acquisition of additional EM induction data at different time points, and (d) expansion of similar coupled geochemical-geophysical studies to the New Rifle former uranium mill tailings site in an effort to compare and contrast characteristics that control elemental fluxes within the two analogous—albeit spatially segregated—alluvial aquifers.

Geostatistical Modeling of Physical and Geochemical Properties for Reactive Transport Modeling, Rifle IFRC

Rifle IFRC (Principal Investigator: Philip Long)

C. Murray (PI, Chris.Murray@pnnl.gov), N. Qafoku, B. Gartman, Y. Bott, K. Draper, J. Greenwood, D. Newcomer, S. Yabusaki—*PNNL*

A coordinated effort has provided initial 3D models of physical and reactive properties for Plot C at the Rifle IFRC. Lithofacies identifications were performed using geologic log data. A rotated grid was defined that is parallel to the main transport direction during biostimulation experiments. Geostatistical modeling of the lithofacies data has been used to generate 250 realizations of the lithofacies on that grid. The petrophysical model developed for Plot A has been used to generate initial grids of hydrologic and reactive properties that will be used for preliminary reactive transport modeling. Laboratory and field measurements have been performed at Plot C and will be used to update the petrophysical model. Preliminary assessment of particle size data from Plot C indicates a good correspondence between geologic log data and particle size distributions. Electromagnetic borehole flowmeter data have been collected in Plot C and calibrated using slug-test data to provide estimates of the absolute hydraulic conductivity. The distribution of EBF hydraulic conductivity within lithofacies indicates slightly higher hydraulic conductivity for the Sandy Gravel lithofacies relative to Muddy Gravel lithofacies. Additional particle size data is being generated to allow for broader comparison of particle size variation with geophysical log data and estimation of petrophysical properties.

We are also working on integrating geochemistry and mineralogy data into the geostatistical model, as well as metal loading data obtained in different sediments and size-fractions separated from them. We have been working with sediments from both oxidized and naturally reduced subsurface zones at La Quinta (Plot D) and Plot C experimental plots. A variety of wet chemical extractions and characterization techniques such as XRD, SEM/EDS, EMPA, μ-XRF, XANES, EXAFS and Mössbauer spectroscopy are being employed in size-fractions separated from the sediments. A series of extraction techniques confirmed the presence of significant amounts of aqueous U(VI), acid volatile sulfide (AVS), co-contaminants such as As, Zn, V, Cr, Cu and Se, and a remarkable assortment of potential host minerals (sorbents and/or electron donors), including Fe oxides (hematite, magnetite, Al-substituted goethite), siderite, reduced Fe(II) bearing clays, sulfides of different types, Zn sulfide framboids and multi-element sulfides. Multi-contaminant, micron size (ca. 5 to 30 μm) areas of mainly U(IV) and some U(VI), and other co-contaminants were present in some sediments, suggesting complex micron-scale (i.e., particle size dependent) system responses to transient redox conditions. We are currently studying phase distribution and contaminant loadings in different particle sizes separated from the sediments.

Collectively, the results improve our understanding of uranium in relationship to complex subsurface behavior caused by physical and mineralogical subsurface heterogeneities; help to unravel mineral-fluid interface complexity and dynamics by identifying key geochemical and hydrological reactions and processes controlling U and other co-contaminant behavior under a variety of conditions; and provide necessary information to develop robust geostatistical models to characterize the complex subsurface sediments and provide the input needed for reactive transport models.

Molecular-Scale Characterization of Natural Organic Matter From A Uranium Contaminated Aquifer and its Utilization by Native Microbial Communities

Rifle IFRC (Principal Investigator: Philip Long)

Paula J. Mouser (PI), *Ohio State U.*; Michael J. Wilkins, *PNNL*; Kenneth H. Williams, *LBNL*; Donald Smith, Ljiljana Paša-Tolić—*EMSL and PNNL*; Philip E. Long, *LBNL*

The availability and form of natural organic matter (NOM) strongly influences rates of microbial metabolism and associated redox processes in subsurface environments. This is an important consideration in metal-contaminated aquifers, such as the DOE's Rifle Integrated Field Research Challenge (IFRC) site, where naturally occurring suboxic conditions in groundwater may play an important function in controlling contaminant mobility, and therefore the long-term stewardship of the site. Currently, the biophysiochemical processes surrounding the nature of the aquifer and its role in controlling the fate and transport of uranium are poorly understood. Using Fourier transform ion cyclotron resonance mass spectrometry (FT-ICR-MS) with electrospray ionization (ESI), we characterized dissolved organic matter (DOM) chemistry for three surface and groundwater sources at Rifle and assessed microbial utilization in batch anaerobic incubation experiments. FT-ICR-MS uniquely offers ultrahigh mass measurement accuracy and resolving power for polar organics, in addition to enabling elemental composition assignments of these compounds.

Samples were collected from the Colorado River, a shallow groundwater aquifer adjacent to the river, and a spring/seep discharge point upgradient from the aquifer. DOM was concentrated and purified from each source and analyzed using FT-ICR-MS with ESI. We identified between 6,000 and 7,000 formulae at each location, with the river sample having the smallest and the spring sample having the largest number of identified peaks. The groundwater and spring samples contained DOM with a large percentage of formulae containing nitrogen and sulfur species, while the river sample was dominated by carbon, hydrogen, and oxygen species. Unsaturated hydrocarbons, cellulose, and lipids were rapidly utilized by indigenous bacteria during a 24-day incubation period, and presumably transformed to more recalcitrant lignins and protein-type molecules. Indeed, inoculation induced a shift in NOM composition from one with unique signatures to one with a larger percentage of shared formulae, suggestive of incipient conversion to the uniform chemical signature reflective of relatively recalcitrant NOM exported to river and marine systems. These findings indicate that FT-ICR-MS with ESI is an effective method for characterizing molecular-scale differences in DOM from complex environments. We also provide preliminary evidence that certain DOM fractions are more efficiently utilized by indigenous microbial communities and likely play an important role in controlling reducing conditions in heterogeneous subsurface environments.

Genome-Centered Analysis of Biogeochemical Cycling

K.C. Wrighton (PI), B.C. Thomas, I. Sharon, C.J. Castille—*U. of California Berkeley*; M.J. Wilkins, *PNNL*; N.C. VerBerkmoes, *ORNL*; C.S. Miller, *U. of California Berkeley*; R.L. Hettich, *ORNL*; M.S. Lipton, *PNNL*; K.H. Williams, P.E. Long—*LBNL*; J.F. Banfield, *U. of California Berkeley*

With the goal of understanding the microbiological and geochemical processes impacting subsurface environments, iron-reducing groundwater samples were collected from the Rifle Integrated Field Research Challenge site and characterized using community proteogenomics. We reconstructed a total of 87 genomes, with most genomes comprising < 1% of the community. 79 of these genomes were Bacterial, the remaining were Bacterial associated phage and mobile elements, with no evidence for Archaea or Eukaryotes in the samples. 49 genomes sampled (57%) were from members of the Bacterial candidate divisions (CD) lineages for which we have none to minimal prior genomic sampling: 21 OD1, 19 OP11, 6 genomes in which UGA (stop) is translated as tryptophan, 5 of which are affiliated with BD1-5, and three that represent a new division (PER). All CD are predicted to ferment, but some augment fermentation with archaeal-like type II/III RuBisCO inferred to couple AMP salvage with CO_2 fixation; others pump protons and reduce sulfur using archaeal-type hydrogenases. Proteomics indicates that fermentative CD lineages convert refractory sediment carbon compounds to acetate, ethanol, and hydrogen, stimulating the activity of respiratory iron, sulfate, and nitrate reducing bacteria. We detected the expression of uptake hydrogenases in the dominant iron (*Geobacter*) and sulfate (*Desufoltalea*-like) organisms, suggesting hydrogen cycling between these trophic groups occurs *in situ*. Other Proteobacterial and Bacteriodetes members have the capacity to oxidize ferrous iron and sulfide produced from these respiratory organisms. Moreover, dissimilatory sulfate reducing and OD1 sulf-hydrogenase proteins were detected throughout the iron-reducing samples, suggesting that biogenic aqueous sulfide produced by sulfate and sulfur reducing metabolisms contributes to abiotic iron reduction in the aquifer during secondary stimulation. The results provide a glimpse into vast phylogenetic diversity, metabolic variety, and integrated physiological networks that persist in subsurface terrestrial anaerobic niches. Rifle IFRC research is supported by U.S. Department of Energy under Contract No. DE-AC02-05CH11231.

Integrating *In Silico* Modeling and Proteomics into Field-Scale Simulations of Uranium Biogeochemical Reactive Transport

Steve Yabusaki (PI), Yilin Fang, Mike Wilkins—*PNNL*; Radhakrishnan Mahadevan, *U. of Toronto*; Tim Scheibe, *PNNL*; Derek Lovley, *U. of Massachusetts*; Phil Long, *LBNL*; and the Rifle IFRC Science Team

The Rifle IFRC project is working towards a holistic understanding of the processes, properties, and conditions controlling uranium behavior as indigenous metal-reducing bacteria are stimulated to enzymatically transform aqueous U(VI) to immobile, solid-associated U(IV). A comprehensive modeling framework is used to systematically represent the impact of acetate biostimulation on the microbial community, terminal electron acceptors, and uranium mobility in the context of the Rifle site geology, hydrology, and biogeochemistry. In this case, three-dimensional, variably-saturated flow and biogeochemical reactive transport modeling is used to simulate the impacts of pulsed acetate amendment, acetate-oxidizing iron and sulfate reducing bacteria, seasonal water table variation, and spatially-variable physical (hydraulic conductivity, porosity) and geochemical (reactive surface area) material properties. A particular challenge is the sensitivity of uranium mobility to pH, Eh, alkalinity, calcium, and reactive surface area, which are impacted directly by the terminal electron accepting process (TEAP) reactions and indirectly by subsidiary reactions involving the biologically-mediated reaction products. We use the eSTOMP subsurface simulator to exploit the large memory and high-performance of massively parallel computers needed to address the high spatial and temporal resolution, large number of reactive species and minerals, and detailed process models.

Our current work focuses on the mechanistic, predictive and quantitative understanding of the bacteria that catalyze bioreduction in the Rifle aquifer. Proteomics data from the 2008 field experiment provided an unprecedented opportunity to assess the capabilities of a genome-scale metabolic ("*in silico*") model of *Geobacter metallireducens,* putatively responsible for the reduction of Fe(III) and U(VI) (Lovley et al., 1991). The *in silico* model of physiological metabolic pathways that was embedded in the field-scale modeling framework is comprised of hundreds of intra-cellular and environmental exchange reactions. One advantage of this multiscale modeling approach is that the TEAP reaction stoichiometry and rate is now a function of the metabolic status of the microorganism, which is affected by acetate and nutrient transport, and biogeochemical conditions. The annotation of *in silico* model reactions to specific *G. metallireducens* proteins and the availability of groundwater proteomic analyses were instrumental to the assessment of model accuracy under evolving hydrologic and biogeochemical conditions. In this case, the largest predicted fluxes through *in silico* model reactions generally correspond to high abundances of proteins linked to those reactions (e.g., some central metabolic pathways). Model discrepancies with the proteomic data, such as the prediction of shifts associated with nitrogen limitation, identified pathways requiring further investigation and potential model refinement to better understand and more accurately predict metabolic processes that occur in the subsurface. The potential outcome of this approach is a predictive understanding of the interplay of key microbial species represented by multiple "*in silico*" models developed, in part, using gene networks identified from metagenomic datasets, and validated using global proteomics.

Temporal Monitoring of Microbial Community Dynamics Under Iron- and Sulfate-Reducing Conditions via "Now-Generation" DNA Sequencing-Enabled Molecular Environmental Microbiology

ANL SFA (Laboratory Research Manager: Carol S. Giometti)

D. Antonopoulos (PI, dion@anl.gov), M. Boyanov, J. Brulc, E. Johnston, M.J. Kwon—*ANL*; P. Long—*LBNL*; T. Marsh, *Michigan State U.*; M. McCormick, *Hamilton College*; F. Meyer, K. Skinner—*ANL*; K. Williams, *LBNL*, D. Sholto-Douglas, E. O'Loughlin, K. Kemner—*ANL*

Understanding the biotic component of any environmental system is challenging, owing to the dynamic spatial and temporal scales that evolving microbial communities exhibit. Over the past 20 years, studies of microbial community composition have been predicated on obtaining inventories of the 16S ribosomal RNA (rRNA)-encoding genes present in a sample as proxies for the organisms present and their relative abundances. Presently, the application of so-called "next-generation" DNA sequencing technologies (effectively state of the art, hence "now-generation") has enabled a new level of relative low-cost, high-throughput sampling that is commensurate with the genomic capacity of the system being studied. Fully exploiting this technological potential is dependent upon realizing scale-effective sampling of the system. One additional benefit of the advent of "now-generation" DNA sequencing is the routine interrogation of all genes present in a sample (effectively the "metagenome" of the microbial community). The underlying computation for annotating the sequencing reads (i.e. comparing them with a database of known genes) at this scale is non-trivial, but strategies developed by members of the Mathematics and Computer Science Division (MCS) and the Institute for Genomics and Systems Biology (IGSB) at Argonne have made this possible. In-house DNA sequencing capabilities (including the Illumina HiSeq2000, GAIIx, and MiSeq platforms, and 454 GS-FLX) and data analysis (via the MG-RAST metagenomics analysis server; http://metagenomics.anl.gov) are unique capabilities at Argonne that can facilitate integration of microbial community dynamics with the synchrotron- and lab-based biogeochemical investigations within the Argonne SBR SFA.

In two recent studies, we have investigated the impact of electron donors (acetate, lactate, and glucose; see companion poster by O'Loughlin et al.) and an electron shuttling compound (2,6-anthraquinone disulfonate [AQDS]) on the evolution of microbial communities over time in iron-rich materials seeded with field sediments from the US DOE SBR Old Rifle IFRC site. For both experiments, mixed batch systems were characterized by microbial community analysis (using 454-based tag sequencing of the V3-V4 region of the 16S rRNA-encoding gene) and geochemical measurements (wet chemical and synchrotron-based analyses) to elucidate natural biogeochemical processes, particularly those related to C, Fe, and S dynamics. Geochemical characterization of an acetate-amended system supplemented with or without AQDS identified an increase in the concentration of reduced iron and a decrease in the concentration of sulfate with time. An increase in the relative abundance of the Deltaproteobacteria was observed early in the experiment (post Day 2) for both systems. For the AQDS-amended system the majority of the community was dominated early by *Geobacter* whereas a greater increase in the relative abundance of Bacteroidetes was observed for the batch not containing AQDS. In both systems a transition occurred (post Day 23) when the Firmicutes became dominant (specifically members of the genus *Desulfosporosinus*). This work is the first detailed laboratory analysis of microbial community development over time in the presence of an exogenous electron shuttle. Many dynamics observed in our experimental batch systems containing acetate as the available electron donor with (or without) the electron shuttle AQDS overlapped with previous observations in the field.

Deep sequencing inventories of the organisms present in a community allows for a more appropriate scale for capturing the complexity of the community structure present in a sample. Standardization of sampling strategies and concomitant automation of sample processing allows the interrogation of a suite of samples at a low cost that spatial and temporal dynamics can now be addressed with the appropriate experimental design. Combining these two key capabilities means that the ebb and flow of individual microbial population abundances within a community can be monitored owing to changes in environmental conditions over time, without *a priori* knowledge of what microorganisms are present. More pointedly, the sensitivity of this overall approach implies that in conjunction with chemical and physical characterizations of the samples, specific triggering events can be identified that dictate assembly of the community.

This research is part of the Subsurface Science SFA at Argonne National Laboratory.

Understanding Uranium Transformations in Reduced Sediments: An Integrated Bottom-Up and Top-Down X-Ray Spectroscopy Approach

ANL SFA (Laboratory Research Manager: Carol S. Giometti)

M. Boyanov (PI, mboyanov@anl.gov), E. O'Loughlin, D. Latta, B. Mishra, K. Skinner—*ANL*; M. Scherer—*U. of Iowa*; W.-M. Wu, C. Criddle—*Stanford U.*; F. Yang, T. Marsh—*Michigan State U.*; R. Sanford—*U. of Illinois Urbana-Champaign*; F. Löffler—*U. of Tennessee and ORNL*; M. Mueller, T. Mehlhorn, K. Lowe, D. Watson, S. Brooks—*ORNL*; K. Kemner—*ANL*

Uranium dynamics in reducing environments are intimately tied to the biogeochemical cycling of the major elements, particularly the redox cycling of C, Fe, and S. The resulting multitude of coupled biotic-abiotic reactions occur in the presence of biological surfaces, minerals, and dissolved ligands, potentially resulting in a distribution of reduced U^{IV} species. However, due to lack of sufficient understanding of U^{IV} speciation, current transport models use only amorphous uraninite ($U^{IV}O_2$) as a reference U^{IV} phase. Our group and others have recently demonstrated the formation of reduced non-uraninite species (i.e., U^{IV} atoms complexed to surfaces or coordinated by ligands) both in laboratory systems and in sediments (e.g., Boyanov et al. GCA 2007; Kelly et al. ES&T 2008; Fletcher et al. ES&T 2010; Boyanov et al. ES&T 2011). The importance of these findings is that non-uraninite U^{IV} species have uncharacterized thermodynamic and kinetic properties that may be significantly different from those of uraninite, resulting in inaccurate descriptions of U transport and subsurface redox dynamics. One of the goals of the Argonne Subsurface Science Focus Area project is to identify the factors and mechanisms that lead to distinct U transformations under reducing conditions, to characterize the structure of reduced U phases and their stability to remobilization, and to use this knowledge to understand the redox transformations of U, Fe, C, and S observed in soils and in sediments from contaminanted field sites.

As part of the "bottom-up" component of these efforts we investigated the reduction of U^{VI} by several gram-positive and gram-negative bacteria (*Shewanella*, *Anaeromyxobacter*, *Desulfitobacterium* spp.) and by several Fe^{II}-containing phases (stoichiometric and partially oxidized magnetite, vivianite, Fe^{II} sorbed to carboxyl functionalized microbeads). Experiments were performed under defined conditions in laboratory batch reactors, and U speciation in the solid phase was determined using synchrotron x-ray absorption spectroscopy (XANES and EXAFS). Results suggest that small amounts of phosphate in the solution phase (as low as P:U = 1:1) inhibit uraninite formation regardless of the method used to reduce U^{VI}. In the absence of phosphate, we observed significant variability in the U^{IV} species formed by the different reductants. *Shewanella* and *Anaeromyxobacter* produced nanoparticulate uraninite, as expected, whereas U^{VI} incubation with five strains of *Desulfitobacterium* spp. and with AH_2DS resulted in a carbonate-complexed, non-uraninite U^{IV} species. Factors such as the chemical conditions at the location of electron transfer can be offered to explain this variability; conversely, the formation of distinct U^{IV} products during U^{VI} reduction may be used to infer the location and mechanisms of electron transfer. In a separate set of abiotic experiments we found that inner-sphere coordination between two or more Fe^{II} atoms significantly enhanced U^{VI}-Fe^{II} reactivity, suggesting that Fe^{II} incorporated in solid phases will be, in general, highly reactive. However, the reactivity of magnetite towards U^{VI} reduction depended on the magnetite's Fe^{II} content in a step-wise fashion, and vivianite (ferrous phosphate) did not reduce U^{VI} over extended periods. Observed U^{IV} products resulting from reduction by Fe^{II} ranged from nanoparticulate uraninite to complexed non-uraninite U^{IV} species, presumably sorbed to surfaces.

The results from the well-defined laboratory systems above are used to understand the speciation of U^{IV} observed in natural sediments. Using XANES and EXAFS spectroscopy at the U L_{III} edge we examined the speciation of U in unmodified sediments from the Oak Ridge IFRC. In one set of experiments, contaminated sediments extracted from surge wells were incubated for 4 years in diffusion-limited columns with or without an initial ammendment of ethanol. Intensive geochemical monitoring revealed the gradual establishment of sulfate- and iron-reducing conditions over a period of 2 years. U speciation was determined *in situ* with EXAFS and shown to evolve from oxidized U^{VI} to reduced U^{IV} as the reducing conditions propagated through the sediment phase. U^{IV} was present as non-uraninite species in all cases. Similar non-uraninite U^{IV} speciation was observed in unmodified sediments extracted from the injection wells of the field-scale biostimulation experiment in Area 2 using emulsified vegetable oil (EVO) as the electron donor. In a separate set of experiments, U^{VI} was reacted with a naturally reduced soil from Hedrick, Iowa. EXAFS analysis revealed that reduced U^{IV} was present as a non-uraninite U^{IV} species (Latta et al., Appl. Geochem. 2012). All of the results above indicate that non-uraninite U^{IV} species are ubiquitous and persistent in natural and biostimulated sediments, suggesting the need for further studies to understand their structure, stability, and the factors controlling their formation.

The Argonne Subsurface Biogeochemical Research Program Scientific Focus Area

Argonne SFA (Laboratory Research Manager: Carol S. Giometti)

K. Kemner (PI, kemner@anl.gov), E. O'Loughlin, M. Boyanov, D. Antonopoulos, D. Latta, T. Flynn—*ANL*; S. Brooks, *ORNL*; E. Carpenter, *Virginia Commonwealth U.*; C. Criddle, *Stanford U.*; J. Fredrickson, *PNNL*; F. Löffler, *U. of Tennessee*; T. Marsh, *Michigan State U.*; M. McCormick, *Hamilton College*; B. Mishra, *Illinois Institute of Tech.*; R. Sanford, *U. of Illinois Urbana-Champaign*; C. Segre, *Illinois Institute of Tech.*; M. Scherer, *U. of Iowa*; W. Wu, *Stanford U.*; J. Zachara, *PNNL*; C. Giometti, *ANL*

The Argonne Subsurface Biogeochemical Research Program (SBR) Scientific Focus Area (SFA) integrates synchrotron-based biogeochemistry with "now-generation" DNA sequencing techniques and bioinformatics approaches, microbiology, and molecular biology to pursue the long-term scientific goal of elucidating the interplay, at the molecular level, between specific microbial metabolic activities, solution chemistry, and mineralogy contributing to the transformations of minerals, heavy metals, and radioactive elements in subsurface environments. Hypotheses developed to achieve this goal are tested by experiments that capitalize on unique Argonne capabilities, together with collaborative efforts at other national laboratories focused on field-scale subsurface biogeochemical questions, as well as several academic institutions. The objective for FY 2013-FY 2015 is to characterize coupled biotic-abiotic molecular-scale Fe, S, heavy metal, and radionuclide transformations, integrated over different length scales, to provide knowledge that is necessary for understanding subsurface processes and predicting contaminant reactivity and transport. This objective guides development and optimization of synchrotron methods for molecular-level measurements pertinent to understanding contaminants, carbon/nutrient forms, and the geochemical character of groundwater in subsurface environments. Argonne SBR SFA research addresses four critical knowledge gaps related to understanding these issues: *(1) an in-depth understanding of molecular processes affecting contaminant speciation*; *(2) an understanding of the role of biogenic and abiotic redox-active products and intermediates in Fe, S, and contaminant transformations*; *(3) an understanding of mass transfer and microenvironment effects on Fe, S, and contaminant transformations*; *and (4) an in-depth understanding of the relationship between microbial community dynamics and function and coupled biotic-abiotic controls and their effects on major/minor element cycling and contaminant transformations.* Addressing these knowledge gaps has driven development of 17 specific hypotheses to be tested within the Argonne SBR SFA.

The science plan focuses on transformation of minerals, uranium, and mercury at different spatial scales and in the context of iron and sulfate reduction in subsurface environments. Researchers at Argonne will collaborate with researchers at PNNL, ORNL. LBNL, Michigan State University, University of Iowa, University of Illinois at Urbana-Champaign, Tufts University, University of Tennessee, Stanford University, Hamilton College, Virginia Commonwealth University, and the Illinois Institute of Technology. Research will emphasize laboratory-based experiments (mixed-batch reactors, thin films for microscopy studies, and columns) with single-crystalline-phase Fe oxide powders, fabricated Fe-rich mineral assemblies designed to mimic mineralogical conditions in subsurface environments in the field, Fe oxide thin films, and geomaterial collected from subsurface field environments. Inocula for promoting iron- and sulfate-reducing conditions will include monocultures of dissimilatory iron-reducing bacteria and dissimilatory sulfate-reducing bacteria representative of organisms identified at these field sites and natural microbial consortia collected from all three of these sites.

Experimental work will drive optimization of techniques at Advanced Photon Source beamlines and increase the availability and productivity of xray beamlines with the characteristics required for the proposed work. This will include (1) development of xray fluorescence (XRF) microspectroscopy (spatial resolution ~100 nm) data correction algorithms to enhance capabilities at the XOR Sector 2 insertion device beamline and (2) optimization of synchrotron-based hard xray capabilities for *in situ* investigations of coupled microbiological and geochemical processes in free-flowing columns.

Ligand and Surface Effects on the Reduction of Hg^{II} by Fe^{II}

Bhoopesh Mishra (PI, bmishra3@iit.edu; bmishra@anl.gov), *Illinois Institute of Tech. and ANL*; Timothy Pasakarnis, *U. of Iowa*; Maxim I. Boyanov, Edward J. O'Loughlin—*ANL*; Michelle M. Scherer, *U. of Iowa*; Kenneth M. Kemner, *ANL*

Abiotic redox transformations of Hg are an integral part of Hg dynamics in reducing environments. The presence of complexing ligands can significantly modify the reduction potential of Hg^{II} and provide an important control on its redox state. We tested the ability of magnetite, a biogenic mineral commonly found in subsurface environments, to reduce Hg^{II} complexed with carboxyl, chloride, and sulfhydryl ligands. These ligands are important constituents of subsurface geomedia and span a wide range of complex formation constants with Hg^{II}. We also investigated the reduction of the Hg-chloride complex by magnetite of varying Fe^{2+} content x (x = Fe^{2+}/Fe^{3+}, for stoichiometric magnetite x=0.50).

Hg^{II} adsorbed to *Bacillus subtilis* at high and low Hg:biomass ratios (corresponding to Hg complexation predominantly with carboxyl and sulfhydryl groups, respectively) was reacted with magnetite under anoxic conditions, and the solid phase was examined by Hg L_{III} edge XAS. When Hg^{II} was bound predominantly to carboxyl groups, reduction of Hg^{II} to Hg^0 occured within 2 h and 2 d at pH 6.5 and 5.0, respectively. When Hg^{II} was bound to sulfhydryl groups, it was not reduced by magnetite after 2 months of reaction at pH 6.5 or 5.0. In the presence of chloride, Hg^{II} was rapidly reduced to Hg^0 by near stoichiometric (x=0.48) magnetite. The reduction of the Hg^{II}-chloride complex by more oxidized forms of magnetite (x=0.38 and 0.28) was kinetically hindered due to the formation of calomel ($Hg^{I}_2Cl_2$) as a stable intermediate reaction product. However, reaction kinetics slowly progressed towards reduced Hg^0 after 4 months of reaction. These results suggest that the complexation of Hg^{II} with carboxyl, chloride, and sulfhydryl exhibits a progressively increased inhibition of the reduction of Hg^{II} to Hg^0 by magnetite. Since Hg is typically present in aquatic and terrestrial systems at low concentrations, binding of Hg^{II} to high affinity sulfhydryl sites on bacteria could have important implications for the potential reduction of Hg^{II} to Hg^0 and the overall mobility of Hg under Fe-reducing conditions.

While the interaction between Hg^{II} and $Fe^{II/III}$ minerals is an important reduction pathway in the Hg cycle, Fe^{II} associated with the surfaces of minerals or biomass is ubiquitously present in reducing environments and may also have a significant influence on Hg^{II} redox transformations. We have tested the ability of Fe^{II} adsorbed to carboxyl-functionalized microbeads to reduce Hg^{II}. Samples were prepared with 0.1 mM Hg^{II}, 1.0 mM Fe^{II}, and 4.2 g/L beads (approx. 0.5 mM surface carboxyl ligands) at pH 7.5 and 8.4. X-ray absorption spectroscopy measurements at the Hg L_{III} edge showed that Hg^{II} in the solid phase was rapidly reduced to Hg^0, regardless of the presence or absence of dissolved chloride. The results suggest that carboxyl-adsorbed Fe^{II} could also act as a reductant for Hg^{II} in the Fe-reducing subsurface environments.

This research is part of the Subsurface Science SFA at Argonne National Laboratory.

Effects of Fe^{III} Oxide Mineralogy and Electron Donor on the Biogeochemical Dynamics of Fe, S, and C under Sulfate- and Iron-Reducing Conditions

ANL SFA (Laboratory Research Manager: Carol S. Giometti)

E. O'Loughlin (PI), M.J. Kwon, D. Antonopoulos, M. Boyanov, J. Brulc, T. Flynn, E. Johnston, K. Skinner—*ANL*; P. Long, K. Williams—*LBNL*; M. McCormick, *Hamilton College*; K. Kemner, *ANL*

The mobility of contaminants, availability of C and nutrients, and the geochemical character of groundwater in subsurface environments is closely tied to the biogeochemical cycling of the major elements, particularly the redox cycling of C, Fe, and S. By definition, redox transformations entail the transfer of electrons between chemical species, and the inherent complexity of natural systems creates a network of pathways for electron transfer that intimately couple the C, Fe, and S cycles. Understanding these complex systems requires a fundamental understanding of highly coupled biotic and abiotic processes that drive the biogeochemical cycling of C, Fe, and S in subsurface environments. Although much is known of the coupling of C, Fe, and S biogeochemistry in general, many fundamental aspects relevant to subsurface environments have yet to be elucidated.

To better understand the effects of electron donor and Fe^{III} oxide mineralogy on the biogeochemical dynamics of Fe, S, and C under sulfate- and iron-reducing conditions, we created bicarbonate-buffered batch systems containing acetate, lactate, or glucose as the electron donor and with ferrihydrite, goethite, or lepidocrocite, in the presence of high (10 mM) or low (0.2 mM) sulfate. The batch systems were inoculated with the native microbial community present in sediment from the Rifle, Colorado, USA, IFRC site. Mineral transformations were monitored by x-ray diffraction (XRD) and x-ray absorption fine structure (XAFS) spectroscopy, and changes in the microbial communities were determined from 16S rRNA-based tag sequence inventories. We examined incubations containing acetate, lactate, or glucose as the electron donor and ferrihydrite and sulfate as electron acceptors. All electron donors tested promoted ferrihydrite reduction to varying extents: glucose >> lactate > acetate. The rates and extents of sulfate reduction were faster with lactate than with acetate, while glucose did not stimulate sulfate reduction. Surprisingly, each replicate of the glucose-amended incubations developed a different color (white vs. brown) over time, as well as different rates and extents of Fe^{II} production and glucose fermentation product profiles; a similar divergence in the replicate glucose bottles was observed when this experiment was repeated. Siderite was the only solid phase detected in the white colored glucose incubation, while there was no significant transformation of ferrihydrite in the brown-colored glucose incubation (consistent with the low levels of Fe^{II} production). Iron sulfide and vivianite were formed in the incubations with lactate or acetate. Unique microbial community profiles were observed according to the availability of specific electron donors. The communities in both of the glucose-amended incubations shifted rapidly and remained stable for the rest of the experiment, consistent with the rapid initial reduction of iron with glucose. However, the community profiles in the incubations with glucose were very different between the replicates, analogous to the differences in the extent of Fe^{II} production in the white vs. brown glucose incubations and the differences in the glucose fermentation product distribution in each. This suggests that the differences in total Fe^{II} production reflect the development of difference glucose-fermenting communities in the replicate glucose incubations. The incubations with acetate and lactate also showed major community shifts over time, but they were different from each other and from the community profiles in glucose amended incubations.

We also examined incubations containing lactate as the electron donor and ferrihydrite, goethite, or lepidocrocite, in the presence of high (10 mM) or low (0.2 mM) sulfate. In the presence of low sulfate, Fe^{III} reduction was slow and limited for all of the Fe^{III} oxides. However, the extent of Fe^{III} reduction increased more than 10 times in the presence of high sulfate. In addition, the extent of Fe^{III} reduction was higher in ferrihydrite and lepidocrocite incubations than in goethite incubations. The concurrence of Fe^{III} and sulfate reduction in the high-sulfate incubations, along with the low levels of Fe^{II} production in the low-sulfate incubations, suggests that Fe^{III} oxide reduction in these systems was primarily the result of abiotic reduction of Fe^{III} by sulfide produced by DSRB and not by direct reduction by DIRB. XAFS analysis confirmed the presence of iron sulfide as the major secondary mineral phase in these incubations. Prior to indications of Fe^{III} or sulfate reduction, lactate was rapidly fermented to acetate and propionate, with subsequent sulfate reduction coupled to complete oxidation of propionate. Distinctly different community profiles were observed for each of the Fe^{III} oxides with high and low sulfate. These results suggest that when DIR is slow and both sulfate and Fe^{III} oxide are available, sulfide produced by microbial sulfate reduction can drive Fe^{III} oxide reduction. However, the rate and extent of the Fe^{III} reduction by sulfide are strongly affected by the specific Fe^{III} oxide.

Experimental Studies and Modeling of Mineral Precipitation in Mixing Zones Controlled by Parallel Flow and Double Diffusion

D. Fox, *INL*; T. Gebrehiwet, *U. of Idaho*; L. Guo, J.R. Henriksen, H. Huang, C. Lu, Y. Fujita—*INL*; A. Tartakovsky, *PNNL*; G. Redden (PI, George.redden@inl.gov), *INL*

The theme for the Idaho National Laboratory (INL) Scientific Focus Area (SFA) is "Understanding and Controlling Precipitation Reaction Fronts in Subsurface Environments." We are investigating how different modes of reactant mixing in porous media affects the spatial-temporal distribution of reaction products in porous media with a special focus on mineral precipitation reactions. The objective is to understand how the nature of mixing of reactants involved in multi-component precipitation reactions affects the rates of precipitation, and reductions in permeability or porosity, in order to predict and control these parameters in subsurface applications.

Precipitation of $CaCO_3$ in the mixing zone between two solutions flowing in parallel, one containing Ca^{2+} and one containing CO_3^{2-} (originally studied in a large flow cell [1]) has been studied using sand-packed flow cells. Reactant solutions were: A) $CaCl_2$, and B) $NaHCO_3$. Both solutions contained a pH indicator (cresol red), were pH adjusted to 9.2, and the densities were matched to less than 0.1% using NaCl. The objective was to use visible pH changes to determine how $CaCO_3$ precipitation reactions in the mixing zone affected changes in the local pH conditions as protons are released. A "pH wedge" appeared, as predicted by modeling, with one edge aligned with the centerline of the mixing zone with the other edge extending into the unbuffered $CaCl_2$ solution. As the reaction progresses, the pH wedge becomes narrow, or disappears, showing that small volume averaged amounts of $CaCO_3$ deposited in the mixing zone can inhibit further precipitation. The results have consequences for predicting volume averaged rates of reactions and changes in transverse permeability.

Double diffusion experiments were conducted in polyacrylamide gels and in fine sand media. The goal is to compare precipitation behavior and reductions in porosity or permeability between the two types of media, and between two chemical systems; calcium carbonate and calcium phosphate. In gel media with zero effective permeability, dramatic differences in precipitation patterns show the system-specific nature of mixing/precipitation patterns. Carbonate precipitation in the gel media initiates with a wide distribution of growing crystals that are widely spaced. In contrast, the phosphate system commences with multiple bands of fine material that evolve in position and width, and that appear to cause a more rapid reduction in porosity. In fine sand media density differences between solutions create mixing patterns that are not orthogonal to the diffusion boundaries. Density effects, which include local changes in density caused by precipitation reactions, can exert additional influences on reactant mixing. It is also likely that the presence of heterogeneous nucleation sites stimulate more rapid nucleation that leads to much finer zones of precipitation.

The ReActive Transport (RAT) code developed at INL has been used to capture the general features of the observed precipitation patterns in the experiments. Cross-platform comparison between RAT and PFLOTRAN has been conducted to confirm that the implementation of the model is accurate.

1. Tartakovsky, A. M., G. Redden, et al. (2008). "Mixing-induced precipitation: Experimental study and multiscale numerical analysis." Water Resources Research 44(6).

Understanding and Controlling Precipitation Reaction Fronts in Subsurface Environments: The Idaho National Laboratory SBR Scientific Focus Area

G. Redden (PI, George.redden@inl.gov), H. Huang, Y. Fujita, D. Fox, L. Guo, J.R. Henriksen, M. McIlwain—*INL*; T. Gebrehiwet, *U. of Idaho*, T. Johnson, *PNNL*; A. Revil, *Colorado School of Mines*; L. Slater, *Rutgers-Newark U.*; R. Smith, *U. of Idaho*, A. Tartakovsky, *PNNL*; C. Zhang, *Rutgers-Newark U.*

Although subsurface environments are repositories for many of the most critical energy, water and mineral resources that sustain the earth's ecosystems and human populations, it remains a persistent challenge to exploit subsurface resources without unintended and undesirable consequences. Geochemical processes in subsurface environments dictate the quality of subsurface resources and the response of the subsurface to contaminants, resource extraction practices or changing ecosphere conditions. Consequently, engineered geo- and biogeochemical processes are now instrumental in efforts to stimulate subsurface reactions to enhance resource recovery or prevent and mitigate damage caused by engineered or accidental interventions in the subsurface.

Possible chemical responses of the subsurface to inputs can be predicted from knowledge based on controlled laboratory studies. However, deliberate stimulation of chemical and biochemical processes in the subsurface usually involves the injection and dispersal of reactants or catalysts where mixing of fluids and reactants become important. The porous and fractured nature of the subsurface creates transient reactant mixing patterns and thermodynamic gradients. The spatial-temporal distribution of reactions is complex particularly when the transport properties of the subsurface are changed through formation of precipitates or biomass.

The theme for the Idaho National Laboratory (INL) Scientific Focus Area (SFA) is "Understanding and Controlling Precipitation Reaction Fronts in Subsurface Environments." We are investigating how different modes of reactant mixing in porous media affects the spatial and temporal distribution of reaction products with a special focus on reactions that include precipitation of mineral phases. The scientific challenge is to understand the relationship between pore-scale processes and their manifestation at large scales. The engineering challenge is to understand how reactions can be propagated in complex heterogeneous media to produce the desired outcomes with respect to targeted outcomes. The INL SFA research program addresses a number of challenging and interrelated topics: The transport and mixing of reactants at multiple scales in porous and fractured media; Relationships between fundamental reaction rates and macroscopically observed and modeled volume averaged reaction rates; The complex behavior of systems where physical processes affecting transport and reactant mixing are tightly coupled to chemical and biogeochemical processes, and; Novel methods that can be used to noninvasively monitor mixing-reaction fronts in subsurface environments.

In the final year of the INL SFA, we are focusing on: 1) how mineral ($CaCO_3$) precipitates are formed within the mixing interface between solutions flowing in parallel, 2) how mineral precipitates are formed in mixing zones controlled primarily by diffusion, 3) $CaCO_3$ precipitation reaction fronts generated when a reactant (carbonate ion) is formed *in situ* by enzymatic hydrolysis of urea, and 4) whether complex resistivity can be used to monitor the position and composition of reaction fronts. Each research area is supported through a modeling platform that is well suited for the simulation of tightly coupled processes because the chemical reactions induce changes in the transport properties of the porous medium. The principles being addressed in the INL SFA will contribute to better predictions for biogeochemical processes where mixing and strong chemical gradients occur in nature or in engineered systems.

Mineral Precipitation Fronts in Porous Media: Modeling Using A Fully Coupled Fully-Implicit Simulator and Monitoring Using Spectral Induced Polarization (SIP)

Chi Zhang (chi.zhang@inl.gov), *Rutgers U. Newark and INL*; Luanjing Guo, George Redden (PI), Hai Huang, Don Fox, Yoshiko Fujita—*INL*; Lee Slater, *Rutgers U. Newark*; Timothy Johnson, *PNNL*

Groundwater contamination by toxic and/or radioactive metals is often untreatable when extraction methods are ineffective or the contaminated environment is inaccessible. This situation has driven the need to develop methods that can immobilize inorganic contaminants *in situ*. Successful development and application of *in situ* remediation requires the ability to simulate the various physical, chemical and biological processes that will govern contaminant state and mobility. These processes are often closely coupled, particularly where precipitation reactions modify physical properties of the media governing transport. It is also necessary to monitor the associated changes in physicochemical properties that are caused by the engineered introduction of amendments in the subsurface.

Experiments involving calcium carbonate precipitation induced by enzyme-driven urea hydrolysis have been carried out in granular silica gel columns where urease enzyme was adsorbed on silica within a defined segment of the column. Experimental measurements were taken for the spatio-temporal distribution of urea, ammonium (NH_4^+), pH and calcium carbonate precipitation. They have been used to investigate the dynamics of mineral precipitation reaction fronts in porous media, and to develop and test approaches for simulating and monitoring the transient features of reaction fronts. A fully–coupled, fully-implicit reactive transport simulator has been applied to investigate the nonlinear coupling effects between the processes of flow, transport and reaction, as well as the interaction between mineral precipitation and medium properties. Simulation results were compared to the lab measurements. Good agreement between most of the experimental and simulated results suggests that the model successfully accounts for the most important processes in the system and can be used to make reasonable predictions of outcomes for scenario testing.

We have been evaluating spectral induced polarization (SIP) for delineating spatio-temporal variations in reaction front chemistry and the properties of the grain surface-fluid interfaces. Complex resistivity was tested as a method for monitoring the progress of the precipitation reaction fronts in the column experiments. Correlations were found between the increased real (σ') and imaginary (σ'') parts of complex conductivity and the increase in hydroxide ion concentrations during urea hydrolysis. Additionally, decreased complex conductivity was observed as calcite precipitation proceeded. The spatiotemporal variations in complex conductivity suggest polarization mechanisms were associated with changes in the interfacial properties of a solid-fluid surface. Based on our observations as well as support from additional experimental work we propose a conceptual model describing hydroxide ion adsorption behavior in silica gel and its control on interfacial polarizability. Our results demonstrate the application of both modeling and geophysical sensing to facilitate an improved understanding of the dynamics of mineral precipitation reaction fronts in the subsurface.

Use of Metagenomic and Meta-Transcriptomic Analysis to Interpret Biogeochemical Processes Mediated by Hanford 100H Aquifer Bacteria (Lab and Field Studies)

LBNL SFA (Laboratory Research Manager: Susan Hubbard)

H.R. Beller (PI), R. Han, U. Karaoz, H.C. Lim, L. Yang, B. Faybishenko, E.L. Brodie—*LBNL*

We are developing the use of biomolecular signatures as part of the LBNL SFA challenge entitled "Unraveling Biogeochemical Reaction Networks Mediating Sustained Chromium Reduction", which focuses on *in situ* reductive immobilization of Cr at DOE's Hanford 100H site. By applying a high-throughput approach that uses metagenomic and meta-transcriptomic data, we hope to identify highly expressed genes in a specific microbial community under conditions of interest, without requiring any *a priori* sequence information or assumptions about what processes might be occurring. A key scientific goal is to determine if there are diagnostic biomolecular signatures indicative of important aquifer biogeochemical processes that can be used to (a) help discriminate between direct (enzymatic) and indirect (abiotic) oxidation-reduction processes relevant to bioremediation and (b) to inform and constrain reactive transport models even when geochemical field measurements do not reveal all relevant processes. We have collected metagenome and meta-transcriptome sequence information from various experimental systems (including flow-through columns and batch microcosms inoculated with Hanford aquifer sediment or groundwater, bacterial isolates from the flow-through columns, and site groundwater) under conditions relevant to *in situ* chromate reduction and re-oxidation at Hanford 100H. Overall, 12 metagenome and 14 meta-transcriptome samples were sequenced, ranging from 0.1 to 1.6 Gb of sequence data per sample. This poster gives an overview of several noteworthy findings from these Hanford studies.

In microcosm studies designed to characterize functional changes in an aquifer-derived, chromate-reducing microbial community as it transitions successively through electron-accepting conditions relevant to the Hanford subsurface, one condition tested was nitrate-dependent oxidation of Fe(II) and reduced S compounds. Meta-transcriptome sequence data revealed expression of nitrate reductase (*nar*) and S oxidation (*sox*) gene clusters from an alpha-Proteobacterial species, whereas routine geochemical (ion chromatography) data did not yield evidence of the S oxidation product. Thus, the meta-transcriptomic data provided insights into biogeochemical processes that would not have been detected by routine geochemical analysis.

In flow-through columns containing Hanford aquifer sediment and reducing Cr(VI) under denitrifying conditions, meta-transcriptome data revealed complete denitrification (with expression of *nar*, *nir*, *nor*, and *nos* genes, as well as the highly expressed pseudoazurin), but the most highly expressed genes encoded proteins of unknown function. This finding stresses an advantage of metagenomic and meta-transcriptomic sequencing over *a priori* approaches, namely, that sequencing can reveal important but unannotated genes/enzymes and focus research on such knowledge gaps. In addition, we isolated a Firmicute (strain HCF1) that dominated the microbial communities of flow-through columns that rapidly reduced Cr(VI) under fermentative conditions; we were able to metabolically reconstruct key pathways (such as lactate fermentation) by examining the genome sequence of strain HCF1.

Metagenome and meta-transcriptome sequencing was carried out on groundwater samples collected during various biogeochemical regimes (e.g., denitrification, sulfate reduction) that followed lactate biostimulation at the 100H site. Among other findings was evidence of nitrogen and phosphorous limitation, which provided information on amendments needed to optimize *in situ* biostimulation.

Following this biomolecular signature discovery phase that involves metagenome and meta-transcriptome sequencing of a range of Hanford-relevant biogeochemical conditions, we are developing meta-transcriptome-based gene expression microarrays that we hope will allow us to rapidly profile the *in situ* gene expression of Hanford microbial communities on a qualitative basis (i.e., what pathways are most highly expressed?) and a semi-quantitative basis.

Field-Scale Estimation and Simulation of Biogeochemical Heterogeneity

J. Chen (PI), *LBNL*; H. Wu, L. Li—*Penn State*; K.H. Williams, M.B. Kowalsky, Carl Steefel, S.S. Hubbard—*LBNL*

Many bioremediation experiments have been conducted at the DOE Rifle (CO) IFRC site to facilitate the reduction of U(VI) to U(IV) and to explore the role of the associated coupled physical and biogeochemical processes. At the Rifle IFRC and elsewhere, it is common to use time-lapse wellbore-based aqueous geochemical data with mechanistic models to assess the progress of the remediation-induced system transformations. In this work, we strive to identify the diagnostic signatures of biostimulation by using hydrological, geochemical, and geophysical data through two different yet complementary approaches.

In the first study, we use a data-driven statistical (or 'top-down') approach to identify system transformations that occur during bioremediation using time-lapse aqueous geochemical data (such as Fe(II), sulfate, sulfide, acetate, and uranium concentrations) and spectral induced polarization (SIP) data. We consider the multivariate geochemical concentrations as hidden random processes (observed at borehole locations but unknown at other locations) and the time-lapse geophysical data as observations at each location along the 2D profiles. The connection between the geophysical observations and geochemical time-series is determined by design matrices that depend upon redox status. We use a Bayesian approach to estimate the unknown parameters and use Markov chain Monte Carlo methods to draw many samples from the joint posterior distribution. We find that the developed statistical approach can provide information about (1) the probability of being in each redox stage over time and space following biostimulation, and (2) diagnostic parameters as functions of aqueous geochemical concentrations and geophysical attributes. The top-down approach is expected to be especially useful for rapid identification of critical system transitions based on streaming monitoring data and for constraining mechanistic transport models where various reaction pathways are possible.

In the second study, we use a mechanistic reactive transport modeling (or 'bottom-up') approach to combine hydrological, geophysical, and geochemical data. We use flowmeter and slug test data to set up the initial distribution of permeability. The initial distribution of porosity was obtained by assuming a correlation between porosity and permeability and by matching bromide breakthrough data and SIP data at the initial time. We use inverse reactive transport modeling of time-lapse geochemical data to determine key parameters that control the reactive transport processes. After obtaining a good match with the geochemical data, we compare the predicted aqueous and solid phase geochemistry from the reactive transport model with the SIP data to understand key controls on the SIP data and whether the SIP data are useful for monitoring and diagnosing changes in the biogeochemical processes during the biostimulation experiments. The established method can be used to link geochemical and geophysical signatures and eventually to help understand and predict subsurface biogeochemical processes using constraints from different types of measurements. This mechanistic approach is complementary to the data-driven, statistical approach in that it allows us to gain a better understanding of the key controls on overall system behavior.

Highly Depleted Gypsum Veins at the Rifle Site Attributed to Multiple Episodes of Redox Cycling

LBNL SFA (Laboratory Research Manager: Susan Hubbard)

Mark E. Conrad (PI), Kenneth H. Williams, Jennifer L. Druhan, Wayne W. Lukens—*LBNL*

The Department of Energy's Old Rifle site is a former uranium mill site situated along a floodplain of the Colorado River in western Colorado. The aquifer underlying the site consists of 6-7 m of Quaternary alluvium overlying the Tertiary Wasatch Formation. Sulfate concentrations in Old Rifle groundwater are elevated (8-10 mM), with unusually low sulfur isotope ratios ($\delta^{34}S$ values from -6‰ to -10‰). Further, higher groundwater uranium concentrations in shallow groundwater at the Old Rifle site are correlated with the higher groundwater sulfate concentrations and lower $\delta^{34}S$ values. To determine the source of the sulfate and its relationship to uranium mobility, we have analyzed the $\delta^{34}S$ values of sulfate minerals found in rock outcrops around the site.

The source of the low $\delta^{34}S$ sulfate in groundwater appears to be gypsum veins within the Wasatch Formation, which outcrops the north and west of the Old Rifle floodplain. Veins of gypsum sampled from outcrops of the upper Wasatch have $\delta^{34}S$ values lower than any previously reported in the literature (as low as -56‰). These veins are located in high permeability shear zones and are associated with secondary Fe-hydroxide minerals including visible iron staining. Fossilized plant material found in several of the shear zones is believed to have created localized reducing zones leading to precipitation of Fe-sulfide minerals from groundwater sulfate. Biologic reduction of sulfate produces a large negative shift in the $\delta^{34}S$ value of the resultant sulfide. After the reducing potential of the organic matter was exhausted, the system converted to oxidizing conditions producing low $\delta^{34}S$ sulfate and Fe oxides from the sulfides, leading to the formation of the gypsum veins. Low $\delta^{34}S$ secondary hydrous Na and Mg sulfate minerals precipitating at active groundwater seeps from outcrops of the Wasatch indicate that this is an on-going process.

Modern analogues of these naturally reduced zones have been found in the Old Rifle groundwater. These reduced zones are characterized by lignitic organic carbon containing abundant framboidal pyrites with $\delta^{34}S$ values as low as -70‰ (Ravi Kukkadapu, Personal Communication). Associated with these pyrites are greatly elevated concentrations of uranium (Qafoku et al., 2009). Oxidation of these reduced zones would lead to mobilization of reduced metals, including uranium, which may explain the high background concentrations of metals in the Rifle groundwater outside of the tailings-impacted area.

[1] Qafoku et al. (2009) Environmental Science and Technology 43, 8528-8534.

Integrating Geochemical, Reactive Transport, and Facies-Based Modeling Approaches to Assess U(VI) Contamination at the Savannah River F-Area

LBNL SFA (Laboratory Research Manager: Susan Hubbard)

S.A. Bea, N. Spycher, H. Wainwright, S. Mukhopadyay, S.S. Hubbard, Carl Steefel, J. Davis (PI)—*LBNL*

Acidic waste solutions containing low level radioactivity from numerous isotopes were discharged to a series of unlined seepage basins at the F-Area of the Savannah River Site, South Carolina, from 1955 through 1989. A nearly 1 km long acidic plume has developed in the groundwater under this site in relatively permeable, mostly sandy sediments. Although the site has gone through many years of active remediation, the groundwater remains acidic, and the concentrations of U(VI) and other radionuclides are still significant. Monitored Natural Attenuation (MNA) is a desired closure strategy for the site, based on the premise that clean background groundwater will eventually neutralize the groundwater acidity and drive natural immobilization of U(VI) through sorption. Understanding key hydrochemical controls and the impact of chemical and physical heterogeneities on contaminant mobility is of particular interest for assessing s MNA and *in situ* treatment over the long term.

The first part of this study involves the development of reactive transport models to explore key controls on the long-term U(VI) plume mobility at this site through considering U(VI) adsorption by sediments and key hydrodynamic processes. Various geochemical, horizontal 1D, and 2D cross-section reactive transport simulations were conducted. These include the saturated/vadose zones and the effects of mineral dissolution and precipitation, as well as H^+ and U(VI) sorption using surface complexation models. The results indicate that H^+ sorption reactions on goethite and kaolinite (the main minerals at the site besides quartz), and the precipitation of Al minerals could delay the pH rebound for decades. Such slow rebound is likely to be exacerbated by residual saturation of the plume below the discharge basins.

The concept of "reactive facies" was explored to spatially distribute linked physical and chemical heterogeneities at local and field scales (see poster by Wainwright et al.). This concept integrates sediment chemical and hydrophysical properties (determined through laboratory and field experiments) with geophysical signatures. Obtained estimates of reactive facies were subsequently used to parameterize our reactive transport models. Because reactive properties at this site relate dominantly to sorption/desorption, we find that heterogeneous distributions of these properties (compared with homogenous distributions) affect the predicted pH and U transport mostly at early times and at plume edges, and over the long term once the concentrations of contaminants have decreased below sorption saturation levels.

The second part of this study involves uncertainty quantification performed in conjunction with the reactive transport simulations in order to: (1) identify the complex physical and geochemical processes that control the migration of the acidic-U(VI) plume in the pH range where it is highly mobile, (2) evaluate those physical and geochemical parameters that are most controlling, and (3) attempt to predict the future plume evolution constrained by historical chemical and hydrological data. The uncertainty quantification analysis shows that model results are most sensitive to the reactive surface area available for sorption, discharge rates, the relative rates of H^+ influx and kaolinite dissolution. The plume behavior also appears to be sensitive to parameters controlling the amount of residual U(VI) in the vadose zone, which acts as a buffering zone in the modeled system.

Isotopic Signature of Calcium and Sulfur Partitioning during Biostimulation: Experiments and Simulations

LBNL SFA (Laboratory Research Manager: Susan Hubbard)

Jennifer L. Druhan (PI), Carl I. Steefel, Kenneth H. Williams, Mark E. Conrad, Donald J. DePaolo—*LBNL*

Stable isotope fractionations of key species in the bioreduction process provide information complementary but distinct from traditional concentration measurements. Detection and modeling of such enrichments therefore provide novel constraints on the rates, progress and secondary mineralization processes associated with *in situ* biostimulation. At the field scale, as with variations in major and trace ion concentrations, stable isotope fractionations are typically subject to reactive path lengths less than the distance between the injection and first row of monitoring wells. Incorporation of stable isotope fractionations into biogeochemical reactive transport models has thus required development of intermediate or meso-scale column studies designed to operate as direct analogs to field conditions with the added benefit of sub-20 cm fluid sampling resolution. This combination of field and laboratory datasets has supported adaptation of the CrunchFlow reactive transport model to accommodate both sulfur and calcium isotope fractionations.

At the Rifle field site, sulfur isotope fractionation has been used to constrain the onset of sulfate reducing conditions. This technique has been applied to multiple years of electron donor amendment in a single well gallery resulting in a previously undocumented trend towards earlier onset of sulfate reduction in subsequent years. In clogged injection wells at the Rifle site, a large enrichment in the stable isotope ratio of aqueous calcium has been documented in association with carbonate precipitation providing a potentially new means of quantifying secondary mineral precipitation rates. In the laboratory, datasets generated from meso-scale column studies indicate sulfur isotope fractionation is only adequately modeled when the dual Monod equation is used to accommodate the rare isotope through the transition from a zero to first order reduction rate. With sulfur isotope fractionation implemented in the CrunchFlow code, a field scale model is developed which reproduces the observed temporal shifts in $\delta^{34}S$ and sulfide as a function of the population density and distribution of sulfate reducing bacteria. Calcium isotopes show a complex relationship between calcite precipitation (enrichment) and ion exchange (mixing) leading to a ~50 cm zone down-gradient of the electron donor source in which the fractionation serves as a novel constraint on both rate and exchange coefficients.

Based on the field and laboratory datasets generated thus far, we are now adequately prepared to develop a reactive transport model at the field scale that fully incorporates the fractionations of sulfur and calcium as independent parameters. This development will yield new constraints on the timing, rates, and pathways of contaminant remediation.

LBNL Sustainable Systems Scientific Focus Area

LBNL SFA (Laboratory Research Manager: Susan S. Hubbard)

S.S. Hubbard (PI), H. Beller, J. Davis, C. Steefel, K.H. Williams, J. Ajo-Franklin, E. Brodie, R. Chakraborty, J. Chen, J. Christensen, M. Conrad, D. DePaolo,W. Dong, B. Faybishenko, M. Kowalsky, B. Moses, P. Nico, D. Silin, N. Spycher, E. Sonnenthal, T. Tokunaga, J. Wan, L. Yang, Y. Wu—*LBNL*; M. Denham, *SRNL*, J. Hunt, *U. of California Berkeley*, J. Istok, *Oklahoma State U.*, Y. Fujita, *INL*, L. Li, *Penn State*

The objective of the LBNL Sustainable Systems SFA is to improve predictive understanding of flow and transport in shallow, heterogeneous, subsurface systems. Our SFA is organized around the following three key challenges, where fundamental (hydrological, biological, geochemical) processes, their couplings, and their macroscopic manifestations are quantified. Although initially geared toward contaminated subsurface environments, the SFA approaches for quantifying multi-scale systems are potentially transferable to a variety of terrestrial systems important for environmental and energy problems.

1. The "Unraveling Biogeochemical Pathways" Challenge focuses on quantifying critical and interrelated microbial metabolic and geochemical mechanisms. A key scientific goal is to determine if there are diagnostic biomolecular signatures indicative of important aquifer biogeochemical processes that can be used to (a) help discriminate between direct (enzymatic) and indirect (abiotic) oxidation-reduction processes relevant to bioremediation and (b) to inform and constrain reactive transport models even when geochemical field measurements do not reveal all relevant processes. Recent work has focused on chromium *in situ* reductive immobilization and reoxidation processes associated with chromium-contamination at the Hanford 100 Site.
2. The "Evolution of Pore Structures and Flowpaths" Challenge focuses on developing a predictive understanding of couplings and feedbacks between microbially facilitated biogeochemical transformations and aquifer flow characteristics, the impact of such feedbacks on overall system behavior, and the discovery of diagnostic signatures of critical system transitions or "tipping points." The research is aligned with and leverages on field experiments that are being conducted at the uranium-contaminated Rifle, Colorado site by the Rifle IFRC team.
3. The "Predicting Contaminant Mobility at the Plume Scale" Challenge explores the impact of a migrating pH gradient and the use of a "reactive facies" concept as an organizing principle to integrate laboratory and field information about properties and mechanisms as needed to make reliable and computationally tractable predictions of U and iodine mobility at the plume scale and over long timeframes. This Challenge also explores the necessary level of detail that is required for adequate predictions of plume mobility. The pore-to-plume scale research is being carried out in collaboration with EM-supported SRNL scientists and the Advanced Simulation Capability for Environmental Management (ASCEM) team at the Savannah River F-Area.

Several cross-cutting scientific themes and a common investigative approach facilitate fertilization across the Sustainable Systems SFA. Recognition of subsurface complex subsurface behavior (which includes emergent processes and feedbacks) is common to all of the SFA challenges, which motivates the quest to explore fundamental processes and their interactions as well as to identify diagnostic (or integrative and often macroscopic) signatures of system responses. Successively larger scale transitions are considered in each of the three SFA Challenges, which spans molecular to plume scales. The SFA investigative approach iterates between laboratory- and field-scale experimentation and observation, hypotheses testing and refinement, all within the context of the reactive transport model. Reactive transport modeling plays an integrative role in the SFA; it allows for transfer of parameters, concepts, and processes across scales, providing a link between the fundamental and system-level research and it is used as a means to formally address emergent phenomena as a result of fundamental process coupling and the hierarchical nature of the complex subsurface.

Reactive Facies: An Approach for Parameterizing Plume-Scale Reactive Transport Models Using Multi-Type Multi-Scale Datasets

LBNL SFA (Laboratory Research Manager: Susan Hubbard)

H.M. Wainwright, D.S. Sassen, S.A. Bea, J. Chen, S.S. Hubbard (PI)—*LBNL*

Predicting subsurface contaminant plume evolution and natural attenuation is challenging due to the difficulty to tractably characterize heterogeneity of flow and transport properties. This study explores a concept of reactive facies, which is based on the hypothesis that we can identify geological units that have unique distributions of reactive transport properties. Because geophysical attributes are often sensitive to delineate such geological units, this concept allows us to take advantage of both laboratory studies and field geophysical/lithological datasets to characterize the spatial distribution of reactive transport parameters. This concept is expected to be especially powerful for characterizing coupled physiochemical parameters over large spatial regions, where it is typically challenging to obtain information about reactive transport parameters with sufficient resolution for numerical reactive transport simulations.

The first part of this study focuses on testing the reactive facies concept at the Department of Energy uranium contaminated Savannah River Site F-Area, where we have analyzed the relationships between laboratory and field (including crosshole radar and seismic, and surface seismic) datasets. First, data mining and iteration with laboratory analysis identified two reactive facies that have unique distributions of mineralogy, texture, hydraulic conductivity and geophysical attributes. We then used these correlations within a Bayesian framework to integrate the crosshole geophysical datasets with the sparse core-based measurements. This yielded high-resolution estimates of reactive facies and their associated reactive transport properties in the scale of crosshole geophysical measurements. To illustrate the value of reactive facies, we simulated migration of an acidic-U plume through this domain. The modeling results suggested that each identified reactive facies exerts a unique control on plume evolution, highlighting the usefulness of the reactive facies concept for spatially distributing reactive transport properties.

The second part of this study presents a stochastic-estimation framework for assimilating multi-source and multi-scale datasets and characterizing a plume-scale subsurface domain. The challenges are to (1) honor the large-scale variability without smoothing out the detailed structure of facies, and (2) assimilate multi-source, multi-scale datasets in a systematic way. To tackle these challenges, we developed a multi-scale Bayesian estimation method to combine disparate wellbore and geophysical datasets having varied resolution and spatial coverage. The model represents multi-scale heterogeneity by a tree-based multi-scale indicator field, and uses Markov-chain Monte-Carlo sampling methods to estimate the marginal posterior distribution of the reactive facies fields. We tested the developed method in synthetic studies and applied to the real field datasets at the F-Area, including wellbore lithology, cone penetration testing, crosshole and surface seismic data. The results showed that the point-scale and crosshole data provide the detailed structure of reactive facies in their vicinity, while the surface seismic data identify the large-scale trend and map facies with increased certainty over a large domain. We found that our methodology effectively integrates different types of data, providing an approach for distributing critical information over plume scales needed for simulating plume migration and remediation. Applying the reactive facies concept to other sites/problems would be needed to test the general utility of this approach as a new paradigm for characterizing reactive transport properties over field-relevant regions.

Pore-Scale Modeling of Permeability Evolution due to Reactive Processes

LBNL SFA (Laboratory Research Manager: Susan Hubbard)

S. Molins (PI), D.B. Silin—*LBNL*

Injection well performance in a bioremediation project may significantly decline due to precipates that accumulate in the pores near the wellbore or to gas bubbles generated by methanogenic bacteria. Although the typical size of a cleanup site is measured in hundreds of meters or even kilometers, the underlying geochemical and hydrologic processes in individual pores eventually define where and how fast the permeability will decline. Understanding these pore-scale mechanisms will help reduce the hindering effect of pore clogging and develop efficient well treatment procedures if the injectivity drops below a minimum tolerance level. Additionally, model-based permeability-porosity correlations for pore space evolution caused by precipitation or dissolution are needed for realistic reservoir-scale numerical simulations.

We employ a sequential approach to model dynamic interaction between reactive transport and evolution of the pore space geometry. First, the flow field is evaluated by solving the Stokes equations. The result is passed as input data to a multicomponent reactive transport code, which computes dissolution and precipitation rates. The changes in the domain geometry caused by the reactive processes are tracked based on mass balance considerations. The flow field is re-evaluated after every domain update. Simulation of dissolution in simple pore geometries allows us to compute porosity-permeability and porosity-tortuosity changes as the pore structure evolves. Simulations of dissolution and precipitation of $CaCO_3$ in simple pore geometries are used to examine the impact of pore structure evolution on permeability, tortuosity and average reaction rates. Three dimensional images of the porous media such as those collected by x-ray computed tomography are used as input data. Two-phase flow simulations evaluate the reduction of permeability by gas bubbles.

Our main finding is that dissolution and precipitation reactions affect the pore space nonuniformly. As a result, a simple porosity-permeability correlation may be insufficient to describe the complexity of the reaction-induced pore space evolution. The relative magnitude of the reaction rate constants in relation to the flow rate affects the evolution of the permeability-porosity relationship. As a result of dissolution, pores become wider, flow paths become less tortuous, and permeability increases faster than porosity. For a given reaction rate constant, this process is more pronounced for faster flow rates. Precipitation is simulated at low degrees of supersaturation and assumed to take place on the carbonate mineral surface. Hysteresis in the porosity-permeability evolution is observed in simulations of dissolution followed by precipitation. Simulations show that in simulation domains with the same average parameters, including column porosity, reactive surface area and flow rate, different pore structures with different flow patterns can result in different average reactions rates. Two-phase flow simulations are used to produce correlations between the relative volume of gas bubbles and permeability in capillary equilibrium.

Competing Evidence for Enzymatic Versus Abiotic Reduction of Cr(VI) in Hanford 100H Flow-Through Columns

LBNL SFA (Laboratory Research Manager: Susan Hubbard)

Charuleka Varadharajan, Ruyang Han, Sergi Molins, Mark Conrad, John Christensen, Markus Bill, Carl Steefel, Joern Larsen, Li Yang, Eoin L. Brodie, Harry R. Beller, Peter S. Nico (PI)—*LBNL*

Remediation of chromium contamination frequently involves reduction of the toxic and soluble hexavalent form, Cr(VI), to the relatively harmless and mostly immobile trivalent state, Cr(III). Microbially mediated Cr(VI) reduction at the Hanford 100H area was investigated by flow-through column experiments. The objective of this study is to identify the biogeochemical reactions that control *in situ* chromium reduction under different dominant electron-accepting conditions, i.e., nitrate-, Fe(III)-, and sulfate-reducing conditions. Replicate columns packed with natural sediments from the site were eluted with artificial groundwater containing lactate (5 mM) and Cr(VI) (5 μM) and kept under anaerobic conditions. Sulfate and nitrate solutions were added to selected columns to promote specific electron-accepting pathways. Native iron and manganese oxides were present in all the column sediments. Effluent concentrations of substrates and metabolites were analyzed regularly over a 1-year period using ICP-MS and IC. X-ray absorption spectroscopy was used to analyze the Cr phases formed during the experiment, while Hanford bacterial isolates were investigated under batch conditions to gain a detailed understanding of microbial metabolism and physiology.

Cr(VI) depletion was observed under all conditions, but the magnitude of the reduction varied significantly. Complete removal of the influent Cr was observed in the denitrifying columns and some of the sulfate-added columns in which fermentation was dominant. Despite the very different biogeochemical regimes in the denitrifying and fermentative columns, spectroscopic studies of both kinds of columns revealed very similar Cr(III)-containing minerals. Analysis of XANES spectra indicates that the Cr(III) particles most closely resemble standards produced by abiotically reacting Cr(VI) with biogenic Fe(II) and are distinct from abiotically synthesized mixed-phase Cr-Fe hydroxides. These results suggest that mixed $Cr_xFe_{1-x}(OH)_3$ material made under realistic subsurface conditions or in active bacterial cultures are structurally different from those materials synthesized through common abiotic synthetic methods.

Formation of these minerals is consistent with bacterial Fe(III) reduction and subsequent abiotic reduction of Cr(VI) by biogenic Fe(II). In contrast, other evidence supports enzymatic Cr(VI) reduction: (1) both denitrifying and fermentative Hanford bacterial isolates catalyze rapid Cr(VI) reduction in iron-free systems, (2) strong correlations between nitrate and chromate reduction suggest that Cr(VI) reduction is co-metabolic with denitrification, and (3) meta-transcriptomic data clearly indicate active denitrification, which is thermodynamically inconsistent with Fe(III) reduction. Current work is underway to understand the ability, or lack thereof, of two newly isolated Hanford organisms, one denitrifier and one fermenter, HCN1 and HCF1 respectively, to catalyze Fe(III) reduction under the column conditions in spite of the prevailing bulk thermodynamic conditions. These experiments will help to determine the extent to which a minor metabolic pathway, e.g., Fe(III) reduction, may or may not be disproportionately responsible for the fate of the redox-active contaminant Cr(VI).

Reactive Transport Modeling of Hanford 100H Lab- and Field-Scale Experiments

LBNL SFA (Laboratory Research Manager: Susan Hubbard)

E.L. Sonnenthal (PI), S. Molins, C. Wanner, C.I. Steefel, H.R. Beller—*LBNL*

The Unraveling Biogeochemical Pathways Challenge of the LBNL SFA focuses on identifying and quantifying the critical and interrelated microbial metabolic and geochemical mechanisms associated with chromium *in situ* reductive immobilization and reoxidation from the molecular to the local field scale at the Hanford 100 site. Here we summarize modeling efforts to simulate the reactive transport processes observed in batch, laboratory flow-through column, and field experiments. A range of capabilities available in the in-house general-purpose reactive transport codes CrunchFlow and ToughReact are brought to bear in this effort. A major thrust of this task has been to develop and incorporate new methods to better constrain the rates of biogeochemical reactions. In particular, rates of respiration and fermentation are calculated with a biomass-explicit approach, with the fraction of carbon going to biomass growth (anabolic pathways) estimated from literature values and/or from the increase in reaction rate over time. In addition, isotope systematics are incorporated that account for fractionation processes during respiration and fermentation.

Modeling of flow-through column experiments focused on the two separate experimental conditions that showed the most removal of Cr(VI) from solution: fermentation and denitrification. In each case, parameters for reaction rate constants were derived from cell suspension experiments carried out with bacterial strains isolated from the site and column experiments. Under denitrifying conditions, Cr(VI) reduction was modeled as co-metabolic with nitrate reduction based on experimental observations and previous studies on a denitrifying bacterium derived from the Hanford 100H aquifer. Under fermentative conditions, the model assumed that Cr(VI) reduction was carried out directly by fermentative bacteria that converted lactate into acetate and propionate.

A 3D reactive transport model of the Hanford 100H site was developed for the field-scale experiment. Thermodynamic, kinetic, and Monod parameters were compiled and calculated based primarily on a wide variety of empirical laboratory data, conceptual models for bacterial growth, and field data. The model successfully captured many aspects of bacterial growth accompanying lactate degradation, propionate and acetate formation and transport, ^{13}C pathways to bicarbonate, and sulfate reduction. Carbon ($^{13}C/^{12}C$) and Sr ($^{87}Sr/^{86}Sr$) isotopes were used to independently constrain rates of microbially mediated processes, mixing with groundwater, and calcite dissolution rate. Cr isotopes were included in order to assess the extent and sustainability of Cr remediation by immobilization. Further, to evaluate the contributions on the overall kinetic Cr isotope fractionation factor, α_{kin}, we modeled Cr(VI) reduction along a 1D flow path using a novel multiple continuum approach. Simulations suggest that for a given reduction mechanism α_{kin} can vary over a large range. The low end of the range (=larger fractionation) is defined by the theoretical equilibrium fractionation factor, while high reduction rates and/or transport limitations induced by Cr(VI) transport to reactive sites can shift α_{kin} to values close to 1 (=no fractionation).

Determining the Plume Source Discharge, Trailing Edge, and Natural Attenuation Timeframe: The F-Area Savannah River Site

T.K. Tokunaga (PI), J. Wan, W. Dong, J.N. Christensen, M.S. Conrad, M. Bill—*LBNL*; M. Denham, *SRNL*; S.S. Hubbard, *LBNL*

At the Savannah River Site (SRS) and many other contaminated facilities, understanding residual drainage from the source zone is essential for predicting attenuation of plumes. Lacking this understanding, the dynamics of a plume's trailing edge remain unknown, and remediation timeframes cannot be predicted. The challenging nature of these problems is reflected in large uncertainties in remediation timeframes at many sites, even after decades of monitoring and research. At the SRS F-Area, large contaminant plumes resulted from decades of radioactive waste disposal into seepage basins. The objective of this work was to predict groundwater plume attenuation through characterizing its current status and developing a mass balance model for source zone drainage and dilution. Here, we combined data from recently acquired field borehole sediment samples with historical waste disposal records, and long-term groundwater and plume monitoring data. Analyses of the sediments reveal the trailing plume edges for tritium and nitrate (Wan et al., in press). We developed a mixing model to predict source zone recharge rates and contaminant concentrations within the plume as functions of time and distance. Our calculations for the plume in F-Area SRS indicate that early stages of post-closure waste drainage occurred with high water fluxes (≈ 0.5 m y^{-1}), and declined over the 20 years since basin closure to low rates of a few cm y^{-1} (Tokunaga et al., in press). While the magnitude of late stage vadose zone drainage is low, its impact is large because of the high concentrations of contaminants it continues to supply to groundwater. The model predictions compared well with measured tritium and nitrate concentrations from monitoring wells 220 and 375 m downstream of the seepage basin. The methodology presented here requires only groundwater monitoring data and a few well-constrained input quantities. Thus, this approach can be useful for gaining better understanding of contaminant dissipation at other sites as well.

We also conducted isotopic studies of U, Sr and nitrate to understand the plume's history. The nitrate isotopic analyses give no indication of biotic denitrification within the plume, although a surface water sample suggests denitrification occurs between the seep line and the stream. Both chemical and systematic isotopic vertical variations of U and Sr isotopes were identified within the upper aquifer. The data suggest that the lower zone represents the effect of the original contaminant fluids, while the upper zone mainly represents recharge of water contaminated by infiltration post-closure through the contaminated vadose zone beneath the basins. The U isotopic compositions of groundwaters collected at the same wells two years apart suggest the migration rate of U from up-gradient portions of the plume of 100 m y^{-1}, below the estimated velocity (123 m y^{-1}) used in our models of basin drainage and plume attenuation.

Tetsu K. Tokunaga, Jiamin Wan, and Miles E. Denham, Estimates of Vadose Zone Drainage From a Capped Seepage Basin, F Area, Savannah River Site. Vadose Zone Journal, in press.

Jiamin Wan, Tetsu K. Tokunaga, Wenming Dong, Miles Denham, and Susan S. Hubbard, Persistent Source Influences on the Trailing Edge of a Groundwater Plume, and Natural Attenuation Timeframes: the F-Area Savannah River Site, ES&T, in press.

U(VI) Mobility in Acidic Waste Plumes: Laboratory Experiments and Surface Complexation Modeling using F-Area Savannah River Site Sediments

Wenming Dong, Jiamin Wan (PI), Tetsu K. Tokunaga, Hua Guo, Patricia M. Fox, James A. Davis—*LBNL*

The mobility of uranium (U) plumes is of great concern under acidic geochemical conditions in many contaminated DOE sites. The mechanisms controlling U mobility under acidic conditions in aquifer sediments are not well understood. Our objective is to understand the mechanisms and factors controlling U adsorption behavior, and predict its mobility under acidic conditions. The acidic U plume (pH < 5) at the F-Area of Savannah River Site (SRS) was selected as the study site. The F-Area sediments were characterized to identify grain size distribution, mineralogy, surface area, and secondary phases present in grain coatings. Laboratory batch equilibrium experiments for U(VI) adsorption onto sediments of different grain sizes (bulk, coarse, fine) and onto reference minerals (goethite, kaolinite) were performed over a range of pH conditions (pH 3.0 – 8.5). To understand the mechanisms of U(VI) adsorption within the grain coatings, a combination of synchrotron and microscopic techniques were used. A component-additivity (CA) based surface complexation model (SCM) was developed to predict U(VI) adsorption under variable geochemical conditions.

Our experimental and modeling results indicate that: (i) the fine fractions (≤ 45 μm) in sediments control U(VI) adsorption due to their large surface areas (relative to the coarse quartz sand); (ii) goethite and kaolinite were identified as the major reactive phases in the fine fractions of sediments. Kaolinite is a more important sorbent for U(VI) at pH < 4.0, while goethite plays a major role at pH > 4.0; (iii) our CA model combines an existing U(VI) SCM for goethite and a modified U(VI) SCM for kaolinite along with estimated relative surface area abundances of these component minerals. The modeling approach successfully predicts U(VI) adsorption behavior on the background F-Area sediments. The model suggests that exchange sites on kaolinite dominate U(VI) adsorption at pH < 4.0, goethite and kaolinite edge sites co-contribute to U(VI) adsorption at pH 4.0 - 6.0, and goethite dominates U(VI) adsorption at pH > 6.0. The coarse fraction (> 45 μm) showed stronger adsorption per unit surface area than goethite and kaolinite under acidic conditions (pH < 5.0). The synchrotron and microscopic studies show that the coatings on quartz grains ranged in size from 1 to 20 microns in thickness and contained a complex mixture of iron oxides and aluminosilicates. Although goethite is the predominant Fe oxide in fine-grained sediments of the F-area, the predominant Fe oxide in the quartz coatings was hematite. Concentration gradients in adsorbed U(VI) within coatings appeared to be only related to the spatial abundance of hematite, not to reaction time (≥2 hr). This implies that U(VI) adsorption by the coatings differs from that of the fines, which may impact U(VI) transport within the sand-dominated, beach barrier reactive facies.

Wenming Dong, Tetsu K. Tokunaga, James A. Davis, and Jiamin Wan, Uranium(VI) Adsorption and Surface Complexation Modeling onto Background Sediments from the F-Area Savannah River Site. Environ. Sci. Technol. 2012, 46, 1565–1571.

Actinide NMR Research at Lawrence Livermore National Laboratory

LLNL SFA (Laboratory Research Manager: Annie B. Kersting)

H. Mason, S. Harley, P. Huang, S. Carroll (PI), R. Maxwell, M. Zavarin, A. Kersting—*LLNL*

As a part of the Transuranic Subsurface Transport Scientific Focus Area at LLNL, we are developing nuclear magnetic resonance (NMR) techniques focused on investigating geochemical and biogechemical reactions with actinide species. The program builds upon the combined expertise of the group and has two major thrusts: *1) The development of surface specific solid-state NMR techniques to investigate the sorption of actinide species to mineral surfaces*; *2) The measurement of reaction rates of actinide solution species, and comparing these to rates calculated from ab-initio atomistic modeling.* The current status of this program has been benchmarking these techniques by investigating systems which allow safe technique development over a larger range of experimental conditions. This benchmarking has yielded results that will allow us to confidently extend these methods to systems containing low concentrations of actinide species. These goals are within reach at LLNL due to new capabilities in the NMR facility which allow us to investigate samples containing up to 10 μCi of ionizing radiation.

Many actinide species (e.g. Pu^{4+}, Pu^{5+}, and Np^{5+}) exhibit paramagnetic electronic ordering which can have a substantial effect on the NMR signal. Therefore, we have developed solid-state cross-polarization magic angle spinning (CP/MAS) NMR as a surface specific technique to probe the sorption of low loadings (1.6 - 54 nmol/m^2) of paramagnetic species (Cu^{2+} and Ni^{2+}) to mineral surfaces. We used statistical methods to provide model-free analysis of the results from variable contact time $^{29}Si\{^1H\}$ CP/MAS NMR spectra on amorphous silica which identified protonated and deprotonated silanol sites. These experiments established the deprotonated surface species as the preferential metal sorption site at pH 8, and show the ability to discern between precipitation of a separate phase and surface sorption. Additional experiments also proved the same results can be obtained under static (non-spinning) conditions, and can, therefore, be safely extended to systems containing low concentrations of paramagnetic actinide species such as Pu^{4+}. Experiments with trivalent lanthanide species (Sm^{3+} and Eu^{3+}) are on-going to further constrain the effective concentration and pH range over which this method is valid.

We also are building on existing expertise in measuring ligand exchange and reaction rates of actinide species using solution state NMR spectroscopy. This work extends previous work in uranyl systems where both the apical oxygen and carbonate counter ion exchange mechanisms were investigated as a function of hydrostatic pressure and temperature. These types of measurements allow for the determination of the activation volume for the exchange process where the magnitude of this value elucidates the mechanism by which the transition state occurs. This is one of the few techniques that allows for direct observation of associative vs. dissociative exchange mechanisms. Further, the unique electronic environment of actinide systems allows for a wide range of NMR techniques to monitor exchange rates. In diamagnetic systems magnetization exchange through the use of tailored excitation allows for the direct detection of exchange rates. In paramagnetic systems it is more difficult to directly monitor exchange; however, the effect of exchange on line widths is well understood and will allow for quantifiable rate determination. Therefore we have accumulated the expertise required to investigate actinide exchange processes at LLNL, and we are moving forward with similar experiments designed to measure the exchange rates for actinide species such as Np^{5+}, Pu^{4+}, Pu^{5+}, and Th^{4+}. By analyzing such reaction rates we gain insight into the limiting reactions which may govern the reactions of these species with minerals surfaces, and complex organic species.

Environmental Transport of Plutonium: Biogeochemical Processes at Femtomolar Concentrations and Nanometer Scales

LLNL SFA (Laboratory Research Manager: Annie B. Kersting)

A.B. Kersting (PI), M. Zavarin, J. Begg, P. Zhao, P. Huang, Z. Dai, R. Tinnacher, R. Kips, H. Mason, S.A. Carroll, R. Maxwell, R. Williams, S. Tumey—*LLNL*; B.A. Powell, J. Wong—*Clemson U.*

The challenge in predicting the mobility and transport of plutonium (Pu) is determining the dominant geochemical processes that control its behavior in the subsurface. The reaction chemistry of Pu (*i.e.*, aqueous speciation, solubility, sorptivity, redox chemistry, and affinity for colloidal particles, both abiotic and microbially-mediated) is particularly complicated. Its migration is known to be oxidation-state dependent and facilitated by transport on particulate matter (*i.e.*, colloidal particles). Despite the recognized importance of colloid-facilitated transport, little is known about the geochemical and biochemical mechanisms controlling Pu-colloid formation and association.

The objective of this program is the identification and quantification of the biogeochemical processes that control the fate and transport of Pu at picomolar to attomolar (10^{-12} – 10^{-18} mol/L) concentrations. Our program is composed of five research elements that are aligned with processes likely to affect Pu transport at environmentally relevant concentrations: 1) Binary sorption to low-site-density, high-affinity surface sites (*e.g.*, surface defects), 2) Stabilization of Pu surface complexes on mineral colloids by natural organic matter, 3) Surface precipitation of Pu polymers (nanocolloids), 4) Co-precipitation with colloids as a result of mineral alteration, and 5) Direct and indirect microbial interactions.

This overview poster highlights this year's results and ongoing effort. They include

- Binary sorption affinity and reversibility. Np(V), Pu(V) and Pu(IV) sorption affinity, reversibility, and morphology on goethite from attomolar to micromolar concentrations was examined. Higher affinities were observed at picomolar concentrations for Np but not Pu. At high concentrations, Pu(IV) and Pu(V) form 2-5 nm PuO_2 and/or Pu_4O_7 nano-colloids. Binary sorption experiments have been extended to other minerals (montmorillonite, bentonite). Sorption/desorption kinetics, reversibility, and stability of the various forms of Pu on mineral surfaces are the focus of ongoing research.
- Pu stabilization by ternary complexes. The influence of natural organic matter on Pu mobility is dependent on behavior and character of the organic ligand. Ternary surface-NOM-Pu surface complexes can form at low pH values where the ligand strongly sorbs. Conversely, at neutral pH values ligand complexation results in higher aqueous Pu concentrations and the potential mobilization of Pu. Stability constants describing humic and fulvic acid complexation with Pu have been determined and formation of ternary complexes on model minerals (goethite, gibbsite) is being investigated.
- Characterization of Pu-contaminated samples from the field. We have developed and tested the use of NanoSIMS imaging for Pu analysis. Sub-micrometer-scale Pu distribution on Hanford sediments located 60 feet beneath a disposal crib has been completed and mineral associations (e.g. Pu-Fe associations) identified. Characterization effort is being expanded to other field sites.
- Development of NMR capability for paramagnetic actinides. We have benchmarked the use of NMR (using Ni and Cu) to probe the surface configuration of paramagnetic species by exploiting the strong response of NMR signals to the presence of paramagnets. This capability is being extended to actinides and will provide a unique facility for probing actinide behavior at the mineral-water interface.
- Ab initio modeling of monomeric adsorption processes. We completed ab initio simulations to model the structure of the hydrated Pu monomer under neutral solution conditions ($Pu(OH)_4$). Successful representation of the tetrahydroxy species is our starting point for examining the monomeric adsorption of Pu on mineral surfaces (goethite, corundum).

Influence of Natural Organic Matter on the Subsurface Fate and Transport of Plutonium

LLNL SFA (Laboratory Research Manager: Annie B. Kersting)

B.A. Powell (PI), N. Conroy, L. Simpkins, J. Wong, T. Zimmerman—*Clemson U.*; A.B. Kersting, M. Zavarin, J. Begg, P. Zhao, R. Tinnacher—*LLNL*

This task within the Transuranic Subsurface Transport SFA is focused on understanding the role of natural organic matter on the fate and transport of plutonium. The task is guided by the hypotheses that NOM can increase Pu mobility by *1) forming NOM coatings on colloids which stabilize Pu surface complexes and 2) formation of aqueous Pu-NOM complexes which prevent sorption of Pu.*

Aqueous stability constants describing complexation of Pu(IV), Th(IV), and Np(V) with IHSS Leonardite Humic Acid and IHSS Suwannee River Fulvic Acid were determined using a combined ultrafiltraton/competitive ligand exchange technique. The stability constants were determined using a four site model of the humic acid and fulvic acid (noted as HL1, HL2, HL3, and HL4) with discrete pKa values of 3, 5, 7, and 9, respectively. The stability constants for Pu(IV) and Th(IV) binding with humic acid were:

$$Pu^{4+} + HL3 + 2H_2O \leftrightarrow Pu(OH)_2L3^+ + 3H^+ \qquad \log K = 6.76$$

$$Th^{4+} + HL3 + 2H_2O \leftrightarrow Th(OH)_2L3^+ + 3H^+ \qquad \log K = 3.58$$

Binding of Pu(IV) was approximately 3 orders of magnitude stronger than Th(IV) indicating that Th(IV) makes a relatively poor choice as an analog for Pu(IV) despite common usage. This was verified by comparison with other common Th(IV) and Pu(IV) organic ligand complexes. Complexation with fulvic acid was examined based on dissolution of PuO_2(s) nanoparticles. Suspensions of PuO_2(s) were prepared in 5mgC/L and 50 mgC/L fulvic acid across the pH range 3 to 9. The aqueous concentration of Pu continuously increased over a 90 day period. Since equilibrium has not yet been achieved, stability constants have not yet been determined. Dissolution rates ranging from 0.5 to 2.0 μg_{Pu}/L/day were determined across the pH range 4 to 7.5.

The influence of organic ligands on sorption of Pu(IV) to gibbsite and goethite was monitored using citric acid, desferrioxamine B, fulvic acid, and humic acid. These ligands were selected to represent a range of molecular weights and sources of NOM. Batch sorption experiments of Pu in the presence of these ligands indicate sorption at low pH values may be due to the formation of ternary surface complexes. For example, sorption of Pu(IV) to gibbsite in the presence of humic acid at pH 4 and 6 was greater than sorption in the absence of humic acid. Furthermore, greater sorption was observed at pH 4 as compared with pH 6. In the absence of humic acid sorption is expected to increase with increasing pH. Thus, humic acid appears to facilitate formation of a ternary surface complex. Modeling the pH 4 and 6 sorption isotherms using the aqueous stability constants listed above yielded a ternary surface complexation constant of:

$$\equiv AlOH + Pu^{4+} + 2H_2O + 2HL3 \Leftrightarrow \equiv AlOH_2(HL3)_2Pu(OH)_2^{3+} + H^+ \qquad \log K = 36.8\ (0.4)$$

Although the ternary surface complexes above indicate the potential for decreased mobility of Pu, batch sorption experiments also indicate that the relatively small siderophores, citric acid and DFOB, reduce sorption most effectively. Citric acid and DFOB decreased the fraction of sorbed Pu when compared with the binary system for all pH values studied. Using continuously stirred flow-through batch reactors, complete desorption of Pu from goethite has been achieved. These results have been verified by observing transport of Pu through a sediment column in the presence of DFOB. Therefore, the presence of DFOB and other small molecular weight, chelating ligands in an environmental system would likely lead to increased mobility of plutonium. However, even in the presence of NOM, Pu sorption increases as the pH is raised, indicating competition between aqueous Pu-NOM complexes and Pu hydrolysis products which generally exhibit strong sorption.

Adsorption and Desorption of Plutonium on Na-Montmorillonite over a Ten Order of Magnitude Range in Concentration

LLNL SFA (Laboratory Research Manager: Annie B. Kersting)

J.D. Begg, M. Zavarin (PI), S.J. Tumey, P. Zhao, A.B. Kersting—*LLNL*

Plutonium (Pu) release to the environment through nuclear weapon development and the nuclear fuel cycle is an unfortunate legacy of the nuclear age. In part due to public health concerns over the risk of Pu contamination of drinking water, predicting the behavior of Pu in both surface and sub-surface waters is a topic of continued interest. It has been suggested that the affinity of Pu for mineral surfaces is significantly greater at low concentrations due to the presence of minor amounts of "high affinity" sorption sites (surface defects, heterogeneity, etc.). Hence the current practice of extrapolating the behavior of Pu at environmental concentrations (10^{-12} to 10^{-16} M), from the results of laboratory experiments which are typically performed at concentrations $>10^{-10}$ M, may not be valid.

Here we present results from batch adsorption experiments performed with Na-montmorillonite in pH 8 background electrolyte spiked with Pu(V) and Pu(IV) at initial concentrations ranging from 10^{-6} – 10^{-16} M. After 30 day's equilibration, Pu concentrations in the supernatant were determined using a variety of analytical techniques: liquid scintillation counting and quadrupole ICP-MS, NuPlasma HR MC-ICP-MS, and accelerator mass spectrometry. The resulting sorption isotherm was found to be largely linear indicating a similar Pu adsorption affinity for montmorillonite over ten orders of magnitude Pu concentration range (10^{-6} to 10^{-16} M). Importantly, these results suggest that, under the conditions of the experimental system, Pu(V) adsorption behavior at typical environmental concentrations (femtomolar) is not significantly different to that at typical laboratory concentrations (nanomolar to micromolar). While Pu affinity for the montmorillonite surface appears to be linear over this concentration range, desorption kinetics may still play an important role in the environmental mobility of Pu. Accordingly, we are investigating the stability of Pu associated with clay surfaces in a series of desorption experiments using flow-cells. The results of these experiments suggest that significant amounts of Pu adsorbed on the surface of clay particles can be desorbed. Modeling of the data is providing insight into the mechanisms controlling the observed environmental colloid-facilitated transport of plutonium. Quantification of desorption kinetics is critical to parameterizing colloid-facilited transport of Pu in the environment.

Biogeochemical and Molecular Mechanisms Controlling Contaminant Transformation in the Environment

Oak Ridge National Laboratory Science Focus Area Program

Laboratory Research Manager: Liyuan Liang (PI, liangl@ornl.gov), *ORNL*
Research Staff: C. Brandt, S. Brooks, S. Brown, D. Elias, B. Gu, F. He, A. Johs, C. Miller, M. Podar, J. Parks—*ORNL*
Current Collaborators: C. Gilmour, *Smithsonian Environmental Research Ctr.*; S. Miller, *U. of California San Francisco*; J.C. Smith, *U. of Tennessee Knoxville*; A. Summers, *U. of Georgia*; J. Wall, *U. of Missouri Columbia*

Mercury (Hg) is a pervasive and highly toxic global pollutant that, in the methylated monomethyl mercury (MeHg), bioaccumulates in the food web, endangering humans and other organisms. The biogeochemical mechanisms controlling MeHg production at contaminated sites present serious knowledge gaps globally, nationally and locally, as at the Oak Ridge Reservation (ORR). The SFA program aims to elucidate fundamental mechanisms governing mercury transformation and behavior in the environment. Its goal is to provide new understanding to facilitate long-term, targeted strategies to significantly mitigate the adverse impacts of mercury at ORR and around the world.

This SFA Program was initiated 3 years ago to provide focus to a diverse portfolio of environmental biogeochemical research. Since its inception in FY 2009, significant progress has been made in addressing the original knowledge gaps. A total of 42 peer-reviewed articles were published in the first phase of the SFA. Of these, 27 result from the new mercury research, and an additional 73 presentations and abstracts exclusively represent our Hg focused study. We presented 5 television, press, and radio interviews and releases, and participated in numerous national and international scientific conferences, often in leadership and planning roles. The SFA program website provides updated information on published work: http://www.esd.ornl.gov/programs/rsfa/index.shtml.

Key areas of progress include: 1. Establishing field research sites at ORR's East Fork Poplar Creek (EFPC) watershed and initiating collection of geochemical and microbial data. 2. Recognition that dissolved organic matter (DOM) dominates Hg speciation and redox/ photochemical reactions, and that DOM exhibits a dual concentration-dependent role in Hg redox chemistry. 3. Demonstrating differences in microbial community structure between Hg-impacted and unimpacted sites, and that *Desulfobulbus* and *Geobacter* spp. dominate at methylating sites. Genomic sequences have been obtained for known Hg-methylators. Hg uptake was shown to be an energy- and thiol-dependent process in *G. sulfurreducens*, but less so in *Dv. desulfuricans* sp. ND132. 4. Construction of a computational framework for understanding subcellular mercury processes. The roles of Hg-thiol interactions and protein dynamics were determined in Hg resistance proteins, including for MerB in demethylation by Hg-C cleavage, MerR in switching on Hg resistance, and MerA in Hg^{2+} reduction. Structural characterization was accomplished for outer membrane proteins of potential importance in microbial Hg reduction.

In the coming summer this SFA will be under the DOE peer-review. In the Renewal Proposal we aim to resolve important new questions revealed by our research, concerning: (1) Exact sites of MeHg production in EFPC, (2) Mechanisms and geochemical controls on Hg and MeHg species transformation and Hg reactivity that lead to its uptake and methylation, (3) Microbial populations at EFPC that participate in Hg methylation and MeHg demethylation, (4) Microbial biochemical pathways, enzymatic mechanisms and genetic controls for Hg methylation and resistance. We therefore propose to continue to our goal of ***elucidating the mechanisms by which inorganic Hg is transformed into MeHg at the sediment-water interface, and in particular the processes that determine net MeHg production at contaminated sites***, by accomplishing the following objectives: I: Examining site biogeochemical processes of the EFPC watershed and identifying key methylation source areas; II: Investigating key mechanisms and geochemical controls on Hg and MeHg species transformation and Hg reactivity leading to its uptake and methylation; III: Identifying microbial species and their biochemical pathways responsible for biological methylation and demethylation; IV: Understanding biogeochemical transformations within and outside microbial cells using structural biology and computational chemistry.

A multidisciplinary systems science approach will be employed to integrate geochemistry, microbiology, molecular biology and molecular simulations to elucidate mercury behavior over multiple scales. In collaboration with other SBR investigators, we are confident that the results of the SFA can make important fundamental progress toward essential goals of assessing and mitigating the effects of mercury at DOE complexes and other contaminated sites both nationally and globally.

Biogeochemical Processes and Hg Cycling in Contaminated Sediments of East Fork Poplar Creek, Oak Ridge, TN (Hg SFA at ORNL)

ORNL SFA (Laboratory Research Manager: Liyuan Liang)

Scott C. Brooks (PI, brookssc@ornl.gov), Carrie Miller, Craig Brandt, David Kocman, Ami Riscassi, Xiangping Yin, Yun Qian—*ORNL*; Rich Landis, Jim Dyer—*DuPont*

Site investigation and geochemical modeling provide key information on major chemical species and processes involved in mercury (Hg) biogeochemical transformations in water and sediment along a longitudinal transect of lower East Fork Poplar Creek (EFPC) in Oak Ridge, TN.

Three sites were established for regular quarterly sampling and detailed characterization of the site biogeochemistry in surface water, interstitial pore water, and creek sediments. Samples are collected from the center of the creek channel and from the creek margins. Similar measurements are being conducted on the adjacent floodplain sediments. Two of the sites (upstream – EFK22; downstream – EFK5) are on the Hg-contaminated EFPC and one is located on a nearby reference stream that receives only atmospheric Hg fallout.

Creek center channel: At both EFK22 and EFK5, 2011 water quality parameters varied little with depth and concentrations were very similar to the surface water. Porewater dissolved Hg (HgD, passes a 0.2 μm filter) showed some trends with depth yet differed between sites. At EFK22 HgD tended to decrease with depth whereas it increased with depth at the downstream location EFK5. MeHgD concentrations were lower in January and the concentration versus depth profiles were relatively uniform in the center channel at both sites in both January and August.

Creek margin: In contrast to the center channel, porewater chemistry vertical profiles exhibited distinct variations at EFK22 and EFK5, with more pronounced changes in warmer months. Changes in concentrations followed the canonical sequence of microbial terminal electron accepting processes: NO_3^- depletion, increased dissolved Mn and Fe, decreasing SO_4^{2-} concentration and increasing sulfide concentration. In intact creek sediment cores from EFK5 collected in August 2011, acid extractable Fe(II) and chrome-reducible sulfur (CRS) also increased with depth. The molar ratio of Fe(II) to sulfide in sediments averaged ~4,000. Using data from all sampling campaigns, sediment-associated MeHg is positively correlated with solid phase total Hg, Fe(II) and organic carbon content. Based on the limited results to date, there is no significant correlation between solid phase MeHg and total solid phase S(II). In general, HgD concentrations in the creek margin porewater showed little systematic variation with depth. MeHgD concentration generally exhibited a peak with depth which was shallower in August than in January. No significant correlation between MeHgD and total dissolved sulfide was observed.

Methylation and demethylation potentials in intact cores of creek sediment: Coupled with the geochemical characterization of intact sediment cores, we are conducting experiments to quantify potential rates of Hg methylation and MeHg demethylation. Methylation potentials in intact sediment cores collected from EFK22 and EFK5 were significantly positively correlated with the ambient MeHg concentration but this relationship is not observed with the EFK22 floodplain samples. The EFK22 floodplain samples exhibit similar methylation potentials to the creek sediment but they have higher ambient MeHg than the creek sediments.

Data management: Due to the volume of data generated, a data management system was adopted for archival and retrieval purposes. Standardized reporting templates, data standards, control vocabulary, and recorded metadata have been adopted. The system helps to achieve consistent reporting of field and laboratory results, including metadata, and facilitates organization and retrieval of results for analysis.

Spatial and Seasonal Relationships Between Surface Water Total and Methylmercury, Dissolve Organic Matter and Particulates in East Fork Poplar Creek, Oak Ridge, TN

Carrie Miller (millercl@ornl.gov), Scott C. Brooks (PI), David Kocman, Ami Riscassi, Xiangping Yin, Yun Qian—*ORNL*

East Fork Poplar Creek (EFPC) in Oak Ridge, TN, USA has elevated mercury (Hg) concentrations as a result of historical Hg use at the Y-12 National Security Complex (Y-12 NSC). . The objective of this work is to examine the relationship between mercury, both total mercury (Hg) and methylmercury (MeHg), particulate concentrations and dissolved organic matter (DOM) in surface waters of EFPC. Longitudinal surveys along the lower 20 kilometers of EFPC were conducted quarterly from October 2010 to October 2011 with sampling frequency increasing to monthly beginning in December 2011. Unfiltered or filter-passing (0.2 μm) MeHg and Hg were not correlated with DOC quantity or total suspended solid (TSS). Concentrations of unfiltered and filter-passing Hg decreased downstream but the fraction of filter-passing Hg remained relatively constant (10-20%). Both unfiltered and filter passing MeHg increased downstream and were generally higher in warmer months. Filter-passing MeHg constituted 40-80% of total MeHg. The increase in net MeHg concentration with increasing downstream distance was constant: no specific reach of EFPC was identified in which there was a significant change in the rate increase. Ultrafiltration was conducted on a limited number of samples collected at several locations along EFPC in April and August 2011 and all of the filter-passing (<0.2 μm) MeHg also passed a 3 kDa cutoff filter. DOM quantity, measured as dissolved organic carbons (DOC), and quality, assessed using UV dependent characteristics of the DOM including slope ratio (SR, ratio of slopes of the log transformed absorption coefficients between wavelengths 275-295 and 350-400 nm, respectively) and DOC-specific UV-absorbance (SUVA-254) were used to examine seasonal and spatial relationships between mercury and DOM. SUVA-254 and SR have been positively and negatively correlated, respectively, with increases in terrestrially-derived DOM. The downstream decrease in filter-passing Hg was not related to changes in DOM concentration or composition. In October 2010 and January and October 2011 filter-passing MeHg was significantly correlated ($p < 0.05$) with the slope ratio and SUVA-254, however these correlations were not significant in April 2011 or August 2011. We attribute this lack of correlation to the decreased influence of the terrestrial environment on DOM inputs during the drier season (summer-fall). The data also suggest that the dominant source of DOM and MeHg input to the creek varies with seasonal changes to local scale hydrology. During wetter months the creek may be better connected to adjacent floodplains and allochthonous, terrestrial inputs may have a greater influence. Conversely, in drier months, adjacent floodplains are hydrologically isolated from the creek and autochthonous DOM and in-stream MeHg production (in sediments and/or periphyton biofilms) may be more important. The increase in sampling frequency initiated in December 2011 will enable a more comprehensive examination of seasonal differences in the relationship between Hg, MeHg and DOM during base flow conditions. A gauged sampling station, with a stilling well and pressure transducer to measure discharge and *in situ* sondes to measure DOM fluorescence, turbidity, pH, conductivity, temperature and dissolved oxygen, has also been established to examining these same relationships under high flow events.

Mercury Methylation: Microbial Communities Involved in Hg Transformations (ORNL Hg SFA, Microbial Genetics and Transformations)

ORNL SFA (Laboratory Research Manager: Liyuan Liang)

James G. Moberly, Richard A. Hurt, Tatiana A. Vishnivetskaya, Steven D. Brown, Craig C. Brandt, Mircea Podar, Anthony V. Palumbo, Dwayne A. Elias (PI, eliasda@ornl.gov)—*ORNL*

We examined microbial communities involved in mercury methylation in streams contaminated from past operations in the Y12 plant at Oak Ridge. In collaboration with the Field Task of the Hg SFA program, we investigated Hg methylating and demethylating microbial communities in Hg contaminated streams and background sites. Initial microcosms suggest active methylation downstream, with this activity being stimulated by sulfate and inhibited by molybdate. Water and sediment samples were analyzed for the microbial community complement phylogenetically via 454 pyrosequencing of the 16S rDNA gene V4 region. We hypothesize that: 1) there is a greater diversity of genes related to pollutants at the contaminated sites; 2) a lower overall phylogenetic diversity is present at these sites, 3) some groups of microorganisms will correlate with areas contaminated with Hg and/or methylmercury (MeHg), 4) specifically, the number of Deltaproteobacteria (the group involved in methylation) will positively correlate with MeHg concentrations. Geochemical principal component analysis of several sites showed that one area, Bear Creek, was substantially different due to the presence of U(VI) and nitrate and this was reflected in the microbial community that was mostly devoid of Proteobacteria. Virtually all of the microbial communities in the other five sites trended towards dissolved Hg. Further, a correlation of the 454 data with geochemistry at the phylum and genus level showed that in areas with higher MeHg, the greatest number of sequences corresponded to the methylating *Geobacter* and *Desulfobulbus* spp. as well as with *Byssovorax* and *Desulfonema* spp. Methylation and demethylation are being investigated with *Desulfobulbus propionicus* under several different culturing regimes to coordinate differences in growth with these activities to point to biochemical methylation pathways.

Efforts to better understand the carbon and electron flux in three methylating and demethylating communities used sediments from intact cores to; a) determine the depth section of the cores with the greatest activity, and b) determine the carbon sources that would stimulate and/or inhibit these activities. Analysis with stable isotopes revealed minimal stimulation with lactate and ethanol while cellobiose inhibited both activities. Ongoing analysis includes a second generation functional gene array with >1000 *mer* gene sequences using DNA and reverse transcribed mRNA, 454 pyrosequencing to correlate differences in organism abundance with DNA and mRNA abundance so as to determine the the organisms and genes responsible for Hg methylation and MeHg demethylation in East Fork Poplar Creek.

Mercury Methylation: Genetics and Physiology of Methylmercury Production (ORNL Hg SFA, Microbial Genetics and Transformations)

ORNL SFA (Laboratory Research Manager: Liyuan Liang)

Andrew M. Graham, *Smithsonian Environmental Research Center*; Romain Bridou, *U. of Missouri*; Richard A. Hurt, Steven D. Brown, Mircea Podar—*ORNL*; Steven D. Smith, *U. of Missouri*; Anthony V. Palumbo, *ORNL*; Judy D. Wall, *U. of Missouri*; Cynthia C. Gilmour, *Smithsonian Environmental Research Center*; Dwayne A. Elias (PI, eliasda@ornl.gov), *ORNL*

In mercury (Hg) contaminated areas, anaerobic bacteria convert Hg(II) to toxic methylmercury ($MeHg^+$); primarily the sulfate-reducing bacteria (SRB) and iron-reducing bacteria (IRB). We identified 11 *Desulfovibrio* strains that constitutively produce MeHg, and 12 strains lacking this ability. Protein-normalized Hg methylation rates varied by ~1 order of magnitude. An updated 16S rRNA phylogeny indicates that Hg-methylators are widely distributed phylogenetically, but closely related species within recent branches show the same capability/inability for Hg methylation. These findings along with more sequenced methylators allows for more refined comparative genomics to predict high value gene targets for methylation and demethylation. We are exploring demethylation rates to evaluate whether non-methylating *Desulfovibrio* have superior demethylation capability. One of the weaker methylators, *D. africanus*, was characterized for methylation and differential gene expression over the growth curve due to extreme pleiomorphology at different growth phases. While no methylating genes were identified, the *feoAB* genes appear to positively correlate with Hg exposure and methylation.

We developed and refined several protocols correlating Hg methylation rates with growth phase, [Hg] and speciation. This is critical for comparisons across chemical conditions and strains. Methylation in our model organism *Desulfovibrio desulfuricans* ND132 is dependent on growth phase, [Hg] and medium chemistry. We found high bioavailability of Hg complexed with diverse thiols, suggesting that ND132 does not take up Hg as intact Hg-thiol complexes. We also found that Hg bioavailability under sulfidic conditions is enhanced by DOM, suggesting HgS nanoparticle bioavailability. This provides a mechanism for observed correlations between DOM and Hg methylation. Further, DOM aromaticity predicted HgS bioavailability, as it predicts nanoparticle growth rates. ND132 is 1 of 2 Hg-methylating SRB with a sequenced genome (JGI). The genome was left in 1 scaffold and 6 contigs and we have now developed a universal procedure to close genomes. To elucidate the genes responsible for Hg-methylation, a random Tn5 transposon library and screening assay were adapted in ND132. Currently, >6,600 mutants have been created. The screening assay was recently modified. Complete sample digestion with 3N HNO_3 (24 h) now overcomes a cell density effect on MeHg recovery (above) with direct ethylation at pH 3.9 with wild type controls at different cell densities allowing for greatly improved discrimination of mutants of interest. Since February 2012, 480 new mutants have been re-assayed to identify mutants using a ratio of methylation potential (MeHg pg.ml-1) and optical density (OD600). These genes will undergo targeted deleted to confirm their involvement in Hg methylation so that the Hg methylation genes and pathways may at last be identified.

Effects of Molecular Structure and Functional Groups of Organic Ligands on Photochemical Transformation of Mercury and Methylmercury

ORNL SFA (Laboratory Research Manager: Liyuan Liang)

Feng He, Yun Qian, Wang Zheng—*ORNL*; Jason Demers, *U. of Michigan*; Balaji Rao, Xiangping Yin—*ORNL*; Joel Blum, *U. of Michigan*; Liyuan Liang, Baohua Gu (PI)—*ORNL*

Photochemical reduction of mercury (Hg) and photo-degradation of methylmercury (MeHg) are among important pathways of elemental Hg(0) production and demethylation in natural and contaminated open surface waters. This transformation is affected by aqueous ionic species, among which aromatic moieties and thiolate functional groups in naturally dissolved organic matter (DOM) are thought to be the most important because of their light-absorbing and Hg-complexing characteristics. However, exact mechanisms by which DOM and organic ligands mediate transformation of Hg or MeHg is not clear owing to our incomplete understanding of the structural arrangement and stoichiometry of reactive functional groups in DOM. In this study, various DOM isolates and naturally-occurring S- or O-containing model ligands were used to systematically investigate the role of various functional groups and their steric arrangements in photochemical transformation of Hg or MeHg. We show that, for O-containing ligands, the photochemical reduction rates of Hg(II) are driven primarily by the secondary reaction and influenced not only by the neighboring functional groups but also their positioning on the aromatic benzene ring structure. On the other hand, photoreduction of Hg(II)-thiolate complexes is driven largely by the direct photolysis (or primary reaction). The presence of dissolved oxygen decreases the photoreduction of Hg(II) but increases reoxidation of Hg(0), in which singlet oxygen rather than hydroxyl radicals formed by the photolysis of thiols drives the photooxidation. We also show that photodegradation of MeHg is enhanced by the presence of DOM isolates and various S- or O-containing ligands in both fresh and saline solutions. However, this enhanced demethylation depended on the chemical structure, concentration, and redox state of the organic ligands. Photodegradation rates of MeHg in ambient water collected from East Fork Poplar Creek at Oak Ridge, Tennessee, are estimated to range from 7.8 to 78 ng m^{-2} d^{-1} at 35°C, suggesting that photodegradation could be an important sink for MeHg in this natural ecosystem. Our findings are thus of critical importance for constructing the mass balance and for improved understanding of the fate of Hg and MeHg in this contaminated environment.

Mercury Redox Cycling and Species Transformation Affected by Complex Interactions with Natural Organic and Thiolate Compounds

ORNL SFA (Laboratory Research Manager: Liyuan Liang)

Baohua Gu (PI), Wang Zheng, Haiyan Hu, Feng He, Balaji Rao, Liyuan Liang—*ORNL*

Mercury (Hg) redox cycling in anoxic environments directly links to the bioavailability of Hg by limiting available Hg(II) species for microbial uptake and mehtylation. However, factors that affect this process are poorly understood. Here we demonstrate that natural organic matter (NOM) and thiolate compounds play critical roles in Hg redox reactions in anoxic environments. We studied the kinetics of reduction and oxidation of Hg by using chemically reduced NOM (NOM_{re}), as well as a range of selected thiolate compounds with varying functional groups and redox state under dark, anaerobic conditions. We show that NOM_{re} simultaneously reduces and oxidizes Hg via different reaction mechanisms. Reduction of Hg(II) is governed by reduced quinones in NOM_{re}, whereas Hg(0) oxidation is primarily controlled by thiol-induced oxidative complexation. This mechanism is supported by the observation that Hg(0) is oxidized by low-molecular-weight thiol compounds, such as cysteine, 2-mercaptopropionic acid, and thiosalicylic acid. The oxidation rate was also found to vary with S oxidation state, substitutional functional groups (e.g. amine), thiol/Hg ratio, and pH. Similarly, depending on NOM oxidation state, NOM:Hg ratio, and the type of NOM, the initial Hg(II) reduction rates vary greatly from 0.4 to 5.5 h^{-1}, which is about 2 to 6 times higher than that observed for photochemical reduction of Hg(II) in open surface waters. However, rapid reduction of Hg(II) by NOM_{re} is offset by oxidation of Hg(0) with an estimated initial rate as high as 5.4 h^{-1}. This dual role of NOM_{re} in Hg redox transformation and the effect of thiol compounds on Hg(0) oxidation are expected to strongly influence the availability of reactive Hg and thus to have important implications for microbial uptake and methylation in anoxic environments.

Structural and Computational Analysis of MerR's Unique Allosteric Activation of *mer* Operon Transcription

ORNL SFA (Laboratory Research Manager: Liyuan Liang)

A. Johs, S.J. Tomanicek, H.-B. Guo, L. Liang (PI)—*ORNL*; A.O. Summers, L. Olliff—*U. of Georgia*; M. Sharp, *ESS Sweden*; J.C. Smith, *U. of Tennessee Knoxville and ORNL*

Mercury resistant (HgR) bacteria strongly influence the bioavailability of toxic methylmercury levels at Hg contaminated DOE sites, most notably the Y-12 NSC. Expression of HgR genes by the *mer* operon is transcriptionally controlled by the repressor-activator MerR [1] which binds its operator-promoter DNA (MerOP) at a dyad between the -10 and -35 RNA polymerase (RNAP) recognition sites [2]. Without Hg(II) MerR binds tightly to MerOP repressing transcription by holding RNAP inactive at the promoter. When Hg(II) appears it binds MerR strongly and, thus activated, MerR transmits its consequent allosteric movement to the DNA of MerOP, underwinding the promoter and enabling RNAP to begin transcription [3]. There are 3D structures for several activated MerR-family regulators, but not as yet for MerR itself, nor are there structures of the repressed form of any MerR-family protein. We have used MerR›s homology to structures of other family members to construct a 3D model of activated Hg-MerR and also collected small-angle X-ray scattering (SAXS) data on MerR alone and Hg-MerR. SAXS showed activated Hg-MerR was more extended than MerR alone. Long timescale molecular dynamics simulations indicated high flexibility of the Hg-MerR[4]. Neutron Spin Echo experiments are performed on Hg-MerR to experimentally determine the internal dynamics, which are important to describe the allosteric transition mechanism. We have also prepared a complex of MerR with a 23bp MerOP and found by dynamic light scattering that this complex forms oligomeric structures in solution. To overcome such oligomerization we devised an alternative buffer that affords a monodisperse solution at high protein concentrations in physiologically relevant thiol buffer levels. Small-angle neutron scattering (SANS) allowed us to probe differences in the conformations of MerR and of DNA in the complex. We included a H_2O/D_2O contrast variation series to obtain complete data sets for the MerR/MerOP complex in the active and repressed conformations. Concurrently, we are optimizing our computational molecular model of the MerR-23bp-MerOP complex by including previous genetic and DNA footprinting data in order to describe the Hg(II)-induced transition from repression to activation.

1. Summers, A. O. (2009). *Curr. Opin. Microbiol.* **12**, 138–144.
2. Park, S. J. et al. (1992). *J. Bacteriol.* **174**, 2160–2171.
3. Ansari, et al. (1992). *Nature*, **355**, 87–89.
4. Guo et al. (2010). *J Mol Biol* **398**(4)**:** 555-568.

ORNL SFA Task 4: Molecular-Scale Interactions and Transformations of Mercury in the Environment

ORNL SFA (Laboratory Research Manager: Liyuan Liang)

A. Johs, J.M. Parks, H.-B. Guo, S.J. Tomanicek, L. Hong, L. Liang—*ORNL*; M. Sharp—*ESS Sweden*; M. Ohl, *FZ Jülich*; L. Shi, *PNNL*, R. Nauss, S.M. Miller—*U. of California San Francisco*; A.O. Summers, L. Olliff—*U. of Georgia Atlanta*; D. Riccardi, J.C. Smith (PI)—*U. of Tennessee Knoxville and ORNL*

As an integral part of the ORNL SFA, this Task investigates subcellular processes, including mechanisms of mercury-ligand interactions, mercury trafficking, and enzyme-catalyzed reactions involved in bacterial mercury resistance, dissimilatory reduction, and methylation.

Our initial focus has been on the biomolecular structure and function of key proteins and enzymes that confer mercury resistance in bacteria and impact mercury speciation and bioavailability in the environment. Expression of mercury resistance genes in the *mer* operon is controlled by the metalloregulator MerR (see poster by Johs et al.). A key component of the *mer* operon, the mercuric reductase MerA, catalyzes the reduction of Hg(II) to Hg(0). Using Neutron Spin-Echo spectroscopy, we are characterizing the interdomain dynamics of MerA at multi-nanosecond time scales. We have also crystallized the N-terminal domain of MerA, NmerA, and obtained X-ray diffraction data to a resolution of 3.25 Å. Solution of the 3D structure using molecular replacement is currently underway.

Understanding the interactions of mercury with various ligands is essential not only for characterizing abiotic reactions but also for complex biological systems. These interactions determine the speciation, biological transport and transformation of mercury in the environment. We have used quantum chemical calculations to carry out quantitative studies of the molecular factors that determine condensed-phase Hg speciation (see poster by Smith et al.). Hg(II) in complex with DOM is known to undergo photoreduction. Using substituted benzoic acids as models of DOM, quantum chemical calculations are being carried out to study photoexcitation of benzoic acids and subsequent photoreduction of Hg(II) upon UV irradiation.

Hg(II) reduction also occurs at low levels as a side reaction of dissimilatory iron reduction in iron-reducing bacteria such as *Shewanella* and *Geobacter*. Many have hypothesized that this reduction is carried out by outer-membrane multiheme cytochromes whose natural role is to transfer electrons to external Fe(III). We purified the decaheme outer-membrane cytochrome OmcA from *Shewanella oneidensis* MR-1 and collected X-ray diffraction data. Solution of the structure of OmcA is currently underway.

Future efforts of this SFA Task will combine biophysical experiments, structural bioinformatics and computer simulations to determine mechanisms of mercury transformations in biotic and abiotic systems.

Quantifying the Influences of Ecological Drift, Selection and Dispersal in Subsurface Microbial Communities

PNNL SFA

J.C. Stegen, X. Lin, J.K. Fredrickson, X. Chen, D.W. Kennedy, C.J. Murray, M.L. Rockhold, A.E. Konopka (PI, allan.konopka@pnnl.gov)—*PNNL*

The microbes that reside within the sediments and groundwater in the Hanford 300 Area can be thought of as a meta-community; that is, a set of ecological communities connected to each other through organismal dispersal. Ecological theory posits that turnover in composition is governed by (ecological) Drift, Selection, and Dispersal Limitation. Quantitative estimates of these processes remain elusive, but would represent a means to evaluate systems-level processes in subsurface environments. Using a novel analytical framework we quantitatively estimate the relative influences of Drift, Selection, and Dispersal Limitation on subsurface, sediment-associated microbial meta-communities. The analysis includes both the Hanford and Ringold formation sediments within the Hanford IFRC well field (~12,500m^3). We find that Drift consistently governs ~25% of spatial turnover in community composition; Selection dominates (governing ~60% of turnover) across spatially-structured habitats associated with fine-grained, low permeability Ringold sediments; and Dispersal Limitation is most influential (governing ~40% of turnover) across spatially-unstructured habitats associated with the Hanford formation's coarse-grained, highly-permeable sediments. Quantitative influences of Selection and Dispersal Limitation may therefore be predictable from knowledge of environmental structure. To develop a system-level conceptual model we extend our analytical framework to compare process estimates across formations, characterize measured and unmeasured environmental variables that impose Selection, and identify abiotic features that limit dispersal. Insights gained here suggest that subsurface microbial community ecology can benefit from a shift in perspective; the quantitative approach developed here goes beyond the 'niche vs. neutral' dichotomy by moving towards a strategy in which estimates of Selection, Dispersal Limitation and Drift can be described, mapped and compared within and across definable elements (e.g., lithofacies) of large-scale subsurface systems.

Biogeochemical Investigations Across Oxidation-Reduction Boundaries at the Hanford Site SFA

PNNL SFA (Laboratory Research Manager: Harvey Bolton)

J.P. McKinley (PI), C.T. Resch, M.D. Miller, R.M. Lund, X. Li, A.E. Konopka, C.J. Murray, J.M. Zachara—*PNNL*

The area near the Columbia River shore at the 300 Area comprises a complex system where microbial populations are controlled by processes occurring across lithologic boundaries where contrasting nutrient availability and mobility impose transitions in oxidation-reduction potential. In addition, while the regional hydrologic gradient is generally from surrounding uplands toward the Columbia River, seasonal and short-term changes in river stage cause rapid fluctuations in the gradient such that the flow direction and velocity change abruptly. River water intrudes the aquifer during abrupt gradient reversals caused by rises in the river stage, imposing extreme fluctuations on local groundwater composition. Our focus is on three biogeochemically distinct formations: the underlying Columbia River basalt flows, intermediate fluviolacustrine Ringold sediments, and uppermost catastrophic flood deposits of the Hanford formation. The uppermost Ringold and the Hanford sediments are the environmentally accessible and impactful stratigraphic components within these strata, and are hydrologically coupled to the Columbia River.

A series of passive multilevel samplers were deployed across known fine-to-coarse lithologic boundaries at the top and bottom of the Ringold formation's uppermost mud. Aqueous and dissolved gas samples were analyzed for the metabolically sensitive solutes O_2, NO_3^-, NO_2^-, SO_4^{2-}, Mn^{2+}, Fe^{2+}, HS^-, N_2O, H_2, and CH_4. Across the gravel-mud boundary from the Hanford to Ringold formations, the concentrations of SO_4^{2-}, Mn^{2+}, NO_2^-, H_2, and CH_4 increased with depth, while the concentrations of O_2 and NO_3^- decreased. At the lower mud-gravel boundary, within the Ringold formation, HS^- increased with decreasing depth (i.e., into the mud). Fe^{2+} and Mn^{2+} were present throughout the sampled Ringold formation, and H_2 and CH_4 increased with depth near the gravel-mud boundary deeper in the section. Anaerobic metabolism within the fine portions of the Ringold formation apparently supported anaerobic microbial populations that actively consumed available electron acceptors. The presence of H_2 and CH_4 suggested that perhaps fermentation reactions drove a supply of electron donors, and the contrast in HS^- and SO_4^{2-} gradients across the lithologic boundary suggested that advection existed from the Ringold into the Hanford formation. PCR analyses showed that nitrate reducers increased in abundance below the gravel-mud boundary, while sulfate and metal reducers were most abundant at the boundary.

We continue to target zones of varying microbial ecology across boundaries within the stratigraphic column that separate strata with varying lithologic contrast, and at locations with varying distance to, and influence by, the Columbia River.

Electron Transfer to the Microbe-Mineral Interface at Nanometer Resolution

PNNL SFA (Laboratory Research Manager: Harvey Bolton)

D.J. Richardson (PI), *U. of East Anglia UK*

A key question regarding electron exchange between a bacterium and extracellular electron acceptors or donors is the mechanism of electron transfer across the outer membrane. We have developed a conceptual model as a framework in which we propose that the multi-heme cytochrome "wires" can embed within an outer-membrane porin sheath to form electrically conductive complexes. These porincytochrome complexes can then interact with various biochemical termini on either side of the outermembrane, depending on their physiological function (e.g., Fe(III) reduction or Fe(II) oxidation). Our objectives are to solve the molecular structure of this complex, reconstitute it into liposomes, study electron transfer to a range of minerals in these artificial membrane systems, and prove that this model applies widely in environmental systems where it is necessary to elucidate the molecular properties of the cytochrome-porin complexes and the termini that interact with them, over a range of environmentally relevant bacterial species. In addressing these broad objectives, we have: (1) obtained 3-Angstrom and 1.8- Angstrom crystal structures of decaheme Fe(III) reducing terminis of an outer-membrane cytochrome-porin wires and used this to explain how electron transfer at the microbe-mineral interface can be direct protein-to-mineral or mediated by soluble electron shuttles such as flaving; (2) incorporated a porin-cytochrome complex into proteoliposomes,enabling us to examine electron exchange with different mineral surfaces, for example hematite,goethite, or birnessite, and study the effectiveness of different outer membrane deca-heme termini inthese processes; (3) undertaken biochemical, spectro-potentiometric; and structural studies on a rangeof outer-membrane electron transport systems to understand functional commonalities and differences and (4) solved crystal structures of outer-membrane cytochromes with Fe(III) complexes bound that give the first nanometer resolution of a cytochrome-ferric iron electron transport complexes.

Relating Differences in Mineral Reaction Rates to Microenvironment Creation and Heterogeneous Pore-Scale Phase Distribution at the Hanford Site

PNNL SFA (Investigators: John M. Zachara; Jim K. Fredrickson)

K. Rosso (PI), A. Felmy, C. Pearce, J. Liu, O. Qafoku—*PNNL*; S. Heald, D. Latta, M. Boyanov, K. Kemner—*ANL*; E. Arenholz, *LBNL*; E. Buck, L. Shi, J. McKinley, D. Moore, T. Resch, T. Schaef, M. Bowden—*PNNL*

This research seeks to unravel effects of mineralogic reactive heterogeneity, local redox and pH gradients, and the resulting distribution of mineralogic and contaminant reaction products in the Hanford subsurface. Hanford sediments are relatively rich in Fe-bearing minerals in the form of magnetite, titanomagnetite, ilmenite, Fe(II)/Fe(III)-phyllosilicates, and Fe(III)-oxides, as well as carbonates, pyroxenes and feldspars. These phases are reactive to different extents with important system species such as O_2, H^+, and Fe(II). These differences in mineral redox reactivity or dissolution rate can generate local microenvironments and a heterogeneous pore-scale mineral or contaminant phase distribution. To investigate these effects, a greater understanding of the reactivity of these phases under dynamic reaction-limited conditions is required.

Towards this goal, natural Fe-rich mineral samples from sediments collected at several locations on Hanford's central plateau were isolated by magnetic separation. This fraction represented ~2 wt% of the total sediment, and was composed of 90% magnetite as determined by XRD. XMP analysis showed that Ti was the most significant impurity, and that these grains could be described with the titanomagnetite formula $Fe_{3-x}Ti_xO_4$ with the dominant composition as $x = 0.15$ by chemical analysis and EPMA in the bulk, and by *L*-edge XAS and XPS at the surface. XMCD showed that octahedral Fe(II) was measurable within 5 nm of the mineral surface. This Fe(II) was highly responsive to the aqueous environment as a result of transitioning from oxic Hanford groundwater to reduced Ringold groundwater. Reaction of magnetically-separated natural phases showed that they are able to reduce Tc(VII) to Tc(IV), and U(VI) to U(IV) with concurrent oxidation of structural Fe(II) to Fe(III), as were synthetic $x = 0.15$ bulk powder and nanoparticle analogue phases developed using EMSL facilities. These studies revealed a wide range of Tc(VII) and U(VI) reduction rates and product form as a function of the Ti content, demonstrating the likelihood for a spatially heterogeneous distribution of products associated with such phases in the subsurface depending on composition. Parallel studies on Pu-containing sediments at the Hanford site that had received high concentrations of acidic waste water showed a complex heterogeneous distribution of precipitates. NanoSims and TEM measurements revealed that these differences were correlated with differences in the basicity of the initially present minerals. Neutralization of the acidic wastes at the reactive mineral surfaces apparently created local higher pH microenvironments that induced precipitation of Pu compounds and other phases selectively at these locations.

Current research is focused on examining relationships between flow, mineral redox and pH neutralization rates, and pore-scale phase distributions. Variations in redox reactivity will be examined by studying the titanomagnetite mineral series with redox probe species (Tc(VII) ,U(VI) and Pu(V)) which are reduced to their insoluble tetravalent state over a broad range of redox potentials. We will also use Fe(II)-oxidizing microbial cytochromes as redox probe species with biogeochemical implications. These studies will be conducted in reaction and microscale flow-through packed porous media, combined with *in situ* spectroscopic quantification of electron transfer progress and synchrotron-based mapping of chemical and valence distributions.

Isolation and Characterization of a Novel Fe(II)-Oxidizing *Alphaproteobacterium* from the Hanford 300 Area Subsurface

PNNL SFA (Laboratory Research Manager: Harvey Bolton)

E. Roden (PI), E. Shelobolina, J. Benzine, E. Percak-Dennett, B. Converse—*U. of Wisconsin*; L. Shi, A. Plymale, S. Reed, J. Fredrickson—*PNNL*

As part of an ongoing study of microbial Fe redox cycling in Hanford 300 Area subsurface sediments, a novel neutral-pH Fe(II)-oxidizing *Alphaproteobacterium* was isolated from Hanford formation groundwater using *in situ* incubation chambers ("i-chips") containing the insoluble Fe(II)-bearing mineral biotite as an energy source. After five months of *in situ* deployment, samples from i-chips were transferred into aerobic liquid medium with biotite the sole energy source. Following several transfers on this medium, the cultures were grown for three generations on medium to which soluble Fe(II) ($FeCl_2$) and air were added repeatedly over time. A pure culture was subsequently isolated on aerobic plates containing acetate and yeast extract. Sequencing of the 16S rRNA gene of the culture showed that it is >99% similar to various strains of *Bradyrhizobium japonicum*. The culture (referred to as *Bradyrhizobium* sp. strain 22, or simply "strain 22") was tested for the ability to grow chemolithoautotrophically with soluble and insoluble forms of Fe(II), as well as other inorganic electron donors. Strain 22 grew in organics-free medium with $FeCl_2$ or Fe(II)-NTA as the electron donor and oxygen or nitrate as the electron acceptor. The organism could also grow repeatedly with biotite (aerobic conditions) or reduced smectite (nitrate-reducing conditions) as the electron donor. Unlike other known chemolithoautotrophic strains of *Bradyrhizobium* (e.g. *B. japonicum* strain USDA 110), strain 22 is not able to grow by oxidation of hydrogen or thiosulfate. A draft whole genome sequence for strain 22 was obtained through the University of Wisconsin-Madison Biotechnology Center. The 7.4 MB sequence underwent de novo assembly and automated annotation through RAST, leading to identification of a total of 7003 coding sequences. The draft genome was searched for genes likely to be involved in chemolithoautotrophic growth with Fe(II). A complete Rubisco system for CO_2 fixation, analogous to that present in other chemolithoautotrophic strains of *Bradyrhizobium*, was identified. Although numerous *c*-type cytochromes were found in the genome, none of them showed homology to the type of outer membrane proteins (e.g. the *mtrAB* system) known to be associated with extracellular electron transfer in some Fe(III)-reducing or Fe(II)-oxidizing organisms. This conclusion was supported by PCR screening of strain 22 genomic DNA for *mtrAB* homologs, which gave negative results. Although verification of the latter finding is pending (by southern blot analysis), information available to date suggest either failure in the annotation of novel outer membrane *c*-type cytochromes, and/or that strain 22 uses a mechanism for Fe(II) oxidation distinct from other known Fe(II) oxidizers. Motivation for more detailed studies of the mechanisms for Fe(II) oxidation in strain 22 (together with other *Bradyrhizobium* isolates from Hanford) comes from the observation of relatively high proportions of *Bradyrhizobium*-related sequences (up to 5-10% of total sequences) in 16S rRNA gene clone libraries constructed with Hanford 300 Area sediments. Development of genetic tools to detect the presence and expression of genes associated with Fe(II) oxidation could provide insight into the role(s) of *Bradyrhizobium*-related organisms in *in situ* biogeochemical processes in 300 Area sediments. Future studies will employ differential gene expression (via RNAseq) and proteomics during organotrophic vs. chemolithoautotrophic growth with Fe(II) as a means for identifying key components of the Fe(II) oxidation system in strain 22.

Identification and Characterization of Microbial Proteins Important for Extracellular Electron Transfer Reactions

Liang Shi (PI), Juan Liu, Kevin M. Rosso—*PNNL*; Gaye White, *U. of East Anglia UK*; Zhi Shi, Alice C. Dohnalkova, Zheming Wang, David W. Kennedy—*PNNL*; Marcus Edwards, Julea N. Butt, Thomas Clarke—*U. of East Anglia UK*; Kathy Byrne-Bailey, John Coates—*U. of California Berkeley*; David J. Richardson, *U. of East Anglia UK*; John M. Zachara, James K. Fredrickson—*PNNL*

Microbial proteins and protein complexes involved in extracellular electron transfer reactions play a critical role in the biogeochemical cycling of metals. These proteins usually form electron transfer pathways that link the extracellular metal redox reactions and metabolic activities inside microbial cells. Our research goal is to establish a molecular-level understanding of the roles of the key proteins of these electron transfer pathways in Fe(II/III) redox transformations in the environment.

Originally discovered in the dissimilatory metal-reducing bacterium *Shewanella oneidensis* MR-1 (MR-1), key components of the Mtr (i.e., metal-reducing) pathway exist in all characterized strains of metal-reducing *Shewanella*. A survey of sequenced microbial genomes has identified homologues of the Mtr pathway in other dissimilatory Fe(III)-reducing bacteria, including *Aeromonas hydrophila*, *Ferrimonas balearica* and *Rhodoferax ferrireducens* and in the Fe(II)-oxidizing bacteria *Dechloromonas aromatica* RCB (RCB), *Gallionella capsiferriformans* ES-2 (ES-2) and *Sideroxydans lithotrophicus* ES-1 (ES-1). The putative Mtr pathways identified from the Fe(II)-oxidizing bacteria are named as Mto (i.e., metal-oxidizing) pathways to distinguish them from those found in the Fe(III)-reducing bacteria. The apparent widespread distribution of Mtr/Mto pathways in both Fe(III)-reducing and Fe(II)-oxidizing bacteria suggests a bi-directional electron transfer role, and emphasizes the importance of this type of extracellular electron transfer pathway in microbial redox transformation of Fe.

The *mtoABCD* and *cymA* genes of the Mto pathways identified from the Fe(II)-oxidizing bacteria ES-1, ES-2 and RCB were cloned for heterologous expression and subsequent characterization. MtoA is believed to be inserted into MtoB and mediates electron transfer across the outer membrane between extracellular Fe(II) and MtoD in the periplasm. Consistent with this prediction, cloned *mtoA* of ES-1 partially complemented an MR-1 mutant without MtrA with regard to ferrihydrite reduction. Purified MtoA of ES-1 was a decaheme *c*-type cytochrome and oxidized soluble Fe(II). Oxidation of Fe(II) by MtoA was pH- and Fe(II)-complexing ligand-dependent. Thermodynamic modeling shows that redox reaction rates for the different Fe(II)-complexes correlated with their respective estimated reaction-free energies. Thus, characterization results are consistent with the prediction that MtoA of ES-1 may be involved in Fe(II) oxidation by ES-1.

In the Mtr pathway of MR-1, MtrABC transfer electrons from the periplasm, across the outer membrane to the surfaces of extracellular Fe(III)-containing minerals. To characterize their interfacial electron transfer rate to solid phase Fe(III) oxides, MR-1 MtrABC were incorporated into proteoliposomes. Immuo-gold localization confirmed that MtrC was exposed at the surfaces of proteoliposomes, which is consistent with the results of proteolytic digestion. Under the conditions tested, MR-1 MtrABC in proteoliposomes facilitated electron transfer between reduced methyl viologen inside proteoliposomes, as the electron donor, to goethite (α-FeOOH) and lepidocrocite (γ-FeOOH) external to the proteoliposomes in the absence of any electron shuttle, such as flavins, at rates of $1288 \pm 39\ s^{-1}$ and $8756 \pm 505\ s^{-1}$, respectively. These results demonstrate the intrinsic ability of MR-1 MtrABC to transfer electrons to solid phase Fe(III) oxides at physiologically relevant rates.

This research is part of the SBR SFA at Pacific Northwest National Laboratory.

Role of Microenvironments and Transition Zones in Reactive Subsurface Biogeochemistry: The PNNL SFA

PNNL SFA (Principal Investigators: John Zachara and Jim Fredrickson)

J.M. Zachara (PI), J.K. Fredrickson (PI)—*PNNL*, J. Davis, *LBNL*; A. Felmy, G. Hammond—*PNNL*; K. Kemner, *ANL*; A.E. Konopka, C. Liu, J. McKinley, C. Murray, C. Pearce—*PNNL*; D. Richardson, *U. of East Anglia UK*; E. Roden, *U. of Wisconsin*; K. Rosso, T. Scheibe, L. Shi, M. Wilkins—*PNNL*; B. Wood, *Oregon State U.*

The PNNL Scientific Focus Area (SFA) is investigating fundamental, Hanford-inspired subsurface science issues through integrated, multi-disciplinary research on the role of microenvironments and transition zones in biogeochemical reactive transport processes. The long-term goals of the SFA are to: i.) develop an integrated conceptual model for microbial ecology and its influence on biogeochemical processes in a complex and hydrologically dynamic subsurface water system; ii.) determine scale transitions of coupled processes from the laboratory to field, causes for scale dependency, and up-scaled parameters for process models; and iii.) advance understanding of field-important electron transfer processes at the molecular and microscopic scale to yield improved process models and their coupling.

Cohesiveness and integration are achieved through focus on vertical redox transition and horizontal groundwater-surface water interaction zones in the field. The Hanford 300A site offers extensive biogeochemical research opportunities as it contains: a dramatic redox interface, a fluctuating water table, a spatially dynamic zone of groundwater-river mixing within the aquifer, and a hyporheic zone where groundwaters discharge to surface water. Findings and concepts from 300A research drive cross-scale SFA investigations that include: field-scale investigation of biogeochemical processes and microbial ecology; laboratory investigations of coupled process interactions at the pore and macroscopic scale; and mechanistic studies of impactful biogeochemical processes.

Future research will emphasize biogeochemical cycling and reaction rate measurements across 300A vertical and horizontal subsurface transition zones, identifying sources of electron donor and their fluxes in different field system compartments, ecological processes controlling microbial community composition and biogeochemical function, and laboratory investigations of key underlying macroscopic and molecular biogeochemical processes. A stochastic multi-scale modeling approach will be implemented that integrates field and smaller scale measurements to understand and predict the behavior of the complex 300 A field system.

SLAC SFA Project Overview: Biogeochemical Processes Governing the Speciation, Dynamics, and Stability of Uranium in Reduced Aquifers

J.R. Bargar (PI), *SLAC*; R. Bernier-Latmani, *ÉPFL*; G.E. Brown Jr., S.E. Fendorf—*Stanford U.*; D.E. Giammar, *Washington U. St. Louis*

The molecular- and nano-scale biogeochemistry of uranium has a profound impact on its fate and transport in complex subsurface systems. While a large body of work has focused on U(VI) behavior in sediments, relatively little is known about the pathways of transformation to U(IV) under reducing conditions *in aquifers*, the identities of the obtained species, their stability, and their dynamics in groundwater. Natural reducing conditions are common at uranium-contaminated aquifers under DOE-EM and DOE-LM management across the Western U.S. Uranium sediment concentrations are significantly elevated in these zones, and uranium solute exchange between these zones and surrounding aquifers is suspected to contribute to the persistence of these large and intractable uranium plumes. The chemical and physical forms of organic carbon, S, and Fe, as well as diffusive solute dynamics, are posited to control U(IV) speciation and release rates from naturally reduced zones (NRZs). U(IV) is also fundamentally important to the performance of redox-based *in situ* aquifer remediation techniques such as stimulated bioremediation.

The SLAC SFA program is using a suite of innovative laboratory and field-based approaches to develop a fundamental understanding of U(IV) speciation in reduced sediments at molecular and nanometer scales, its impact on uranium dynamics in aquifers, and its relationship to biogeochemical C, S, and Fe cycling. In the past year, we have focused on the following research questions: (1) What is the occurrence, nature, and stability of U(IV) species in time and space in naturally and artificially reduced *aquifers*?; (2) What geochemical and microbiological factors control the production of biomass-bound noncrystalline forms of U(IV)?; (3) What is the stability of different forms of U(IV) under aquifer conditions? And, (4) What controls the structure and reactivity of poorly crystalline iron oxides, and how do they impact uranium attenuation?

Work in the past year has shown that both uraninite and biomass-bound U(IV) are important in field-reduced sediments. In-aquifer experiments show the latter to be the least stable form under aquifer conditions. Laboratory-based work has shown that both phosphate and calcium solute concentrations help to govern the production of noncrystalline U(IV), and that solutes such as Ca retard uraninite oxidative dissolution. Going forward, we will examine the impact of organic carbon, S and Fe mineralogy, and sediment heterogeneity on the formation of NRZs and naturally reduced U(IV), the chemical and physical form of the obtained U(IV), its distribution over nano- to millimeter scales, and its stability under seasonally variable aquifer conditions. Research performed by the SLAC SFA is providing new concepts for uranium dynamics in aquifers and quantitative parameters that provide the basis for improved biogeochemical models.

SLAC SFA: Speciation of Uranium in Biologically Reduced Sediments During Iron and Sulfate Reduction in the Old Rifle Aquifer

J.R. Bargar (PI), J.S. Lezama Pacheco, N. Janot—*SLAC*; J.E. Stubbs, *U. of Chicago*; D.S. Alessi, E.I. Suvorova, G.M. Stylo, R. Bernier-Latmani—*ÉPFL*; K.H. Williams, P.E. Long, J.A. Davis, P.M. Fox—*LBNL*; Kim M. Handley, *U. of California Berkeley*; Jose M. Cerrato, Daniel E. Giammar—*Washington U. St. Louis*

The speciation and dynamics of uranium(IV) in naturally and artificially bioreduced sediments, as well as its local nanometer to millimeter scale physical and chemical environment, controls its stability, susceptibility to oxidation, and subsequent transport behavior in aquifers. Uraninite is widely believed to be the most stable and therefore desirable form of uranium in bioreduced sediments. However, non-polymerized forms of U(IV), generally referred to as monomeric U(IV), also have been observed in laboratory axenic culture, column, and microcosm studies. Similar types of studies generally have not been performed in reduced aquifers but are required to develop a better understanding of U(IV) reaction products produced in these complex subsurface systems. For those studies where U(IV) products were observed in sediment systems, it has not been certain if U(VI) reduction was accomplished by organisms (*i.e.*, direct enzymatic reduction) or via reaction with inorganic reductants such as magnetite or FeS. Knowledge of mechanisms, species, chemical/physical environment, stability, and dynamics, is required to construct biogeochemical models that can predict uranium behavior under varying aquifer conditions.

We have studied the speciation of U, Fe, and S following electron donor amendment to aquifers at the Rifle IFRC. This technique uses *in situ* columns to obtain direct access to sediment U(IV) species, aquifer microbial populations, reaction rates, groundwater compositions, temperature, and pH, among other natural controls. A major advantage of the Old Rifle site for this study is the ability to temporally distinguish between iron- and sulfate-reducing conditions and therefore to study U(IV) transformation products across these regimes. We have studied U(IV) bioreduction over periods of 4 to 55 days and subsequent aging in the aquifer up to 1 year. Whole sediments were examined using x-ray and electron microscopy, x-ray absorption spectroscopy, and chemical extractions in order to determine the speciation and spatial distributions of U, Fe, and S. Under sulfate-reducing conditions, U(IV) was found to be associated with Fe- and S-rich coatings on the grain scale, but to be coordinated to oxygen atoms. The dominant mineral in the coatings was mackinawite with some FeS_2 also present. At the scale of and within individual coatings (tens of μm down to hundreds of nm), U and Fe concentrations were not correlated, and EXAFS spectra were consistent with U(IV) bound to biomass, suggesting a primarily biological U(VI) reduction pathway. The presence of sulfide minerals intimately associated with U(IV) implies substantially retarded reoxidation. Under Fe reducing conditions, U(IV) again appeared to be bound to biomass, although grain coatings were not observed. Uraninite was present as a minority species during and after bioreduction, but in some cases became enriched in relative concentrations during subsequent aging in the aquifer. This work establishes the importance of both monomeric U(IV) complexes and uraninite as bioreduction products in the Old Rifle aquifer and provides conceptual models of U(VI) bioreduction and U(IV) fate in complex subsurface systems.

SLAC SFA: U(IV) Biomineralization and Stability of Monomeric U(IV) Species

Rizlan Bernier-Latmani (PI), Daniel S. Alessi, Paul P. Shao, Malgorzata Stylo—*ÉPFL*; Juan S. Lezama-Pacheco, Noemie Janot, John R. Bargar (lead PI, bargar@slac.stanford.edu)—*SLAC*; Philip E. Long, Luis R. Comolli—*LBNL*

In situ immobilization of uranium in a reduced form is the goal of bioremediation approaches. Additionally, reduced uranium is found associated with natural reduced zones at the Rifle IFRC. In the last year, we have expanded our work on the products of biological and abiotic U(IV) reduction in several ways. We probed the chemical species that led to preferential monomeric U(IV) formation, microscopically characterized biogenic formation of both products preserved in a frozen hydrated state, investigated the role of extracellular polymeric substances (EPS) and explored the *in situ* reactivity of monomeric U(IV) at the Rifle IFRC site.

The ratio of UO_2 to monomeric U(IV) produced by *Shewanella oneidensis* MR-1 is strongly dependent on the chemical composition of the medium in which U(VI) reduction occurs. Uranium L_{III} edge XAS and the wet chemical extraction technique we developed allowed the identification of PO_4^{3-} and Ca^{2+} as critical components promoting monomeric U(IV) formation. Surprisingly, the aqueous concentration of these solutes during U(VI) bioreduction remains constant, suggesting little binding of these solutes to biomass. This may suggest an indirect influence of the presence of phosphate and calcium in solution on biological properties of cells that, in turn, impact the product of U(VI) reduction.

Cryo-TEM images of high pressure frozen and cryo-sectioned *Shewanella oneidensis* captured during U reduction to form either UO_2 or monomeric U(IV) reveal discrete nucleation points on the surface of the outer membrane. Cryo-tomographic reconstructions of the same phenomena further confirm the exterior localization of electron-dense U. The 3D profiles contrast the nanocrystalline uraninite, observed in clumps and the monomeric U(IV), which forms tufts. Additionally, we are investigating the role of biomolecules in promoting the formation of monomeric U(IV) vs. UO_2 using scanning transmission X-ray microscopy (STXM). A protein core and phospholipid membranes typical of bacteria were identified along with additional lipids and polysaccharides representative of EPS located on the exterior of the cell. When U was localized in the same region using SEM/EDX, U could be detected in EPS-containing regions. Further work is ongoing to confirm these initial findings.

To study the reactivity of monomeric U(IV) in an aquifer, agarose gel pucks containing monomeric U(IV) were deployed in wells at the Rifle IFRC site for up to 3 months. Two types of monomeric U(IV) were studied: that associated with a *Shewanella sp.* isolated from the Rifle site, and monomeric U(IV) associated with a biogenic magnetite that was treated with phosphate prior to U(VI) reduction. U loss from monomeric U(IV) gel pucks is significantly faster than that from uraninite pucks. Digestion and X-ray absorption spectroscopy (XAS) analyses on the recovered gels reveals that the chemistry and oxidation state of the groundwater impacts the rate of U loss from the gels, as well as its oxidation and retention as U(VI) within the gels.

Monomeric U(IV) is an important research topic due to its relevance in the subsurface. Its formation is promoted by the presence of phosphate and calcium. Biomass-associated monomeric U(IV) occurs at discrete locations on the outer membrane and appears to co-localize with EPS. Finally, it is significantly more labile than nanoparticulate UO_2 *in situ*.

SLAC SFA: Biogeochemical Processes and Diffusive Transport Limitations Affecting the Stability of Biogenic U(IV)

Daniel E. Giammar (PI), Jose M. Cerrato, Mathew N. Ashner, Zimeng Wang, Vrajesh Mehta—*Washington U. St. Louis*; Juan S. Lezama-Pacheco, John R. Bargar (lead PI)—*SLAC*; Daniel S. Alessi, Rizlan Bernier-Latmani—*ÉPFL*

Fundamental knowledge about the molecular-scale speciation and reactivity of U(IV) products of microbial U(VI) reduction is crucial for the success of *in situ* bioremediation strategies in uranium-contaminated sites and can provide information about the fate of uranium present in naturally reducing zones. Recent studies have shown that U(IV) products of microbial reduction of U(VI) include uraninite (UO_2) and U(IV) bound to biomass (i.e., monomeric U(IV)). UO_2 is the most desirable product of *in situ* bioremediation because it is orders of magnitude less soluble than other U species. Biogeochemical processes, molecular structure and composition, and diffusive transport limitations can affect the stability of U(IV) species in subsurface environments. The focus of this portion of the SLAC SFA project was to assess the reactivity of uraninite under carefully controlled conditions.

The relative lability of different forms of U(IV) have been probed in a series of chemical extractions that target U(IV) fractions that are water soluble, ion exchangeable, amenable to complexation by a ligand, and oxidizable. Biogenic UO_2 and molecular U(IV) had similar low degrees of mobilization to chemogenic UO_2 in all of the extractions except for the oxidizing one (oxygen or persulfate) in which the biogenic U(IV) species were more easily extracted.

Laboratory experiments were performed to evaluate adsorption and precipitation reactions occurring in the presence of groundwater cations that can affect UO_2 dissolution. Oxidative UO_2 dissolution rates were 1450 times lower in the presence of Zn^{2+} and 7 times lower in the presence of Ca^{2+} than in water free of divalent cations. Electron microscopy and x-ray absorption spectroscopy analyses of UO_2 solids recovered from the experiments suggest that adsorbed or precipitated phases of calcium and zinc can block the surface of UO_2 and inhibit its oxidative dissolution. We posit that the UO_2 solid may facilitate the formation of a Ca-U(VI) phase through adsorption of Ca^{2+} and subsequent surface precipitation. A Zn carbonate phase precipitated on the UO_2 solids recovered from experiments performed in the presence of Zn. Interactions with divalent groundwater cations have implications for the longevity of UO_2 and the mobilization of U(VI) from these solids in remediated subsurface environments.

The effects of diffusive transport limitations on the dissolution of UO_2 were investigated using a synthetic groundwater prepared to simulate the conditions at the Old Rifle site. The dissolution of UO_2 was measured in the absence and presence of diffusive limitations exerted by permeable sample cells. Dissolution rates of UO_2 at diffusion-limited conditions were two orders of magnitude lower than those measured in well-mixed systems, suggesting that transport processes could affect the fate of U immobilized during *in situ* bioremediation. Characterization of unreacted and reacted UO_2 solids suggest that oxidative dissolution was more evident in the absence of diffusive limitations. A 1-D transport model successfully simulated diffusion-limited UO_2 dissolution with the dominant rate-limiting process being the transport of U(VI) out of the permeable sample cells. These findings advance our overall understanding of the coupling of geochemical and transport processes that can lead to differences in dissolution rates measured in the field and in laboratory experiments.

SLAC SFA: Structural Basis for Ferrihydrite Reactivity in Subsurface Environments

F.M. Michel (PI), J.S. Lezama-Pacheco, J.R. Bargar—*SLAC*; A.C. Cismasu, G.E. Brown Jr.—*Stanford U.*; K.H. Williams, P.E. Long—*LBNL*

Ferrihydrite is a reactive and relatively abundant Fe-oxyhydroxide phase that coats subsurface sediments at redox transition zones in aquifers, such as occur in and around artificially and naturally bioreduced zones, hyporheic boundaries, and near the surface of the water table. In these environments, ferrihydrite plays important roles in mediating the cycling of carbon, sulfur, and contaminants such as uranium. The reactivity of ferrihydrite derives from its exceptionally large surface area, high sorptive capacity for organic carbon, metal ions, silicate and phosphate, and from its poor crystallinity and metastability. Ferrihydrite forms in the presence of natural organic matter (NOM, *e.g.*, humic and fulvic substances), aluminum and silica, all of which are common in aquifers and interfere with its crystallization. These interactions profoundly modify the reactivity and stability of ferrihydrite. In spite of its importance, a structural basis that conceptually and quantitatively relates these constituents to the behavior of ferrihydrite and linked elemental cycles in aquifers is lacking. This portion of the SLAC SFA is addressing the fundamental molecular- and nano-scale physico-chemical factors that control ferrihydrite reactivity in complex subsurface environments.

We have evaluated the structural and physico-chemical characteristics of ferrihydrite formed in the subsurface at the Rifle, CO IFRC site. Rifle ferrihydrite was found to be closely associated with Si and NOM. Synchrotron-based X-ray diffraction (XRD), X-ray total scattering, and Pair Distribution Function (PDF) analysis show that Rifle ferrihydrite is smaller in size and more structurally disordered than pure synthetic ferrihydrite. When structural details are combined with compositional analyses, we find that NOM and Si appear to be responsible for these structural perturbations. Surprisingly, Rifle ferrihydrite bears close structural resemblance to ferrihydrites formed in natural environments ranging from acid mine drainage systems to deep-sea microbial mats, which also contain significant amounts of NOM, Si, and/or Al.

We have subsequently explored the individual and combined effects of organic matter, Si, and Al on synthetic ferrihydrite structures. In the case of Al, X-ray scattering/PDF, scanning transmission X-ray microscopy, and nuclear magnetic resonance (NMR) spectroscopy show that up to ~25 mol.% Al^{3+} replaces Fe^{3+} in octahedral sites in the ferrihydrite structure. Si, on the other hand, does not appear to structurally incorporate in ferrihydrite but rather forms as a poorly ordered Si-rich surface coating. Si strongly impacts the crystal size of ferrihydrite and increases lattice strain. Finally, we have used hydroxybenzoic acids as well-defined model substances to probe the impact of structural organics on the formation and structure of ferrihydrite. Here, we have found that hydroquinone structures in particular strongly impact ferrihydrite formation and size, as well as also increasing strain. This information is providing a fundamental scientific basis to account for ferrihydrite stability and reactivity in sediments.

Early Career Awards

Multi-System Analysis of Microbial Biofilms

M.J. Marshall (PI, matthew.marshall@pnnl.gov), S.M. Belchik, E.A. Hill, L.A. Kucek, A.C. Dohnalkova—*PNNL*
Collaborators: H. Beyenal, *Washington State U.*; B. Cao, *Nanyang Technological U.*

Direct examination of natural and engineered environments has revealed that the majority of microorganisms in these systems live in structured communities termed biofilms. In addition to microbial cells, biofilms are comprised of a poorly characterized organic matrix commonly referred to as extracellular polymeric substance (EPS) that may play roles in facilitating microbial interactions and biogeochemical reactions including extracellular electron transfer. Using high-resolution electron microscopy (EM) imaging, we have shown copious amounts of highly hydrated bacterial EPS to be produced during microbial metal reduction. The juxtaposition of extracellular electron transfer proteins and nanoparticulate reduced metal suggested that EPS played a key role in metal capture and precipitation. Here we present a multi-faceted approach to determine the composition of biofilm-associated EPS using a combination of synchrotron-based X-ray and infrared microimaging techniques combined with high-resolution EM and nano-secondary ion mass spectroscopy (nanoSIMS) imaging at the Environmental Molecular Sciences Laboratory (EMSL) to construct a high spatial resolution, complex chemical image of a biofilm community. To produce ultrathin sections of biofilms for scanning transmission X-ray microscopy (STXM) and synchrotron infrared microimaging, we developed a cryo-sample preparation technique where the traditional sample processing chemicals that interfere with carbon edge spectra or produce interfering infrared signatures were omitted. Biofilms were grown to 200 μm thick in a constant-depth (bio)film fermenter (CDFF) and samples were cryo-preserved by flash-freezing. Frozen biofilms sections were prepared using a cryo ultramicrotome and collected on formvar coated alpha numeric grids. EM analysis confirmed that an excellent depth-resolved biofilm morphology and cell ultrastructure was well preserved. After EM imaging, 100 nm thin sections were imaged by STXM followed by nanoSIMS to obtain chemical information at the nanometer scale that could be correlated to high-resolution images. In initial studies, we investigated the carbon chemistry and found that several differences existed between the cell surface and the EPS matrix encompassing biofilm cells. Concurrent with these studies, synchrotron-based infrared imaging was employed on 1.0 μm thick sections to produce high spatial resolution (0.54 μm) images with infrared spectral data showing the localizations of key biofilm components (i.e., proteins EPS, nucleic acids, and membrane lipids) to further construct our chemical image of biofilms. The integration of these techniques will provide detailed, high-resolution visualizations and corresponding chemical information that will help us to understand how biofilms influence local biogeochemical reactions in their environment.

This work was funded by a U.S. Department of Energy (DOE) Office of Science Early Career Research Program Award (DOE National Laboratory Announcement 10-395).

Nanoscale Mercury Sulfide-Organic Matter Interactions: Implications for Mercury Methylation Potential in Sediments

H. Hsu-Kim (PI), A. Morris, T. Zhang, K. Kucharzyk, Y. Liu, M.A. Deshusses—*Duke U.*

Mercury contamination of soil and sediment is a concern at several Department of Energy facilities due to the long-term risks for human exposure. In sediments, anaerobic bacteria (mainly sulfate reducers) are capable of converting inorganic forms of mercury to methylmercury, a highly bioaccumulative form of the metal. One factor controlling the production of methylmercury (MeHg) is the chemical speciation of inorganic Hg in sediments (e.g., Hg-sulfides) and the amount of mercury that is bioavailable to methylating bacteria. Our previous work has demonstrated that nanoparticulate forms of $HgS_{(s)}$ can be an important portion of mercury in sediments, particularly in locations containing dissolved organic matter (DOM) that facilitates the stabilization of nanoparticles in porewater. This research aims to develop a framework for linking mercury speciation to methylation potential in sediments. The objectives are to characterize the structure and reactivity of nanoscale compounds formed during the precipitation of HgS in DOM-containing water and then relate these properties to their bioavailability to methylating bacteria.

In the first part of this work, we performed precipitation experiments in solutions containing Hg, sulfide, and dissolved humic acid. These mixtures resulted in aggregates of nanoparticles (~3 to 4 nm) with metacinnabar-like mineralogy. Pure cultures of sulfate reducing bacteria were then exposed to these nanoparticles and also to bulk scale HgS. The experiments demonstrated greater amounts of MeHg production in cultures exposed to nanoparticles than in cultures exposed to the same concentration or the same surface area of microscale $HgS_{(s)}$ particles. These results indicated that the nanoparticles provided an extra source of bioavailable mercury (perhaps via enhanced dissolution rates of nanoparticles relative to microscale particles). The methylation experiments also showed that the methylation potential of nanoparticles decreased with the 'age' of the original nano-HgS stocks.

We utilized a wide variety of tools to assess changes to the size and crystallinity of HgS nanoparticles in their original stock solution. Measurements of monomer diameter and crystallite diameter by TEM and X-ray diffraction did not show large changes over 1 to 7 days. However, small angle X-ray scattering data suggested that the Hg-S-humic acid mixtures initially comprised of small scattering units (~1 nm) that would correspond to multinuclear Hg-S cluster type compounds in solution. Small clusters or amorphous particles would not be detected in TEM or XRD analysis. These small scattering units disappeared over one day as the HgS particles ripened and aggregated in solution. We also employed extended X-ray absorption spectroscopy to investigate the short-range order of HgS species in these mixtures. Our preliminary data suggest that the particles consisted of metacinnabar-like structure. However, Hg-S coordination numbers were less than bulkscale metacinnabar, indicating the presence of nanoscale HgS particles or clusters in the sample. Overall, the characterization of the nanoparticle stock solutions demonstrated that the smallest entities (e.g., HgS cluster compounds) may have some bioavailability to methylating bacteria (perhaps via dissociation directly outside the cell membrane surface prior to uptake). The next steps will be to apply models to the SAXS and EXAFS data and extract quantitative information regarding particle size distribution. We hope to apply the results to an overall framework that can link the kinetics of Hg-S-DOM transformations to mercury methylation rates in sediments.

Student Abstracts

Hg Stable Isotope Measurements in Fish Tissue as Indicators of Hg Chemical Transformations in East Fork Poplar Creek, TN

G. Bartov,* T.M. Johnson (PI)—*U. of Illinois Urbana-Champaign*

Mercury (Hg) is a highly toxic heavy metal with complex biogeochemical cycling. Hg occurs in two chemical forms in the environment; Hg(0) which is insoluble, and less toxic, and Hg(II), the highly soluble and reactive form of Hg. The complex biogeochemical cycle of Hg complicates our understanding of Hg interactions in contaminated DOE sites. The East Fork Poplar Creek (EFPC), which flows from the DOE Y-12 complex near Oak Ridge, TN, and empties into the Clinch River in Tennessee, has been contaminated by historic Hg emissions from the plant. Remediation efforts have reduced the Hg input into the creek significantly; however, methylmercury (MeHg) concentrations in the water and fish have not decreased.

Hg stable isotope measurements provide a unique potential to identify and quantify sources and chemical transformations of Hg, such as breakdown of MeHg and reduction of Hg(II) to Hg(0). Hg has seven stable isotopes (^{196}Hg, ^{198}Hg, ^{199}Hg, ^{200}Hg, ^{201}Hg, ^{202}Hg, ^{204}Hg). There are two known mechanisms to alter the relative abundances of the Hg isotopes. One, the kinetic isotope effect (KIE), enriches the product of Hg(II) reduction, methylation, demethylation and a few other processes, with lighter Hg isotopes relative to the reactant pool. This mass dependent fractionation (MDF) mechanism is due to the fact that lighter isotopes tend to react more readily than heavier isotopes. The second mechanism to alter the relative abundances of Hg isotopes is mass independent fractionation (MIF). Studies have shown that photochemical transformations of Hg cause the odd isotopes of Hg to act differently than what theoretical calculations based on MDF would predict. This effect, known as the magnetic isotope effect, allows ^{199}Hg and ^{201}Hg to back-react during photochemical reactions, and get depleted in the product of a reaction. The relative abundances of Hg isotopes are reported relative to NIST SRM 3133, an accepted inter-laboratory standard.

We analyzed fish tissue taken from upstream (close to the Y-12 complex) and downstream (18.5 km downstream from the plant) of the EFPC. The measured ^{202}Hg/^{198}Hg ratios show a weak positive trend from -0.59±0.06‰ (n=4) upstream to -0.31±0.14‰ (n=4) downstream. Fish are believed to be integrators of Hg over time, so the positive trend they exhibit may be indicative of some chemical transformation of Hg in the EFPC waters. Odd isotope anomalies were also detected in the fish samples. The slope calculated when the ^{199}Hg anomalies are plotted against the ^{201}Hg anomalies is consistent with previous studies' observations of photochemical MeHg reduction to Hg(0). Overall, the results suggest that the Hg taken up by the fish has experienced little redox cycling, and specifically we see no evidence for extensive Hg(II) reduction or photochemical demethylation.

*Student Presenter

Characterizing the Biological Mechanism of Uranium Reduction Using Novel Voltammetric Techniques

Keaton Belli,* *Georgia Institute of Tech.*; Philippe Van Cappellen, *U. of Waterloo Canada*; Thomas DiChristina, Martial Taillefert (PI)—*Georgia Institute of Tech.*

Uranium bioreduction represents a unique *in situ* remediation strategy which harnesses the ability of native microbial communities from contaminated sediments to utilize U(VI) as a terminal electron acceptor during anaerobic respiration. In this process, soluble U(VI) is reduced to sparingly soluble U(IV) followed by precipitation of U(IV) minerals to limit the mobility of this contaminant. Thus far, the biological mechanism of this bioremediation strategy has not been characterized in detail in a single organism. A recent study detected U(V) as a transient intermediate during uranium bioreduction, suggesting that uranium reduction proceeds via an initial one-electron transfer step from U(VI) to U(V) followed by either 1) a second biotic reduction of U(V) to U(IV) or 2) abiotic disproportionation of U(V) to regenerate U(VI) and precipitate U(IV). This mechanism opposes previously proposed pathways which describe uranium bioreduction as a single two-electron transfer step. Understanding all biotic and abiotic transformations of this radionuclide, including any chemical intermediates in these processes, is imperative to assess and implement this remediation strategy at contaminated sites. Unfortunately, the mechanism of U(VI) bioreduction continues to remain elusive due in part to the lack of analytical techniques able to measure the speciation of uranium in solution across multiple oxidation states at a high frequency.

To address these limitations, a voltammetric technique was developed using a hanging mercury drop electrode (HMDE) to quantify aqueous U(VI) and U(V), and qualitatively detect U(IV) species. Linear calibration curves were obtained for $U^{VI}O_2^{2+}$, $U^{VI}O_2(CO_3)_3^{4-}$, and $U^{V}O_2(CO_3)_3^{5-}$ with limits of detection of 1.2, 1.9, and 2.0 μM, respectively. In a medium composed of >99% $UO_2(CO_3)_3^{4-}$ species, *Shewanella putrefaciens* strain 200 reductively precipitated 2 mM U(VI) from solution at an initial rate of 7.54×10^{-10} mM/hr/cell. Au/Hg microelectrode measurements of $UO_2(CO_3)_3^{4-}$ correlated with total dissolved uranium measurements by ICP-MS thereby validating the newly developed voltammetric technique for quantifying U(VI) speciation during uranium bioreduction incubations. To assess the reactivity of a U(V) intermediate, abiotic U(V) disproportionation was investigated using kinetic isolation experiments in bicarbonate media at environmentally relevant pH. U(V) disproportionation was demonstrated to be first order with respect to $U^{V}O_2(CO_3)_3^{5-}$ with an observed rate constant of $0.174 \pm 0.025\ s^{-1}$. This finding supports a previously proposed mechanism involving two unique U(V)-carbonate species and sheds light on the behavior of the U(V) bioreduction intermediate in relevant geochemical conditions.

Overall, these results demonstrate that voltammetry can be used to rapidly quantify both U(VI) and U(V) as a function of time. This technique will be used to test the hypothesis that a pentavalent U(V) intermediate is formed during the bioreduction of U(VI). Simultaneously, fundamental rate laws for U(VI) bioreduction and U(V) disproportionation will be developed and incorporated into reactive transport models to predict the fate of uranium in diverse geochemical conditions, a crucial step in implementing U(VI) bioreduction as an effective bioremediation strategy.

*Student Presenter

Studies on Abiotic Mechanisms and Kinetics of Chemogenic Uraninite Oxidation in the Presence of Mackinawite and its Implication in Uranium Remediation

Yuqiang Bi,* *U. of Michigan Ann Arbor*; Kim Hayes (PI)

This research seeks to identify the potential of iron sulfides (primarily mackinawite) in inhibiting the reoxidation of U(IV) solids and evaluate the protective nature of mackinawite for long-term sequestration of uranium at DOE contaminated sites. Over the past three years, abiotic studies have been extensively conducted and thoroughly examined to 1) identify and quantify dominant geochemical mechanisms that protect uranium against mobilization in the presence of mackinawite under moderate oxic conditions; 2) evaluate the influence of a range of groundwater conditions on the ability of iron sulfides to inhibit reoxidation and remobilization of uranium; 3) assess the impact of post oxidation products of iron sulfides on uranium stability and mobility.

For this study, a continuously mixed batch reactor system has been developed and utilized along with an array of analytical methodologies to examine the mechanism and kinetics of FeS protection against UO_2 oxidation. Experimental results show that mackinawite serves as an effective oxygen scavenger to inhibit the fast oxidation of chemogenic uraninite under simulated groundwater conditions. The kinetic profiles of dissolved uranium indicate that 5 g/L mackinawite inhibits UO_2 oxidative dissolution for about 60 hr under pH = 7, P_{O2} = 0.02 atm, and P_{CO2} = 0.05 atm. During the lag time, oxidation of structural Fe(II) and S(-II) of mackinawite control the DO levels, leading to the formation of iron hydroxides and elemental sulfur, respectively, as determined by X-ray diffraction (XRD), Mössbauer and X-ray absorption spectroscopy (XAS). The redox potential of the reaction system appears to accurately track the stages of mackinawite oxidation. After FeS is depleted, DO levels increase and UO_2 oxidative dissolution occurs at a faster initial rate relative to the control experiments where mackinawite is absent. Oxidized U(VI) formed stable ternary Ca-UO_2-CO_3 complexes and dominates aqueous U(VI) species based on thermodynamic simulations. Approximately 20% - 40% of soluble U(VI) products are adsorbed by iron hydroxides (i.e. nanogoethite and ferrihydrite) formed from FeS oxidation depending on Fe:U molar ratio and calcium concentration. The kinetic data, along with XRD and XAS characterization of reaction products, suggests that the rapid uptake of U(VI) by FeS oxidation products during the initial stages of UO2 oxidation is responsible for the accelerated rate of UO_2 oxidative dissolution compared to the control in absence of FeS. Ongoing research is testing other groundwater conditions (including pH, pCO_2, pO_2) to understand the effects of these geochemical constraints in uranium reoxidation.

A completely mixed flow reactor (CMFR) is currently under development to study the rate of UO_2 oxidative dissolution in the presence of FeS under various experimental conditions. Dissolution reactions in flow-through systems are kept far from equilibrium by constantly refreshing reactant solutions and preventing accumulation of U(VI) products. The newly designed reactor system has advantages of better pH control and flexibility of varying influent compositions, and of providing accurate UO_2 dissolution rates more efficiently in comparison to the batch studies.

This research has benefited from active collaborations with multiple institutions, including Arizona State University, Synchrotron Radiation Lightsource and Pacific Northwest National Laboratory. The collective effort has resulted in the production of joint publications and constructive intellectual exchange. This work, while providing the mechanistic basis for the role of FeS in the long-term uranium sequestration, also facilitates the identification of the controlling redox reactions when natural systems comprised of iron sulfides and reduced uranium are subjected to oxidants in the subsurface.

*Student Presenter

Microbial Oxidation of Hg(0): Its Effect on Hg Stable Isotope Fractionation and Methylmercury Production

Matthew Colombo,* Nathan Yee, Juyoung Ha, John Reinfelder—*Rutgers U.*; Tom Johnson, *U. of Illinois Urbana-Champaign*; Tamar Barkay (PI), *Rutgers U.*

Background: The methylation of inorganic Hg is known to be mediated by microorganisms under anoxic conditions. Previous studies have elucidated the forms of mercuric Hg [Hg(II)] that are bioavailable to methylating microbes. It is generally assumed that elemental Hg [Hg(0)] is unavailable for biologic methylation, however the uptake and transformation of Hg(0) by anaerobic Hg-methylating bacteria have never been tested. In this project, we will conduct laboratory experiments to examine the oxidation of Hg(0) by anaerobic bacteria, and investigate the effect of microbial Hg(0) oxidation on Hg stable isotope fractionation and MeHg production.

Hypotheses: We will test the following hypotheses:

1. In anoxic environments, anaerobic bacteria catalyze the oxidization of Hg(0) to Hg(II).
2. Microbial oxidation of Hg(0) to Hg(II) imparts a mass-dependent fractionation of Hg stable isotopes.
3. Anaerobic Hg-methylating bacteria produce MeHg when provided with Hg(0) as the sole Hg source.
4. MeHg formed from Hg(0) is isotopically distinct from MeHg produced directly from Hg(II).

Research Plan: To test these hypotheses, we will carry out Hg(0) oxidation and methylation experiments using Hg-methylating iron-reducing and sulfate-reducing bacteria. Hg(0) oxidation experiments will be performed by exposing *Desulfovibrio desulfuricans* ND132 and *Geobacter sulfurreducens* PCA to a constant source of Hg(0) in the dark, and then monitoring the formation of non-purgeable Hg. To determine the chemical speciation of cell-associated Hg, the cells will be collected and examined using X-ray absorption near edge structure spectroscopy. The production of methylmercury will be determined by a distillation and ethylation-gas chromatography method. Finally, the fractionation of Hg stable isotopes by microbial Hg(0) oxidation will be investigated using state-of-the-art multi-collector inductively coupled mass spectrometry.

Results: The anaerobic bacterium *Desulfovibrio desulfuricans* ND132 exhibited a rapid transformation of Hg(0), with bacterial cultures producing 700 μg/L of Hg of non-purgeable Hg after 24 h of incubation. Comparison of the Hg L_{III}-edge energy position for the bacterial samples with reference compounds showed that Hg associated with *D. desulfuricans* ND132 was in the oxidized [Hg(II)] form. MeHg analyses revealed that after 24 h of incubation, *D. desulfuricans* ND132 produced up to 50 μg/L of MeHg. Our results indicate that anaerobic Hg-methylating bacteria can catalyze the oxidization of Hg(0) to Hg(II), and produce MeHg when provided with Hg(0) as the sole Hg source.

*Student Presenter

Quantifying the Enthalpy and Entropy of Europium-Hematite Surface Species Using Variable Temperature Batch Experiments and EXAFS

Shanna L. Estes,* Yuji Arai (co-PI)—*Clemson U.*; Rodney C. Ewing (co-PI), Jiaming Zhang—*U. of Michigan*; Tomohiro Shibata—*Illinois Institute of Tech., ANL*; Brian A. Powell (PI)—*Clemson U.*

The environmental fate of actinides is greatly influenced by interfacial reactions, including sorption to solid surfaces where the sorption of trivalent and tetravalent actinides is generally a very strong and potentially irreversible reaction. We hypothesize that the strong interactions of actinides with mineral surfaces result from the formation of inner sphere complexes with a limited number of high-energy surface sites, and that displacement of solvating water molecules from the actinide and mineral surface during sorption is energetically favorable and results from a large increase in entropy. The goal of this research is to provide both a qualitative conceptual model and a quantitative thermodynamic speciation model describing plutonium partitioning to sediments, which is based upon a mechanistic understanding of sorption processes as determined from both molecular-, microscopic- and macro-scale experimental techniques.

Due to its strong hydration sphere and utility as a chemical analog of trivalent actinides, we selected trivalent europium (Eu) as a model case, and studied the sorption of Eu(III) to synthetic hematite (α-Fe_2O_3) using variable temperature batch sorption experiments and extended x-ray absorption fine structure spectroscopy (EXAFS) analysis. The variable temperature batch experiments, conducted at 15, 25, 35, and 50 °C, demonstrated increasing Eu(III) sorption with increasing temperature, and yielded Eu(III)-hematite sorption edge data over the pH range ~3–7.5. We modeled the sorption edge data at each temperature using FITEQL 4.0 and the equilibrium constants for dissociation of water, protonation of the hematite surface (derived from potentiometric titrations of a hematite suspension), and hydrolysis of Eu. Under the experimental conditions, several Eu(III) surface species were possible, and the FITEQL models for each species fit the experimental data equally well. EXAFS analysis indicated the presence of inner-sphere bidentate mononuclear hematite surface complexes with a decrease in the coordination number for the Eu-O shell from 8 to 5 after sorption and a radial distance of the Eu-Fe shell at ~3.1Å. Additionally, we observed no evidence of Eu surface/bulk precipitates in high-resolution transmission electron microscopy (HRTEM) and EXAFS analysis. In a separate experiment, there was no net pH change after reacting Eu(III) with hematite. Based on the results of multi-scale geochemical analyses, we postulate the following surface reaction:

$$2SOH+Eu^{3+} = (SOH)_2Eu^{3+}$$

Using a plot of the surface complexation constants versus T^{-1} (K^{-1}), we calculated sorption enthalpy and entropy values of 104.2 kJ·mol^{-1} and 705.3 J·K^{-1}·mol^{-1}, respectively, for $(SOH)_2Eu^{3+}$. This implies that the entropy term ($-T\Delta S$) at 25 °C is -210 kJ·mol^{-1} and is the driving force behind this chemical reaction. This observation of the dominant entropy term is consistent with our experimental hypothesis that the energetic favorability of actinide surface complex formation is strongly influenced by positive sorption entropies, which are mechanistically driven by displacement of solvating water molecules from the actinide and mineral surface during sorption.

*Student Presenter

Chromium Responses and Biofilm Formation in *Desulfovibrio vulgaris* RCH-1, a Sulfate-Reducing Bacterium Isolated from 100H Chromium-Contaminated Groundwater, are Temperature-Dependent

L.C. Franco,* *Montana State U.*; Y.A. Gorby, *U. of Southern California*; M.W. Fields (PI), *Montana State U.*

Desulfovibrio vulgaris RCH-1 is a sulfate-reducing bacterium that was isolated from chromium-contaminated groundwater at the 100H Hanford Site. Reduction of chromium(VI) to the insoluble and less toxic chromium(III) could help prevent migration of chromium-contaminated groundwater to the Colombia River, a valuable drinking water source. Biostimulation of chromium-reducing organisms by injecting electron donors into the subsurface can create unbalanced ratios of electron donor to acceptor and here we show that these ratios affect *D. vulgaris* RCH-1 ability to reduce Cr(VI). Additionally, growing *D. vulgaris* RCH-1 at a temperature that is relevant to the *in situ* subsurface temperature affects chromium tolerance, reduction rates, and presence of extracellular filaments. Growth experiments were initiated in batch growth mode with electron donor-limited, electron acceptor-limited, and electron donor/acceptor balanced ratios. Washed *D. vulgaris* RCH-1 cells were exposed to 0, 20, 50, and 100 μM K_2CrO_4 and chromium(VI) levels were monitored during growth. Growth in electron acceptor-limited and electron donor-limited cultures was effected and had increased lag-times compared to cultures with electron donor/acceptor balanced ratios. *D. vulgaris* RCH-1 grows optimally at 30°C, but to understand if the chromium response is different at *in situ* temperatures, experiments were also carried out at 20°C. *D. vulgaris* RCH-1 was more susceptible to chromium at 20°C than at 30°C and cells could only tolerate 50 μM as opposed to 100 μM K_2CrO_4. *D. vulgaris* RCH-1 was also grown as a biofilm under electron acceptor-limited conditions at 30°C and 20°C and extracellular filaments were observed at 20°C, but not at 30°C. The presence of extracellular filaments at a field-relevant temperature suggests that the filaments play a role *in situ*. Current studies are focused on the determination of function and composition for extracellular structures. Studies of recent field isolates provide valuable insights into the metabolic potential of organisms that are present in the environment of interest as opposed to a model organism. Assessing chromium reduction at *in situ* temperatures rather than optimal growth temperatures and under electron donor- and acceptor-limitation provides field relevant insight into chromium toxicity and reduction for respective field sites.

*Student Presenter

Effects of Temporal Error Correlation on Quantification of Predictive Uncertainty in Groundwater Reactive Transport Modeling

Dan Lu,* Ming Ye—*Florida State U.*; Gary P. Curtis (PI), *USGS*; Philip D. Meyer, Steve Yabusaki—*PNNL*

Quantifying uncertainty of reactive transport simulations in groundwater can be conducted by using multiple conceptual models because groundwater flow and reactive processes are complex and subject to multiple interpretations. Consideration of alternative models results in broader but more realistic estimates of predictive uncertainty because the alternatives capture different plausible conceptual uncertainties. When quantitatively comparing model simulations it is important to separate error introduced by the inherent random processes in a groundwater aquifer from the structural error introduced by considering an alternative plausible conceptual model. Model structural error is likely to present a high degree of temporal correlation for breakthrough data collected sequentially along time. It has been long recognized that the error correlation may affect parameter estimation and predictive uncertainty quantification. However, methods for accurately describing the correlation structure of the errors and to incorporate it into groundwater reactive transport modeling is an open question. In conventional groundwater modeling, the errors are assumed to be multivariate Gaussian with zero mean and independent with a diagonal covariance matrix by considering only variances of measurement errors. This assumption has been found invalid in reactive transport modeling, and may lead to significant underestimation of predictive uncertainty. This is particularly true in multimodel analysis when alternative reactive transport models are considered. Use of a diagonal covariance matrix of the measurement errors in the calibration can cause one model to have an overwhelmingly high model probability (even 100%), which cannot be justified by the available data and knowledge.

In this study, we developed a statistical method to identify the temporal correlation structure using time series theories. The method considers both measurement errors and model structural errors. Unlike the measurement errors, the model structural errors present a high degree of temporal correlation. Therefore, unlike the conventional assumption, the correlation structure of the total errors is characterized by a full covariance matrix instead of the diagonal one. The full covariance matrix is obtained by simulating the correlated errors with autoregressive models and is incorporated into groundwater modeling by an iterative method with two stages of parameter estimation. We applied this method to a set of synthetic and real-world surface complexation models developed to simulate uranium transport based on a series of column experiments. Our results demonstrated that (1) the errors are highly temporally correlated due to model structural errors; (2) the temporal correlation can be properly considered by our method; (3) if the error correlation is disregarded, model uncertainty is underestimated, and predictive uncertainty bound is narrow, hardly covering the true values; and (4) with the error correlation considered by using our method, the predictive uncertainties of individual models become larger, and the model probabilities become distributed more evenly and realistically among the models, thus leading to better predictive performance with considering model uncertainty. Our method is mathematically general and theoretically can be applied to any reactive transport models. Our future research is to further evaluate and develop the method for multi-scale models and datasets.

*Student Presenter

Formation and Stability of Uranium(VI) Phosphates under Groundwater Conditions

Vrajesh Mehta,* Dan Giammar (PI)—*Washington U. St. Louis*

Phosphate addition to uranium-contaminated subsurface environments is a promising approach for *in situ* remediation. Addition of phosphate amendments can result in uranium sequestration in its oxidized +VI state without requiring chemically reducing conditions as needed for *in situ* immobilization via biogeochemical reduction of U(VI) to less soluble U(IV) species. Phosphate addition can be used as a stand-alone process or as a complementary process to bioremediation-based methods. The U(VI)-phosphate-sediment groundwater system is complex owing to the fact that uranium can adsorb to substrate minerals in addition to precipitating in uranyl phosphate solids. Furthermore, the solids that form may be metastable phases instead of those predicted by equilibrium calculations. The conditions that determine the dominant immobilization mechanisms are not well understood, and improvements in our knowledge can enable the design of more efficient remediation strategies.

To gain a better understanding of molecular scale interactions between U(VI) and phosphate, batch precipitation experiments were conducted at various pH conditions with solutions equilibrated with the atmosphere. As would be done in practice, phosphate was added in molar excess to U(VI) [ratio of PO_4^{3-} : U(VI) of 10:1] to enhance the precipitation reactions. Samples collected at various time intervals were used to measure the aqueous phase concentrations of uranium and phosphate using ICP-MS. In the presence of phosphate, more than 90% of uranium was sequestered in the solid phase under acidic conditions (pH= 4, 6) where there otherwise would not have been any uranium precipitation. At higher pH (pH= 7.5), the formation of soluble uranium-carbonate complexes prevented any precipitation. Solids collected on membrane filters were characterized using scanning electron microscopy with energy dispersive X-ray spectroscopy (SEM-EDX) and X-ray diffraction (XRD). In the presence of phosphate, precipitates of thin 1-5 μm square plates were observed. These analyses suggest the formation of chernikovite [$UO_2HPO_4.4H_2O$], which probably formed as a metastable phase since uranyl phosphate [$(UO_2)_3(PO_4)_2$] is calculated to be the thermodynamically most favorable phase under these conditions. The stoichiometry of the solid was examined by digestion of the solids and corroborates the formation of chernikovite [U(VI) : PO_4^{3-} ratio of ~ 1:1] in the presence of phosphate.

Current experiments are studying the specific effects of dissolved inorganic carbon and common groundwater cations (Na, Ca, Mg etc.) on the formation of precipitates in the presence and absence of phosphate. Ultimately, these experiments on precipitation of uranium-containing solids following homogeneous nucleation will be extended to conditions relevant to field sites by examining precipitation and adsorption in the presence of iron oxides, clays, and actual sediments. These studies will advance our fundamental understanding of molecular-scale mechanisms of uranium immobilization and their impact on uranium fate and transport in the subsurface.

*Student Presenter

Dynamics of Mercury Release in Flooded Soils from Oak Ridge, Tennessee

Brett A. Poulin,* *U. of Colorado Boulder and USGS*; George R. Aiken, *USGS*; Joseph N. Ryan, *U. of Colorado Boulder*; Kathryn L. Nagy (PI), *U. of Illinois Chicago*

Mercury transport from contaminated East Fork Poplar Creek (EFPC) floodplain soils in Oak Ridge, TN contributes to downstream mercury pools available for methylation, but the environmental controls of soil-to-stream mercury release are not well understood. Factors such as soil mercury speciation, fluctuations in soil redox status, soil geochemistry, and dissolved organic matter may control the mobilization and subsequent transport of mercury from contaminated soils to nearby streams. Our objectives were to identify the dominant source(s) and molecular controls on mercury release from contaminated soils, and characterize the hydrologic conditions (i.e., rising and falling water table) that may enhance or mitigate contaminant transport. In this study, mercury release was assessed from two EFPC soils, obtained from a stream bank site and a floodplain site, under saturation conditions. Characterization of the soils, from 0-65 cm depth at 10 cm intervals, included total mercury concentration, mercury physiochemical speciation via selective sequential extraction, organic matter content, elemental composition, cation exchange capacity, and soil mineralogy. Undisturbed, intact soil cores were collected at the sample sites from the O through A (0-30 cm depth) horizons which encompass the depth of historical contamination. Soil cores were artificially flooded with deionized water, and O- and A-horizon porewaters were sampled at 8-72 h intervals. To simulate the effects of a fluctuating water table, cores were drained at the end of the initial flooding event, allowed to dry for 7 d, and subjected to a second flooding event. Porewater analyses included pH, total dissolved mercury (0.45 μm filtered), total dissolved metals (Fe, Mn, Al), anions (Cl^-, NO_3^-, SO_4^{-2}) and cations (Ca^{+2}, Mg^{+2}, K^+, Na^+), dissolved inorganic carbon, and dissolved organic carbon. Additionally, porewater dissolved organic matter was characterized via UV/vis and fluorescence spectroscopy, and fluorescence excitation-emission matrix (EEM) spectra were modeled using parallel factor analysis (PARAFAC).

Results from streambank soil cores show that during initial flooding events, a rapid release (t = 3 d) of dissolved mercury was observed in O-horizon porewaters following inundation, suggesting that the release mechanism is independent of redox-sensitive processes. Conversely, slow mercury release kinetics (t = 14 d) were observed in A-horizon soils, inferring a release mechanism coupled to redox-sensitive processes. This hypothesis was supported by a robust positive relationship between porewater Mn(II) concentrations, which is an indicator for reductive dissolution processes, and dissolved mercury. Mercury release from the O-horizon during the second flooding events was much slower, suggesting that the labile mercury pool was exhausted during the first saturation period. A-horizon soils exhibited similar mercury release trends during second flooding events, signifying that these soils have a mercury pool that is accessible for a longer time under strongly reducing conditions. Mercury release trends were not explained by changes in dissolved organic matter concentration or composition. The effects of saturation events on soil cation exchange capacity were evaluated to identify potential modifications of mineral and/or mineral coating structures. Future objectives are to expand our experimental investigation to soils from the floodplain site, and complement intact core experiments with mercury release batch experiments.

*Student Presenter

Biostimulation at Rifle, CO: Impacts on Aqueous Arsenic Geochemistry

Valerie K. Stucker,* *Colorado School of Mines*; Kenneth H. Williams, *LBNL*; James F. Ranville, *Colorado School of Mines*; Brian Mailloux (PI), *Barnard College*

Biostimulation to reduce aqueous uranium (VI) to immobile uranium (IV) has been the main focus for uranium remediation at the former uranium mill site in Rifle, CO. While this technique has been shown to decrease aqueous uranium concentrations downgradient of acetate injection wells, it has also increased arsenic concentrations from around 1 uM upgradient to 6 uM downgradient. In order to determine the effects of uranium remediation on arsenic chemistry, groundwater samples were collected and preserved for concentration and speciation analysis during the 2009 and 2011 experiments. A Dionex AS/AG-16 column was used to separate arsenic species using a sodium hydroxide gradient eluent. Inductively coupled plasma mass spectrometry was used as an arsenic specific detector and to separately measure total concentrations of arsenic, uranium and other redox sensitive elements. The highest arsenic concentrations observed at the Rifle site were found when the system was in sulfate reduction and the sulfide concentrations were highest. Prior analyses of arsenic speciation focused solely on arsenate, arsenite and methylated species, but more recent research has shown that systems with high sulfide concentrations have additional thiolated arsenic species. Thioarsenates (mono-, di-, tri- and tetra-thio), and specifically trithioarsenate, dominate the arsenic speciation when the concentrations are highest. Stopping biostimulation before sulfate reduction begins could prevent the formation of thioarsenates and high arsenic release. Other uranium remediation techniques such as bicarbonate flushing will also help with uranium remediation without creating a problem with arsenic release.

*Student Presenter

Facilities

EMSL: A DOE Scientific User Facility for Biogeochemical and Subsurface Science Research

Donald Baer (EMSL Chief Scientist), Nancy Hess (Science Lead for Geochemistry/Biogeochemistry and Subsurface Science)—*EMSL*

http://www.emsl.pnl.gov/

To address current and emerging national and DOE challenges, including subsurface contamination from former weapons production activities, long-term underground storage of nuclear waste, and climate change, scientists need to develop credible, predictive models of the impact of biogeochemical processes on contaminants, carbon, and nutrient cycles in subsurface and terrestrial ecosystems. Robust models of subsurface processes are based on understanding the key geochemical and biogeochemical reactions that control the mobility of these elements, cells and other materials. The ability to identify and adequately probe dynamic processes at the molecular scale can provide information needed to accurately simulate these reactions using computational models, thereby leading to the incorporation of the reaction rates and kinetics into reactive flow and transport models. This linking of experimental and theoretical information from the molecular to the field scale requires the integration of diverse experimental and computational techniques and collaboration with experts from multiple disciplines.

EMSL, a DOE scientific user facility in Richland WA, provides both premier experimental tools and high performance computing (HPC) resources and expertise for scientific research and discovery in subsurface biogeochemical research to users free of charge. Three sets of EMSL capabilities are particularly relevant for biogeochemical research: 1) **Next generation imaging and surface characterization experimental capabilities,** 2) **quantitative proteomics/metabolomics platforms and related genome- and epigenome-directed applications,** and 3) **a suite of capabilities to study flow and transport at multiple scales**. The imaging and surface characterization experimental capabilities can be used to provide the spatially resolved elemental analysis, oxidation state determination, chemical speciation, mineral identification, and microbe-mineral associations needed to understand the chemical fate and mobility of contaminants in the biogeochemical environment. The comprehensive quantitative proteomics/metabolomics platforms and related genome- and epigenome-directed applications enable users to unravel the interplay between microbial communities and geochemistry. Capabilities for studying flow and transport from the micron to the intermediate scale are made possible by in-house scientists who assist with all steps of the research process from pre-experiment modeling to hydraulic characterization, analytical chemistry, numerical modeling, and post-process analysis on custom-built flowcells. On-site lithographic fabrication capabilities are available for the creation of custom pore-scale micromodels in a variety of materials.

In 2013, two additional sets of capabilities will be fully available: 1) a new **Radiochemistry Annex** and 2) a **next generation HPC system**. The Radiochemistry Annex will greatly expand the range of experimental capabilities for analysis of environmental samples contaminated with radionuclides. The new facility will have a surface analysis-imaging suite that contains FIB-SEM, TEM-EELS, SPM, XPS and EMP. The magnetic resonance suite will house wide-bore 100 and 750 MHz NMR spectrometers and an EPR spectrometer. EMSL's current HPC system is available to users, but EMSL is in the process of obtaining the next generation HPC system. The next system is likely to be available to users in the Spring of 2013. EMSL scientists continue to collaborate with external user groups to enhance NWChem, EMSL's premier computational modeling code, which is now open source.

A Liquid Sample Interface for Rapid 14C Analysis by Accelerator Mass Spectrometry

T.P. Guilderson (PI), T. Ognibene, A. Thomas, P. Daley, G. Bench—*LLNL*

Current Accelerator Mass Spectrometry (AMS) measurement has typically required that carbon containing materials be converted to graphite for analysis. Considerable human handling is required, and the process suffers from low sample throughput (<100 samples processed per day) and long turnaround times (~2 days) at a current cost of hundreds of dollars per sample. Many users have been slow to adopt AMS because of the high cost and complexity of sample preparation and resulting slow turnaround times for analysis.

A technological need, widely voiced by industrial and academic investigators in recent years, has been for a user-friendlier AMS interface, including far less cumbersome sample preparation. To facilitate sample preparation and reduce analysis times from days to minutes, we have developed an online, directly-coupled, liquid sample interface that allows analysis without first converting a sample to graphite. The liquid sample interface rapidly converts the carbon content of samples suspended or dissolved in a liquid to CO_2 gas and directly transports the gas to a gas-accepting ion source for real-time 14C AMS analysis. This interface eliminates complex and time-consuming human handling of samples and enables direct coupling of an HPLC or other liquid separation technology to the spectrometer for real-time AMS analysis. The ability to handle liquid samples and continuous flows of liquid will enable more widespread and routine use of AMS in biological and environmental applications.

Participants

As of April 18, 2012

Dion Antonopoulos
Argonne National Laboratory

Todd Anderson
U.S. Department of Energy

Elizabeth Armstrong
University of Illinois at Urbana-Champaign

Estella Atekwana
Oklahoma State University

Don Baer
Pacific Northwest National Laboratory

Greg Baker
University of Tennessee

Enrica Balboni
University of Notre Dame

Jill Banfield
University of California, Berkeley

Reema Bansal
Pennsylvania State University

John Bargar
SLAC National Accelerator Laboratory

Mark Barnett
Auburn University

Gideon Bartov
University of Illinois at Urbana-Champaign

Anirban Basu
University of Illinois at Urbana-Champaign

Paul Bayer
U.S. Department of Energy

Udo Becker
University of Michigan

James Begg
Lawrence Livermore National Laboratory

Harry Beller
Lawrence Berkeley National Laboratory

Keaton Belli
Georgia Institute of Technology

Graham Bench
Lawrence Livermore National Laboratory

Rizlan Bernier-Latmani
Ecole Polytechnique Fédérale de Lausanne

Haluk Beyenal
Washington State University

Andrew Binley
Lancaster University

Diane Blake
Tulane University School of Medicine

Joel Blum
University of Michigan

Harvey Bolton
Pacific Northwest National Laboratory

Curt Bolton
U.S. Department of Energy

Maxim Boyanov
Argonne National Laboratory

Robin Brinkmeyer
Texas A&M University

Eoin Brodie
Lawrence Berkeley National Laboratory

Scott Brooks
Oak Ridge National Laboratory

Peter Burns
University of Notre Dame

Liz Butler
University of Oklahoma

Andres Campiglia
University of Central Florida

Cindy Castelle
Lawrence Berkeley National Laboratory

Jeff Catalano
Washington University in St. Louis

Jose Cerrato
Washington University in St. Louis

Skip Chamberlain
U.S. Department of Energy

Clara Chan
University of Delaware

Jinsong Chen
Lawrence Berkeley National Laboratory

Xingyuan Chen
Pacific Northwest National Laboratory

Jon Chorover
University of Arizona

John Christensen
Lawrence Berkeley National Laboratory

Dena Cologgi
Michigan State University

Matt Colombo
Rutgers University

Rick Colwell
Oregon State University

Luis R. Comolli
Lawrence Berkeley National Laboratory

Mark Conrad
Lawrence Berkeley National Laboratory

Craig Criddle
Stanford University

Gary Curtis
U.S. Geological Survey

Frederick Day-Lewis
U.S. Geological Survey

Participants

Evan DeLucia
University of Illinois at Urbana-Champaign

Hailiang Dong
Miami University

Wenming Dong
Lawrence Berkeley National Laboratory

Dwayne Elias
Oak Ridge National Laboratory

Shanna Estes
Clemson University

Toby Ewing
Iowa State University

Jeremy Fein
University of Notre Dame

Andy Felmy
Pacific Northwest National Laboratory

Scott Fendorf
Stanford University

Sandra Fernando
University of Michigan

Matthew Fields
Montana State University

Mary Firestone
University of California, Berkeley

Jim Fredrickson
Pacific Northwest National Laboratory

Mark Freshley
Pacific Northwest National Laboratory

Tsigabu Gebrehiwet
University of Idaho-Idaho Falls

Gary Geernaert
U.S. Department of Energy

Franz Geiger
Northwestern University

Kurt Gerdes
U.S. Department of Energy

Robin Gerlach
Montana State University

Dan Giammar
Washington University in St. Louis

Yuri Gorby
University of Southern California

Robin Graham
Argonne National Laboratory

Susan Gregurick
U.S. Department of Energy

April Gu
Northeastern University

Baohua Gu
Oak Ridge National Laboratory

Thomas Guilderson
Lawrence Livermore National Laboratory

Hao-Bo Guo
Oak Ridge National Laboratory

Hong Guo
University of Tennessee, Knoxville

Juyoung Ha
Rutgers University

Brian Haliena
Auburn University Graduate Student

Glenn Hammond
Pacific Northwest National Laboratory

Kim Hayes
University of Michigan

Terry Hazen
University of Tennessee and Oak Ridge National Laboratory

Feng He
Oak Ridge National Laboratory

Florencio Hernandez
University of Central Florida

Nancy Hess
Pacific Northwest National Laboratory

Bob Hettich
Oak Ridge National Laboratory

Helen Hsu-Kim
Duke University

Max Hu
The University of Texas, Arlington

Susan Hubbard
Lawrence Berkeley National Laboratory

Kim Hayes
University of Michigan

David Hyndman
Michigan State University

Gary Jacobs
Oak Ridge National Laboratory

Peter Jaffe
Princeton University

Danielle Jansik
Pacific Northwest National Laboratory

Qusheng Jin
University of Oregon

Tim Johnson
Pacific Northwest National Laboratory

Tom Johnson
University of Illinois at Urbana-Champaign

David Johnston
Harvard University

Alexander Johs
Oak Ridge National Laboratory

Morris Jones
Stanford University

Ram Kannappan
U.S. Geological Survey

Daniel Kaplan
Savannah River National Laboratory

Kristina Keating
Rutgers University, Newark

Lisa Kelly
Lawrence Berkeley National Laboratory

Ken Kemner
Argonne National Laboratory

Timothy C. Kenna
Lamont-Doherty Earth Observatory of Columbia University

Annie Kersting
Lawrence Livermore National Laboratory

Allan Konopka
Pacific Northwest National Laboratory

Carla Koretsky
Western Michigan University

Joel Kostka
Georgia Institute of Technology

Kate Kucharzyk
Duke University

Randall Laviolette
ASCR, U.S. Department of Energy

Hope Lee
Pacific Northwest National Laboratory

David Lesmes
U.S. Department of Energy

Juan Lezama Pacheco
SLAC National Accelerator Laboratory

Li Li
Pennsylvania State University

Hsiu-Ping Li
Texas A&M University at Galveston

Yueyun Li
Northeastern University

Liyuan Liang
Oak Ridge National Laboratory

Mary Lipton
Pacific Northwest National Laboratory

Chongxuan Liu
Pacific Northwest National Laboratory

Frank Loeffler
University of Tennessee
and Oak Ridge National Laboratory

Vijay Loganathan
Oak Ridge National Laboratory

Phil Long
Lawrence Berkeley National Laboratory

Derek Lovley
University of Massachusetts

Yi Lu
University of Illinois at Urbana-Champaign

Dan Lu
Florida State University

Craig Lundstrom
University of Illinois at Urbana-Champaign

Krishna Mahadevan
University of Toronto

Fabien Maillot
Washington University in St. Louis

Brian Mailloux
Barnard College

Terence Marsh
Michigan State University

Matthew Marshall
Pacific Northwest National Laboratory

Sheryl Martin
Oak Ridge National Laboratory

Robert Martinez
University of Alabama

Chris Marx
Harvard University

Harris Mason
Lawrence Livermore National Laboratory

Melanie Mayes
Oak Ridge National Laboratory

David Mays
University of Colorado, Denver

James McKinley
Pacific Northwest National Laboratory

Vrajesh Mehta
Washington University in St Louis

Barbara Methe
J. Craig Venter Institute

Philip Meyer
Pacific Northwest National Laboratory

Marc Michel
SLAC/Stanford University

Susan Miller
University of California, San Francisco

Carrie Miller
Oak Ridge National Laboratory

Richard Mills
Oak Ridge National Laboratory
and University of Tennessee

Bhoopesh Mishra
Illinois Institute of Technology

Sergi Molins
Lawrence Berkeley National Laboratory

Francois Morel
Princeton University

Jessica Morrison
University of Notre Dame

Duane Moser
Desert Research Institute

Stephen Moysey
Clemson University

Karl Mueller
Pacific Northwest National Laboratory

Chris Murray
Pacific Northwest National Laboratory

Satish Myneni
Princeton University

Kathryn Nagy
University of Illinois at Chicago

Anke Neumann
The University of Iowa

Thomas Nicholson
U.S. Nuclear Regulatory Commission

Peter Nico
Lawrence Berkeley National Laboratory

Peggy O'Day
University of California, Merced

Edward O'Loughlin
Argonne National Laboratory

Tullis Onstott
Princeton University

Jerry Parks
Oak Ridge National Laboratory

Catherine Peters
Princeton University

Susan Pfiffner
University of Tennessee

Elizabeth Phillips
U.S. Department of Energy

Eric Pierce
Oak Ridge National Laboratory

Brett Poulin
University of Colorado, Boulder

Brian Powell
Clemson University

Amy Pruden
Virginia Tech

Nik Qafoku
Pacific Northwest National Laboratory

Harihar Rajaram
University of Colorado, Boulder

George Redden
Idaho National Laboratory

Gemma Reguera
Michigan State University

Andre Revil
Colorado School of Mines

Participants

Demian Riccardi
University of Tennessee, Knoxville

David Richardson
University of East Anglia

William Riley
Lawrence Berkeley National Laboratory

Eric Roden
University of Wisconsin

Derrick Rodriguez
Colorado School of Mines

Kevin Rosso
Pacific Northwest National Laboratory

Eric Roth
University of Colorado, Denver

Joe Ryan
University of Colorado, Boulder

Kathleen Salome
Georgia Institute of Technology

Robert Sanford
University of Illinois at Urbana-Champaign

Peter H. Santschi
Texas A&M University at Galveston

Kaye Savage
Wofford College

Christopher Schadt
Oak Ridge National Laboratory

Jeffra Schaefer
Princeton University

Tim Scheibe
Pacific Northwest National Laboratory

Michelle Scherer
University of Iowa

Kathy Schwehr
Texas A&M University

Paul Shao
Ecole Polytechnic Federale de Lausanne

Jonathan (Josh) Sharp
Colorado School of Mines

Henry Shaw
Lawrence Livermore National Laboratory

Liang Shi
Pacific Northwest National Laboratory

Alyssa Shiel
University of Illinois at Urbana-Champaign

David Shuh
Lawrence Berkeley National Laboratory

David Singer
Lawrence Berkeley National Laboratory

Gargi Singh
Virginia Tech

Kamini Singha
Pennsylvania State University

Karen Skubal
U.S. Department of Energy

Jeremy Smith
Oak Ridge National Laboratory

Patricia Sobecky
University of Alabama

Eric Sonnenthal
Lawrence Berkeley National Laboratory

Carl Steefel
Lawrence Berkeley National Laboratory

James Stegen
Pacific Northwest National Laboratory

Dan Stover
U.S. Department of Energy

Valerie Stucker
Colorado School of Mines

Anne Summers
University of Georgia

Ryan Swanson
Pennsylvania State University

Jim Szecsody
Pacific Northwest National Laboratory

Martial Taillefert
Georgia Institute of Technology

Guoping Tang
Oak Ridge National Laboratory

Brad Tebo
Oregon Health and Science University

Michael Thompson
U.S. Department of Energy

Ming Tien
Pennsylvania State University

Tetsu Tokunaga
Lawrence Berkeley National Laboratory

Paul Tratnyek
Oregon Health and Science University

Wooyong Um
Pacific Northwest National Laboratory

Al Valocchi
University of Illinois at Urbana-Champaign

Philippe van Cappellen
University of Waterloo

Ravi Vannela
Arizona State University

Madeline Vargas
College of the Holy Cross
University of Massachusetts

Roelof Versteeg
Sky Research

Haruko Wainwright
Lawrence Berkeley National Laboratory

Judy Wall
University of Missouri

Jiamin Wan
Lawrence Berkeley National Laboratory

Kai-tak Wan
Northeastern University

Xin Wang
Northeastern University

Scott Wankel
Woods Hole Oceanographic Institution

David Watson
Oak Ridge National Laboratory

Karrie Weber
University of Nebraska, Lincoln

Dawn Wellman
Pacific Northwest National Laboratory

Mike Wilkins
Pacific Northwest National Laboratory

Ken Williams
Lawrence Berkeley National Laboratory

Mark Williamson
U.S. Department of Energy

Jennifer Wong
Clemson University

Nick Woodward
U.S. Department of Energy

Kelly Wrighton
University of California, Berkeley

Weimin Wu
Stanford University

Ernest Wylie
University of Notre Dame

Huifang Xu
University of Wiscosnsin, Madison

Qin Xu
University of Tennessee and
Oak Ridge National Laboratory

Chen Xu
Texas A&M University at Galveston

Steve Yabusaki
Pacific Northwest National Laboratory

Fan Yang
Michigan State University

Yu Yang
University of Notre Dame

Ming Ye
Florida State University

Chris Yeager
Los Alamos National Laboratory

Nathan Yee
Rutgers University

John Zachara
Pacific Northwest National Laboratory

Mavrik Zavarin
Lawrence Livermore National
Laboratory

Tong Zhang
Duke University

Saijin Zhang
Texas A&M University at Galveston

Jiao Zhao
University of Toronto

Chen Zhou
Arizona State University

Jizhong Zhou
University of Oklahoma

Ming Zhu
U.S. Department of Energy

Author Index

Indexed by Page Number

A

Agarwal, Reema Bansal 64
Aiken, George R. 42, 159
Ajo-Franklin, Jonathan 38, 116
Albrecht-Schmitt, T. 3
Alessi, Daniel S. 144, 145, 146
Alexandrov, V. 55
Anderson, Brian J. 2
Anitori, R. 65
Antonopoulos, D. 103, 105, 107
Anwar, R. 54
Arai, Yuji 46, 155
Arenholz, E. 139
Artsimovitch, I. 60
Ashner, Mathew N. 146
Asta, Maria Pilar 43
Atekwana, Estella A. 1

B

Baars, O. 54
Baer, Donald 161
Baker, Greg S. 85, 86, 89, 93
Balboni, Enrica 7
Banfield, Jillian F. 2, 94, 97, 101
Bargar, John R. 13, 14, 20, 56, 62, 96, 97, 143, 144, 145, 146, 147
Barger, M. 55
Barkay, Tamar 60, 154
Barlett, Melissa 31
Barnett, M.O. 3, 53
Bartov, G. 151
Basu, A. 30
Bea, S.A. 114, 117
Beard, B. 55
Becker, U. 46
Begg, J.D. 124, 125, 126
Belchik, S.M. 149
Beller, Harry R. 43, 111, 116, 119, 120
Belli, Keaton 152
Bench, G. 162
Bender, Kelly S. 68
Benzine, J. 140
Berman, Elena 98
Bernier-Latmani, Rizlan 62, 143, 144, 145, 146
Beyenal, Haluk 4, 149
Bi, Yuqiang 153
Bill, Markus 119, 121
Binley, Andrew 73
Bishop, Michael 6
Bi, Yuqiang 20
Bjornstad, B.N. 83
Blum, Joel D. 5, 60, 132
Bott, Y. 99
Bowden, M. 139
Boyanov, Maxim I. 4, 30, 55, 86, 103, 104, 105, 106, 107, 139
Brandt, Craig C. 86, 127, 128, 130
Brantley, Susan 64
Bridou, Romain 131
Brinkmeyer, R. 51
Brodie, Eoin L. 15, 111, 116, 119
Brooks, Scott C. 9, 85, 86, 87, 89, 90, 91, 92, 93, 104, 105, 127, 128, 129
Brown Jr., G.E. 14, 143, 147
Brown, Roslyn N. 4
Brown, S. 127
Brown, Steven D. 130, 131
Bruckner, J.C. 39
Brulc, J. 103, 107
Buck, E. 139
Burgos, William D. 6
Burns, Peter C. 7
Butler, E. 8
Butt, Julea N. 141
Byrne-Bailey, Kathy 141

C

Cabaniss, Kevin 11
Campiglia, A.D. 9
Cao, B. 149
Cao, Bin 4
Carpenter, E. 105
Carpenter, Julian 20
Carroll, S.A. 123, 124
Carroll, S.L. 90
Castelle, Cindy J. 2
Castille, C.J. 101
Catalano, J.G. 10
Celia, M.A. 44
Cerrato, Jose M. 144, 146
Chakraborty, R. 116
Chan, Clara 11
Chang, H.S. 24
Chemnasiry, W. 9
Chen, J. 112, 116, 117
Chen, L. 8
Chen, R. 40
Chen, X. 77, 78, 136
Chorover, Jon 12
Chourey, K. 45
Christensen, John N. 83, 116, 119, 121
Cismasu, A.C. 147
Clarke, Thomas 141
Clifford, Jeremy 73
Coates, John 141
Cologgi, Dena L. 48
Colombo, Matthew 154
Comolli, Luis R. 2, 97, 145
Conrad, Mark E. 113, 115
Conrad, Mark S. 39, 83, 98, 116, 119, 121
Conroy, N. 125
Converse, B. 50, 140
Criddle, Craig S. 13, 86, 104, 105
Csencsits, Roseann 2
Curtis, Gary P. 71, 72, 157
Czerwinski, K. 39

D

Dafflon, Baptiste 58, 98
Dai, Z. 124
Daley, P. 162
Daly, Rebecca A. 15
Davis, James A. 20, 72, 95, 96, 97, 114, 116, 122, 142, 144
Day-Lewis, Frederick D. 72, 73
Dean, D. 40
Delwiche, M. 58
Demers, J. 5
Demers, Jason 132
Deng, Ye 70
Denham, M. 116, 121
DePaolo, Donald J. 115, 116
Deshusses, M.A. 22, 150
Detwiler, Russell 47
Diaz, C. 9
Diaz, V. 9
DiChristina, Thomas 152
DiDonato, Nicole 52
Dixon, Paul 74
Dohnalkova, Alice C. 141, 149
Doktycz, C.M. 90
Dong, Hailiang 6

Dong, Wenming 116, 121, 122
Draper, K. 99
Drennan, D. 56
Druhan, Jennifer L. 98, 113, 115
Du, X. 13
Dyer, Jim 128

E

Earles, J. 92, 93
Edmunds, M. 85
Edwards, Marcus 141
Elias, Dwayne A. 90, 127, 130, 131
Emerson, H. 46
Estera, Katerina 15
Estes, Shanna L. 46, 155
Ewing, Robert P. 23
Ewing, Rodney C. 46, 155

F

Fakra, Sirine C. 2, 97
Fan, D. 65
Fang, Yilin 31, 102
Faybishenko, B. 111, 116
Fein, J. 41
Felmy, A. 139, 142
Fendorf, S.E. 13, 14, 143
Fernando, S. 46
Fields, M.W. 18, 156
Figueroa, Linda 37
Findlay, R. 50
Finneran, Kevin T. 16
Finsterle, Stefan A. 74
Firestone, Mary K. 15
Fisher, J.C. 39
Flach, Gregory 74
Flanagan, Kelly 32
Flury, Markus 17
Flynn, T. 105, 107
Fox, Don 108, 109, 110
Fox, Patricia M. 95, 96, 97, 122, 144
Franco, L.C. 156
Fredrickson, James K. 4, 83, 105, 136, 140, 141, 142
Freedman, Vicky L. 74
Freshley, Mark D. 74, 82, 83
Frischkorn, Kyle R. 2
Fritz, B.G. 82
Fujita, Yoshiko 58, 108, 109, 110, 116

G

Gallagher, A.K. 72
Gartman, Brandy 21, 99
Gasperikova, E. 85
Gebrehiwet, T. 58, 108, 109
Gee, Glendon 17
Giammar, Daniel E. 10, 62, 143, 144, 146
Gihring, T.M. 90
Gilbert, Benjamin 38
Gilchrist, A. 28
Gilmour, Cynthia C. 127, 131
Giloteaux, Ludovic 33
Ginn, T.R. 58
Giometti, C. 105
Glasser, Paul 6
Gorby, Y.A. 18, 156
Gorton, Ian 74
Graham, Andrew M. 131
Green, Stefan J. 87
Greenwood, J. 99
Greenwood, W. 79
Greskowiak, Janek 95
Gross, J.D. 60
Gu, April Z. 19
Gu, Baohua 5, 54, 60, 86, 89, 127, 132, 133
Guo, H. 57, 60
Guo, H.-B. 134, 135
Guo, Hua 96, 122
Guilderson, T.P. 162
Guo, Luanjing 108, 109, 110
Gupta, Manish 98

H

Ha, Juyoung 154
Haggerty, Roy 73, 83
Hammond, G. 77, 78, 83, 142
Han, Ruyang 111, 119
Handley, Kim M. 97, 144
Hansel, Colleen M. 8, 67
Hao, N. 40
Harley, S. 123
Harsh, Jim 17
Hatcher, Patrick G. 52
Hay, M. 72
Hay, Michael B. 95
Hayes, Kim 153
Hayes, Kim F. 20, 96
He, Feng 5, 127, 132, 133
He, Zhili 15, 70
Heald, S. 139
Heider, E.C. 9
Helmus, Ruth A. 64
Henriksen, J.R. 58, 108, 109
Hernandez, F.E. 9
Herron, M.M. 27
Herr, S. 46
Hess, Nancy 161
Hettich, R.L. 45, 97, 101
Hill, E.A. 149
Hixon, A. 46
Hochella Jr., Michael F. 21
Hollenback, S. 56
Holmes, Dawn E. 33
Hong, L. 135
Howe, J. 93
Hsu-Kim, H. 22, 150
Hu, Bill 80
Hu, Haiyan 133
Hu, Qinhong 23
Huang, Hai 108, 109, 110
Huang, P. 123, 124
Hubbard, Susan S. 49, 58, 74, 85, 86, 89, 93, 98, 112, 114, 116, 117, 121
Hunt, J. 116
Hurt, Richard A. 130, 131
Hyun, Sung Pil 20, 96

I

Ihms, Hannah E. 35
Isern, Nancy G. 4
Istok, J. 116

J

Jaffe, P.R. 24, 25, 97
Janot, Noemie 144, 145
Jansik, D. 65
Jasrotia, Puja 87, 89
Jin, Q. 50
Johnson, C. 55
Johnson, M.K. 61
Johnson, Timothy C. 73, 79, 83, 109, 110
Johnson, Tom M. 30, 36, 151, 154
Johnston, David T. 67
Johnston, E. 103, 107
Johs, A. 57, 127, 134, 135
Jones, K.W. 44
Jones, M. 14
Jung, Hun-Bok 69

K

Kanematsu, Masa 12
Kaplan, D.I. 24, 46, 51
Karaoulis, M. 49
Karaoz, U. 111
Kearney, K. 42
Keating, Kristina 26, 40, 73
Keimowitz, Alison Spodek 37

Kelly, Shelly 48
Kemner, Kenneth M. 4, 6, 30, 55, 69, 86, 89, 103, 104, 105, 106, 107, 139, 142
Kenna, T.C. 27
Kennedy, David W. 4, 136, 141
Kent, Douglas 80, 83
Kerkhof, L. 25
Kerley, M.K. 90
Kersting, A.B. 123, 124, 125, 126
Kim, Yongman 15
Kips, R. 124
Kocman, David 128, 129
Kohler, M. 72
Konishi, Hiromi 69
Konopka, A.E. 83, 136, 137, 142
Koretsky, C.M. 28
Koster van Groos, P. 24
Kostka, Joel E. 86, 87, 89, 90, 93
Kowalsky, M.B. 112, 116
Krumholz, L. 8
Kucek, L.A. 149
Kucharzyk, K.H. 22, 150
Kukkadapu, Ravi K. 14, 20, 21, 96
Kumar, Jitendra 88
Kwon, M.J. 103, 107

L

Lampa-Pastirk, Sanela 48
Landis, Rich 128
Lane Jr., John W. 72, 73
Larsen, Joern 119
Latta, D. 104, 105, 139
Laubach, P. 36
LaVoie, S. 61
Layton, A. 45
Lee, S.-W. 62
Lei, Tim C. 38
Lezama, J. 14
Lezama-Pacheco, Juan S. 62, 144, 145, 146, 147
Li, B. 13
Li, D. 24
Li, H-P. 51
Li, Li 29, 112, 116
Li, X. 137
Li, YueYun 19
Li, Yusong 68
Liang, Liyuan 54, 57, 60, 127, 132, 133, 134, 135
Lichtner, Peter C. 17, 83, 88
Lim, HsiaoChien 15, 111
Lin, Chaofeng 11
Lin, X. 136
Lindquist, W.B. 44
Lipton, Mary S. 2, 4, 61, 97, 101
Liu, Chongxuan 80, 83, 142
Liu, Juan 139, 141
Liu, W-T. 66
Liu, X. 45
Liu, Y. 150
Löffler, F.E. 30, 45, 104, 105
Loganathan, Vijay A. 75
Lollar, B. Sherwood 39
Long, Philip E. 21, 25, 36, 62, 84, 95, 97, 98, 100, 101, 102, 103, 107, 144, 145, 147
Lovley, Derek R. 31, 32, 33, 34, 97, 102
Lowe, K. 13, 85, 93, 104
Lu, C. 108
Lu, Dan 157
Lu, Yi 35
Luan, Fubo 6
Luef, Birgit 2, 97
Lukens, Wayne W. 113
Lund, Rachael M. 81, 137
Lundstrom, C.C. 30, 36

M

Ma, Eugene 31
Mackley, R.D. 82
MacLeod, A. 28
Madden, A. 8
Mahadevan, Radhakrishnan 31, 102
Maillot, F. 10
Mailloux, Brian J. 37, 160
Majors, Paul D. 4, 80
Malvankar, Nikhil S. 32
Manceau, A. 42
Marshall, Matthew J. 4, 149
Marsh, Terence L. 63, 70, 103, 104, 105
Mason, H. 123, 124
Massey, M. 14
Mattson, Earl 17
Maxwell, R. 123, 124
Mayes, Melanie A. 75
Mays, David C. 38
McCormick, M. 103, 105, 107
McGuinness, L. 25
McIlwain, M. 109
McKinley, James P. 65, 81, 82, 83, 137, 139, 142
McLean, Jeffrey S. 4
Mehlhorn, T.L. 13, 85, 90, 104
Mehta, Vrajesh 10, 146, 158
Merryfield, J.R. 30, 90
Meyer, F. 103
Meyer, Philip D. 71, 157
Michel, F.M. 147
Miller, Carrie 127, 128, 129
Miller, C.S. 101
Miller, Micah D. 81, 137
Miller, S.M. 57, 60, 61, 127, 135
Miller, T. 46
Mills, Richard T. 88
Mishra, Bhoopesh 4, 41, 104, 105, 106
Moberly, James G. 130
Molins, Sergi 118, 119, 120
Momany, C. 60
Moore, A.F. 9
Moore, D. 139
Morel, F.M.M. 54
Morris, A. 150
Morrison, Jessica M. 7
Moser, D.P. 39
Moses, B. 116
Moulton, J. David 74
Mouser, Paula J. 100
Moysey, S. 40
Mueller, Karl 12
Mueller, M. 104
Muftu, Sinan 19
Mukhopadyay, S. 114
Mullin, Sean W. A. 2
Murray, Christopher J. 77, 81, 83, 97, 99, 136, 137, 142
Myneni, S.C.B. 41

N

Nagy, Kathryn L. 42, 159
Nakshatrala, K. 66
Nauss, R. 135
Neumann, A. 55
Nevin, Kelly P. 34
Newcomer, D. 99
Nico, Peter S. 14, 116, 119
Nissen, S. 45
Ntarlagiannis, D. 26, 40

O

O'Day, Peggy A. 12, 43
Ognibene, T. 162
Ohl, M. 135
Olliff, L. 61, 134, 135
O'Loughlin, Edward J. 55, 103, 104, 105, 106, 107
Ong, J.B. 72
Onstott, T.C. 39
Oostrom, M. 66

Orellana, Roberto 34

P

Palumbo, Anthony V. 130, 131
Pan, Don 68
Parker, Jack C. 86, 91
Parker, K.R. 82
Parks, J.M. 57, 127, 135
Pasakarnis, Timothy 106
Paša-Tolić, Ljiljana 100
Patel, Pranav 32
Patrauchan, Mariana 1
Peacock, A.D. 24, 25
Pearce, C. 139, 142
Pennell, K. 30
Percak-Dennett, E. 140
Perdrial, Nico 12
Peters, C.A. 44
Peterson, John 58, 93, 98
Pfiffner, S.M. 45
Phillips, D. 93
Plathe, K.L. 62
Plymale, A. 140
Podar, Mircea 127, 130, 131
Polacco, B. 61
Poulin, Brett A. 42, 159
Poweleit, Eric 12
Powell, Brian A. 46, 124, 125, 155
Prakash, Om 87
Pratt, L.M. 39
Pruden, Amy 21
Purvine, S.O. 61

Q

Qafoku, Nikolla P. 21, 99
Qafoku, O. 139
Qian, Yun 128, 129, 132
Qin, Yujia 70

R

Rajaram, Harihar 47
Ranville, James F. 37, 160
Rao, Balaji 132, 133
Redden, George 108, 109, 110
Reed, S. 140
Reguera, Gemma 48
Reich, T.J. 28
Reinfelder, John 154
Resch, Thomas C. 81, 137, 139
Revil, Andre 1, 49, 109
Riccardi, D. 57, 135
Richardson, David J. 138, 141, 142
Riquelme Breazeal, Maria V. 21
Riscassi, Ami 128, 129
Rishishwar, Lavanya 87
Ritalahti, K. 30, 45
Rittmann, Bruce E. 20
Roberts, K.A. 51
Rockhold, M.L. 44, 79, 83, 136
Roden, Eric E. 50, 69, 140, 142
Rodriguez, D. 71, 72
Romine, Margaret F. 4
Rosso, Kevin M. 55, 139, 141, 142
Roth, Eric J. 38
Rubin, Y. 83
Russell, C. 39
Ryan, Joseph N. 42, 159

S

Saiers, J. 3
Sanford, R.A. 30, 36, 66, 104, 105
Santschi, Peter H. 51, 52
Sassen, D.S. 117
Savage, K. 53
Sayler, G. 45
Schadt, Chris W. 86, 87, 89, 90, 91, 93
Schaefer, J.K. 54
Schaef, T. 139
Scheckel, K. 24
Scheibe, Timothy 31, 102, 142
Scherer, Michelle M. 55, 104, 105, 106
Schwehr, Kathleen A. 51, 52
Scott, R.A. 60, 61
Segre, C. 105
Shah, M. 45
Shang, Jianying 80
Shao, Paul P. 145
Sharma, Manju L. 32
Sharon, I. 101
Sharp, J.O. 56
Sharp, M. 134, 135
Shelobolina, E. 50, 140
Shi, JiaYi 19
Shi, Liang 4, 135, 139, 140, 141, 142
Shi, Zhi 80, 141
Shibata, Tomohiro 155
Shiel, A.E. 36
Sholto-Douglas, D. 103
Shuh, D. 3
Silberman, Jeffrey D. 33
Silin, D.B. 116, 118
Silverman, D. 56
Simpkins, L. 125
Singer, David M. 96
Singer, Steven W. 2
Singha, Kamini 73
Singh, Andrea 94
Singh, Gargi 21
Skinner, K. 103, 104, 107
Skold, M. 49
Slater, Lee 26, 79, 109, 110
Smith, Donald 100
Smith, J.C. 57, 60, 127, 134, 135
Smith, R. 109
Smith, R.W. 58
Smith, Steven D. 131
Sonnenthal, E.L. 116, 120
Speers, Allison M. 48
Spycher, N. 49, 114, 116
Stallings, K. 42
Stanford U. 13, 14, 86, 89, 91, 104, 105, 143, 147
Steefel, Carl I. 12, 43, 74, 112, 114, 115, 116, 119, 120
Stegen, J.C. 136
Stoliker, Deborah 80
Storniolo, R. 93
Strathmann, Timothy 16
Stroud, R. 60
Stubbs, J.E. 144
Stucker, Valerie K. 37, 160
Stylo, G.M. 144
Stylo, Malgorzata 145
Summers, A.O. 57, 60, 61, 127, 134, 135
Suvorova, E.I. 144
Swanson, Ryan D. 73
Szecsody, J. 65

T

Taillefert, Martial 152
Tan, H. 25
Tan, Zheng Huan 68
Tang, Guoping 75, 89, 91, 92
Tang, Yuanzhi 67
Tartakovsky, A. 31, 108, 109
Tartakovsky, G. 31
Taylor, J.L. 58
Tebo, B.M. 62, 65
Thomas, A. 162
Thomas, Brian C. 94, 101
Thompson, K.M. 83
Tiedje, James M. 63, 70
Tien, Ming 64
Tinnacher, R. 124, 125
Tokunaga, Tetsu K. 15, 116, 121, 122
Tomanicek, S.J. 57, 134, 135
Traina, Samuel 43
Tratnyek, P. 65
Tremblay, Pier-Luc 32

Trieu, K. 9
Tumey, S.J. 124, 126

U

Ueda, Ken-ichi 94
Ulrich, Craig 93, 98
Um, W. 44
Um, Wooyong 12

V

Valocchi, A.J. 66
Van Cappellen, Philippe 152
Vannela, Raveender 20
Van Nostrand, Joy D. 70
Varadharajan, Charuleka 119
Vargas, Madeline 32
Veeramani, Harish 21
VerBerkmoes, N.C. 97, 101
Vermeul, Vince R. 81, 82, 83
Versteeg, R.J. 79, 83, 84
Vishnivetskaya, Tatiana A. 45, 130

W

Wainwright, H.M. 114, 117
Wallin, E. 79
Wall, Judy D. 127, 131
Walshe, G. 30
Wan, Jiamin 15, 116, 121, 122
Wan, KaiTak 19
Wang, Guohui 12
Wang, Li 29
Wang, Xin 19
Wang, Zheming 10, 141
Wang, Zimeng 62, 146
Wankel, Scott D. 67
Wanner, C. 120
Ward, A. 27
Watson, David B. 13, 49, 85, 86, 87, 89, 90, 91, 92, 93, 104
Webb, S.M. 56
Weber, Karrie A. 68
Werth, Charles 16
Werth, C.J. 66
White, Gaye 141
Wilkins, Michael J. 2, 33, 97, 100, 101, 102, 142
Williams, Kenneth H. 11, 25, 26, 33, 34, 36, 37, 62, 95, 97, 98, 100, 101, 103, 107, 112, 113, 115, 116, 144, 147, 160
Williams, R. 124
Wong, J. 124, 125
Wood, B. 142
Wrighton, Kelly C. 2, 33, 94, 97, 101
Wu, H. 112
Wu, L. 55
Wu, Liyou 70
Wu, T. 50
Wu, W. 105
Wu, Wei-Min 13, 86, 89, 91, 104
Wu, Y. 49, 116
Wylie, Ernest M. 7
Wyman, D. 28

X

Xiang, Yu 35
Xie, Y. 46
Xiong, Yijia 4
Xu, Chen 51, 52
Xu, Huifang 69
Xu, Q. 57

Y

Yabusaki, Steve 71, 97, 99, 102, 157
Yang, F. 63, 104
Yang, L. 111, 116
Yang, Li 119
Yang, Z.K. 90
Ye, Ming 71, 157
Yeager, C. 51
Yee, Nathan 154
Yin, Xiangping 128, 129, 132
Young, S. 39

Z

Zachara, John M. 12, 75, 77, 78, 79, 80, 81, 82, 83, 84, 105, 137, 141, 142
Zavarin, M. 39, 123, 124, 125, 126
Zhang, Changyong 66, 80
Zhang, Chi 109, 110
Zhang, Fan 86
Zhang, Fred 17
Zhang, J. 46
Zhang, Jiaming 155
Zhang, Ping 15, 70
Zhang, S. 51
Zhang, T. 13, 22, 150
Zhang, Xiaoying 80
Zhao, Jiao 31
Zhao, P. 124, 125, 126
Zheng, C. 83
Zheng, Wang 5, 132, 133
Zhou, Chen 20
Zhou, Jizhong 13, 15, 63, 70, 86
Zhou, Peng 43
Zhuang, Kai 31
Zhu, Wenyi 53
Zimmerman, Trevor 86, 89, 125
Zink, E.M. 61

Institutional Index

Indexed by Page Number

Institutions determined by affiliations provided by authors

Argonne National Laboratory (ANL) 4, 6, 30, 41, 55, 69, 86, 89, 103, 104, 105, 106, 107, 139, 142, 155
Auburn University 3, 53
Barnard College 37, 160
Brookhaven National Laboratory (BNL) 44
Centre National de la Recherche Scientifique (CNRS) 42
Clemson University 16, 40, 46, 124, 125, 155
College of the Holy Cross 32
Colorado School of Mines 1, 37, 49, 56, 71, 72, 109, 160
Desert Research Institute 39
DOE-RL 83
Duke University 22, 150
DuPont 128
École Polytechnique Fédérale de Lausanne (ÉPFL) 62, 143, 144, 145, 146
Environmental Molecular Sciences Laboratory (EMSL) 21, 61, 100, 161
ESS Sweden 134, 135
EXAFS Analysis 48
Florida State University 71, 80, 86, 87, 157
FZ Jülich 135
Georgia Institute of Technology 87, 89, 90, 93, 152
Hamilton College 103, 105, 107
Harvard University 8, 67
Idaho National Laboratory (INL) 17, 58, 108, 109, 110, 116
Illinois Institute of Technology 105, 106, 155
Indiana University 39
Iowa State University 23
J. Craig Venter Institute 4
Lamont-Doherty Earth Observatory 27
Lancaster University 73
Lawrence Berkeley National Laboratory (LBNL) 2, 3, 11, 12, 14, 15, 21, 25, 26, 33, 34, 36, 37, 38, 39, 43, 49, 58, 62, 72, 74, 83, 85, 86, 89, 93, 95, 96, 97, 98, 100, 101, 102, 103, 107, 111, 112, 113, 114, 115, 116, 117, 118, 119, 120, 121, 122, 139, 142, 144, 145, 147, 160
Lawrence Livermore National Laboratory (LLNL) 123, 124, 125, 126, 162
Los Alamos National Laboratory (LANL) 17, 51, 74, 83, 88
Los Gatos Research, Inc. 98
Miami University 6
Michigan State University 48, 63, 70, 90, 103, 104, 105
Microbial Insights 24, 25
Montana State University 18, 156
Nanyang Technological University 149
Northeastern University 19
Oak Ridge National Laboratory (ORNL) 5, 9, 13, 30, 45, 49, 54, 57, 60, 75, 85, 86, 87, 88, 89, 90, 91, 92, 93, 97, 101, 104, 105, 127, 128, 129, 130, 131, 132, 133, 134, 135
Ohio State University 60, 100
Oklahoma State University 1, 116
Old Dominion University 52
Oregon Health and Science University (OHSU) 62, 65
Oregon State University 73, 83, 142
Pacific Northwest National Laboratory (PNNL) 2, 4, 10, 12, 14, 17, 21, 27, 31, 33, 44, 55, 61, 65, 66, 71, 73, 74, 75, 77, 78, 79, 80, 81, 82, 83, 96, 97, 99, 100, 101, 102, 105, 108, 109, 110, 135, 136, 137, 139, 140, 141, 142, 149, 157
Pennsylvania State University (Penn State) 6, 12, 29, 64, 73, 112, 116
Princeton University 24, 25, 39, 41, 44, 54
Queens University 93
Rutgers-Newark University 26, 40, 109
Rutgers University 60, 73, 79, 110, 154
Savannah River National Laboratory (SRNL) 24, 46, 51, 74, 116, 121
Sky Research 79, 83, 84
SLAC National Accelerator Laboratory 13, 62, 143, 144, 145, 146, 147
Smithsonian Environmental Research Center 127, 131
Southern Illinois University 68
Stanford Synchrotron Radiation Lightsource (SSRL) 14, 56, 96, 97
State University of New York (SUNY), Stony Brook 44
Texas A&M University at Galveston (TAMUG) 51, 52
Tufts University 30
Université Joseph Fourier 42
University of Alabama 50
University of Arizona 12
University of Arkansas 33
University of California, Berkeley 2, 15, 33, 94, 97, 101, 116, 141, 144
University of California, Davis 58
University of California, Irvine 47
University of California, Merced 12, 43
University of California, San Francisco 57, 60, 61, 127, 135
University of Central Florida 9
University of Chicago 144
University of Colorado, Boulder 42, 47, 159
University of Colorado, Denver 38

University of Delaware 11
University of East Anglia, United Kingdom 138, 141, 142
University of Georgia 24
University of Georgia, Atlanta 57, 60, 61, 127, 134, 135
University of Hong Kong 13
University of Houston 66
University of Idaho 58, 108, 109
University of Illinois, Chicago 42, 87, 159
University of Illinois, Urbana-Champaign 30, 35, 36, 66, 104, 105, 151, 154
University of Iowa 55, 104, 105, 106
University of Massachusetts 31, 32, 33, 34, 97, 102
University of Michigan 5, 46, 60, 96, 132, 153, 155
University of Missouri, Columbia 127, 131
University of Nebraska 68
University of Nevada, Las Vegas 39
University of Notre Dame 3, 7, 41
University of Oklahoma 8, 13, 15, 63, 70, 86
University of Oldenburg, Germany 95
University of Oregon 50
University of Southern California 18, 156
University of Tennessee 30, 45, 57, 60, 85, 86, 89, 90, 91, 93, 104, 105, 127, 134, 135
University of Texas 23
University of Toronto 31, 39, 102
University of Waterloo, Canada 152
University of Wisconsin 50, 55, 69, 140, 142
U.S. Environmental Protection Agency (EPA) 24
U.S. Geological Survey (USGS) 42, 71, 72, 73, 80, 83, 95, 157, 159
Vassar College 37
Virginia Commonwealth University 105
Virginia Polytechnic Institute and State University (Virginia Tech) 21
Washington State University 4, 17, 149
Washington University, St. Louis 10, 62, 143, 144, 146, 158
Western Michigan University 28
Wofford College 53
Yale University 3